The Dissertation Committee for David Justice Lampert Certifies that this is the approved version of the following dissertation:

An Assessment of the Design of *In Situ* Management Approaches for Contaminated Sediments

Committee:

Danny Reible, Supervisor

Robert Gilbert

Lynn Katz

Kerry Kinney

Paul Montagna

An Assessment of the Design of *In Situ* Management Approaches for Contaminated Sediments

by

David Justice Lampert, B.S.; M.S.E.

Dissertation

Presented to the Faculty of the Graduate School of

The University of Texas at Austin

in Partial Fulfillment

of the Requirements

for the Degree of

Doctor of Philosophy

The University of Texas at Austin

May 2010

Dedication

I wanted to dedicate this dissertation to something that I believe in, so I decided to go with the sport of triathlon, which has become my main extra-curricular activity the last few years. In a day and age where most people drive their car everywhere, eat junk food, and few exercise at all, triathletes out there are up early in the morning swimming, cycling, and running to shave a few minutes off their time. This activity provides a fun way for people to stay in shape, meet fulfilling personal goals, and to alleviate our over-burdened health care system. So here's to the growth of the sport.

Acknowledgements

There are so many people to thank. I have to start with my advisor Danny Reible. I feel fortunate the have been one of his first PhD students at UT. I joined "Team Reible" quite ignorant to the problems associated with contaminated sediments and with a limited understanding of the underlying phenomena associated with our field. I now see many of the gaps in the current state of the practice and I feel confident about my ability to pursue future research in this area. The downturn in the economy left many graduate students scrapping for funding, and I feel very grateful to have had good financial support over the last five years (has it been that long?).

Next I have to thank the other professors who've contributed to my academic growth over the years. I'll start with my committee. I feel like I have the most diverse PhD committee—Dr. Reible (chemical engineering), Dr. Kinney (environmental engineer), Dr. Katz (ok, she's also an environmental engineer but has a great chemistry background), Dr. Gilbert (geotechnical engineer), and Dr. Montagna (marine biologist). I guess the diversity speaks to the wide variety of issues associated with contaminated sediments. Then there are other great professors who have helped in my academic growth—Dr. Hughes for getting me started in civil engineering, Dr. Wilber for introducing me to environmental engineering, Dr. Speitel for serving as my Master's

Degree advisor, and Dr. Lawler, Dr. Truskett, Dr. Guy, Dr. Wheeler, and Dr. Sepehrnoori for their great courses.

Of course it's been great to have so much help in the Reible group. Dr. Lu's preliminary work with the PDMS fibers, the worms, and of course, the HPLC has made it easier for me to conduct my experiments over the years. YS, Tony, and Nate—it's been quite an experience for us over the years as the first wave of PhD students in this group. We've had to struggle through some things but it looks like we're all moving on to great careers. I have had great help from other M.S. students in our group—Brian, Wil, Alison, Matt, and Liz—they've helped me collect some good data. I also had help from some great undergraduates—Sameer Kamal, May Sun, Ashley Tallent, Sam Rendon, Erika Kase, and Charles Perng. I know I'm leaving some people out. Everyone in the group has helped me at some point.

Then there's the rest of EWRE and the associated community. Andrew Davidson (homebrewing and general debauchery), Dave Ostrowski (basketball and homebrewing), Eric Hersh (cycling and camping), Mike Konieczki (golf and imbibing), Dan Obenour (cycling and gamenight), Ben Bayer (homebrewing and poker), Amanda Van Epps (happy hour and wine tasting), John Fardall (gamenight), Tyler Jantzen (gamenight and hiking), Brad Eck (math stuff and office gossip), Tim Chess (triathlon), Ashwin Dalvi (the supercomputer), Gabe Trejo (intramural sports and sports gossip), Lee Blaney (China, gamenight and fixie riding), and finally Tony Solina and Constance Danner (a general distraction but particularly golf and trivia night). I know I've left some people out, but it's a long list and there are so many of you to mention.

Last I have to thank my family. They've been supportive and kept the "big life questions" to a dull roar. Well I better wrap it up. Thanks to all of you for making the last five years a successful and enjoyable experience.

An Assessment of the Design of In Situ Management Approaches for Contaminated Sediments

Publication No._____

David Justice Lampert, PhD

The University of Texas at Austin, 2010

Supervisor: Danny D. Reible

Sediments serve as the ultimate sink for many hydrophobic organic compounds and thus present a residual environmental risk many years after sources of contamination are eliminated. Monitored natural attenuation and *ex situ* treatment processes are often ineffective for treatment; as such *in situ* remediation technologies (i.e., capping) are under review.

A conventional *in situ* remediation technology for refractory sediment contaminants is placement of a clean layer of material as a cap. A series of design models was developed to predict the performance of caps composed of the traditional material, sand. A passive sampling method using polydimethylsiloxane (PDMS) fibers for evaluating the performance of caps was developed and tested in the laboratory. The results of the laboratory analysis showed the ability to measure pore water concentration profiles in caps, the consistency of profiles with design model predictions, and correlation of PDMS-derived concentrations with contaminant uptake in test organisms.

Potentially more effective caps composed of permeable adsorptive materials (to retard contaminant migration) and impermeable materials (to divert groundwater flow) were placed along with a conventional sand cap in the Anacostia River in Washington DC in 2004. Field tests of this site showed the ability to measure *in situ* pore water concentration profiles in caps using a field-deployable version of the PDMS passive sampling device and demonstrated the necessity of pore water-based approaches for analyzing caps.

A model for assessing the uptake rates of HOCs within PDMS fibers was developed and shown to predict the kinetics of HOC sorption into fibers. The model is based on external-mass transport processes, which through a series of analyses were shown to be more significant than internal diffusion in PDMS fibers.

Using the PDMS approach, field bioaccumulation tests at the Anacostia site as well as at San Diego Bay and Hunters Point Naval Shipyard showed stronger correlation of PDMS-based pore water concentrations than solid-phase concentrations with observations of bioaccumulation. The overall conclusions suggest that pore water concentrations can often be a better indicator of risk than bulk solid concentrations.

Table of Contents

List of Tables

List of Figures

List of Acronyms

AES	—	atomic emission spectroscopy
AWTA	—	Anacostia Watershed Toxic Alliance
ARCS	—	assessment and remediation of contaminated sediments
BAA	—	benz[a]anthracene
BAP	—	benzo[a]pyrene
BBF	—	benzo[b]fluoranthene
BKF	—	benzo[k]fluoranthene
CETCO	—	Colloid Environmental Technologies Company
CHR	—	chrysene
CSO	—	combined sewer overflow
BSAF	—	biota-sediment accumulation factor
DDD	—	dichloro-diphenyl-chloroethylene
DDE	—	dichloro-diphenyl-dichloroethylene
DDT	—	dichloro-diphenyl-trichloroethylene
DOC	—	dissolved organic carbon
ECD	—	electron capture detection
EPA	—	Environmental Protection Agency
ERDC	—	U.S. Army Corps of Engineers Research and Development Center
ERT	—	Earth Resource Technology
ETWG	—	Engineering/Technology Work Group
FD	—	fluorescence detection
FG	—	Fiber Guide Industries
GC	—	gas chromatography
HC	—	hard carbon
HOC	—	hydrophobic organic compound
HPLC	—	high performance liquid chromatography
ICP	—	inductively coupled plasma
LC	—	labile carbon
MATLAB	—	matrix laboratory
MLLW	—	mean lower low water
MNR	—	monitored natural recovery
MS	—	mass spectroscopy
NOAA	—	National Oceanic and Atmospheric Administration
NRC	—	National Research Council
OC	—	organic carbon
PAH	—	polycyclic aromatic hydrocarbon
PCB	—	polychlorinated biphenyl
PDMS	—	polydimethylsiloxane
PE	—	polyethylene
PFOA	—	perfluorooctanoic acid
PFOS	—	perfluorooctane sulfonate
PHE	—	phenanthrene

PM	—	Poly Micro Industries
POM	—	polyoxymethylene
PYR	—	pyrene
RAMWG	—	Risk Assessment/Modeling Work Group
RCM	—	reactive core mat
RTDF	—	Remediation Technology Development Forum
SITE	—	Superfund Innovative Technology Evaluation
SPMD	—	semi-permeable membrane device
SPME	—	solid-phase microextraction
SRC	—	Syracuse Research Corporation
TCWG	—	Toxicity/Chemistry Work Group
TOC	—	total organic carbon
TPAH	—	total PAH concentration (sum of 16 priority compounds)
USCS	—	Unified Soil Classification System
UT	—	The University of Texas at Austin

List of Symbols

α	=	dispersivity
β	=	$\sqrt{Pe_1^2/4 + Da_1}$
γ	=	$\sqrt{Pe_2^2/4 + Da_2}$
A	=	left-hand side coefficient matrix for finite difference system
B	=	right-hand side coefficient matrix for finite difference system
Bi	=	Biot number (relative importance of internal to external diffusion)
C	=	aqueous-phase concentration
C_{bio}	=	cap-bioturbation interfacial pore water concentration
$(C_{bio})_{avg}$	=	average bioturbation layer pore water concentration
C_{bl}	=	boundary layer concentration
C_{PE}	=	polyethylene concentration
C_w	=	water concentration
C_0	=	initial sediment pore water concentration
C_1	=	pore water concentration in Layer 1
C_2	=	pore water concentration in Layer 2
∇^2	=	Laplacian operator
$\Delta\zeta$	=	dimensionless grid spacing
$\Delta\tau$	=	dimensionless time spacing
δ_j	=	D_j / D_0
D	=	effective diffusion coefficient
D_0	=	effective diffusion coefficient in Layer 0
D_1	=	effective diffusion coefficient in Layer 1
D_2	=	effective diffusion coefficient in Layer 2
D_{bio}	=	biodiffusion coefficient
D_j	=	effective diffusion coefficient in Layer j
D_w	=	molecular diffusivity in water
Da	=	Damkohler number (relative importance of reaction to transport)
Da_1	=	Damkohler number in Layer 1
Da_2	=	Damkohler number in Layer 2
ε	=	porosity
ε_0	=	porosity in Layer 0
ε_1	=	porosity in Layer 1
ε_2	=	porosity in Layer 2
ε_j	=	porosity in Layer j
f_{hc}	=	fraction hard carbon
f_{lc}	=	fraction labile carbon
f_{lipid}	=	fraction lipid content
f_{oc}	=	fraction organic carbon
$(f_{oc})_{bio}$	=	fraction organic carbon in bioturbation layer
F	=	flux

F_0	=	initial flux
$F_{bio}{}^{p}$	=	flux from bioturbation
$F_{bio}{}^{pw}$	=	flux from bioirrigation
F_w	=	flux to overlying water
g	=	acceleration due to gravity
h_{bio}	=	bioturbation layer thickness
$h_{channel}$	=	channel depth
h_{eff}	=	chemical isolation layer thickness
h_{cap}	=	cap thickness
h_j	=	layer j thickness
h_{tot}	=	total domain thickness
i	=	$\sqrt{-1}$
k_{bl}	=	benthic boundary layer mass transfer coefficient
k_h	=	sediment particle release rate
K_d	=	solid-water partition coefficient
$(K_d)_j$	=	solid-water partition coefficient in j^{th} layer
K_{doc}	=	dissolved organic carbon partition coefficient
K_f	=	fiber-water partition coefficient
K_{fr}	=	Freundlich coefficient
K_{hc}	=	hard carbon partition coefficient
K_{lc}	=	labile carbon partition coefficient
K_{lw}	=	lipid-water partition coefficient
$K_n(x)$	=	modified Bessel function of the second kind of order n
K_{oc}	=	organic carbon partition coefficient
K_{ow}	=	octanol-water partition coefficient
K_{PEW}	=	polyethylene-water partition coefficient
λ_0	=	decay rate constant in Layer 0
λ_1	=	decay rate constant in Layer 1
λ_2	=	decay rate constant in Layer 2
λ_j	=	decay rate constant in Layer j
l_j	=	$(\varepsilon_j\lambda_j)/\ (\varepsilon_j\lambda_j)$
L	=	characteristic length scale
L_{lake}	=	fetch of lake in wind direction
M	=	mass in sampling device
M_w	=	molecular weight
$\overline{M}$	=	Laplace domain mass in sampling device
υ_w	=	kinematic viscosity of water
n	=	Manning's n
N	=	Freundlich exponent
O	=	order of approximation
π	=	3.14159265…
p	=	number of grid points
p_1	=	grid point corresponding to the bottom of Layer 1
p_2	=	grid point corresponding to the bottom of Layer 2

p_3	=	grid point corresponding to the bottom of Layer 3
p_j	=	grid point corresponding to the bottom of Layer j
Pe	=	Peclet number (relative importance of advection to diffusion)
Pe_1	=	Peclet number in Layer 1
Pe_2	=	Peclet number in Layer 2
q	=	solid-phase concentration (mass per unit mass)
q_{hc}	=	hard carbon-phase concentration (mass per unit mass)
q_j	=	$\frac{\delta_j}{\psi_j}\frac{\Delta\tau}{2\Delta\zeta^2}$
q_{lc}	=	labile carbon-phase concentration (mass per unit mass)
q_{lipid}	=	lipid-normalized tissue concentration (mass per unit mass)
q_{oc}	=	organic carbon-phase concentration (mass per unit mass)
$q_{organism}$	=	organism concentration (mass per unit mass)
$q_{predicted}$	=	predicted lipid-phase concentration (mass per unit mass) = $K_{ow} * C_w$
$q_{sediment}$	=	sediment concentration (mass per unit mass)
ρ_{doc}	=	dissolved organic carbon concentration
ρ	=	particle bulk density
ρ_a	=	air density
ρ_p	=	particle density
ρ_j	=	bulk density in j^{th} layer
ρ_w	=	water density
r	=	radial distance
r_1	=	radius of glass fiber core
r_2	=	radius of glass fiber core plus PDMS coating
r_j	=	$\frac{1}{\psi_j}\frac{Pe\Delta\tau}{12\Delta\zeta}$
R	=	retardation factor (total mass divided by mass in mobile phase)
R_0	=	retardation factor in Layer 0
R_1	=	retardation factor in Layer 1
R_2	=	retardation factor in Layer 2
R_j	=	retardation factor in Layer j
σ	=	internal to external diffusion parameter = $\sqrt{D_{PE}/D/(\varepsilon + f_{oc}K_{oc})}K_{PEW}$
s	=	complex Laplace domain dimensionless time
s_j	=	$\frac{l_j}{\psi_j}\frac{Da\Delta\tau}{2}$
Sc	=	Schmidt number (relative rate of momentum to mass diffusion)
Sh	=	Sherwood number (relative rate of mass transfer to advection)
τ	=	dimensionless time
t	=	time
t_{adv}	=	characteristic advection time
$t_{adv/diff}$	=	characteristic advection/diffusion time
t_{diff}	=	characteristic diffusion time

$t_{internal}$	=	characteristic internal diffusion time
u	=	dimensionless pore water concentration
$\boldsymbol{u}$	=	dimensionless discretized solution matrix
u_i	=	discretized solution value of dimensionless pore water concentration
$\bar{u}$	=	Laplace domain dimensionless pore water concentration
v	=	dimensionless solid-phase concentration
$\bar{v}$	=	Laplace domain dimensionless solid-phase concentration
U	=	Darcy velocity
U_{bl}	=	boundary layer Darcy velocity
v_a	=	wind velocity
v_x	=	river velocity
V	=	pore water upwelling flow rate per unit area
V_{dep}	=	deposition velocity
W	=	Solid-phase concentration (mass per unit volume)
W_{bio}	=	bioturbation layer solid-phase concentration
$(W_{bio})_{avg}$	=	average bioturbation layer solid-phase concentration
ψ_j	=	R_j/R_0
ξ	=	dimensionless distance
x	=	distance
ζ	=	dimensionless depth
z	=	depth

Chapter 1: Introduction

1.1 Background and Problem Statement

As mankind has advanced technologically, new methods have been developed to fabricate materials, create energy, and mass produce items. Demand for these goods and increases in population have resulted in exponential increases in manufacturing and industry. The by-product of this activity has been mankind's increasingly significant impact on the environment. This impact is manifested in many forms, including loss of species, wetlands, and rainforest; global warming; and pollution. Before the 20th century pollution was considered a nuisance and often ignored. However, its effect has become significant and the scope of the problem so large that it can no longer be overlooked. In the United States, the Environmental Protection Agency (EPA) was formed in 1970 to repair damage done to the environment and enforce regulations to protect it in the future. The Federal Water Pollution Control Act was passed in the United States in 1972 in part to introduce measures for reducing pollution from point sources. Subsequently, many pollution sources have been reduced or eliminated. However, despite removal of these sources, many places in the world have become contaminated.

Because much of the pollution in the environment stems from chemicals that have been introduced to ecosystems where they have not existed historically, the natural processes in these ecosystems are not capable of degrading the contaminants rapidly enough to prevent buildup. In addition, the organisms in these ecosystems have begun to biologically accumulate these contaminants, often with adverse effects. As these chemicals are introduced into the food chain, they can ultimately have a negative effect on human health.

One example of this is in contaminated sediments. Sediments often serve as a sink for organic contaminants due to their high organic carbon content. The surfaces of sediments also often contain binding sites that interact with heavy metals. Because of the slow degradation rates and affinity of these contaminants for sediments, the contamination may persist many years after the sources have been contained. The Water Resources Development Act of 1992 calls for assessment of the quality of sediments in the United States. As a result, assessment and remediation of contaminated sediments is a major issue facing environment policy-makers, scientists, and engineers today.

1.2 Current State of Knowledge

1.2.1 Remediation Technologies

Few alternatives exist for contaminated sediment management; at this time, these include monitored natural attenuation, dredging, *in situ* stabilization with activated carbon, capping, and active capping. Natural attenuation is reduction in contaminant exposure risk through natural processes such as degradation and deposition. Natural attenuation processes are often very slow. Dredging has several disadvantages that often limit its effectiveness, including creation of significant acute risks to downstream receptors during dredging activity and minimal effectiveness at surficial sediment concentration reduction. *In situ* stabilization is a new technology that seeks to reduce exposure risks through amendments to the sediment column; the long-term success of this technology is unknown, particularly as it does not physically isolate the contamination from the receptors. For these reasons, capping and active capping are under evaluation as potential remediation technologies for contaminated sediment sites.

Capping contaminated sediments with a clean layer of material is an increasingly attractive method for *in situ* remediation. The most cost-effective material is sand; it is easy is to place due to its large particle diameter, inexpensive, and suitable for re-

colonization of *benthos* after enough time has passed for deposition of fresh sediment (to provide organic matter for organism growth). While exhibiting minimal adsorption capacity in comparison to organic-rich particles, sands often possess some ability to retard contaminant migration of highly hydrophobic compounds. Sand caps also present a physical barrier between benthos and the contamination, since the macro-organisms that dictate contaminant uptake typically only populate the top few cm of the sediment column. As one of the chief risks associated with contaminated sediments is re-suspension during high flow events, a properly designed cap can help to armor sediments and prevent contaminant mobilization and release during floods. The costs associated with sediment capping are generally much less than dredging. For all these reasons, capping appears to be a promising technology for contaminated sediment remediation.

Under some situations (such as high rates of groundwater seepage), however, achievement of the desired reductions in contaminant flux and concentration may require the use of a layer that can more effectively sequester or degrade contaminants. These types of caps are often termed active caps to differentiate them from passive sand caps. Active cap materials include phosphate minerals for metals control, sorbents such as activated carbon or coke for organic contaminant control, and clays for permeability control. Laboratory testing has shown the potential for such materials to effectively control contaminants that might migrate through a conventional cap, primarily by retarding contaminant migration by sorption (Murphy et al. 2006, Kaplan and Knox 2004, Hull et al. 1998). In some cases, degradation can also be enhanced, but the opportunities for incorporating degradative layers into cap materials are not well developed.

1.2.2 Assessment of Contaminated Sediment Risks

Contaminated sediments pose risks to human health and the environment through a variety of pathways. Perhaps the most significant is as a route of entry into the food chain, which has been well-documented (Young et al. 1977, Augenfeld et al. 1982, Reynoldson 1987). The bulk solid-phase concentration is an easily characterized parameter, but correlates poorly with observed bioaccumulation (Burton 1991). Freely-dissolved pore water concentrations have been linked to bioaccumulation (Kraaij et al. 2003, Lu et al. 2003, Lu et al. 2004a, Lu et al. 2004b, Lu et al. 2006). A current research focus has been to estimate pore water concentrations through passive sampling devices such as semi-permeable membrane devices (SPMDs, Booij et al. 1998), polyoxymethylene (POM) sheets (Jonker and Koelmens 2001), polyethylene (PE) sheets (Vinturella et al. 2004), and polydimethylsiloxane (PDMS)-coated glass fibers (Mayer et al. 2000a). These technologies appear to have promise for assessing risks associated with hydrophobic organic compounds (HOCs) in sediments. However, a number of questions linger regarding experimental observations using these devices and more successful applications in laboratory and field settings are needed to validate this approach for contaminated sediment management.

1.3 Outstanding Research Needs for *In Situ* Contaminated Sediment Management

A growing body of evidence suggests the potential effectiveness of *in situ* management approaches (i.e., capping technologies) for contaminated sediments. There is a pressing need to develop appropriate tools for assessing caps. However, several gaps exist in the current understanding of capping as applied. To effectively design sand caps, it is critical to identify the key processes that govern the migration of contaminants within caps. Due to the relatively low sorption capacity of sand, the bulk solid-phase concentration may be a poor metric for assessing cap performance. More appropriate

methodologies are needed for assessing the long-term performance of capping. Passive sampling methods for estimated *in situ* pore water concentrations show promise as a surrogate assessment technique, but remain to be applied within the context of capping and are in need of further field validation. In addition, contaminant uptake kinetics within these devices is not well understood.

1.4 Approach

A major step in the development of capping and active capping into viable treatment technologies is evaluation at the field scale. The introduction of active capping materials into the environment has been limited as a result of the lack of precedent and costs. To encourage the consideration of active capping materials for sediment caps, a field demonstration of selected active capping technologies has been conducted in the Anacostia River in Washington DC. The sediments in the Anacostia contain a wide variety of contaminants of concern including metals, polychlorinated biphenyls (PCBs) and polycyclic aromatic hydrocarbons (PAHs). Selected active capping materials include AquaBlok^{TM}, a clay material for permeability control; apatite, a phosphate mineral for metals control; coke, an organic sequestration agent; sand, material for a control cap. One of the primary objectives in this dissertation was to assess the potential effectiveness of various capping and active capping technologies at this site.

Another key component of assessment of any environmental system and of engineering design is mathematical modeling. A modeling approach is presented herein for design and evaluation of sediment capping and to make predictions about the effects of sediment capping on contaminant concentrations. The modeling approach is applied to a series of laboratory experiments and found to predict contaminant behavior accurately. These results demonstrate the underlying processes that are significant in a

cap and provide useful insight into the development of performance predictions for cap design and assessment.

Appropriate metrics are needed for assessing the performance of sediment caps. The relative insignificance of the solid-phase concentration and the subsequent importance of the interstitial water concentrations are demonstrated in this dissertation. Passive sampling with PDMS-coated fibers is a promising technology for quantifying these concentrations in sediment environments. Herein, the PDMS passive sampling technique is shown to be capable of measuring pore water concentration profiles for HOCs in caps and to correlate well with field-measured organism tissue concentrations. Finally, the kinetics of contaminant uptake within the sampling device are investigated and found to be predicted well by a diffusion model.

1.5 Dissertation Structure

To evaluate the effectiveness of capping and active capping of contaminated sediments, the following dissertation is proposed. The dissertation is divided into the following chapters:

1. a literature review of previous studies on HOC-contaminated sediments, including risk assessment and research motivation, sorption of contaminants to sediments, potential remediation strategies, laboratory studies on capping and potential active capping materials, previous modeling work related to sediment contaminants, and techniques for assessing bioaccumulation of HOCs from contaminated sediments.
2. the development of a mathematical modeling approach for predicting contaminant fate and transport in capping and active capping systems, determining model parameters, and estimating the importance of various parameters in cap design and effectiveness

3. a description of the results from the Anacostia project, including an evaluation of the ability to implement sand and active caps, the costs associated with different capping technologies, and the ability of caps to contain contaminants in the bulk solid phase
4. a comparison of pore water concentration profiles to solid phase concentration profiles in caps that shows the ability of the PDMS passive sampling technique to measure pore water concentration profiles and demonstrates the potential effectiveness of thin-layer capping of contaminated sediments
5. the development of a model for assessing contaminant uptake kinetics in passive sampling devices
6. a demonstration of the applicability of the passive sampling kinetics model to predict uptake rates in PDMS fibers
7. a discussion of the application of the PDMS sampling device for predicting bioaccumulation of HOCs in sediments through application at three sites: the Anacostia River in Washington DC, Naval Station San Diego in San Diego Bay, CA, and Hunters Point Naval Shipyard in San Francisco Bay, CA
8. a summary of findings and recommendations for future investigations

Chapter 2: Literature Review

Contaminated sediments pose a risk to human health and the environment through direct exposure to sediments and as a source of entry into the food chain through benthic receptors. Due to the affinity of many contaminants to sediments, sediments can serve as a source of pollution long after the original source of the pollution is stopped. Hydrophobic organic compounds (HOCs) compose one major class of sediment contaminants. In this chapter, background on the toxicology and sources of these sediment contaminants are presented first, followed by background on sorption (how these contaminants have become associated with sediments), risks associated with contaminated sediments, regulatory responses to these risks, management strategies for contaminated sediments, mathematical modeling, and techniques for measuring pore water concentrations to familiarize the reader with the overall issues associated with sediment contamination.

2.1 Sediment Contaminants

2.1.1 Polycyclic Aromatic Hydrocarbons (PAHs)

PAHs are fused ring aromatic compounds that are produced from such sources as coke production, petroleum refining, and other high temperature industrial processes. PAHs are generally hydrophobic; the partition coefficients for PAHs onto natural organic matter range from hundreds to hundreds of thousands (Schwarzenbach et al. 2003). Figure 1 shows the name and chemical structure of several common PAHs. Kennaway (1930) and Cook (1932) were some of the first to show that PAHs cause cancer in mice. PAHs were subsequently shown to produce tumors in Syrian hamsters (Salley 1954).

Many studies were performed in the 1950s and 60s on the sources, fate, and treatment of PAHs. Andelman and Suess (1970) provide a comprehensive overview of

the literature on PAH pollution; in summary, PAHs were discharged in industrial and municipal effluents and enter the hydrological cycle directly or indirectly through atmospheric deposition. The only effective treatment method for removal was adsorption onto activated carbon, which is impractical for removal of trace concentrations in such complex mixtures as municipal and industrial wastewaters.

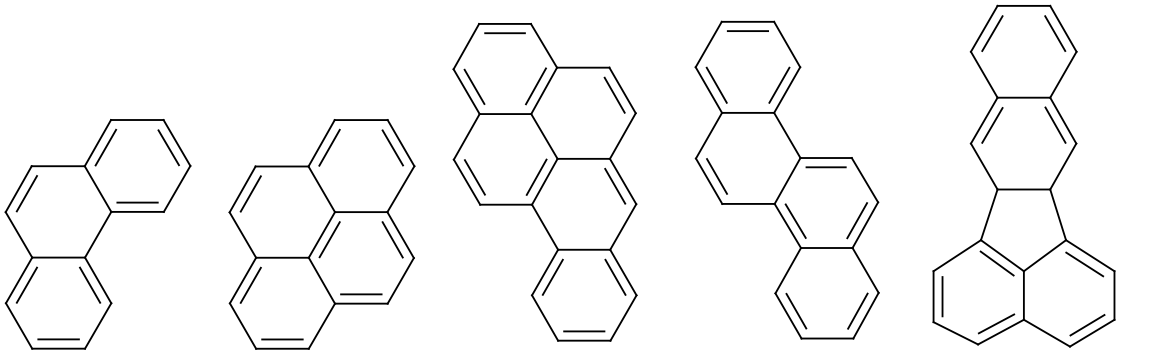

Figure 1. Some typical PAHs.

Today, the United States Environmental Protection Agency (EPA) has determined that benz[a]anthracene, benzo[a]pyrene, benzo[b]fluoranthene, benzo[k]fluoranthene, chrysene, dibenz[a,h]anthracene, and indeno[1,2,3-c,d]pyrene are probable human carcinogens (EPA 2008). Sixteen of the PAHs have now been classified as priority pollutants by the EPA. PAHs are regulated to some degree under the National Primary Drinking Water List, the Hazardous Constituent List, the Ground Water Monitoring List, and the Contract Laboratory Target Compounds and Analytes List. The latter is used for monitoring PAH levels in sediments.

2.1.2 Polychlorinated Biphenyls (PCBs)

PCBs are a class of organic compounds consisting of two fused biphenyl rings with various degrees of chlorination (one to ten atoms). There are theoretically 209 different arrangements of chlorine atoms on the two phenyl rings. PCBs are ubiquitous contaminants that are found in soils, sediment, air, and water. They were produced in the United States from 1929 to 1977 for a number of industrial applications due to their low reactivity and high stability (Farrington et al. 2001). Like many other synthetic chemicals, however, these very properties have resulted in their accumulation in the environment. PCBs are generally hydrophobic; the partition coefficients for PCBs onto natural organic matter range from hundreds to millions (Schwarzenbach et al. 2003). Figure 2 shows the nomenclature system and chemical structure of several PCBs.

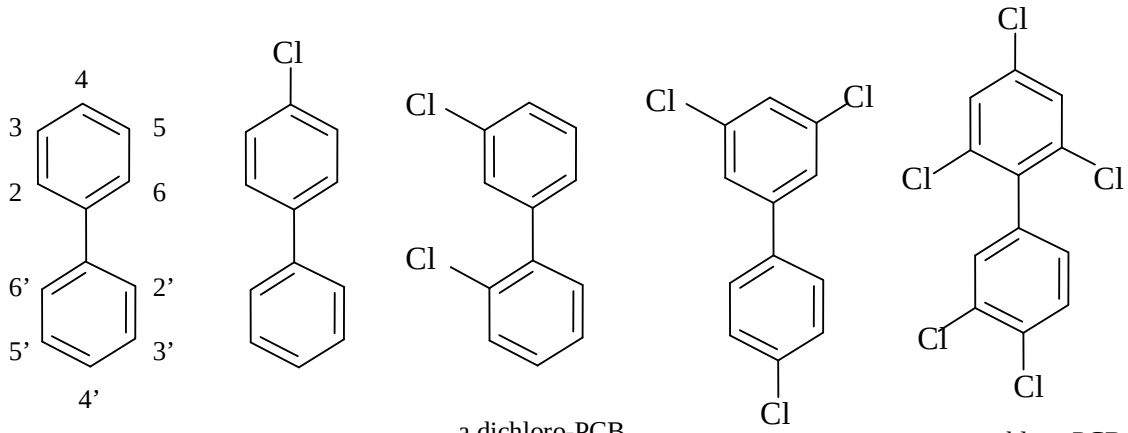

Figure 2. PCB chemical structures and nomenclature.

In 1966, PCBs were first recognized as an environmental contaminant (Jensen 1966). PCBs were later demonstrated to accumulate in a wide variety of marine organisms, particularly white-tailed eagles (Jensen et al. 1969). Hansen et al. (1971)

determined that chronic exposure of pinfish to PCBs resulted in spot disease, while Jonsson et al. (1975) demonstrated that high levels of PCBs abolished reproduction in rats. Thus, after extensive research on accumulation and toxicity of PCBs, the U.S. government banned essentially all the production and use of PCBs under the Toxic Substances Control Act in 1976.

2.1.3 Other Organic Compounds

While the most common sediment contaminants are PAHs and PCBs, other compounds have been shown to accumulate in sediment that present a residual risk to the environment. Polychlorinated dibenzodioxins, or simply dioxins, have been found in sediments (Bopp et al. 1991) at levels of concern. One of the chief sources of dioxins in the environment has been as a combustion by-product from compounds used in the synthesis of Agent Orange (Hay 1982). Dibenzofurans exhibit similar properties to dibenzodioxins, and are often grouped together with dibenzodioxins under the "dioxin" label. Van den Berg et al. (1994) showed that dioxins bioaccumulate in humans in blood, tissues, and milk. Different dioxin compounds exhibit different toxicity; however, the literature has established toxicity levels for all dioxin compounds that are important for risk assessment associated with sediment contamination (Haws et al. 2006).

Dichloro-diphenyl-trichloroethylene (DDT) is a synthetic pesticide that has been used to kill mosquitoes. DDT was first synthesized in 1874, although its pesticide properties were not discovered until later. It has subsequently been used as a pesticide worldwide. Carson (1962) suggested that DDT usage may cause cancer and that its usage has a large negative effect on wildlife, particularly birds. DDT usage was eventually banned in the United States in 1972, although it is still used in some countries. Dichloro-diphenyl-dichloroethylene (DDE) and dichloro-diphenyl-chloroethane (DDD) are by-products in the synthesis and degradation of DDT that are now commonly found

in DDT-polluted areas. DDT, DDE, and DDD have been found in sediments in New Jersey estuaries (Gillis et al. 1995), of the coast of China (Ma et al. 2001), and in Southern California (Young and McDermott-Ehrlich 1977). Management of DDT, DDE, and DDD contaminated sediments is hence a worldwide issue.

Perfluorinated surfactants, including perfluorooctanoic acid (PFOA) and perfluorooctane sulfonate (PFOS), represent an emerging class of contaminants in sediments. These compounds have been used in Teflon, in flexible food packing, to improve stain-resistance in clothing, in fire-fighting foams, and in semiconductor manufacturing. Nakata et al (2006) found levels of perfluorinated surfactants in sediments in the Ariake Sea in Japan. Pefluorinated surfactants display a remarkable stability in the environment (Hansen et al. 2001) and have been determined to bioaccumulate (Renner 2001). The long-term health effects associated with exposure to perfluorinated surfactants are still being evaluated, but it has been hypothesized that they cause liver cancer (Upham et al. 1998).

Clearly, there are many synthetic organic chemicals that display environmental stability, represent unacceptable risk, and demonstrate a tendency to bioaccumulate. In addition to the ones highlighted here, other chemicals that were at one time deemed harmless are found to present adverse environmental effects. Sediments serve as the ultimate sink for many of these contaminants due to their hydrophobic properties.

2.2 Binding of Contaminants to Sediments

Recognizing the risks associated with the chemicals discussed in 2.1, next the mechanisms of how these contaminants become associated with sediments are developed. Understanding the binding behavior of sediment contaminants is a critical part of assessing their fate, transport, bioavailability, and risks, which are concepts developed

later in this review. In this section, a brief review of the theories and models of sorption and desorption of contaminants to sediments are presented.

It was recognized very early in the study of sorption in natural systems that organic matter was primarily responsible for the accumulation of organic compounds in soils and sediments (Goring 1962). An organic carbon-normalized approach to sorption in natural systems was further developed by Goring (1967), Hamaker and Goring (1972), Lambert et al. (1965), and Lambert (1967), who suggested that organic carbon partitioning should be analogous to that of an immiscible solvent to water in liquid-liquid extraction. For organic contaminants in sediment, the organic fraction dictates sorption behavior.

Organic matter in sediments is composed of a complex mixture of different biochemical compounds including proteins, nucleic acids, lipids, cellulose, and lignin. In addition to these, the processes of degradation, re-arrangement, and recombination of the original biochemical compounds, collectively termed diagenesis, create new compounds in sediment environments. As a result, natural organic matter in sediment may contain many different domains, some hydrophobic, some hydrophilic, with different sorption characteristics. In addition to the natural organic matter present in sediments, other organic sorbents that are derived from anthropogenic sources can also be present. An increasing body of evidence suggests the so-called “black” or “hard” carbon fraction (HC), which is derived from incomplete combustion processes, significantly affects sorption processes in sediments.

Karickhoff et al. (1979) presented the widely accepted linear adsorption model for partitioning of hydrophobic organic compounds onto sediments. The partition coefficients were later shown to be related to octanol-water partition coefficients (Karickhoff 1981). Under this model, the pore water concentration, C, is linearly related

to the sediment-phase concentration, q, through the fraction organic carbon in the sediments, f_{oc}, and the organic carbon partition coefficient, K_{oc}. Mathematically:

$$q = f_{oc} K_{oc} C \tag{2.1}$$

Schwarzenbach et al. (2003) present a summary of empirical correlations for estimating the value of K_{oc} for various compounds.

Because sediments now serve as a source of contamination, desorption of organic compounds from sediments is equally as important as sorption. Curiously, desorption behavior from sediments has been found to be very different than sorption behavior. While adsorption is predicted well by the linear model (2.1), desorption generally demonstrates a different equilibrium relationship. The aqueous-phase concentrations in equilibrium with the solid phase are often much lower than those described by the classic model. This desorption resistance has been characterized in numerous studies (Kan et al. 1997, Kan et al. 1998, McGroddy and Farrington 1995, Chen et al. 2000). Several hypotheses exist to explain this phenomenon, including interaction with black carbon, hole filling, and physical entrapment within the organic matter.

Several researchers (Accardi-Dey and Gschwend 2002, Lohmann et al. 2005) have studied the sorption characteristics of sediments onto the HC fraction, which has been defined as the organic carbon that remains after 24 hours of combustion at 375°C. In this work, the researchers hypothesized that HC is responsible for the observed hysteresis in the sediment-water partitioning.

Kan et al. (1998) proposed that some of the sorption compartments are reversible while others are irreversible to explain this observed hysteresis in the adsorption and desorption curves. Desorption from the reversible sites is assumed to follow the classic linear model, while desorption from the irreversible compartment is assumed to follow a

Langmuir relationship. This model has been termed the dual-equilibrium desorption model.

2.3 Sediments as a Source of Environmental Risk

Nimmo et al. (1971) were the first to study bioaccumulation of PCBs directly from contaminated sediments. In this study, the authors established that fiddler crabs and shrimp exposed to PCB-contaminated sediments accumulated PCBs proportional to the concentrations in the sediment. Young et al. (1977) concluded that sediments can act as a source of pollution in a study of PCB contamination in Southern California coastal waters.

Augenfeld et al. (1982) were the first to show accumulation of PAHs directly from sediments. Sediments were spiked with ^{14}C-labeled PAHs, after which *M. inquinata*, a detritus feeding clam and *A. pacifica*, a burrowing polychaete, were exposed to the contaminated sediment. In this study, the authors observed concentrations higher in the organism tissue than in the sediments.

Throughout the 1980s, more focus was placed on the importance of sediment-associated contaminants, and many different theories began to develop to explain the observed bioaccumulation of these contaminants. Reynoldson (1987) performed a survey of this literature, and pointed out the need for better understanding of uptake in the lower trophic levels of the food web. Researchers proposed absorption from overlying water, direct sediment ingestion, external contact, and interstitial pore water as the predominant mechanism for bioaccumulation of sediment contaminants. Burton (1991) also observed that chemical concentrations in the sediment phase do not correlate well with observed bioaccumulation.

Bierman (1990) suggested using equilibrium partitioning theory to predict the accumulation of organic contaminants in benthos from sediment. This concept assumes

that a contaminant will distribute among the sediment, pore water, and organisms according to a predictable partitioning relationship. The biota-sediment accumulation factor (BSAF) is a useful measure of the bioaccumulation potential that is essential to this theory was first presented by McFarland (1984):

$$\mathrm{BSAF} = \frac{q_{lipid}}{q_{oc}} = \frac{q_{organism} / f_{lipid}}{q_{sediment} / f_{oc}} \tag{2.2}$$

Where q_{lipid} represents the contaminant lipid-phase concentration of the organism, q_{oc} is the contaminant concentration in the sediment organic matter, $q_{organism}$ is the contaminant concentration in the organism, $q_{sediment}$ is the contaminant concentration in sediment, f_{lipid} is the lipid fraction of the organism, and f_{oc} is the organic carbon fraction in sediment. In equilibrium partitioning theory, the BSAF is theoretically the same for a particular contaminant in different sediments because bioaccumulation of a contaminant is dictated by the contaminant sediment-phase concentration. However, due to the complex relationship between solid-phase concentrations and pore water concentrations in sediments (summarized in 2.2), prediction of pore water concentrations by simple linear models may be inaccurate.

DiToro et al. (1991) presented guidelines for establishing sediment quality criteria. In this paper, the authors noted that organism accumulation is correlated with sediment pore water concentrations. This approach prevents issues associated using sediment-phase concentrations as standards, since they are not well correlated with bioaccumulation (Burton 1991). Ankley and Shubauer-Berigan (1994) suggested that pore water concentrations should be used as the criteria for evaluation of contaminated sediments. Other more recent studies have confirmed that pore water concentrations, and not bulk sediment concentrations, dictate bioaccumulation and should therefore be used

to evaluate sediments (Kraaij et al. 2003, Lu et al. 2003, Lu et al. 2004a, Lu et al. 2004b, Lu et al. 2006).

Drake (2007) evaluated the uptake of PAHs and PCBs in benthic organisms and studied the correlation of tissue concentrations to both sediment and pore water concentrations. To assess the importance of pore water in bioaccumulation, in this study the BSAF was predicted using the observed pore water concentrations to predict q_{oc} with Equation (2.1). The authors plotted the measured BSAF and the predicted BSAF and found that the BSAF based on the measured pore water concentrations provided a stronger correlation than the BSAF from the solid-phase concentrations. These results provide more evidence to support the theory that bioaccumulation is driven by the pore water concentrations and not the sediment-phase concentrations.

2.4 Regulatory Responses to Concern about Contaminated Sediments

In response to the increasing concern over contaminated sediments, in 1987 the EPA authorized a five-year study and demonstration project to determine appropriate treatment of toxic contaminants in bottom sediments. This program was termed the Assessment and Remediation of Contaminated Sediments (ARCS) Program. ARCS was divided into three technical work groups: the Toxicity/Chemistry Work Group (TCWG), the Engineering/Technology Work Group (ETWG), and the Risk Assessment/Modeling Work Group (RAMWG). The job of the TCWG was to characterize the chemical and toxicological properties of contaminated sediments. The purpose of the ETWG was to evaluate the feasibility of remediation and technologies. The RAMWG was formed to provide a framework for evaluating the ecological and health risks and benefits associated with remedial alternatives. Some of the major findings of the program were (EPA 1994):

1. sediment cores provide more information than surficial grab samples and should be used to evaluate chemical concentration profiles
2. chronic exposure tests (28 days) should be used to evaluate sediment toxicity
3. toxicity tests to determine appropriate endpoints should consist of multiple species, endpoints, and response pattern groups
4. comparisons between concentrations of simultaneously extracted metals, total PAHs, and total PCBs and benthic invertebrate abundances demonstrate a consistent pattern of decreasing abundance with increasing contamination
5. measurements of chemical and physical variables should be made on sub-samples of the sediments from which invertebrates are collected to avoid the potential problems associated with heterogeneous distributions of organisms and contaminants
6. additional research is needed to evaluate the specific contaminant factors that control invertebrate abundance in contaminated sediments
7. long-term monitoring is essential to any sediment remediation project due to the time scales involved in transport of the contaminants

The committee determined that management of contaminated sediments requires an integrated sediment assessment approach that combines chemical analyses, toxicity testing, and benthic community surveys to define the magnitude and extent of the sediment contamination at a site. In 1992, Congress authorized the EPA under the Water Resources Development Act to develop a biennial report to Congress on sediment quality.

In response to the Congressional mandate, in 1998 the EPA released *Contaminated Sediment Management Strategy*. In this report, it was concluded that seven percent of all U.S. watersheds, including every state in the country, are sufficiently

contaminated to present risks to the environment. The EPA established four primary goals for management of contaminated sediments (EPA 1998):

1. prevent the volume of contaminated sediment from increasing
2. reduce the volume of existing contaminated sediment
3. ensure that sediment dredging and dredged material disposal are managed in an environmentally sound manner
4. develop scientifically sound sediment management methods

Goals (2), (3), and (4) require treatment strategies and assessment techniques that represent an important challenge for environmental science, policy, and engineering community today.

2.5 Strategies for Managing Contaminated Sediments

There is no panacea for management of contaminated sediments due to the complex nature and variety of different sites. The risks, costs, benefits, and design goals for each site are different. Several different possibilities are being evaluated for management of the contaminated sediments, including monitored natural attenuation, dredging, *in situ* stabilization with black carbon, capping, and active capping.

2.5.1 Monitored Natural Recovery

Monitored natural recovery or attenuation (MNR) is the assessment of ongoing natural recovery processes such as biodegradation or irreversible sorption to reduce contaminant bioavailability. A critical part of the success of MNR is demonstrating that natural processes are capable of this reduction, which requires that contaminants are either destroyed by these processes or that they become less bioavailable. Due to the ubiquitous nature of sediment contamination, any form of sediment remediation involves MNR to some extent. The processes that affect bioavailability are dispersion, sorption, and contaminant transformation (either biotic or abiotic). Dispersion in this context

refers to dilution to acceptable levels, which can result from mixing into the overlying water, loss to the atmosphere, and decreased availability due to deposition of new (and presumably clean) sediment. The sorption of contaminants on sediments is discussed extensively in (2.2). A brief summary of the studies on biological degradation of contaminants in sediments is presented here.

Shiaris and Sayler (1982) studied biological degradation of PCBs by freshwater microorganisms, but found that only the lower chlorinated compounds could be degraded aerobically. Bedard et al. (1987) showed that more highly chlorinated PCBs can be degraded anaerobically by reductive dechlorination to lower chlorinated compounds that can be degrdaded aerobically subsequently. Thus, the authors suggested a two-stage process for PCB decay. However, in most natural systems the necessary conditions for these decay mechanisms to occur are rare, which means that MNR is not likely to reduce contaminant environmental risk associated with PCBs.

Herbes and Schwall (1978) studied the transformation rates of PAHs in sediments using ^{14}C-labeled molecules. In these experiments, the authors observed degradation of PAHs, although the rate decreased with increasing molecular weight. They attributed the slow degradation rates to hydrophobicity, which was hypothesized to decrease bioavailability and slow diffusion into the cell membranes due to the large molecular size.

The degradation of PAHs under aerobic conditions in sediments was subsequently demonstrated by many researchers (Bauer and Capone 1985, Durant et al. 1995, Sepic et al. 1995). It was initially thought that anaerobic degradation of PAHs did not occur, however, which is significant because only the very top of the sediment column is aerobic (Cerniglia 1992). Several researchers (Hayes et al. 1999, Rockne and Strand 1998, McNally et al. 1998) observed PAH degradation under sulfate-reducing conditions,

although at rates 1-2 orders of magnitude lower than aerobic conditions. Beckles et al. (2007) showed that bioavailability may be the source of persistence of PAHs in sediments. In this study PAH degradation was linked to pore water concentrations predicted by the dual-equilibrium desorption model, which indicated that desorption resistance also limits bioavailability. PAH presence in sediments can persist due to the lack of appropriate bacteria species, lack of availability, or other inhibitory effects, such as the presence of co-contaminants.

2.5.2 Dredging

Dredging is the process of gathering up sediments and moving them to a different location. Dredging has been used for hundreds of years for improving the navigability of waterways throughout the world. Due to increased awareness about the high levels of contamination in sediments, dredging has been proposed as a remediation alternative for managing contaminated sediments. As one of the four stated goals of the EPA's *Contaminated Sediment Management Strategy* (EPA 1998) is to reduce the volume of contaminated sediments in the United States, removing contaminated sediments by dredging appears to be an effective strategy for achieving this goal. However, risks associated with contaminated sediments are primarily driven by accumulation in benthic receptors, and these risks are driven by the concentrations at the top of the sediment column. If surficial sediment concentrations are not decreased, dredging may prove ineffective at risk reduction. The United States National Research Council (NRC) later stated that the primary concern over PCBs in sediments is to human health and the environment (NRC 2001). The effectiveness of dredging as a remediation technology for contaminated sediments is still under review.

In addition to concerns over the actual benefits associated with dredging, the process is very expensive. Dredging residuals must be dewatered to reduce volume and

disposal costs. The remnant is then transported to a landfill, often a hazardous waste landfill (depending on the level of contamination) for final disposal. Thus the costs associated with dredging can be very high relative to other treatment technologies and are highly site-specific. Dredging results in suspension of many of the targeted contaminated sediments into the water column; this effect presents an acute risk to aquatic receptors that must also be considered when managing a contaminated sediment site.

Thibodeaux and Duckworth (2001) evaluated the effectiveness of dredging at three sites. The effectiveness was evaluated by quantifying contaminant release, short term aquatic effects, and long-term effects. The authors found that dredging is effective at removing large quantities of contaminants, although they concluded that it is impossible to remove 100% of the contamination. The surficial sediment concentrations were typically reduced by 50-75%, and the short-term effects on fish were consistently negative.

In the NRC report on PCB contaminated sites, the effectiveness of dredging was evaluated by looking at the Grasse River in Massena, New York (NRC 2001). In this study, as many as 32 passes were required to reduce PCB concentrations below target cleanup levels. It was concluded that dredging combined with capping would be the most effective means of managing the contaminated sediments.

2.5.3 *In Situ* Stabilization with Activated Carbon

The so called “black: or “hard” carbon fraction of sediments (carbon remaining after combustion at 375°C) has been linked to contaminant desorption hysteresis in sediments (described in 2.2). As pore water concentrations have also been linked to bioavailability, several researchers have proposed intermixing activated carbon into contaminated sediments as a means of reducing the pore water concentration (Zimmerman et al. 2004, Millward et al. 2005). These studies showed a 70% or greater

reduction in organism uptake with minimal effects on organism from the presence of the activated carbon molecules. This technology is relatively new and is now being evaluated at the field scale (Cho et al. 2007), but holds promise as it is one of the few *in situ* technologies for contaminated sediment remediation.

2.5.4 Capping

The primary option for *in situ* treatment of contaminated sediments is capping with clean material. Capping provides a physical barrier between benthic receptors near the sediment-water interface and can reduce contaminant concentrations by retarding migration through sorption onto the cap material. Sand caps can also provide a new habitat to areas where transport of coarse-grained sediments has been reduced due to reduction in high flow events (due to dams and other man-made interferences).

Thibodeaux and Bosworth (1990) proposed capping with clean material as a mechanism of reducing the concentration and flux from PCB-contaminated sediments. In this study, a clean sediment cap was observed to retard diffusion of contaminants from contaminated sediments. Wang et al. (1991) studied sediment capping of 2,4,6-trichlorophenol in the laboratory by evaluating its migration through clean sediment. These studies showed the potential effectiveness of capping as a remediation technology for managing contaminated sediments.

Capping with sand has been evaluated throughout the past two decades in various studies. Zeman and Patterson (1997) discuss the successful implementation of a sand cap in Hamilton Harbor, Ontario, Canada. A capping project in the St. Paul Waterway near Tacoma, Washington successfully demonstrated habitat restoration (Parametrix 1998). Ten years of monitoring showed minimal cap disturbance and the ability of capping to contain contaminants. As an added benefit, sand capping restored shallow-water habitat that had been reduced by 90% over the past 100 years. Simpson et al. (2002) found that

capping was successful at reducing metal fluxes, particularly due to organism-induced mixing (bioturbation) in the clean cap material rather than in the sediments.

2.5.5 Active Capping

Due to the permeable and relatively inert nature of sand, questions have arisen over the long-term effectiveness of sand caps for contaminated sediment management. As an alternative to traditional capping, active capping has been proposed. Active capping can be broadly defined as capping with materials that encourage degradation or sequestration of the contaminants. Active cap materials, while effective for contaminant sequestration, may be unsuitable habitats for benthos; as such, a clean sand layer often serves as both an erosion armoring and habitat restoration layer.

Apatites represent a class of naturally-occurring minerals that have been investigated as a sorbent for metals in soils and sediments (Chen et al. 1997, Peld et al. 2004). Apatites generally consist of a matrix of calcium phosphate and various other common anions, including fluoride, chloride, hydroxide, and occasionally carbonate. The mechanism of the sorption is a matter of some debate, with the two main theories suggesting that either direct ion exchange of a metal for the calcium atom (Miyake et al. 1986, Takeuchi and Arai 1990) or dissolution of hydroxyapatite followed by precipitation of lead apatite (Ma et al. 1993, Xu and Schwartz 1994) are the dominant mechanism of metal immobilization. Whatever the mechanism, apatite minerals are capable of sequestering metals and as such present a possible material for active capping of metal-contaminated sediment.

Crannell et al. (2004) investigated apatite for sediment capping in a series of pilot-scale experiments. In these experiments, 10-cm apatite caps were placed on two different contaminated sediments in 40-L tanks. Natural estuarine waters were run over the sediments, and the tanks were monitored for 400 days. In addition, 10-day

bioaccumulation experiments were performed on *Chironomus tentans*. The results showed significant reduction in lead, cadmium, and zinc pore water concentrations versus control (sand) caps and reduced biouptake of cadmium.

Jacobs and Forstner (1999) developed the concept of an active barrier system for containment of metals using zeolite. They also suggested exchanging a cationic surfactant onto the surface charges to create a hydrophobic, sorbing layer for non-polar organics. Organoclay is a modified bentonite containing such substitutions that is under evaluation for control of non-aqueous phase liquids and other organic contaminants (Parrett and Blishke 2005, Reible et al. 2005).

Hull et al. (1998) studied the effectiveness of AquaBlok^{TM}, a clay and polymer-based mineral around an aggregate core, as a capping material to reduce pore water upwelling to improve the performance of sediment caps. The authors found that AquaBlok^{TM} was capable of settling to the bottom of the water column and forming a cohesive boundary with minimal intermixing with the underlying contaminated sediment. In another study, Hull et al. (1999) compared the effectiveness of sand to AquaBlok^{TM} in a laboratory study, recognizing that the highly permeable nature of sand created susceptibility to migration in systems with high upwelling. The AquaBlok^{TM} cap was found to significantly reduce upwelling versus the sand cap.

Organic sorbents such as activated carbon are another potential active capping material for sequestering HOCs. One of the concerns over the applicability of these materials is cost. McDonough et al. (2007) discuss the idea of using thin-layer caps for implementation of high-cost cap materials. Murphy et al. (2006) proposed using thin-layer caps of highly sorptive materials, such as coke, organic rich soil, and activated carbon, as a means of reducing contaminant concentrations and fluxes. In this study, sorption isotherms were developed for the different materials and used with mathematical

models to predict the long-term effectiveness of sorbent-amended caps at reducing surficial sediment concentrations.

This body of research has supported the idea of using sorbent materials to enhance cap performance. The studies to date have shown the effectiveness of these approaches in a laboratory setting. Now there is a pressing need to demonstrate the effectiveness of active capping at a field scale.

2.6 Modeling of Contaminant Transport in Sediment Caps

To evaluate the effectiveness of sediment capping, it is critical to be to predict concentrations and fluxes of contaminants in the future. The transport of contaminants through engineered porous containment layers has been modeled extensively over the past 30 years (Rowe and Booker 1985, Rubin and Rabideau 2000, Malusis and Shackelford 2002). Typically, estimations of chemical migration in a containment barrier are made with a transient advection-diffusion model as described by Bear (1972). An analytical solution to the mass conservation equation can be obtained if the cap is assumed semi-infinite. These models can also be extended to reactive contaminants (van Genuchten, 1981).

The majority of this work done on engineering barriers applies to soil containment; sediment environments possess some different transport mechanisms that limit the applicability of this work to sediment capping. The difference between contaminant transport in sediment caps and soil containment barriers lies in the transport processes near the sediment-water interface. The sediment zone near this interface is where macrobenthic biological activity takes place and is commonly known as the bioturbation layer. The water directly overlying the sediment-water interface is commonly referred to as the benthic boundary layer.

The bioturbation layer is subject to significantly different transport processes and physical and chemical characteristics than in the underlying sediment and cap layers, such as increased organic carbon content and sharp gradients in redox conditions. The organisms that reside in this zone re-work sediment particles, significantly affecting chemical transport near cap-water interface. It is also within this region that chemical reactivity is highest due to the exchange of nutrients, labile organic matter and electron acceptors with the overlying water. The benthic boundary layer or diffusive sub layer is the part of the water column directly above the sediment-water interface and is important for transport modeling to account for water-side mass transfer limitations at the surface of the bioturbation layer.

The chemical reactions that take place near the sediment-water interface are collectively known as diagenesis. Marine and soil scientists have studied diagenesis extensively and developed many models for predicting transport behavior of chemicals in this region (Berner 1980, Boudreau 1997, Boudreau and Jorgensen 2003). As sediment contamination has become a larger issue, environmental engineers and scientists have recognized the importance of incorporating diagenetic reactions into contaminant fate and transport modeling in sediments. Thibodeaux (1996) presents a number of useful relationships for fate and transport modeling of contaminants in sediments.

Thoma et al. (1993) presented several models for evaluating the effects of sediment capping on contaminant concentrations and fluxes. This work did not incorporate bioturbation in the capping layer, however. Palermo et al. (1998) provided guidance for modeling of contaminant transport in sediments. In this approach, the flux associated with semi-infinite transport due to advection, diffusion, dispersion, and decay from the chemical containment layer (below the bioturbation zone) was estimated. Transport through the bioturbation layer was assumed to be dictated by the combined

processes of bioturbation, advection, diffusion, and dispersion. The flux through the water side of the benthic boundary layer was modeled as a mass transfer reaction. The authors then used a simple combination of these fluxes and mass transport resistances to estimate the concentration in the bioturbation layer. This approach, while not unreasonable, is very simplistic and is need of extension for performing simulations of more robust systems.

2.7 Approaches for Measuring Pore Water and Bioaccumulation Potential

As discussed in 2.3, contaminant sediment-phase concentrations, while relatively easy parameter to measure, often correlate poorly with bioaccumulation. A growing body of evidence suggests that pore water concentrations are a better predictor of bioaccumulation from sediments. Water is the mobile phase in sediment treatment systems; as such concentrations in the aqueous phase are more representative of contaminant migration than solid-phase concentrations. For example, due to the limited sorption capacity of sand, bulk solid levels in a sand cap never reach the levels seen in sediments. The pore water, however, is unaffected and represents an unbiased measurement of success. Several approaches have been examined for measuring pore water concentrations and are discussed below.

2.7.1 Centrifugation

Ankley and Schubauer-Berigan (1994) compared the effectiveness of different techniques for measuring pore water concentrations. These techniques included centrifugation at low (2,500 *g*) and high speed (10,000 *g*), syringe extraction, compression, and dialysis. The authors concluded that the best technique for pore water extraction was with high speed centrifugation. Concentrations measured using this technique, however, do not enable pore water profiling and are often below detectable levels.

2.7.2 Dialysis Membranes

Hesslein (1976) described an *in situ* pore water profiling device using a dialysis membrane capable of achieving 1-cm resolution that has been widely used for studying diagenesis. This technique reduced to the need to filter and clean up the pore water prior to analysis. However, for many sediment contaminants the concentrations are low and therefore require significant volumes of water for adequate mass to meet instrument detection limits. Collecting such large volumes significantly reduces the resolution capabilities of this technique.

2.7.3 Semipermeable Membrane Devices (SPMD)

Huckins et al. (1990) were some of the first researchers to explore the idea of passive sampling for assessing bioaccumulation of contaminants from sediments. In the approach presented by these authors, low density polyethylene tubing containing a thin film of lipids was placed into contaminated aquatic environments, and then removed for analysis. The authors termed the lipid-filled tubing a semipermeable membrane device (SPMD). The concept of the study was to simulate the bioconcentration of non-polar organic contaminants by aquatic organisms with a more consistent and less costly approach. The authors believed this technique would provide insight into the concept of equilibrium partitioning theory between the sediment, pore water, and biological tissue phases.

SPMD excludes contaminants associated with humic acid or sediments, therefore a pre-filtration step is unnecessary (Huckins et al. 2006). The primary disadvantages of SPMD are the time consuming dialysis procedure required and the difficulty in identifying toxic agents from the lipid extract (Namiesnik et al. 2005). SPMD is also problematic in the field due to possible tearing and loss of triolein, which makes accurate

measurements difficult (Namiesnik et al. 2005). Due to the success of SPMD, other "passive sampling" methods have been proposed and investigated.

2.7.4 Polyethylene (PE) Sheets

Adams et al. (2007) used polyethylene sheets (PE) as an alternative to SPMD for passive sampling of organic contaminants in sediments. Polyethylene devices passively accumulate HOCs in proportion to freely dissolved concentrations similar to SPMD. Thin strips of low-density PE provide a simple and effective method for passive *in situ* sampling (Adams et al. 2007). Clean PE is woven in an accordion fashion on a steel wire which is woven to a nylon rope and can be deployed in an aquatic environment. After equilibrating, the PE sheets are recovered and extracted to measure contaminants.

2.7.5 Polyoxymethylene (POM) Extraction

Polyoxymethylene solid-phase extraction (POM) is another emerging method of passive sampling. The POM method is similar to other solid phase extraction techniques in that the POM is inserted into a aqueous and solid sediment phase or slurry, left to equilibrate for a previously determined amount of time, removed, extracted and analyzed using appropriated analytical techniques (Jonker and Koelmans 2001). The POM method is capable of strongly extracting the natural sorbent due to the larger capacity of POM and is also capable of detecting low aqueous concentrations. POM utilizes a clean-up step which removes complex interfering environmental matrixes since POM is not a selective method and all compounds with an affinity for the plastic are absorbed (Jonker and Koelmans 2001).

2.7.6 Polydimethylsiloxane (PDMS) Fibers

Mayer et al. (2000) described a technique for measuring pore water concentrations using a glass fiber core surrounded by a cross-linked polydimethylsiloxane (PDMS) coating, which is commonly used in fiber optic cables.

The cross-linked PDMS material has a hydrophobic surface which repels both water and alcohols and can absorb HOCs. The PDMS material may adsorb both organic solvents and solutes, however.

PDMS extracts HOCs from sediment pore water into the fiber coating using the sediment particles as a reservoir, which for sufficiently small coatings remains essentially unchanged over the duration of the equilibration period. The compounds on the PDMS fiber can then be extracted rapidly using a non-polar solvent, which is capable of swelling the fiber matrix and rapidly releasing the contaminants. The pore water concentrations can be determined using an appropriate partition coefficient, which is generally linear. At this point in time, PDMS fibers appear to be a promising technique for measuring pore water profiles of caps *in situ* and have the potential to evaluate the success of sediment caps.

2.8 Summary

This chapter has broadly discussed the issue of HOCs in sediments. Once associated with sediments, these chemicals present a long-term risk to the environment that requires further analysis. A summary of the current strategies for managing sediments was presented with particular emphasis on capping and active capping. These technologies present considerable promise as they are relatively inexpensive and appear effective at reducing environmental risk. There is now a pressing need for long-term assessments of the effectiveness of capping and active capping. A critical portion of this evaluation is predicting contaminant fate and transport in the environment using mathematical models. Another key need for assessment and remediation of contaminated sediments is measuring contaminant pore water concentrations through passive sampling devices. The freely dissolved pore water concentration is believed to dictate transport and bioavailability of contaminants in sediment environments.

Chapter 3: An Analytical Modeling Approach for Evaluation of Capping of Contaminated Sediments[1]

David J. Lampert[2], Danny Reible[2]

3.0 Abstract

An analytical design tool is developed to predict performance of a cap for containment of contaminated sediments. Transient conditions within a cap can be modeled by advection, diffusion, and reaction within the typically homogeneous chemical isolation layer for which analytical models exist. After contaminant penetration of the chemical isolation layer, a steady state model is proposed that incorporates pore water advection and diffusion, sediment erosion and deposition, sediment re-working and pore water pumping via bioturbation, and reaction. The steady state model allows the complexities of the biologically active layer to be considered while maintaining an analytical form for convenient and rapid evaluation. In this paper, the model framework, behavior, and limitations are presented.

[1]Published in: Soil and Sediment Contamination, 18(4):470-488, 2009. Reprinted here with permission of the journal.

[2]Department of Civil, Architectural, Environmental Engineering, The University of Texas, Austin, TX

3.1 Introduction

Remediation of contaminated sediments is one of the most challenging problems in environmental engineering today. One of the primary risks associated with contaminated sediments is bioaccumulation in benthic organisms, which is a route of entry into the food chain. Thus an important goal of sediment remediation is reducing concentrations to these organisms.

Few alternatives exist for management of contaminated sediments. One promising technology for reducing exposure and risk to contaminated sediments *in situ* is through the use of capping with clean media. Capping with clean media has been shown to reduce surficial sediment concentrations in the lab and to agree well with traditional mass transport models (Thoma et al. 1991). In a field study, Azcue et al. (1998) found that the flux of metals was reduced significantly one year after capping. Zeman and Patterson (1997) discuss the successful implementation of a sand cap in Hamilton Harbor, Ontario, Canada. A capping project in the St. Paul Waterway near Tacoma, Washington successfully demonstrated habitat restoration (Parametrix 1998). Ten years of monitoring showed minimal cap disturbance and the ability of capping to contain contaminants. As an added benefit, sand capping restored shallow-water habitat that had been reduced by 90% over the past 100 years. Simpson et al. (2002) found that capping was successful at reducing metal fluxes, particularly due to organism-induced mixing (bioturbation) in the clean cap material rather than in the sediments.

The primary purposes of a cap over contaminated sediments are:

1. Armoring contaminated sediments to ensure they are not re-suspended in high flow conditions

2. Physically isolating contaminated sediments from benthic organisms that typically populate only the upper few cm of sediment
3. Providing resistance to transport processes that result in chemical release from the sediments

Because many sediment contaminants are highly sorptive, their migration through a cap can be retarded due to accumulation on the clean cap material. A portion of the cap is typically compromised by the following processes: intermixing between sediment and the lower layer of the cap, expression of contaminated pore water by consolidation of underlying sediment, and bioturbation (organism-related mixing) of the near surface layer. The remaining layer is termed the chemical isolation layer. It has been estimated that the time for typical sediment contaminants to migrate through strongly sorbing chemical isolation layers may be hundreds or thousands of years (Murphy et al. 2006). For other less sorbing caps where the breakthrough time is shorter, capping can serve as a mass transport resistance to reduce the steady state flux and surficial concentrations near the sediment-water interface.

Evaluation and design of sediment caps requires a model to predict the relationship of design parameters to chemical fate and transport processes that take place within the contaminated sediment cap containment system. Chemical migration in porous containment layers can be estimated using a transient advection-diffusion model as described by Bear (1972). For example, numerous approaches to the transport of contaminants through soil containment layers have been presented (e.g., Rowe and Booker 1985, Rubin and Rabideau 2000, Malusis and Shackelford 2002). The majority

of this work has been applied to soil slurry liners, which differ from sediment caps in several important ways.

The top of the sediment cap (hereafter referred to as the bioturbation layer) is subject to significantly different transport processes and rates than in the underlying cap layer and may exhibit significantly different physical and chemical characteristics, such as increased organic carbon content and sharp gradients in redox conditions. The organisms that reside in this zone also re-work sediment particles; this process significantly affects chemical transport. It is also within this zone that chemical reactivity is highest due to the exchange of nutrients, labile organic matter and electron acceptors with the overlying water. The thickness of the cap may increase due to deposition or decrease due to erosion. Finally, mass transport at the sediment-water interface requires different boundary conditions than those used in soil slurries due to the presence of turbulent motion in the overlying surface water.

The EPA has provided guidance for *in situ* cap design (Palermo et al. 1998). The important considerations for cap design are minimizing erosion, reducing contaminant flux to biological receptors, and providing appropriate thickness to account for consolidation of the surficial sediments. The EPA guidance document presents a simplistic approach for evaluating contaminant fluxes and concentrations in a sediment cap. In this approach, the transient migration and flux through the cap system is assumed to be controlled by the chemical isolation layer and estimated by advection or diffusion. This approach does not include important processes such as degradation and cannot predict contaminant concentrations or fluxes in the biologically active zone that is often of primary importance.

In this paper, an approach is presented to address these limitations. The result is a set of analytical models that can be used for initial screening and evaluation of sediment capping. Because the models are analytical, they can be used for rapid evaluation across a range of parameter values and can be used as a check for more complex numerical models which may be applied to situations where no exact solution to the governing equations exists.

The models developed herein enable an assessment of the concentration within the chemical isolation layer of a cap at any time, the time over which a cap is effective, and the potential exposure in the biologically active zone after contaminant penetration of the chemical isolation layer. The recommended approach is to employ a one-layer analytical transient model under the assumption of a semi-infinite domain until penetration of the chemical isolation layer occurs (i.e., while the assumption is valid). Upon penetration of the chemical isolation layer, the relatively rapid transport processes in the surface layer will subsequently quickly lead to steady state conditions. Under steady state conditions it is possible to consider the complexities of the upper boundary and still employ relatively simple analytical solutions to the chemical transport equations. Through use of a steady state model, it is possible to estimate the maximum contaminant concentration and flux that may ever be achieved within the biologically active zone. Thus the model can be used to determine a conservative cap design through estimation of the maximum concentrations and fluxes in the biologically active zone. The transient model presented here is equivalent to the one presented in the EPA guidance document (Palermo et al. 1998) but is included for completeness and discussion of how to adapt the model to evaluate other processes such as burial by sediment deposition. The

combination of the transient model for the chemical isolation layer and the steady state model for the chemical isolation and bioturbation layers presented here provide:

1. the concentration profiles during contaminant migration through the chemical isolation layer
2. the time of complete separation of the benthos from the contaminants
3. the maximum concentration and flux that will be achieved after penetration of the cap assuming constant concentration in the underlying sediment

3.2 Conceptual Model

The conceptual model divides the system into five different parts: the underlying sediment, the chemical isolation layer, the biologically active or bioturbation layer, the sediment-water interface (benthic boundary) layer, and the overlying water column. The placed cap layer, with thickness h_{cap}, consists of both the chemical isolation layer, with thickness h_{eff}, and the bioturbation layer, with thickness h_{bio}. The underlying sediment layer also includes the zone in which cap and sediment have intermixed during placement as the pore water concentrations in this region are essentially indistinguishable from those in the underlying sediment. In transient calculations any portion of the cap compromised by chemical migration due to consolidation should also be considered part of the underlying sediment (Palermo et al. 1998). Under steady state conditions, however, pore water expression and consolidation do not influence contaminant behavior.

The underlying sediment concentration is assumed constant. In a real sediment capping system, as contaminants are transported from the former sediment-water interface to the clean cap material the concentrations in the underlying sediment would change. The concentration at the bottom of the cap would likely decrease with depletion

of mass to the capping materials. However, as shown by Rabideau and Kandelwahl (1998), the most conservative boundary condition for the underlying contaminated material in a containment system is constant concentration. Any change in the actual concentration would likely be a decrease as mass is lost to the cap material, which provides further conservatism to this assumption. An alternative to constant concentration in the sediment would be to model the entire sediment layer; this approach is more robust but would require numerical simulation to describe behavior in the sediment column and capping layer.

The transport processes in the chemical isolation layer are advection, diffusion/dispersion, and decay. For the bioturbation layer, bioturbation-induced movement of particles and bioirrigation of pore water are also considered. Bioturbation-related processes are considered quasi-diffusive and hence are assumed to increase the effective diffusion/dispersion coefficient. Transport through the aqueous boundary layer is dictated by the benthic boundary layer mass transfer coefficient (Boudreau and Jorgensen 2001). Benthic boundary layer mass transfer is controlled by the turbulence in the overlying water. For river systems, this process is controlled by parameters such as current and water depth. In lake systems, this coefficient is typically controlled by lake mixing processes. Imberger and Hamblin (1982) provide an excellent overview of mechanisms of mixing processes in lakes; these include wind, wave and buoyancy-driven circulation. Figure 3 shows the conceptual model of the sediment cap system along with the model coordinate system.

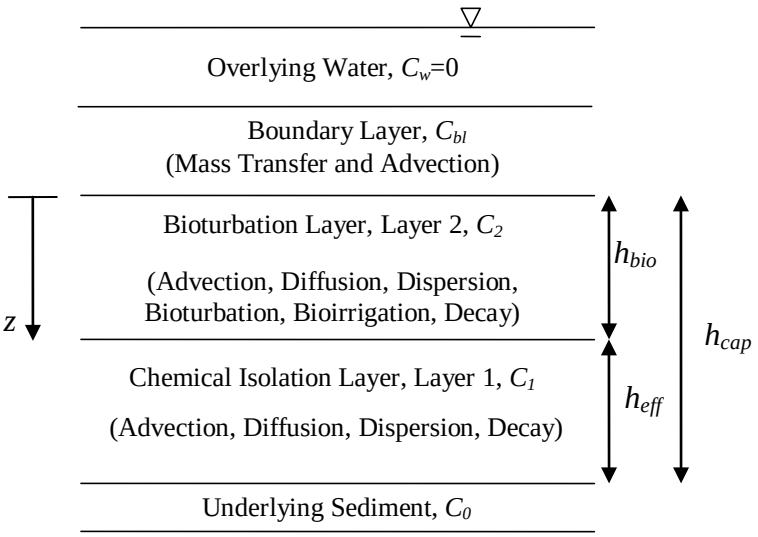

Figure 3. Sediment cap system and parameter definition.

Due to the low solubility of most sediment contaminants, the bulk sediment loading, *q*, (mass of contaminant on solid phase per mass of solid phase) is the parameter that is typically used for quantifying contaminant levels in sediments instead of the pore water (mobile phase) concentration. The value of *q* depends upon the sorption properties of the sediment or cap layer, however, and is potentially discontinuous while the pore water concentration is both continuous across interfaces and directly represents the mobile phase contaminants. Under the assumption of linear partitioning, the bulk sediment loading can be related to the pore water concentration, *C*, through the following relationship, assuming local equilibrium:

$$q = K_d C \tag{3.1}$$

Where K_d represents the effective sediment-water partition coefficient in the cap material. It is generally reasonable to assume local equilibrium with the pore water at some

effective (measured) partition coefficient due to the relatively slow contaminant migration rates within the sediment bed. Of critical importance to the rate of migration of contaminants in the cap material is the ratio of the total concentration (mass per unit volume) in the porous cap matrix to that of the mobile phase concentration, or the retardation factor, R_l (defined in terms of model parameters subsequently).

For organic contaminants, the contaminant partition coefficient is often estimated as the product of the fraction organic carbon f_{oc} and the organic carbon partition coefficient, K_{oc}. This is likely a crude assumption in the underlying sediment which has been shown to exhibit a different relationship due to desorption resistance (McGroddy and Farrington 1995) but may be a good assumption for the cap material and the new (clean) sediment. For typical sand, the organic carbon fraction tends to be less than 0.1%. At these low organic carbon contents, mineral sorption tends to become important even for organic compounds; so, the assumption of 0.01-0.1% organic carbon is likely a lower bound to the effective sorption of organic contaminants on sandy cap materials (Schwarzenbach et al. 2003).

Due to the limited sorptive capacity of sand caps, permeable adsorptive caps, sometimes referred to as active caps, have been proposed (Reible et al. 2007, McDonough et al. 2007). These caps may contain organic sorbents such as activated carbon, organo-modified clays, coke, or metal sorbents such as apatite. These could be incorporated in the modeling approach herein by using the appropriate effective partition coefficient, although for sorbents exhibiting nonlinear sorption behavior such as activated carbon, the model results are only approximate. Permeable reactive caps with enhanced

degradation characteristics have also been proposed although their long-term efficacy has not been demonstrated.

The approach presented here is developed using pore water concentrations, which represent the mobile contaminant phase in a stable cap and may be more closely related to the contaminants available for bioaccumulation (e.g., Lu et al. 2006, Beckles et al. 2007). Based on the assumptions listed above, the domain of the model for the cap system consists of two layers: the chemical isolation layer and the bioturbation layer. The underlying sediment, benthic layer, and overlying water are utilized to develop boundary conditions.

3.3 Transient Model and Containment Breakthrough Time

The governing transport equation for the chemical isolation layer (Layer 1) is:

$$R_1 \frac{\partial C_1}{\partial t} - U \frac{\partial C_1}{\partial z} = D_1 \frac{\partial^2 C_1}{\partial z^2} - \varepsilon_1 \lambda_1 C_1 \tag{3.2}$$

Where C_1 is the pore water concentration in the isolation layer, z is the depth downward from the cap-water interface, t is the time, λ_1 is the decay rate constant, R_1 is the retardation factor in the layer (defined here as the ratio of the total concentration to that in the mobile phase), U is the effective advective velocity (assumed to be directed upward although a negative value is still appropriate), and ε_1 is the porosity in the layer. The decay of the contaminant is assumed to be first-order and to occur only in the pore water. Thus seemingly large decay rate constants may have only a minimal impact on mass degradation rate since only a small fraction of the contaminants resides in the pore water.

The strong sorptive nature of most sediment contaminants limits the rate of degradation due to limited bioavailability (Hyun et al. 2006, Beckles et al. 2007).

For an active capping system, the chemical isolation layer must be further subdivided into sand and active layer(s), which would require introduction of additional governing and appropriate boundary conditions (continuity of concentration and flux) for each layer. The transport equation for each layer would be essentially the same, with the primary difference arising from the retardation term. For sorbing cap materials such as organoclays and peats that obey linear partitioning relationships, the governing equations would differ only in the value of the retardation factor. For a nonlinear sorption model (such as activated carbon) the governing equations would be almost the same, although the retardation factor would no longer be constant but a function of concentration. Note that in either case at steady state that the sorption term disappears and the steady state model developed herein still applies.

For the chemical isolation layer, the bottom boundary condition is assumed to be a first-type or Dirichlet boundary with a concentration of C_0:

$$C_1 (z = h_{cap}) = C_0 \tag{3.4}$$

For modeling during the transient period, i.e., before significant penetration of the overlying biologically active layer, the chemical isolation layer may be approximated as semi-infinite, which produces the second boundary condition:

$$\lim_{z \to -\infty} \frac{\partial C_1}{\partial z} = 0 \tag{3.5}$$

For an initially clean cap, the initial condition is:

$$C_1 (t = 0) = 0 \tag{3.6}$$

The transient behavior can be estimated using an analytical solution to Equation (3.2) subject to the conditions in (3.4), (3.5), and (3.6). The solution to this problem was presented by van Genuchten (1981):

$$C(z,t) = \frac{C_0}{2}\left\{ \begin{array}{l} \exp\left[\frac{(U-u)(h_{cap}-z)}{2D_1}\right]\mathrm{erfc}\left[\frac{R_1(h_{cap}-z)-ut}{\sqrt{4D_1R_1t}}\right]+ \\ \exp\left[\frac{(U+u)(h_{cap}-z)}{2D_1}\right]\mathrm{erfc}\left[\frac{R_1(h_{cap}-z)+ut}{\sqrt{4D_1R_1t}}\right] \end{array} \right\} \tag{3.7}$$

$$u = \sqrt{U^2 + 4\varepsilon\lambda_1 D_1}$$

The transient model (3.7) is appropriate until the time when the isolation layer is completely compromised by migration from below by the processes of advection, diffusion, and dispersion. For a diffusion-dominated problem with no decay, Equation (3.7) reduces to the well-known complementary error function solution:

$$C = C_0\,\mathrm{erfc}\left(\frac{R_1^{0.5}(h_{cap}-z)}{\sqrt{4D_1t}}\right) \tag{3.8}$$

This equation can be assumed valid while the concentration at the boundary of the containment and bioturbation layers is small; the complementary error function is equal to about 0.01 when the argument is about two (i.e., when the concentration predicted at the top of the cap layer is 1% of the underlying sediment concentration). Therefore, a conservative estimate of penetration time for a diffusion-dominated system is:

$$t_{diff} = \frac{R_1 h_{eff}^2}{16D_1} \tag{3.9}$$

For an advection-dominated system with no decay, Equation (3.7) reduces to a front or step function with velocity U/R_1; hence an appropriate time for penetration is:

$$t_{adv} = \frac{R_1 h_{eff}}{U} \tag{3.10}$$

Because advection and diffusion/dispersion act together to compromise the chemical isolation layer, the time for penetration of the layer can be estimated by assuming the processes act in parallel. Thus, a time scale characteristic of the advective-diffusive migration through the isolation layer can be written:

$$t_{adv/diff} \approx \frac{1}{1/t_{diff} + 1/t_{adv}} \approx \frac{1}{16D_1/(R_1 h_{eff}^2) + U/(R_1 h_{eff})} \approx \frac{R_1 h_{eff}^2}{16D_1 + U h_{eff}} \tag{3.11}$$

For times long compared to $t_{adv/diff}$ a steady state model will describe concentrations and fluxes in the cap. The transient time through the biologically active layer is typically negligible compared to that in the chemical isolation layer due both to its small thickness (5-15 cm) and the rapid sediment reworking and contaminant migration rates in this layer. Thus for times long compared to $t_{adv/diff}$, a steady state model is applicable to both the chemical isolation layer and the overlying bioturbation layer.

To verify the applicability of the relatively simple approach in Equation (3.11), the time required to achieve a concentration at the top of the chemical isolation layer equal to 1% of the concentration at the sediment-cap interface (C/C_0 =0.01) and the time required to achieve a flux at the top of the chemical isolation layer 1% of the flux at the sediment-cap interface, F/F_0 =0.01, were calculated from a full advection-diffusion model and compared to the prediction of Equation (3.11). The ratio of the flux at the top of the chemical isolation layer to the flux at the sediment-cap interface was calculated by,

$$F / F_0 = \frac{F(z = h_{bio}, t)}{F(z = h_{cap}, t)} = \frac{UC(z = h_{bio}, t) + D_1 \dfrac{\partial C(z = h_{bio}, t)}{\partial z}}{UC(z = h_{cap}, t) + D_1 \dfrac{\partial C(z = h_{cap}, t)}{\partial z}} \tag{3.12}$$

The results were computed for dimensionless time, τ, in terms of the dimensionless Peclet number, *Pe*, which is defined as:

$$\tau = \frac{tD_1}{R_1 h_{eff}^2} \tag{3.13}$$

$$Pe = \frac{Uh_{eff}}{D_1} \tag{3.14}$$

The times to concentration or flux equal to 1% of that at the bottom of the sediment were calculated for two solutions to Equation (3.2), a semi-infinite cap layer and a finite cap layer with a zero concentration at the cap-water interface (z=0). The calculated times were identical for both boundary conditions, since the top boundary does not affect the solution until significant penetration of the complete chemical isolation layer has occurred. The results in Figure 4 show that the prediction of breakthrough based on Equation (3.11) fall between those based on flux and concentration at low *Pe*, while at high *Pe* Equation (3.11) slightly over-predicts breakthrough for both cases. The maximum over prediction compared with an F/F_0 value of 0.01 basis was 23%. It appears that Equation (3.11) provides a reasonable estimate for penetration time for a non-reactive solute over the entire range of *Pe* and, in particular, provides a good estimate of the time before conditions in the biologically active layer will begin to influence concentration profiles within the cap. Any decay would retard the

breakthrough time and as a result the predictions from Equation (3.11) would be conservative.

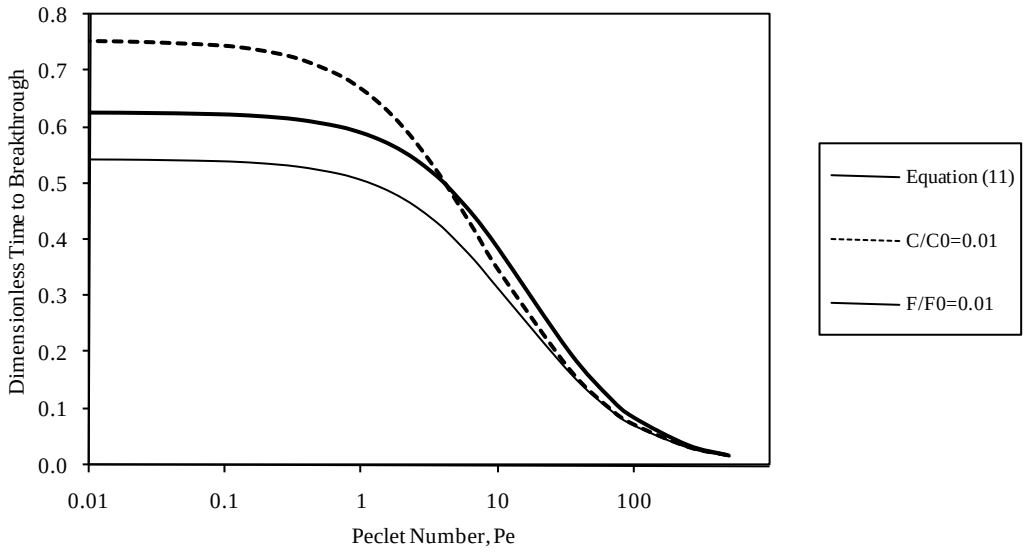

Figure 4. Comparison of breakthrough time approaches.

The times required to achieve concentration (C) or flux (F) at top of the chemical isolation layer equal to 1% of the concentration (C_0) or flux (F_0) at the bottom of the layer from full solutions of Equation (3.2) were computed. The predictions from Equation (3.11) closely matched the values obtained through the numerical approach.

3.4 The Bioturbation Layer and the Sediment-Water Interface

The transport equation for the bioturbation layer has the same general form as the chemical isolation layer; however, the processes of bioturbation are assumed to increase the effective diffusion/dispersion coefficient. The decay rate and retardation factor in the bioturbation layer may also be different than that observed in the chemical isolation layer. The Darcy velocity U must be the same for water (assumed incompressible). The transport equation for the bioturbation layer (Layer 2) is:

$$R_2 \frac{\partial C_2}{\partial t} - U \frac{\partial C_2}{\partial z} = D_2 \frac{\partial^2 C_2}{\partial z^2} - \varepsilon_2 \lambda_2 C_2 \qquad (3.15)$$

Where C_2 is the concentration in the bioturbation layer, R_2 is the retardation factor in the bioturbation layer, D_2 is the effective diffusion/dispersion coefficient for the bioturbation layer, λ_2 is the decay rate for the bioturbation layer, and ε_2 is the porosity in the layer.

At the interface between the chemical isolation layer and the bioturbation layer, the concentrations and fluxes in the two layers must be equal. Recognizing that the advective flux is the same in each layer, the following represent appropriate boundary conditions at the interface between the bioturbation and underlying containment layers (here C_{bio} is defined as the concentration at the interface):

$$C_1 (z=h_{bio}) = C_2(z=h_{bio})=C_{bio} \tag{3.16}$$

$$-D_1 \frac{\partial C_1(z=h_{bio})}{\partial z} = -D_2 \frac{\partial C_2(z=h_{bio})}{\partial z} \tag{3.17}$$

The boundary condition at the cap-water interface is the most complex, as it essentially requires the effluent boundary condition from a porous medium, which has a long history and is the subject of many papers (Hulbert 1944, Danckwerts 1953, Wehner and Wilhelm 1956). The concept of a benthic boundary layer mass transfer resistance composed of a laminar (diffusive) sublayer above the sediment-water interface has long been used for modeling mass transport from surficial sediments and is widely accepted in soil and marine science (see Boudreau 1997). A complete mass balance on the interface results in the following expression (Boudreau and Jorgensen, 2001):

$$UC_2(z=0^+) - D_2 \frac{\partial C_2(z=0^+)}{\partial z} + R' = U_{bl} C_{bl}(z=0^-) + k_{bl}(C_{bl} - C_w) \tag{3.18}$$

Where *R'* represents transport of contaminants from the exposed surficial sediment to the overlying water, and U_{bl}, $k_{bl,}$, and $C_{bl}(z)$ represent the effective advective velocity,

effective mass transfer coefficient, and concentration in the benthic boundary layer, respectively. The value of *R'* has been shown to be small relative to the other processes (Boudreau and Jorgensen 2001). The effective mass transfer coefficient in the benthic boundary layer can also be thought of as the diffusion in a laminar sub layer of thickness, δ, separating the cap-water interface from the bulk overlying water of concentration, C_w:

$$k_{bl}(C_{bl} - C_w) = D_{bl}\frac{C_{bl} - C_w}{\delta} \tag{3.19}$$

The value in the overlying surface water is taken to be zero without loss of generality (all other concentrations are taken relative to this surface water concentration). Combining these assumptions results in the following boundary condition of the third kind (Boudreau and Jorgensen, 2001):

$$D_2\frac{\partial C_2(z=0^+)}{\partial z} = k_{bl}C_{bl}(z=0^-) = k_{bl}C_2(z=0^+) \tag{3.20}$$

3.5 Steady State Model

To evaluate the concentrations in the combined layers of a containment layer and a bioturbation layer, the relative importance of the different transport mechanisms can be evaluated with the following dimensionless numbers, which are defined as:

$$Pe_1 = \text{Peclet number in chemical isolation layer} = \frac{Uh_{eff}}{D_1} = \frac{\text{Rate of advection}}{\text{Rate of diffusion}} \tag{3.21}$$

$$Da_1 = \text{Damkohler number in chemical isolation layer} = \frac{\varepsilon_1\lambda_1 h_{eff}^2}{D_1} = \frac{\text{Rate of decay}}{\text{Rate of diffusion}} \tag{3.22}$$

$$Pe_2 = \text{Peclet number in bioturbation layer} = \frac{Uh_{bio}}{D_2} \tag{3.23}$$

Da_2 = Damkohler number in bioturbation layer = $\frac{\varepsilon_2 \lambda_2 h_{bio}^2}{D_2}$ (3.24)

Sh = Sherwood number at cap-water interface = $\frac{k_{bl} h_{bio}}{D_2} = \frac{\text{Rate of mass transfer}}{\text{Rate of diffusion}}$ (3.25)

Under steady state conditions the time derivatives in Equations (3.2) and (3.15) disappear. Equations (3.2) and (3.15) can be re-written in terms of the dimensionless parameters introduced above:

$$h_{eff}^2 \frac{\partial^2 C_1}{\partial z^2} + Pe_1 h_{eff} \frac{\partial C_1}{\partial z} - Da_1 C_1 = 0 \tag{3.26}$$

$$h_{bio}^2 \frac{\partial^2 C_2}{\partial z^2} + Pe_2 h_{bio} \frac{\partial C_2}{\partial z} - Da_2 C_2 = 0 \tag{3.27}$$

By assuming a solution of an exponential form, the general solution of (3.26) and (3.27) can be obtained. At steady state the concentrations at the boundaries of the domain are constant and assumed to have values of C_0 at the cap-sediment interface, C_{bio} at the boundary of the chemical isolation and bioturbation layers and C_{bl} at the cap-water interface. The solutions to the governing ordinary differential equations are thus:

$$C_1 = \frac{C_{bio} e^{-Pe_1/2} - C_0 e^{-\beta}}{2\sinh\beta} \exp\left[\left(\frac{Pe_1}{2} + \beta\right)\frac{h_{cap} - z}{h_{eff}}\right] + \frac{C_0 e^{\beta} - C_{bio} e^{-Pe_1/2}}{2\sinh\beta} \exp\left[\left(\frac{Pe_1}{2} - \beta\right)\frac{h_{cap} - z}{h_{eff}}\right] \tag{3.28}$$

$$\beta = \sqrt{\frac{Pe_1^2}{4} + Da_1}$$

$$C_2 = \frac{C_{bl}e^{-\frac{Pe_2}{2}} - C_{bio}e^{-\gamma}}{2\sinh\gamma}\exp\left[\left(\frac{Pe_2}{2}+\gamma\right)\frac{h_{bio}-z}{h_{bio}}\right] + \frac{C_{bio}e^{\gamma} - C_{bl}e^{-\frac{Pe_2}{2}}}{2\sinh\gamma}\exp\left[\left(\frac{Pe_2}{2}-\gamma\right)\frac{h_{bio}-z}{h_{bio}}\right] \tag{3.29}$$

$$\gamma = \sqrt{\frac{Pe_2^2}{4} + Da_2}$$

The values of C_{bio} and C_{bl} can be determined by applying the boundary conditions (3.17) and (3.20) to Equations (3.28) and (3.29):

$$C_{bio} = \frac{C_o\frac{Pe_2}{Pe_1}e^{\frac{Pe_1}{2}}\beta\sinh\gamma}{\frac{Pe_2}{Pe_1}\beta\cosh\beta\sinh\gamma + \gamma\sinh\beta\cosh\gamma - \frac{\gamma^2\sinh\beta}{\left(Sh+\frac{Pe_2}{2}\right)\sinh\gamma + \gamma\cosh\gamma}} \tag{3.30}$$

$$C_{bl} = \frac{C_0 e^{\frac{Pe_1+Pe_2}{2}}}{\left(\frac{Pe_1}{2}+\frac{Pe_1Sh}{Pe_2}\right)\frac{\sinh\beta\cosh\gamma}{\beta} + \left(\frac{Pe_2}{2}+Sh\right)\frac{\cosh\beta\sinh\gamma}{\gamma} + \frac{Pe_1\gamma\sinh\gamma\sinh\beta}{Pe_2\beta} + \cosh\beta\cosh\gamma} \tag{3.31}$$

The concentration of contaminants in the bioturbation layer is of particular interest, as benthic organisms in the layer often provide the primary route of entry of contaminants into the food chain. Hence, another important parameter is the average concentration in the bioturbation layer. This concentration can be used to evaluate the potential long-term effectiveness of a sediment cap. Integrating Equation (3.29) over the bioturbation layer and dividing by the depth of the bioturbation layer provides the average value:

$$(C_{bio})_{avg} = \frac{C_{bl}e^{-\frac{Pe_2}{2}} - C_{bio}e^{-\gamma}}{2\sinh\gamma}\frac{e^{\frac{Pe_2}{2}+\gamma}-1}{\frac{Pe_2}{2}+\gamma} + \frac{C_{bl}e^{\gamma} - C_{bio}e^{-\frac{Pe_2}{2}}}{2\sinh\gamma}\frac{e^{\frac{Pe_2}{2}-\gamma}-1}{\frac{Pe_2}{2}-\gamma} \tag{3.32}$$

The average solids loading in the bioturbation layer, $(W_{bio})_{avg}$, can be determined from the partitioning relationship between the pore water and the sediment, where $(f_{oc})_{bio}$ is the expected fraction of organic carbon in the newly deposited sediment:

$$(W_{bio})_{avg} = (f_{oc})_{bio} K_{oc} (C_{bio})_{avg} \tag{3.33}$$

Additionally, the flux to the overlying water column, F_w, may be of interest. This can be evaluated by:

$$F_w = (k_{bl} + U) C_{bl} \tag{3.34}$$

3.6 Numerical Model Comparison

To check the validity of the analytical solutions for both the transient and steady state models, Equations (3.2) and (3.15) subject to boundary conditions (3.4), (3.16), (3.17), and (3.20) and initial condition (3.6) were solved independently by numerical analysis. A finite differencing scheme using the Crank-Nicolson method (Crank and Nicolson, 1947) with a forward difference for the advection term and central difference for the diffusion term was employed for the analysis. Reasonable estimates for the parameters were assumed for two cases using the methods described above. Simulations were performed for low and high values of Pe_1. Figure 5 shows that results of the simulations and the analytical solutions (3.7) and (3.28-3.31) are equivalent. Thus the analytical solutions can be used to predict concentrations within the chemical isolation layer during the transient period and to predict the steady state behavior. For estimation of cap behavior in the transition time between $t_{adv/diff}$ and steady state, a numerical model must be employed to approximate the solution to the governing equations.

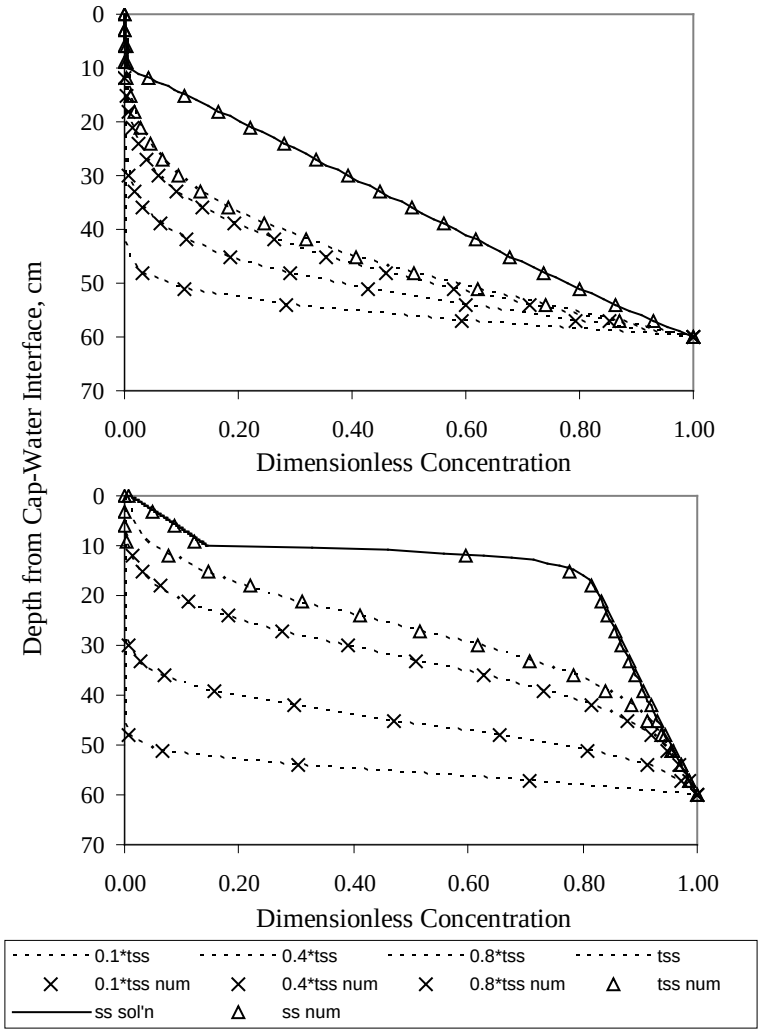

Figure 5. Transient and steady state concentration profiles throughout cap: comparison of analytical with numerical solution.

Top: low flow (Pe_1=0.66); Bottom: high flow (Pe_1=32.8).

3.7 Characterization of Transport Parameters

The factors R_1 and R_2 as defined here are the ratios of the total concentration in an elementary sediment volume (stationary phase) to that in the pore water (mobile phase) for the containment and bioturbation layers, respectively. A significant proportion of the total concentration in the pore water may be present in colloidal organic matter (Baker et

al. 1985, Chin and Gschwend 1992, Schlautman and Morgan 1993). Chin and Gschwend (1992) found this relationship to be linear. Thus partitioning onto the total organic carbon in the pore water, ρ_{doc}, with a colloidal organic carbon partition coefficient, K_{doc} serves to increase the effective solubility of the compounds. Coupling this assumption with the linear partitioning onto the cap material, and recognizing that the fractional organic carbon in the bioturbation layer, $(f_{oc})_{bio}$ will over time be different from that in the containment layer, $(f_{oc})_{eff}$, produces the following relationships for R_1 and R_2 in terms of ρ_{oc}, K_{doc}, ε_1, ε_2, the particle density ρ_p, and K_{oc}:

$$R_1 = \frac{\varepsilon_1 + \varepsilon_1 \rho_{doc} K_{doc} + (1-\varepsilon_1)\rho_p K_{oc}}{1 + \rho_{doc} K_{doc}} \tag{3.35}$$

$$R_2 = \frac{\varepsilon_2 + \varepsilon_2 \rho_{doc} K_{doc} + (1-\varepsilon_2)\rho_p K_{oc}}{1 + \rho_{doc} K_{doc}} \tag{3.36}$$

The Darcy velocity, U, here accounts for both groundwater upwelling and the effect of erosion/deposition. In a coordinate system fixed relative to the cap-water interface, deposition or erosion changes the net advective flux. Because particle deposition effectively buries both pore water and solid associated contaminants, the effective advective flux also encompasses both. The effective advective velocity associated with both the Darcy pore water upwelling, V, the velocity of sediment deposition, V_{dep}, and the retardation factor applicable to the cap-sediment layer, R, is:

$$U = V - RV_{dep} \tag{3.37}$$

Note that although new sediment is typically deposited at the cap–water interface, the mixing in this region is rapid and governed by bioturbation, or particle mixing

processes that are not subject to retardation by pore water transport. Transient migration in the underlying cap containment layer is delayed by burial with new sediment and the apparent shifting of the sediment interface. For estimation of the time delay associated with burial, R in Equation (3.37) can be conservatively estimated by R_1 (the retardation in the underlying sand), despite the fact that typically more sorbing sediment is deposited at the cap-water interface (characterized by R_2). In the event of net erosion rather than deposition the value of V_{dep} is negative. For the purposes of conservative estimates and due to uncertainties over future deposition rates, it is often assumed that the deposition of new sediment is negligible despite the fact that contaminated sediments have typically accumulated in net depositional areas.

The advective flow is perhaps the most important parameter in this analysis, as it will dominate in many natural systems. The flow may be upward or downward, in which case the value is negative. In the absence of direct measurements, the flow may be modeled using Darcy's Law. This approach requires an understanding of the hydrogeology of the area, including the effective hydraulic conductivity of the sediment/groundwater system and the local groundwater elevation levels driving the flow rate. For direct measurement of groundwater flux, seepage meters such as the one described by Lee (1977) may be used to measure the groundwater seepage rate. Alternatively, Cook et al. (2003) describe methods for estimating flux using different kinds of tracers. The local effective hydraulic conductivity for the sediment-cap system is dictated by the layer with the lowest hydraulic conductivity. The hydraulic conductivity of the system is generally unaffected by the presence of a cap (since it is often composed of relatively coarse granular media) although the cap could be

constructed to control permeability or may cause consolidation in the underlying sediment, reducing its permeability.

The value of D_1 is the sum of the diffusion and dispersion coefficients. Diffusion through granular porous media is often characterized by an effective diffusion coefficient D_{diff} given by the molecular diffusivity D_w times the porosity (the available diffusion area) and divided by a hindrance parameter (the lengthening of the diffusion path by the media). The model of Millington and Quirk (1961), where the hindrance parameter is taken to be the porosity to the negative one-third power, is widely used for diffusion in granular porous media such as a typical sand cap:

$$D_{diff} = \varepsilon_1^{4/3} D_w \tag{3.38}$$

Boudreau (1997) suggests an alternative that may be more applicable for fine-grained sediments:

$$D_{diff} = \frac{\varepsilon_1 D_w}{1 - \ln \varepsilon_1^2} \tag{3.39}$$

The molecular diffusivity is a function of temperature and molecular weight and can be estimated from the literature (e.g., Lyman et al. 1990). Mechanical dispersion characterized by D_{disp} of the contaminant through the cap can be modeled as the product of the velocity through the cap and some length scale defined as the dispersivity, α:

$$D_{disp} = \alpha U \tag{3.40}$$

Thus, the effective diffusion/dispersion coefficient in the containment layer can be determined by:

$$D_1 = \varepsilon_1^{4/3} D_w + \alpha U \tag{3.41}$$

After placement of a sediment cap, new sediment is deposited at the cap surface. As this deposition occurs, the top of the sediment cap is re-colonized by benthic organisms (worms and other macro invertebrates). These organisms blend the sediments at the top of cap, resulting in relatively rapid transport of contaminants from the bottom of the layer to the overlying water. Provided that the movement of particles and pore water by these organisms is essentially random, the length scale of the movement of the particles is smaller than that being studied (i.e., the cap thickness), and time scale between mixing events is smaller relative to other processes, the transport processes can be taken as quasi-diffusive (Boudreau 1986). The diffusion-like mixing of particles is known as bioturbation, while the diffusion-like mixing of pore water is bioirrigation. These processes increase diffusion/dispersion coefficient from the containment layer, D_1, to that in the bioturbation layer, D_2. The flux of a chemical species, F_{bio}^{p}, associated with the diffusion of these particles associated with a bioturbation coefficient of F_{bio}^{p} and a solid-phase concentration (mass of chemical species per unit volume sediment particle) of W is:

$$F_{bio}^{p} = -D_{bio}^{p} \frac{\partial W}{\partial z} \tag{3.42}$$

If the time for movement of the sediment particles plus the time between particle movement events is large compared with that of desorption of contaminants, local equilibrium can be assumed, and the value of W can be re-written in terms of pore water concentration (noting that ε, ρ_p, $(f_{oc})_{bio}$, and K_{oc} are independent of depth):

$$F_{bio}^{p} = -D_{bio}^{p} (1-\varepsilon)\rho_p (f_{oc})_{bio} K_{oc} \frac{\partial C_2}{\partial z} \tag{3.43}$$

In addition to particle mixing, organisms also irrigate the surficial sediments through direct pore water exchange from the underlying sediments to the overlying water. The transport of contaminants associated with this process can be modeled by:

$$F_{bio}^{pw} = -D_{bio}^{pw} \frac{\partial C}{\partial z} \tag{3.44}$$

Thus the processes of bioturbation and bioirrigation serve to increase the effective diffusion/dispersion coefficient. The values of $D_{bio}{}^{p}$ and $D_{bio}{}^{pw}$ can be measured using radioactive tracers, such as described by McCafree et al. (1980). Thoms et al. (1995) provide an extensive review of measured biodiffusion coefficients at different locations in the United States. The effective diffusion coefficient for the bioturbation layer, D_2, can be determined from the following:

$$D_2 = D_1 + D_{bio}^{pw} + D_{bio}^{p}(1-\varepsilon)\rho_P (f_{oc})_{bio} K_{oc} \tag{3.45}$$

The decay rates λ_1 and λ_2 are highly compound and site specific. The model taken here is based on first-order kinetics, which may not be appropriate as the degradation may depend on many factors other than the contaminant concentration but provides a relatively simple way of incorporating this important mechanism into a mathematical model. In the absence of a site-specific study, the literature may be used to estimate a degradation rates.

Transport at the cap-water interface is dictated by the benthic boundary layer mass transfer coefficient, which is a function of the turbulence and shear of the overlying water column. Boudreau and Jorgensen (2001) and Thibodeaux (1996) present empirical correlations for k_{bl} based on mixing conditions in the overlying water. The value of k_{bl}

should be conservatively estimated, as its value directly affects the surficial sediment concentrations.

3.8 Steady State Model Behavior

The steady state model presented in (3.28-3.31) is a function of only the five parameters (3.21-3.25) and the depth of the two layers. To illustrate the behavior of the solution, consider a one foot (30 cm) thick sand cap with an expected bioturbation depth of 10 cm. For Case I, consider a conservative ($Da_1 = Da_2 = 0$) contaminant, with $Sh = 10$ (minimal mass transfer limitations) and $D_2 = 10D_1$ ($Pe_2 = 0.05Pe_1$). Figure 6 shows the dimensionless concentration profiles for $0.1<Pe_1<200$. For low Pe_1, the solution approaches a straight line in each layer, which is the expected result of a diffusion-dominated steady state profile. The increased diffusivity in the bioturbation layer results in lower concentrations in that layer. This behavior makes sense physically because the increased mixing rate in the layer reduces the concentrations there (contaminants are transported more rapidly in the bioturbation layer). If advection dominates (high Pe_1), the concentration profile approaches unity; again this is the expected result for an advection problem at steady state. The deviation near the boundary layer is a result of the simplifying assumptions made in the formulation of the top boundary condition. For high advection a more appropriate boundary condition would be a zero gradient. However, the profiles still approach the expected result and provide a reasonable estimation of cap performance even under these conditions. Clearly, at steady state in a high upwelling velocity system a cap will have limited effectiveness.

Now consider a system with degradation (Case II). For simplicity, the Damkohler number in the chemical isolation layer is assumed to be four. The value of D_2 was again

taken as $10D_1$, and again it is assumed that Sh=10. The decay rate in the bioturbation layer is taken as ten times that in the chemical isolation layer, a reasonable assumption due to higher levels of nutrients, organic matter, and electron acceptors. These assumptions result in $Pe_2 = 0.05Pe_1$ and $Da_2 = 0.25Da_1 = 1$. Figure 6 shows the dimensionless concentration profiles for $0.1<Pe_1<200$. When compared with the no decay situation, the concentration profiles are lower, as expected. In general, the graphs perform as anticipated mathematically. The concentrations in the bioturbation layer are significantly decreased versus the underlying sediment concentrations. Hence, if it can be proven that a contaminant will decay in a cap, capping is an extremely attractive alternative for remediation.

To evaluate the effects of mass transfer resistance on model output, consider the systems presented in Cases I and II with Sh=0.1 rather than 10 (Cases III and IV). Figure 6 also shows the results for these parameters. For Case III, the concentrations in the cap are minimally reduced even when diffusion-dominated (low Pe_1). The performance is as expected theoretically, with a linear profile in the containment layers at low Pe_1 which approaches a uniform profile for high values of Pe_1. In Case IV, the importance of decay on long term capping success is demonstrated. For a diffusion-dominated system, the bioturbation layer concentrations are drastically reduced over pre-cap levels, even with mass transfer resistance at moderately high advection ($Pe_1 = 5$). Again, as the upwelling velocity is increased, the cap performance is limited.

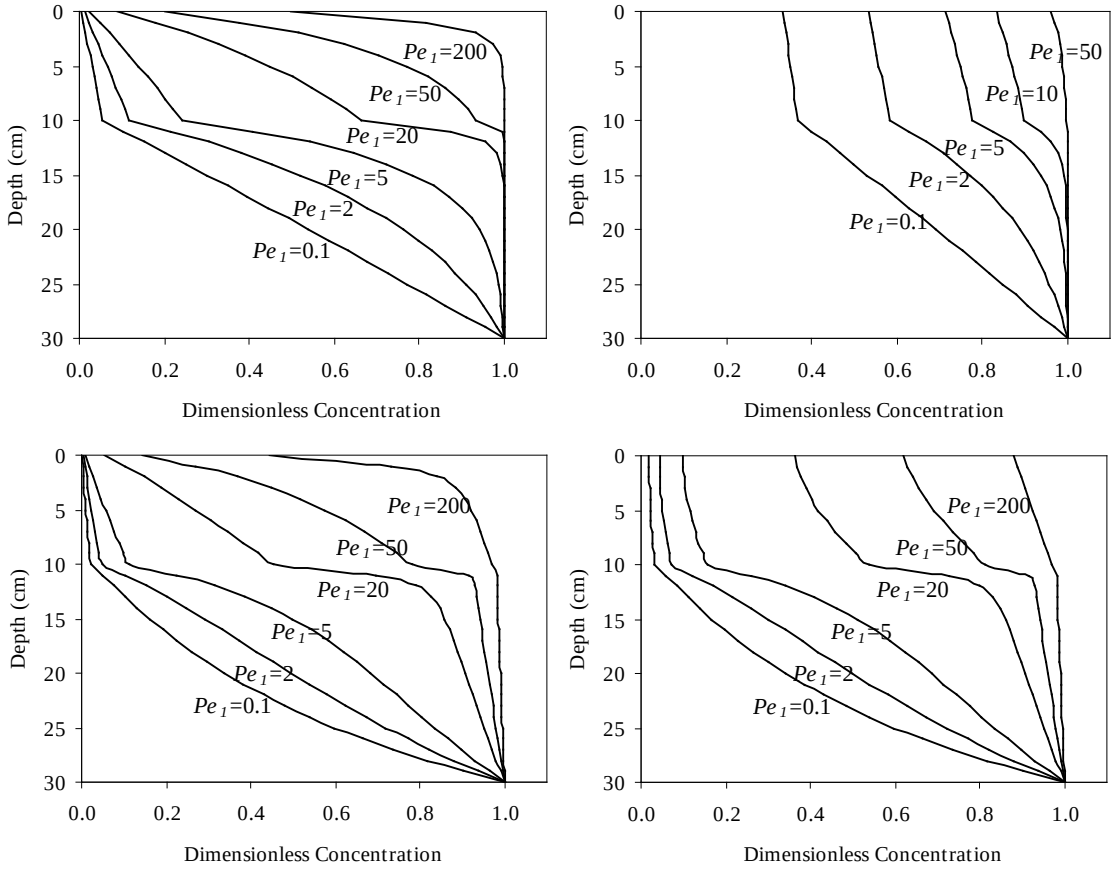

Figure 6. Steady state model behavior.

Top left, Case I (Da_1=Da_2=0, Sh=10). Bottom left, Case II (Da_1=4, Da_2=1, Sh=10). Top right Case III (Da_1=Da_2=0, Sh=0.1). Bottom right, Case IV (Da_1=4, Da_2=1, Sh=0.1). The dashed lines represent the interface between the chemical isolation and the bioturbation layers.

It is important to note that the model presents steady state concentrations, which may not be realized for many years. Capping may still be a viable option in a case where the transient migration through the containment layer is sufficiently long that natural attenuation processes not included in the models are expected to render the contaminants inconsequential. Steady state predictions beyond this time frame may not be considered important.

These results show the importance of the ground water upwelling velocity in the effectiveness of a cap. The upwelling velocity is a critical parameter in a transient analysis as well as it often controls the steady state flux. Upwelling velocities of the order of cm/day or more may be high enough to effectively negate the effectiveness of a cap even for moderately sorbing contaminants. In addition, the local equilibrium assumption may fail under the influence of extremely high upwelling. So, if capping is under consideration for management of contaminated sediments, it is important for the designer to measure or make a good estimate of the upwelling velocity before making a final decision. Due to the inherent heterogeneity in this parameter, it is also important to evaluate a range of values of upwelling velocity for predicting concentrations that will be used in design and decision making.

The traditional material used for capping sediment is clean sand. However, as demonstrated by these modeling results, a passive sand cap may not be an effective long-term approach for contaminated sediment management for high seepage/low degradation systems. For this reason, one current research focus (Reible et al. 2007, McDonough et al. 2007) is on active capping; that is, capping with materials that may enhance sequestration/degradation in situ or decrease the seepage flow rates through a sediment cap.

3.9 Conclusions

In this paper, the key processes controlling chemical migration in a cap isolation layer and in the overlying biologically active layer have been highlighted. A simple means for incorporating these processes into an analytical modeling approach has been developed. The approach is subject to a number of limitations. First, several of the

models for individual processes are simplistic (e.g., deposition, linear pore water partitioning, first-order decay). The underlying sediment is assumed to maintain a constant concentration. A more robust approach to assessing the concentration in the sediment would be to model fate and transport within the layer based on an initial concentration profile. However, this approach would normally require a numerical simulation in the full advection-diffusion case. Finally, the model is based on two homogeneous layers. Predicting transient concentration profiles in more complex sediment caps with more than two homogeneous layers or with nonlinear sorption would require a more robust approach. The steady state model presented here, however, would still be valid provided the values of diffusion/dispersion coefficients and decay rates were the same. For predicting transient performance of a cap under these scenarios, a numerical solution to the governing equations would be required. The exact solutions presented here represent an important check for future models of this kind.

The model presented here allows calculation of the steady state concentration profile and flux in a sediment cap. When coupled with a transient model of advection, diffusion, and reaction in the chemical isolation layer, this approach forms a relatively simple means of evaluating sediment caps. If the steady state condition is sufficient for achieving remediation objectives, there is no need for a more complicated transient approach. A spreadsheet that computes the analytical model output is available at: http://www.caee.utexas.edu/reiblegroup/downloads.html for interested parties.

3.10 References

1. Azcue, J.M., Zeman, A.J., Mudroch, A., Rosa, F., and Patterson, T. 1998. "Assessment of sediment and porewater after one year of subaqueous capping of contaminated sediments," Water Science and Technology, 37:323-329.
2. Baker, J.E., Capel, P.D., Eisenreich, S.J. 1985. "Influence of Colloids on Sediment-Water Partition Coefficients of Polychlorobiphenyl Congeners in Natural Waters," Environmental Science & Technology, 20:1136-1143.
3. Bear, J. 1972. Dynamics of Fluids in Porous Media. Elsevier, New York.
4. Beckles, D., Chen, W., Hughes, J. 2007. "Bioavailability of Polycyclic Aromatic Hydrocarbons Sequestered in Sediment: Microbial Study and Model Prediction," Environmental Toxicology and Chemistry, 26:878-883.
5. Boudreau, B. 1986. Mathematics of Tracer Mixing in Sediments, I. Spatially-Dependent, Diffusive Mixing, American Journal of Science, 286:161-198.
6. Boudreau, B. 1997. Diagenetic Models and Their Implementation: Modeling Transport Reactions in Aquatic Sediments. Springer-Verlag, New York.
7. Boudreau, B. and Jorgensen, B. 2001. The Benthic Boundary Layer. Oxford University Press, New York.
8. Chin, YP, Gschwend, P.M. 1992. "Partitioning of Polycyclic Aromatic Hydrocarbons to Marine Pore Water Organic Colloids," Environmental Science & Technology, 26:1621-1626.
9. Cook, P.G., Favreau, G., Dighton, J.C., Tickell, S. 2003. "Determining Natural Groundwater Influx to a Tropical River Using Radon, Chlorofluorocarbons, and Ionic Environmental Tracers," Journal of Hydrology, 277:74-88.

10. Crank, J. and Nicolson, P. 1947. "A Practical Method for Numerical Evaluation of Solutions of Partial Differential Equations of the Heat Conduction Type," Proceedings of the Cambridge Philosophical Society, 43:50-64.
11. Danckwerts, P.V. 1953. "Continuous Flow Systems," Chemical Engineering Science, 2:1-13.
12. Hulburt, H.M. 1944. "Chemical Processes in Continuous-Flow Systems: Reaction Kinetics," Industrial and Engineering Chemistry, 36:1012-1017.
13. Hyun, S., Jafvert, C., Lee, L., and Rao, P. 2006. "Laboratory Studies to Characterize the Efficacy of Sand Capping a Coal Tar-Contaminated Sediment," Chemosphere, 63:1621-1631.
14. Imberger, J. and Hamblin, P. 1982. "Dynamics of Lakes, Reservoirs, and Cooling Ponds," Annual Review in Fluid Mechanics, 14:153-187.
15. Lee, D.R. 1977. "A Device for Measuring Seepage Fluxes in Lakes and Estuaries," Limnology and Oceanography, 22:140-147.
16. Lu, X., Reible, D.D., and Fleeger, J.W. 2006. "Bioavailability of Polycyclic Aromatic Hydrocarbons in Field-Contaminated Anacostia River (Washington, DC) Sediment," Environmental Toxicology and Chemistry, 25:2869-2874.
17. Lyman, W.J, Reehl, W.F. and Rosenblatt, D.H. 1990. Handbook of Chemical Property Estimation Methods: Environmental Behavior of Organic Compounds. American Chemical Society, Washington DC.
18. Malusis, M. and Shackelford, C. 2002. "Theory for Reactive Solute Transport through Clay Membrane Barriers," Journal of Contaminant Hydrology, 59:291-316.

19. McDonough, K., Murphy, P., Olsta, J. Zhu, Y., Reible, D., and Lowry, G. 2007. "Development of a Sorbent-Amended Thin Layer Sediment Cap in the Anacostia River," Soil & Sediment Contamination, 16:313-322.
20. McGroddy, S.E. and Farrington, J.W. 1995. "Sediment Porewater Partitioning of Polycyclic Aromatic Hydrocarbons in Three Cores from Boston Harbor, Massachusetts," Environmental Science & Technology, 29:1542-1550.
21. McCafree, R.J., Myers, A.C., Davey, E., Morrison, G., Bender, M., Luedtke, N., Cullen, D., Froelich, P., and Klinkhammer, G. 1980. "The Relation between Pore Water Chemistry and Benthic Fluxes of Nutrients and Manganese in Narragansett Bay, Rhode Island," Limnology and Oceanography, 25:31-44.
22. Millington, R.J., and Quirk, J.M. 1961. "Permeability of Porous Solids," Transactions of the Faraday Society, 57:1200-1207.
23. Murphy, P., Marquette, A., Reible, D. and Lowry, G.V. 2006. "Predicting the Performance of Activated Carbon-, Coke-, and Soil-Amended Thin Layer Sediment Caps," Journal of Environmental Engineering, 132:787-794.
24. Palermo, M., Maynord, S., Miller, J. and Reible, D. 1998. Guidance Document for In Situ Subaqueous Capping of Contaminated Sediments, EPA 905-B96-004.
25. Parametrix. 1998. St. Paul Waterway Area Remedial Action and Habitat Restoration Project. Final 1998 Monitoring Report.
26. Rabideau, A., and Khandelwal, A. 1998. "Boundary Conditions for Modeling Transport in Vertical Barriers," Journal of Environmental Engineering, 124:1135-1139.

27. Rowe, P.K. and Booker, J.R. 1985. "1-D Pollutant Migration in Soils of Finite Depth," Journal of Geotechnical Engineering, 111:479-499.
28. Rubin, H. and Rabideau, A. 2000. "Approximate Evaluation of Contaminant Transport through Vertical Barriers," Journal of Contaminant Hydrology, 40:311-333.
29. Reible, D.D, Lampert, D.J., Constant, D., Mutch, R., and Zhu, Y. 2006. "Active Capping Demonstration in the Anacostia River in Washington DC," Remediation Journal, 17:39-53.
30. Schlautman, M.A. and Morgan, J.J. 1993. "Effects of Aqueous Chemistry on the Binding of Polycyclic Aromatic Hydrocarbons by Dissolved Humic Materials," Environmental Science & Technology, 27:961-969.
31. Schwarzenbach, R., Gshwend, P., and Imboden, D. 2003. Chapter 9, Sorption I: Introduction and Sorption Processes Involving Organic Matter and Chapter 11: Sorption III: Sorption Processes Involving Inorganic Surfaces. Environmental Organic Chemistry, 2nd Edition, 275-330 and 387-458. Wiley & Sons, Hoboken, New Jersey.
32. Simpson, S., Pryor, I., Mewburn, B., Batley, G., and Jolley, D. 2002. "Considerations for Capping Metal-Contaminated Sediments in Dynamic Estuarine Environments," Environmental Science & Technology, 36:3772 -3778.
33. Thibodeaux, L.J. 1996. Chapter 5: Chemical Exchange between Water and Adjoining Earthen Material. Environmental Chemodynamics, 255-368. J. Wiley, New York.

34. Thoma, G., Reible, D., Valsaraj, K., and Thibodeaux, L. 1991. "Efficiency of Capping Contaminated Bed Sediments In Situ. 1. Laboratory-Scale Experiments on Diffusion-Adsorption in the Capping Layer," Environmental Science & Technology, 25:1578-1584.
35. Thoms, S.R., Matisoff, G., McCall, P.L., and Wang, X. 1995. Models for Alteration of Sediments by Benthic Organisms, Project 92-NPS-2, Water Environment Research Foundation, Alexandria Virginia.
36. Van Genuchten, M. 1981. "Analytical solutions for chemical transport with simultaneous adsorption, zero order production and first order decay," Journal of Hydrology, 49:213-233.
37. Wehner, J. and Wilhelm, R. 1956. "Boundary Conditions of Flow Reactor," Chemical Engineering Science, 6:89-93.
38. Zeman, A. and Patterson, T. 1997. "Preliminary Results of Demonstration Capping Project in Hamilton Harbour," Water Quality Research Journal of Canada, 32:439-452.

Chapter 4: Active Capping Demonstration in the Anacostia River, Washington DC[3]

Danny Reible[4], David Lampert[4], David Constant[5], Robert D. Mutch, Jr.[6], and Yuewei Zhu[7]

4.0 Abstract

An active capping demonstration project in Washington DC is testing the ability to place sequestering agents on contaminated sediments using conventional equipment and evaluating their subsequent effectiveness relative to conventional passive sand sediment caps. Selected active capping materials include: (1) AquaBlok™ a clay material for permeability control (2) apatite - a phosphate mineral for metals control (3) coke - an organic sequestration agent and (4) sand material for a control cap. All of the materials, except coke, were placed in 8,000 ft^2 test plots by a conventional clamshell method during March and April 2004. Coke was placed as a 1.25-cm layer in a laminated mat due to concerns related to settling of the material. Post-capping sampling and analysis was conducted during the first, sixth and eighteenth months after placement. Although post-cap sampling is expected to continue for at least an additional 24 months, this article summarizes the results of the demonstration project and post-cap sampling efforts up to 18 months. Conventional clamshell placement was found to be effective for placing relatively thin (6-inch) layers of active material. The viability of placing high value or difficult to place material in a controlled manner was successfully demonstrated

[3]Published in *Remediation Journal*, 17(1):39-53, 2006. Reprinted here with permission of the journal.
[4]Department of Civil, Architectural and Environmental Engineering, The University of Texas, Austin, TX
[5]Department of Civil and Environmental Engineering, Louisiana State University, Baton Rouge, LA
[6]Hydroqual, Inc. , Mahwah, NJ

with the laminated mat. Post-cap monitoring indicates that all cap materials effectively isolated contaminants, but it is not yet possible to differentiate between conventional sand and active cap layer performance. Monitoring of the permeability control layer indicated effective reductions in groundwater seepage rates through the cap, but also showed the potential for gas accumulation and irregular release. All of the cap materials show deposition of new contaminated sediment on to the surface of the caps, illustrating the importance of source control in maintaining sediment quality.

[7]Horne Engineering Services, Falls Church, VA

4.1 Introduction

In situ containment of contaminated sediments is often achieved through capping, typically with a passive sand layer to physically separate contaminants from benthic receptors and to reduce the flux of contaminants to the overlying water. Under some situations, however, such as high rates of groundwater seepage, achievement of the desired reductions in flux may require the use of a layer that can sequester or degrade contaminants. These types of caps are often termed active cap layers to differentiate them from passive sand layers. Active cap materials include phosphate minerals for metals control, organoclays and sorbents such as activated carbon or coke for organic contaminant control, and clays for permeability control. Laboratory testing has shown the potential for such materials to effectively control contaminants that might migrate through a conventional cap, primarily by retarding contaminant migration by sorption. In some cases, degradation can also be enhanced, but the opportunities for incorporating degradative layers into cap materials are not well developed.

Active cap layers that sorb or sequester contaminants more effectively than conventional sand caps increase the capacity of a cap to control finite contaminant sources and the period of effectiveness for continuous sources. This results in more effective containment for a given cap thickness or allows a certain degree of containment to be achieved with a thinner cap, thereby reducing the impact of a cap on water depth or strength and consolidation concerns in the underlying sediment.

Although effective, the introduction of active capping materials into the environment has been limited as a result of the lack of precedent and potentially increased cost. In order to encourage the consideration of active capping materials for

sediment caps, a field demonstration of selected active capping technologies was conducted for the Anacostia River in Washington DC. The Anacostia River is a freshwater tidal system that drains an urban watershed encompassing 176 square miles in Maryland and the DC. The river suffers from overall poor water quality caused by numerous pollutants, including suspended solids, excess nutrients, toxics, trash, and debris. This pollution results in chronically low dissolved-oxygen levels and high bacterial levels. The low dissolved oxygen threatens aquatic life while the bacterial levels make recreational water activities, such as swimming, unsafe. The sediments contain a large inventory of contaminants of concern including metals, polychlorinated biphenyls (PCBs) and polycyclic aromatic hydrocarbons (PAHs). Additional contaminants are introduced, particularly after rainfall events, from combined sewer overflows (CSOs). The combination of continuing sources and past sources are reflected by the poor sediment quality.

A range of potential sediment remediation approaches is being considered for the river, including capping. Conventional sand capping may be effective for many of the areas of concern in the river, but it was felt that alternative approaches to increase the effectiveness of capping (i.e., active capping) might also be applicable. This article presents the results from a demonstration project designed to better assess the applicability of active capping. The site for the demonstration project is an area with elevated contaminant concentrations as indicated by the site investigation data (SRC/NOAA 2000 and Horne 2003). In addition, the site is downstream of an active CSO site. The contaminants of concern (i.e., PCBs, PAHs, and metals), near to and downstream of the CSO, are well documented. The area selected for the demonstration is

also identified for potential remedial action by the Anacostia Watershed Toxic Alliance (AWTA, 2002).

The demonstration project was implemented by a team led by Danny Reible, then at Louisiana State University but currently at the University of Texas, in cooperation with the prime on-site contractor, Horne Engineering Services, with the active support and contributions from AWTA and its members including the DC Department of Health. The Environmental Protection Agency (EPA) Superfund Innovative Technology Evaluation (SITE) program also provided extensive field support as part of a supplemental and complementary analysis of the AquaBlok™ cap. The lead project team was from the EPA supported Hazardous Substance Research Center/South and Southwest, a multi-university research consortium of Louisiana State University, Rice University, Georgia Tech University, Texas A&M University and the University of Texas. A variety of other groups also contributed to the overall project and their contributions are acknowledged at the end of this paper and at http://www.hsrc-ssw.org/ana-index.html.

As a result of the site characterization efforts, active capping materials appropriate for the site contaminants and conditions were selected for the demonstration. The materials included AquaBlok™, coke and apatite. AquaBlok™ is a bentonite clay material formed around a granular core and manufactured by Hull and Associates in Toledo, Ohio. The granular core encourages settling of the clay through the water column. After settling to the bottom, the clay absorbs water and swells, thereby reducing the permeability of the surface layer. In this manner, the AquaBlok™ is expected to reduce tidal pumping of porewaters in the contaminated sediment and divert groundwater upwelling away from the contaminated sediments to other, presumably less

contaminated, portions of the site. The EPA SITE program participated in a separate characterization and evaluation of the use of AquaBlok^{TM} as a result of their interest in this capping material.

Coke was included in the demonstration as an organic sequestration agent. Coke is a petroleum pyrolysis product that is widely available at low cost. The coke employed in this project was provided by U.S. Steel/Clairton Works of Clairton, Pennsylvania. The material exhibits particle sizes of 0.425 to 2 mm (10 - 40 mesh). Sorption measurements showed that the coke is similar in sorptive capacity to moderate organic carbon sediments while other sequestration agents (e.g., activated carbon) may exhibit 10-100 times greater adsorption capacity (Murphy et al., 2006). Coke contains residual PAH levels, but pre-demonstration leaching tests showed low levels of mobile PAHs due to the organic sequestration properties of the coke. Because cost was of paramount concern, the original plan was to place the coke in bulk, and ignore more sorptive (but more expensive) cap materials, such as activated carbon. Initial investigations, however, showed that the coke contained a significant fraction (10-20 percent) of nonsettleable material, raising concerns about its bulk placement. An alternative placement approach was discussed with CETCO (Arlington, Illinois) and ultimately selected. This alternative involved placing coke within a mat (also referred to as a reactive core mat (RCM)) in a high void fraction polyester core with two filtering polyester laminate layers on each side. The mats were constructed in a roll approximately 10 feet wide and approximately 100 feet long. Although used in this study for coke placement, the inclusion of this technology in the demonstration also served to illustrate its use for the controlled, thin layer placement of any high cost or nonsettleable granular material.

The final capping material demonstrated was apatite, manufactured by PCS Phosphate Company, Inc. in Aurora, North Carolina. Apatite is a phosphate material with the ability to preferentially adsorb certain metals. The material has the consistency of coarse sand and was delivered and placed in bulk. To provide a comparison of the effectiveness of the active capping materials, a fourth 8,000 ft^2 capping plot was used to place sand. A fifth area slightly outside of the four capping areas was used as an uncapped control area. All cap materials were placed between March 8, 2004 and April 23, 2004. Sampling for the evaluation placement performance was conducted in May 2004 while additional sampling for post-cap monitoring was conducted in the Fall 2004 and Fall 2005. Additional sampling is planned for Fall 2006 and Fall 2007. This article summarizes the cap construction activities and results of post-placement monitoring through Fall 2005.

4.2 Site Characteristics

The Anacostia River is a freshwater watershed located within the Potomac River Drainage Basin, which discharges to the Chesapeake Bay. The high volume-to-influx ratio in the Anacostia River results in a flow rate frequently described as sluggish. Under normal conditions, river currents are driven by tidal fluctuations. Tidal amplitudes are typically 1 to 2 feet. Median magnitudes for the average current velocity ranged from 0.13 ft/s for high slack to 0.21 ft/s for maximum flood. Maximum magnitudes ranged between 0.64 ft/s at high slack to 1.29 ft/s at maximum ebb, while all minimum magnitudes for all tide stages were 0.01 ft/s. The estimated cumulative flushing time, based solely on a tidal prism model (i.e., no river inflow), is 23 days (Katz et al. 2000). As a result of the relatively low flow in the river, the cap demonstration area is net

depositional. Vertical profiles of cesium (^{137}Cs), lead (^{210}Pb) and beryllium (^{7}Be) were measured in three cores collected from the river (Bentley, 2004). Vertical profiles of ^{137}Cs were consistent with a uniform deposition rate over at least the past 50 years of 0.68±0.21 cm/yr based upon 3 cores. ^{210}Pb in the same cores showed a similar deposition rate of 0.76±0.21 cm/yr. Vertical profiles of ^{7}Be indicated that the surface 4 to 5 cm in these cores was mixed via biodiffusion or other processes at an effective diffusion coefficient of approximately 29±5 cm^2/yr. Taken together, this information suggests that the upper 4 to 5 cm of the sediment was expected to be relatively well mixed with deposited contaminants, but that sediments below this depth were placed at least 5 to 10 years previously and were unlikely to be exposed or incorporated into the surface layer.

The cap demonstration area is generally featureless and exhibits a gentle slope with water depths ranging from approximately 5 ft to 20 ft below North American Vertical Datum 88 (NAVD 88) or 3.6 ft to 18.6 ft below Mean Lower Low Water (MLLW). The bathymetric data and geophysical survey tracklines are depicted in Figure 7. The topography in the eastern half of the area shows that the riverbed is steeper in the vicinity of a CSO. The cap demonstration was focused in the area of a gentler slope west of this region and east of a storm water outfall to the west. The surficial sediment consisted of high-plasticity silty clay, classified as CH according to the Unified Soil Classification System (USCS). From the mud line to at least 10 feet below this elevation, these soils were very soft, extremely weak, and highly compressible. Compressibility was enhanced by the presence of significant amounts of gas in the sediments due to denitrifying and methanogenic bacterial activity in the sediments.

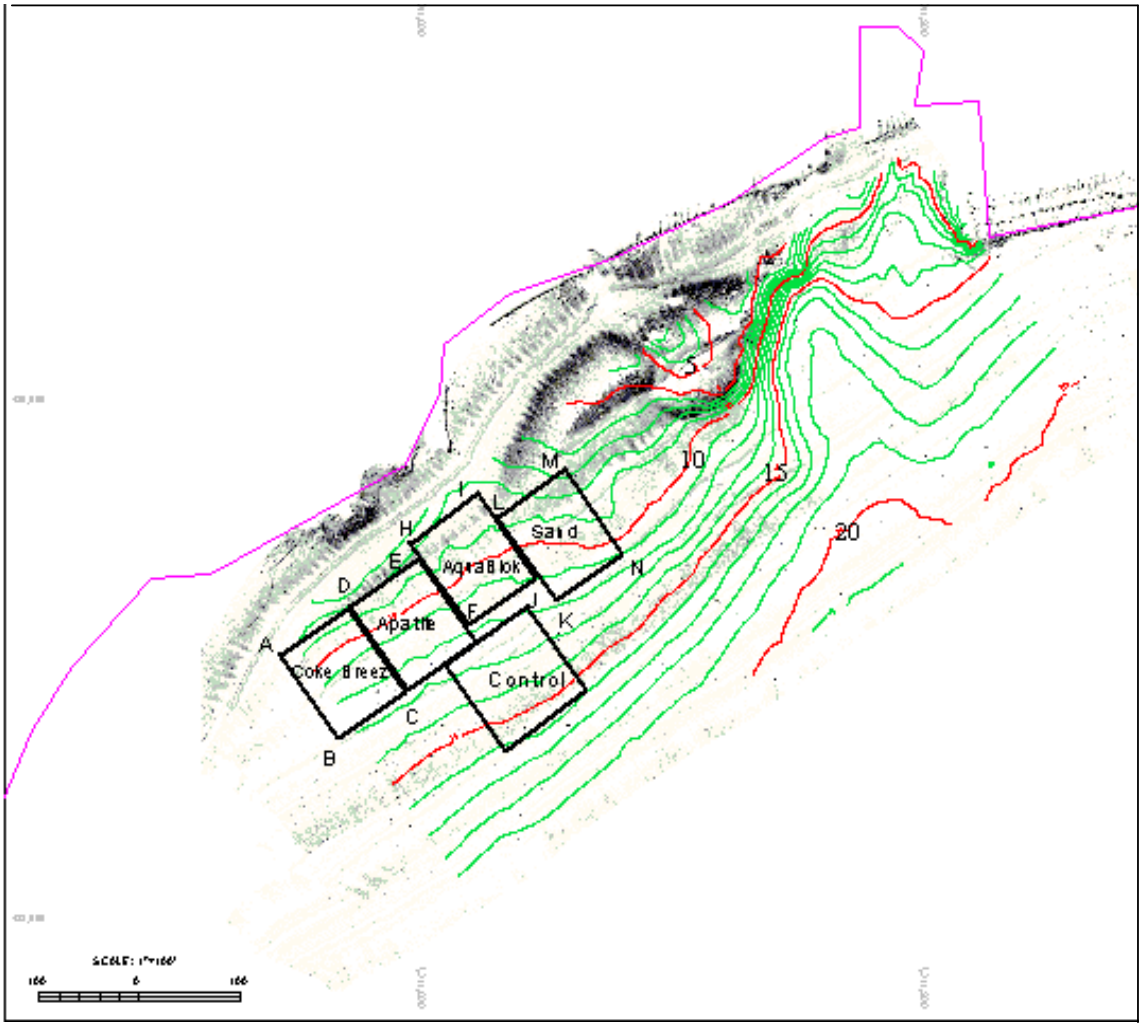

Figure 7. Map of study area showing bathymetry (feet), sediment surface relief, cap locations and potential local sources of continuing contamination.

Tidal fluctuations in the river give rise to hypopheric zone exchange between sediment porewaters and the overlying water. In addition, groundwater upwelling gives rise to transport from deeper sediments to the overlying waters. Net groundwater outflows from the river were measured in September 2003 prior to cap placement. The measurements averaged 4 cm/day at the east end of the demonstration area, but were effectively 0 cm/day at the west end (Matrix, 2003, Horne, 2003). Tidally driven pore

water pumping caused a cyclic fluctuation in this mean velocity with amplitude in both locations of about 1 cm/day.

A complete description of the site characterization delineating the sediment contamination is presented in the site characterization report (Horne, 2003). The chemical concentrations were characterized across the site from a CSO outfall to the east to a storm water drainage area to the west. Although the concentrations were highly variable across this area, as noted below, the variations within the cap demonstration area, which is a subset of the overall characterization area and not immediately adjacent to either CSO or storm water drainage outfall, were more homogeneous. The surficial sediment characterization results over the entire site are summarized below.

Polychlorinated biphenyls: Sediment samples were analyzed for Aroclors. The total PCB in the surficial sediment ranged from 25 µg/kg to 2,400 µg/kg. Within the demonstration area, most of the concentrations were in the range of 500 to 2,000 µg/kg. The dominant Aroclors in the sediment were Aroclor 1248, 1254, and 1400. None of the Aroclors 1016, 1221, or 1232 were detected.

Polycyclic Aromatic Hydrocarbons: Surficial sediment PAHs were characterized according to the EPA regulated 16 PAH compounds expressed as "total PAH" (TPAH). The 16 regulated PAHs are acenaphthene, acenaphthylene, anthracene, benzo(a)anthracene, benzo(b)fluoranthene, benzo(k)fluoranthene, benzo(g,h,i)perylene, benzo(a)pyrene, chrysene, dibenzo(a,h)anthracene, fluoranthene, fluorine, indeno(1,2,3-cd)pyrene, naphthalene, phenanthrene and pyrene. The TPAH concentrations detected in the surficial sediment samples from across the entire site ranged from 470 µg/kg to 82,360 µg/kg dry weight. The highest TPAH concentration (82,360 µg/kg) was detected

near the CSO. The TPAH concentrations within the demonstration area were typically 10,000 to30,000 μg/kg.

Metals: Sediment samples from across the site were analyzed for the EPA 13 priority pollutant metals, including antimony, arsenic, beryllium, cadmium, chromium, copper, lead, mercury, nickel, selenium, silver, thallium and zinc. The detected metal concentration ranges in the surficial sediment samples were as follows, in mg/kg dry weight: antimony, 0.33 to 5.0; arsenic, 1.6 to 10.8; beryllium, 0.31 to1.5; cadmium, 0.32 to 3.8; chromium, 11.3 to 94.8; copper, 18 to 437; lead, 29.3 to 726; mercury, 0.033 to 10.7; nickel, 15.3 to 69.8; selenium, non detect to 1.9; silver, 0.29 to 22.5; thallium, non detect to 2.0; and zinc, 109 to 892.

4.3 Cap Placement

Material was provided to the site in various forms. AquaBlok™ was packaged into approximately 2-ton capacity SuperSacks (bags) for a total of 55 bags shipped to the site. Each bag was placed on a pallet at the manufacturing site and delivered to the site via flatbed trailer. Upon arriving at the site, the bags were unloaded with a forklift onto a 20-mil polyethylene sheet and covered with a 6-mil polyethylene sheet to prevent contact with precipitation because of the highly water-sensitive nature of this product. Apatite was delivered to the site by trucks. Approximately 235 tons of apatite were delivered to the site in 11 truckloads, each load being about 21 tons. Once arriving at the site, the dump truck unloaded the apatite onto a 20-mil polyethylene sheet with a size of 20 feet by 100 feet. Sand was delivered to the site by trucks. Approximately 1,355 tons of sand were delivered to the site in about 64 truckloads (each truckload was about 21 tons capacity). Apatite and sand were also covered with a 6-mil polyethylene sheet, primarily

to maintain ease of handling. Bulk materials were conveyed to a barge, which was then towed to the cap demonstration area for placement by conventional clamshell. Placement was achieved by filling a two yd^3 bucket with the material and gradually opening the bucket, while swinging the crane arm through an arc of approximately three yards. The bucket placement was controlled from the crane through a Windows Offshore Positioning Software system that tracked each bucket placed. Each cap was placed with a nominal cap thickness of approximately six inches and covered with a sand layer of six inches. The sand cap control area was covered with two layers each of a nominal thickness of 6 inches.

As indicated previously, coke was incorporated within the laminated mat due to its near neutral buoyancy relative to water and to the presence of fines that might not be adequately contained by near surface placement. Coke was packaged into an approximately 10-foot by 100-foot porous mat (less than one inch in thickness) and provided as a roll. The delivered coke-filled roll was approximately five feet in diameter, ten feet in length and covered with a plastic sheet. Once at the site, the coke-filled rolls were unloaded to a 20-mil polyethylene sheet, then covered with a 6-mil polyethylene sheet. A total of 12 rolls were delivered to the site although only 11 were used to cover an area of approximately 80 feet x 100 feet. Rolls were placed with use of the crane. Placement was achieved by tacking one end of a roll at the desired location on the bottom with sand and then unrolling by swinging the crane over the placement area. Each roll was overlapped with a previous roll by approximately 1 to 2 feet. In other applications that would entail capping all the way to shore, the rolls could be tacked from shore without the use of divers and unrolled by swinging the crane. After placement of the

coke-filled rolls, a sand layer with a nominal 6-inch thickness was placed as described previously.

The locations of the placed cap materials are shown in Figure 7 as an overlay on a side scan sonar image of the site (geophysical support from Ocean Survey, Inc., Old Saybrook, CT). Note that the AquaBlok^{TM} was not placed over the entire design cap area due to placement at greater than design thickness. AquaBlok^{TM} was the first active cap placed and the crane operator had not yet developed an optimal placement procedure. In addition, the target AquaBlok^{TM} thickness was less than the other cap materials to allow for swelling of the clay layer after placement.

4.4 Monitoring Immediately after Cap Placement

Monitoring immediately after the cap placement (1 to 4 months after placement) was designed to characterize cap placement effectiveness and define initial conditions with which to compare subsequent cap monitoring. Sediment cores were collected to confirm and characterize the cap layer thicknesses. Geophysical measurements, including bathymetry and side scan sonar were used to characterize the bottom conditions including each cap's placement. Survey methods were also employed to estimate the thickness of each cap. Seepage measurements were conducted to evaluate the influence of cap placement on groundwater movement.

Bathymetry measurements were not sufficiently precise to adequately evaluate cap thicknesses. A large number of hand driven cores (greater than 50), however, were collected and believed to provide the best indication of the thickness of each cap and thickness variations across the site. Table 1 summarizes the cap thicknesses and standard deviations measured by hand driven cores. As stated previously, the AquaBlok^{TM} cap

was greater than its design thickness and, therefore, there was incomplete coverage of the design area. AquaBlok^{TM} swells in water, however, and thus accurate comparison of the measured and placed thickness of AquaBlok^{TM} is not possible. The average and standard deviations in cap layer thicknesses show that the vast majority of the cap layers were near to design despite the effort to place relatively thin layers and the use of conventional clamshell bucket placement. Presumably greater uniformity in cap layer thickness could be achieved through placement by methods such as hydraulic broadcasting of the material (at least for sand and apatite that could be effectively placed as a slurry). Although the vast majority of the observed cap thicknesses were near to design, occasional cores showed little or no cap material or a layer of cap material that was excessively thick. The areal average effectiveness of a cap, however, is proportional to the area covered and thus small areas left exposed would not significantly compromise the overall effectiveness of the cap. This fact should be considered when setting performance standards for field capping efforts, for example, by evaluating placement performance on the basis of 95 percent confidence limits in observed cap thickness rather than by requiring all measurements of cap thickness to exceed a specified value.

Table 1: Targeted and Observed Cap-Layer Thicknesses

Cap	Materials Placed	Target Thickness (in)	6-Month Minimum (in)	6-Month Maximum (in)
Sand	Sand	12	3	18
AquaBlok	AquaBlok Sand	4 8	3	18
Apatite	Apatite Sand	6 6	3	15
Coke Breeze	Coke Sand	0.5 8	3	12

A review of the target and achieved cap thicknesses suggest that the goal of placing active capping materials in relatively thin lifts (6 inches) using conventional clamshell bucket equipment was met. In addition, the ability to place high value or difficult to place materials in a laminated mat was also demonstrated.

Settlement plates were used to assess consolidation of the underlying sediment. Total settlement of 0.75 to 2.25 inches was noted within 5 to 20 days of cap placement. Ultimate consolidation was much less than the total cap thickness placed (nominally 12 inches for the sand, AquaBlok^{TM} and sand, and apatite and sand caps and 1+6 inches for the coke mat with sand). Some of the initial consolidation was associated with gas release due to the disturbance of cap placement. Gas generated by denitrification and methanogenesis in the sediments had accumulated in pockets of the sediments and occasionally significant amounts of gas were released after the disturbance associated with a single bucket placement of cap materials. In at least one instance, gas was released for 20 to 30 seconds after placement of a single bucket, as noted by vigorous bubbling at the surface.

Groundwater seepage measurements after the placement of the caps showed little or no change in the rate of pore water exchange in any of the cap areas except in and outboard of the AquaBlok^{TM} cap. The presence of the AquaBlok^{TM} cap showed effectively no groundwater outflow in an area that exhibited 2 to 4 cm/day net outflow prior to the cap placement. In addition, the control area immediately outboard of the AquaBlok^{TM} cap area showed increases in groundwater seepage with effectively no specific discharge prior to cap placement to as much as 5 to 10 cm/day post cap placement. This is illustrated in Figure 8, which includes the sand cap (no change in

specific discharge), AquaBlok™ (significant decrease in specific discharge) and the control area (significant increase in specific discharge).

There were concerns that hydraulic forces as a result of groundwater gradients, tidal forces and gas accumulation, might cause vertical motions in the AquaBlok™ since its low permeability might limit relief from such forces. Immediately after placement of the AquaBlok™, an array of ten inclinometers (Slope Indicator, Inc., Mukiltea, Washington) were placed on top of the AquaBlok™ and covered by sand.

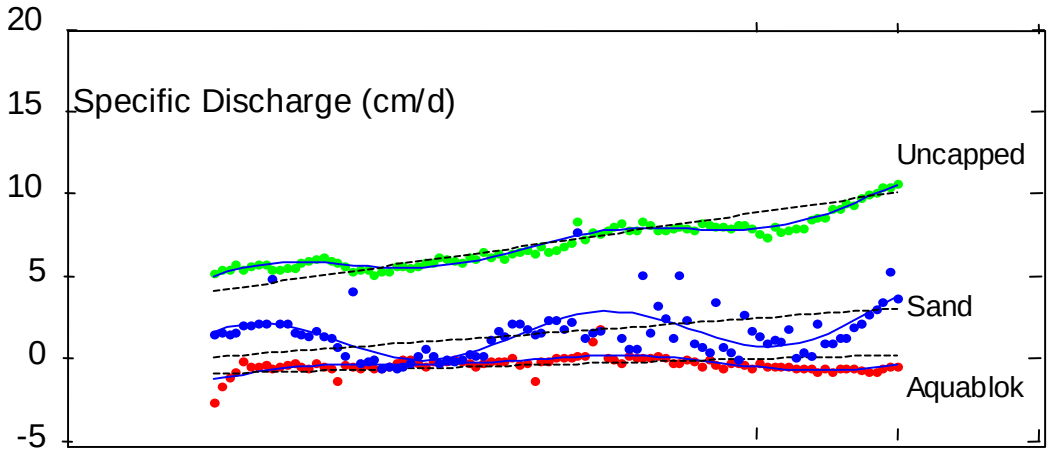

Figure 8. Specific discharge at three locations in the cap demonstration area.
Note: AquaBlok™ significantly reduced the specific discharge relative to the adjacent sand cap area, while the specific discharge in the uncapped area was significantly enhanced by diversion of flow from the AquaBlok™.

The inclinometers embedded within the cap allowed for the measurement of vertical motions of the cap. As shown in Figure 9, tidal level changes were observed to cause sub-mm heaving of the AquaBlok™ cap. Some sensors showed a continuous increase over time, although several showed significant decreases due to consolidation.

A slow increase in elevation with time was especially significant in the outboard end of the inclinometer and vertical uplift of approximately 20 mm was noted over a 2-month period as shown in Figure 10. On May 25, 2004, however, somewhat less than 2 months after placement, the inclinometer showed a sudden deflection of 0.75 m. This was apparently due to the release of gas that had accumulated over time underneath the AquaBlok^{TM}. It was not known why the gas accumulated at the outboard end of the cap or what caused its rapid release, although the AquaBlok^{TM} is thinnest near its outboard edge. The outboard end of the inclinometer was subject to similar rapid deflections every 30 to 45 days throughout the summer and then vertical motions effectively ceased, presumably due to the onset of cooler conditions and the resulting reduction in microbial gas generation. No similar deflections were noted during the subsequent summer although some deterioration of the inclinometer sensors was expected by that time. In addition, the presence of the cap would eliminate the deposition of new organic matter, reducing and eliminating significant microbial activity over time.

4.5 Chemical Containment Effectiveness

In addition to demonstrating the ability to effectively place active cap materials in relatively thin lifts, a project objective was to measure the chemical containment effectiveness of the active caps relative to conventional caps or uncapped sediments. This effort is ongoing and will continue through 2007. A major impediment to demonstrating greater chemical containment effectiveness is the high degree of effectiveness of conventional sand caps. The differences between the caps with active sequestration agents and conventional sand cap are expected to be small initially but to slowly grow with time. The primary tool employed to assess contaminant containment

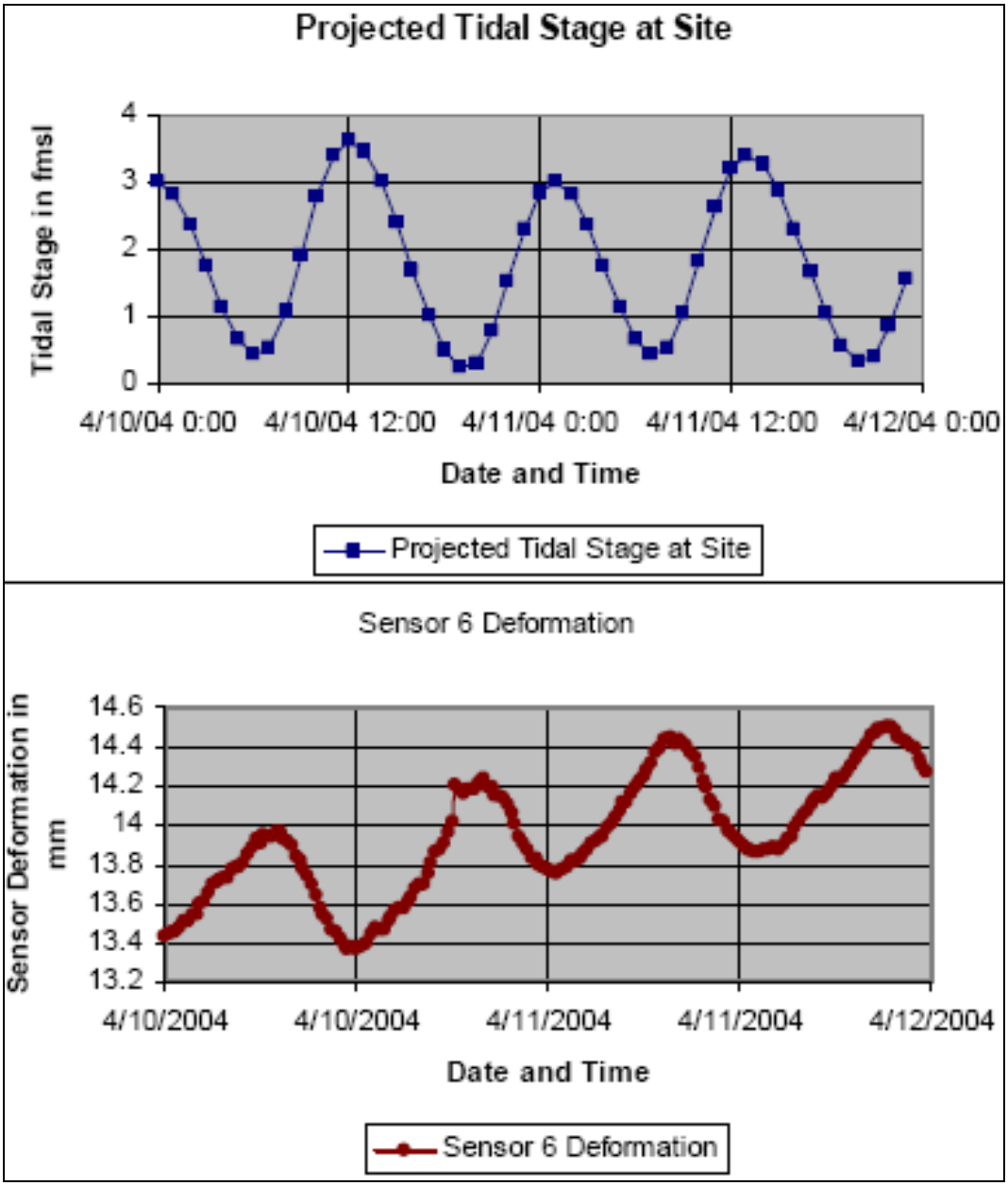

Figure 9. Tides and resulting deformation of the AquaBlok™ cap.

Note: feet above mean sea level

is the chemical concentration profile in cores. The ability to differentiate between the various cap treatments in such cores, however, is limited by the vertical resolution of the

core samples, intermixing between cap layers and the underlying sediments and the low sorption associated with the sand cap layers.

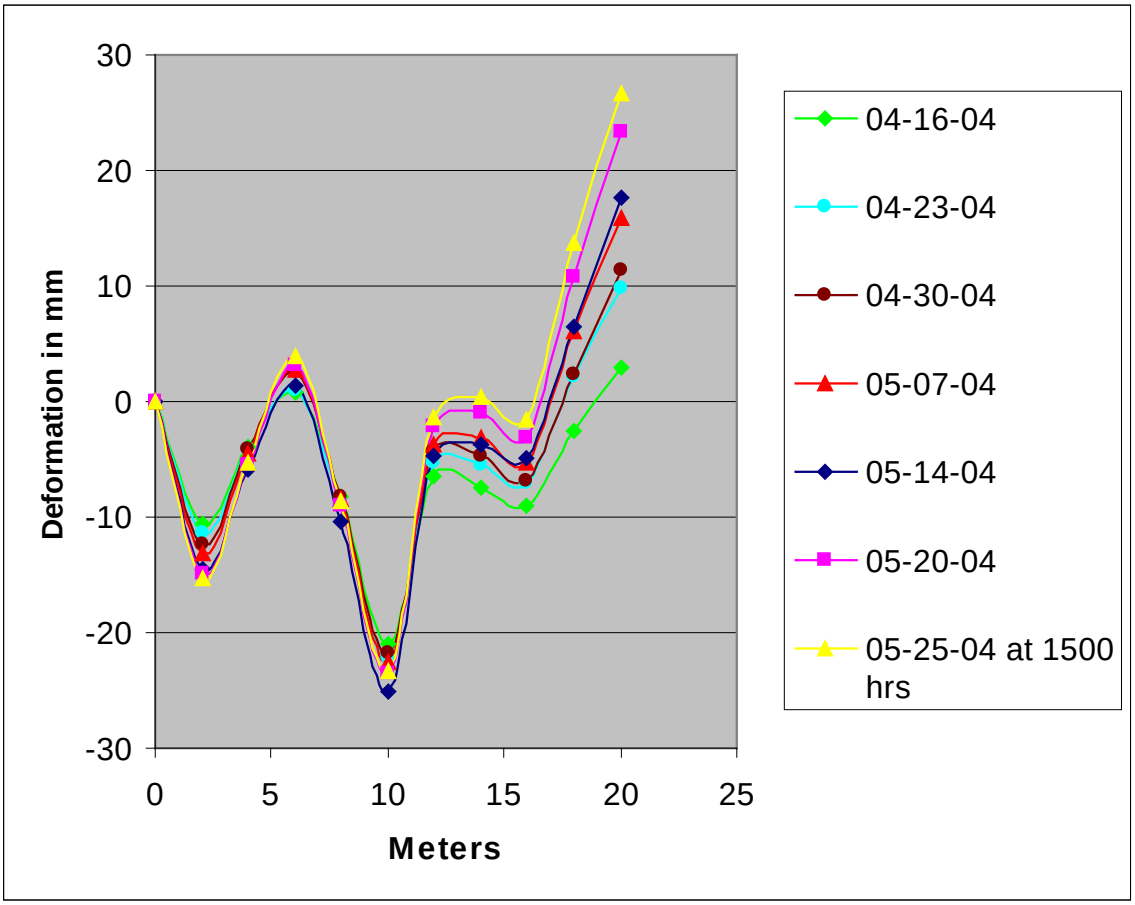

Figure 10. Deformation of the AquaBlok™ as a function of distance into the river at various times after placement.

Note: There was a steady rise of the outboard end of the cap until a sudden gas release at 4:00 pm on 5/25/04.

Conventional cores were collected with 2-inch sample resolution. The large sample thickness was to ensure sufficient sample quantity for PAH and metal analyses and physical characterization by commercial laboratories. Such a large sample thickness can be relevant at the exposed sediment (or cap) water interface where bioturbation may

cause effective mixing over at least that depth. At the cap-sediment interface, however, there exists no bioturbation and chemical migration processes are much slower. Figure 11 shows a typical vertical profile collected at this resolution. The concentration profile shows no measurable movement into the cap layer or the sand above the active capping layer but the vertical resolution is insufficient to clearly identify any migration that might occur within 18 months of cap placement. Note that the concentration profile shows elevated concentrations at the top of the cap layer or at the cap-water interface. There appears to be no connection with the contamination beneath the cap. It is believed that the higher contaminant concentration at the surface is the result of deposition of new sediment and contaminants. Contaminant sources, including combined sewer overflows and storm water drains have not been controlled along the Anacostia thus additional contamination is to be expected. The recontamination of the surface of the capping materials appears to be widely variable across the site presumably due to the presence of specific sources outside of the cap area, such as a CSO on the east end of the site and a storm drain at the west end. Although the storm drain should exhibit minimal contaminant loading, sheens are regularly observed from this drain and, in addition, the latest monitoring shows significant new sediment deposition in this area. Up to 2 to 4 inches of new deposition has occurred on the coke cap while less than 1 inch was observed elsewhere.

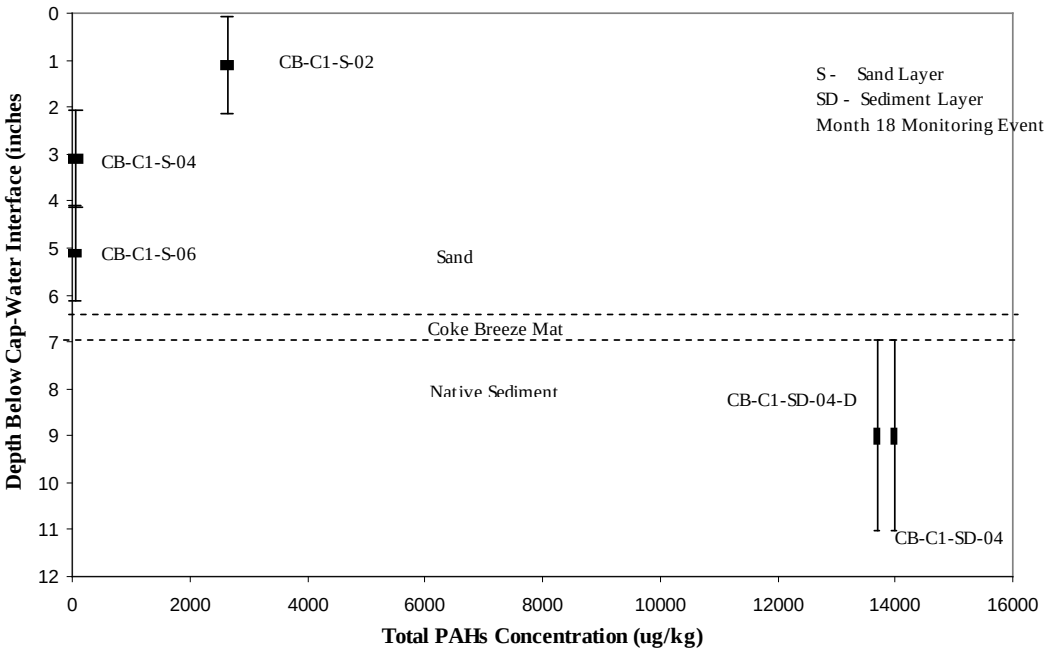

Figure 11. Coke core 1 total PAHs versus depth – October 2005.

Note: The vertical PAH profile in the coke mat area shows excellent containment of sediment contaminants and recontamination from unremediated areas of the river at the surface.

Higher resolution cores were collected 18 months after placement in an attempt to gain a better understanding of the chemical migration to date. Figure 12 shows one such profile in which PAH concentrations are measured in the sand cap with a resolution of 5 mm. A grain size analysis was also conducted for each sample in an attempt to identify the effect of intermixing between the sand and the sediment. The intermixing zone was defined as the zone between the samples which exhibited a sand fraction identical to that of the underlying sediment (approximately 30 percent sand) and effectively 100 percent sand, which meant that the sample was all cap material and contained no underlying sediment. The PAH concentrations in this interval are consistent with the sediment fraction in each sample indicating that the PAH concentrations at each interval were the

result of intermixing between the underlying sediment and the sand cap and not PAH migration. This does not necessarily exclude the potential for PAH migration in pore water since the sand has little sorption capacity for PAHs relative to the sediment. In order to better understand dissolved PAH migration, pore water profiling using diffusion samplers is currently being tested. The results from these studies are not yet available.

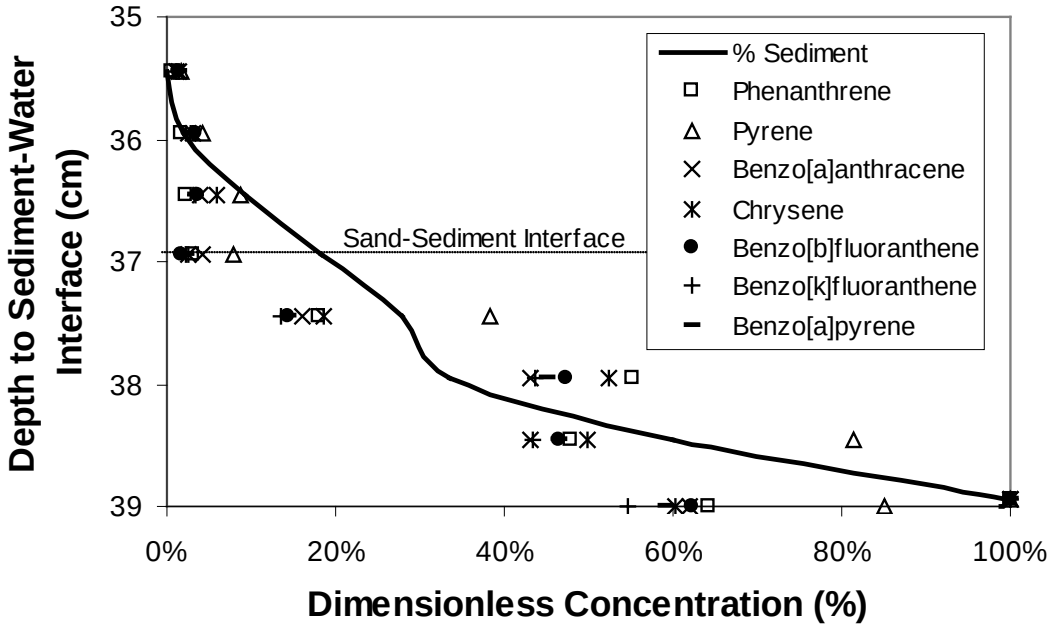

Figure 12. PAH concentrations versus depth in the sand cap 18 months after placement.

Note: The graph indicates that intermixing at the sand-sediment interface accounted for the observed PAH distribution.

4.6 Summary and Preliminary Conclusions

The Anacostia active capping demonstration successfully demonstrated the ability to place selected capping materials including AquaBlok^{TM} (for permeability control), apatite, (for enhanced metals sorption and control), and coke (for enhanced organic sorption and control). Apatite and AquaBlok^{TM} were successfully placed using a

conventional clamshell in layers of six inches or less. The coke was successfully placed in a laminated mat demonstrating that high value and/or difficult to place material can be placed in a controlled fashion. Sand was successfully placed by conventional clamshell in 6-inch layers on top of the active cap materials to act both as an armoring layer and as a better bottom substrate. The placement efforts demonstrated that active capping materials could be effectively placed with conventional equipment in relatively thin layers. Subsequent monitoring has shown deposition of additional fine grained material and no loss of cap material due to erosion or other processes have been noted.

The deposition of additional fine grained material, at rates expected to be similar to historical depositional rates of approximately 0.75 cm/yr ± 0.2 cm/yr has led to the recontamination of the top of the capping layers since sources have not yet been completely controlled in the Anacostia. It is expected that this re-deposited sediment contains contaminant levels similar to the surficial pre-cap concentrations. Deposition of new sediments is especially significant near a storm water outfall near the western edge of the cap.

Post-capping performance monitoring has shown no measurable contaminant migration in any of the caps, including the sand cap control. Observed concentration profiles are consistent with intermixing of the cap material in the soft sediment during the cap placement. Monitoring will continue for at least another year and include pore water measurements in an effort to better differentiate the performance of the various cap layers.

The AquaBlok^{TM} cap has been shown to effectively halt groundwater upwelling in the capped area, with subsequent increases in upwelling in surrounding uncapped

areas. The low permeability of this layer, however, also led to a slow uplift due to the accumulation of gas beneath the cap and the rapid release of this accumulated gas several times during the first summer after placement. This release is expected to subside over time due to the elimination of organic matter deposition that drives gas ebullition in the sediments protected by a cap. When gas ebullition processes are active, however, gas accumulation and release will occur and a cap design should consider its implications. In this case, no effect on contaminant release, or cap layer integrity, has been noted.

4.7 Acknowledgements

The planning, placement and subsequent monitoring of the capping demonstration project depended upon the support of a number of people and groups beyond the authors of this article. The oversight and support of the District of Columbia Department of Health and the Anacostia Watershed Toxics Alliance were critical to the success of the project. The US EPA through the Hazardous Substance Research Center/South and Southwest, the Remediation Technology Development Forum (RTDF) and the EPA SITE program were instrumental in the design and monitoring stages of the project. The supplemental monitoring of the AquaBlok^{TM} cap being conducted by the EPA SITE program will improve the understanding of the performance of that cap material and also allowed the overall project team to more effectively focus monitoring efforts. In addition, the efforts of Ocean Surveys, Inc for geophysical support, Chris Smith and Matrix for seepage measurements, Bob Diaz for sediment profiling imaging, and Earth Resource Technology (ERT) for field support of Horne Engineering, the prime site contractor. The assistance of various teams of researchers providing laboratory data assisting in the cap design is also gratefully acknowledged including Greg Lowry,

Carnegie Mellon University (coke evaluation), Jeff Melton and Brad Crannell of the University of New Hampshire (apatite evaluation), and Hull and Associates, (AquaBlok^{TM} support and evaluation). Finally the success of the field operations is largely due to the efforts of the construction contractor, Sevenson Environmental Services, and the prime field contractor, Horne Engineering.

4.8 References

1. The Anacostia Watershed Toxics Alliance (AWTA), 2002. Chartering a Course Toward Restoration: A Toxic Chemical Management Strategy for the Anacostia River. Draft Report, Washington, DC
2. Bentley, S. 2004. Radiochemical Analysis of Anacostia Sediment. Draft Report January 2004. Retrieved on October 2, 2006 from http:www.hsrc-ssw.org/ana-index.html.
3. Horne Engineering Services (Horne). 2003. Site Characterization Report for Comparative Validation of Innovative "Active Capping" Technologies Anacostia River Washington, DC. Prepared for the Hazardous Substance Research Center/S&SW. Retrieved on October 2, 2006 from http:www.hsrc-ssw.org/ana-index.html.
4. Horne Engineering Services (Horne). 2004a. Cap Completion Report for Comparative Validation of Innovative "Active Capping" Technologies Anacostia River, Washington, DC. Prepared for the Hazardous Substance Research Center/S&SW. Retrieved on October 2, 2006 from http:www.hsrc-ssw.org/ana-index.html.

5. Horne Engineering Services (Horne). 2004b. Month 1 Monitoring Report Comparative Validation of Innovative "Active Capping" Technologies Anacostia River, Washington, DC. Prepared for the Hazardous Substance Research Center/S&SW. Retrieved on October 2, 2006 from http:www.hsrc-ssw.org/ana-index.html.
6. Matrix Environmental and Geotechnical Services (Matrix) 2003. Final Report - Quantifying Specific Discharge across the Sediment–Water Interface within a Test Area of the Anacostia River, Washington, D.C.: a Pre-Capping Evaluation. November 2003. Submitted to Horne Engineering Services, Inc. Submitted by Matrix Environmental and Geotechnical Services, Florham Park, NJ 07932.
7. Matrix Environmental and Geotechnical Services (Matrix) 2004. Draft Report-Quantifying Specific Discharge across the Sediment –Water Interface within a Test Area of the Anacostia River, Washington, D.C. a Post-Capping Evaluation. July 2004. Submitted to Battelle. Submitted by Matrix Environmental and Geotechnical Services, East Hanover, NJ 07936.
8. Murphy, P. A. Marquette, D. Reible, and G. V. Lowry. 2006. "Predicting the Performance of Activated Carbon-, Coke-, and Soil-Amended Thin Layer Sediment Caps," Journal of Environmental Engineering, 132:787-794.
9. Syracuse Research Corporation and National Oceanic and Atmospheric Administration (SRC and NOAA). 2000. Interpretive Summary of Existing Data Relevant to Potential Contaminants of Concern within the Anacostia River Watershed. SRC#FA292, June 2000.

Chapter 5: Demonstration of PDMS Passive Sampling for Measuring Contaminant Pore Water Concentration Profiles in Sediment Caps: Implications for Remediation[8]

David Lampert[9], Wil Sarchet[10], and Danny Reible[9]

5.0 Abstract

Passive samplers with a sorbent phase such as polydimethylsiloxane (PDMS)-coated fibers provide a means of estimating contaminant pore water concentrations in sediments. In this paper, the ability to measure *in situ* pore water concentrations is demonstrated using a PDMS-based device. The low detection limits possible with the PDMS device enable high resolution vertical concentration profiles that can be used to infer contaminant migration rates and mechanisms. The approach was used to show that thin layer capping can be effective at reducing benthic exposure to bioaccumulation of polycyclic aromatic hydrocarbons (PAHs) as long as the thickness of the cap layer exceeds the depth of organism interaction with the sediments. Finally, it is concluded that the dilution of surficial sediment concentrations with inert sands by organism mixing does not reduce bioaccumulation.

[8]Manuscript in preparation for submission.

[9]Department of Civil, Architectural, Environmental Engineering, The University of Texas at Austin, 1 University Station C1786, Austin, TX 78712-0273

[10] Staff Engineer, Carollo Engineers, 8911 N Capital of Texas # 2200, Austin, TX 78759

5.1 Introduction

Sediments serve as the ultimate sink for many hydrophobic organic compounds (HOCs) such as polycyclic aromatic hydrocarbons (PAHs) and polychlorinated biphenyls (PCBs). As a result, the presence of HOCs in sediments often presents a residual environmental risk many years after sources of contamination are eliminated. Because of poor understanding of the ecological risks associated with contaminated sediments and the ubiquitous nature of the problem, assessment and remediation of contaminated sediments presents a major research challenge for the environmental community (US EPA, 1998).

5.1.1 Sediment Capping

One of the primary alternatives for *in situ* treatment of contaminated sediments is capping with clean material. Capping provides a physical barrier between benthic receptors near the sediment-water interface and can reduce contaminant concentrations by retarding migration through sorption onto the cap material. Sand caps can also provide a new habitat in areas where transport of coarse-grained sediments has been reduced due to reduction in high flow events (due to dams and other man-made interferences). Numerous laboratory studies have demonstrated the ability of sand to act retard contaminant fluxes from sediments (Thibodeaux and Bosworth 1990, Wang et al. 1991, Thoma et al. 1993, Zeman and Patterson 1997).

Due to the permeable and relatively inert nature of sand, questions have arisen over the long-term effectiveness of sand caps for contaminated sediment management. As an alternative to traditional capping, active capping with materials that strongly sorb contaminants has been proposed (Murphy et al. 2006, Reible et al. 2006, McDonough et

al. 2007). However, such materials may be unsuitable habitats for *benthos* and would thus require a clean sand layer for erosion armoring and habitat restoration. To assess the effectiveness of various capping materials at retarding contaminant migration, it is necessary to quantify concentration profiles in such systems and ultimately the impact of these concentrations on bioaccumulation of contaminants.

5.1.2 Assessing Bioaccumulation

In situ pore water concentrations have been linked to bioaccumulation of HOCs in sediment environments (Kraaij et al. 2003, Lu et al. 2006, Meloche et al. 2009). However, direct measurement of HOC concentrations in the aqueous phase is frequently difficult due to analytical limitations; thus the bulk solid-phase concentration is often used for assessment of sediment quality (Doucette 2003). The bulk solid-phase concentration is not always an appropriate metric for assessing bioavailability (Burton 1991), as the release of contaminants from the sediment organic carbon may over-predicted by the classic theory of instantaneous linear partitioning with sediment organic carbon (McGroddy and Farrington 1995, Kan et al. 1997, Accardi-Dey and Gschwend 2002). As a result, a current research thrust is the use of passive sampling devices for assessing pore water concentrations of HOCs in sediments.

Various passive sampling approaches have been tested for estimation of *in situ* HOC pore water concentrations, including semi-permeable membrane devices (SPMDs) (Booij et al. 1998), polyoxymethylene (POM) sheets (Jonker and Koelmens 2001), polyethylene (PE) sheets (Vinturella et al. 2004), and polydimethylsiloxane (PDMS)-coated glass fibers (Mayer et al. 2000a). These techniques estimate the mass that is accumulated on a sorbent sampling device to estimate *in situ* concentrations. The pore

water concentration is then back-calculated from an established partitioning relationship. The accumulation on the sorbent can also be used as a biomimetic sampler and compared directly to contaminant effects or bioaccumulation.

Glass fibers coated with a thin layer of PDMS are readily available commercially and particularly convenient to insert into sediments with minimal disturbance. They are thus well-suited for an *in situ* approach where the sorbent can be inserted, removed after attainment of equilibrium or a known fraction thereof, and segmented to determine high precision concentration profiles. The PDMS-coated glass fibers can be manufactured to very small sizes (e.g., 110 µm glass diameter with 30 µm PDMS coating, Mayer et al. 2000a) or at other sizes to maximize uptake kinetics (10 µm layer on 210 µm diameter core). Because of this relatively small size, the method does not significantly deplete the neighboring sediment particles, and hence does not affect the equilibrium chemistry. In addition, equilibrium may be attained relatively rapidly (Mayer et al. 2000a). The ability to determine high resolution vertical pore water concentration profiles provides an opportunity to infer availability, rates, and potentially mechanisms of transport that are not available from bulk solid concentration measurements.

5.1.3 Research Objectives

This paper has four primary objectives:

1. to demonstrate the potential effectiveness of a thin layer of sand for capping contaminated sediments
2. to develop appropriate metrics for assessing the effectiveness of capping (i.e., pore water concentrations)

3. to validate theoretical model predictions of contaminant concentrations in these caps
4. To demonstrate the insignificance of dilution of particle-phase concentrations by inert sands

To meet these objectives, the results of a series of laboratory microcosm experiments and a field demonstration are presented and analyzed. The laboratory microcosms simulated migration of PAHs from contaminated sediment through thin layer sand caps to a test organism, *Ilyodrilus templetoni*, an annelid oligochaete. The data from these experiments were taken from Sarchet (2008). PDMS-coated glass fiber passive sampling devices were used to quantify contaminant concentration profiles in the caps. The results were analyzed to assess the effectiveness of such caps and demonstrate the ability of the PDMS sampling device to measure concentration profiles. Following the success of this method, the device was used to measure pore water concentration profiles in the sediment capping demonstration area described by Reible et al. (2006). The field-measured pore water profiles showed a large discrepancy when compared to bulk solid phase profiles that can be explained by the relative differences in sorption capacity of the capping materials. The study provides an indication of the appropriateness of using the PDMS sampling device to infer near surface bioaccumulation as well as demonstrate a practical means of measuring profiles in the field.

5.2 Materials and Methods

5.2.1 Analytical Methods

PAHs were chosen as target analytes in the study due to their ubiquitous nature and relative sensitivity. PAH analysis was performed using high performance liquid

chromatography for separation with fluorescence detection (HPLC/FD) for quantification. All analyses were performed in accordance with EPA Method 8310: Polynuclear Aromatic Hydrocarbons using a Waters 2795 Separations Module. An isocratic flow rate of 1.0 mL/min composed of 3:7 water:acetonitrile (v:v) was used for separation of the target analytes. Detection was achieved using a Waters 2475 multiwavelength fluorescence detector. The optimal excitation and emission wavelengths used for quantification of each of the PAHs were taken from Futoma et al. (1981). All analyses utilized linear calibration curves with a minimum of five points. Check standards and blanks were used with every sample set to ensure performance. Seven PAHs were analyzed in all of these studies: phenanthrene (PHE), pyrene (PYR), benz[a]anthracene (BAA), chrysene (CHR), benzo[b]fluoranthene (BBF), benzo[k]fluoranthene (BKF), and benzo[a]pyrene (BAP).

PAHs were extracted from the solid phase (sediments as well as cap materials) using EPA Method 3550B: Ultrasonic Extraction. This technique is used for extracting nonvolatile and semivolatile compounds from solid matrices. Approximately two grams of sample were mixed with anhydrous sodium sulfate in thoroughly pre-cleaned glassware until a free-flowing powder was formed. Next, 60 mL of a 1:1 (v:v) hexane:acetone solution were then added to the jar. The samples were then placed into a water bath in a Branson (Danbury, CT) Model 2200 Ultrasonicator for 30 minutes to dismember the particles. Samples were equilibrated overnight, after which an aliquot of the extract was separated, blown down with nitrogen gas using a Labconco (Kansas City, MO) Model 79100 RapidVap N_2 Evaporation System, and finally reconstituted with acetonitrile for final analysis. The solid-phase concentrations were determined by back-

calculation using mass, which was measured at each step in the extraction. Method blanks were used to check for contamination with every set of samples. A sample was periodically spiked as a check on extraction efficiency.

The total organic carbon of sediment samples was determined by elemental analysis on a Carlo-Erba 1108 according to Hedges and Stern (1984) modified according to Harris et al. (2001) (i.e., overnight vapor acidification with a hydrochloric acid atmosphere to remove inorganic carbon from samples). The oxidation column was run at 1020°C, while the reduction column was run at 650°C. The oven temperature was maintained at 60°C. Each sample was measured in triplicate and the results averaged to obtain the final values used for analysis.

Lipid content was assessed using the method first described by Herbes and Allen (1983) to convert wet worm tissue loadings to lipid-phase concentrations. Twenty worms (~100 mg wet weight) were transferred to pre-weighed 15 mL centrifuge tubes and then re-weighed to assess worm mass. Five mL of a 1:1 (v:v) solution of reagent grade methanol and reagent grade chloroform (Fisher Scientific, Waltham, MA) were added to each tube for lipid extraction. The samples were then sonicated for 30 seconds and allowed to equilibrate for four hours. The tubes were centrifuged, and the supernatant was transferred to a new tube. An addition five mL of the methanol-chloroform solution were added to the original tube to remove any remaining extract. The extract was then equilibrated with two mL of water to remove tissue protein. The extract was then dried at 50°C and weighed to assess the lipid mass in the original sample. Method blanks were evaluated and showed no solvent residuals.

5.2.2 PDMS Fibers

Two different PDMS fibers were used in these studies. The first fiber (hereafter referred to as PM 170/110) was obtained from Poly Micro Industries (Phoenix, AZ) and had a 110 µm core with a 30 µm PDMS coating or outer diameter of 170 µm, which equates to a specific volume of 13.55 µL/m fiber. The second fiber (hereafter referred to as FG 230/210) was obtained from Fiber Guide Industries (Stirling, NJ) and had a 210 µm core with a 10 µm PDMS coating or outer diameter of 230 µm, which equates to a specific volume of 6.91 µL/m fiber. Both of the fibers were very thin, brittle, and nearly transparent.

5.2.3 Laboratory Characterization of PDMS Fibers

Both of the PDMS fibers were tested in the laboratory to verify their ability to quantify sediment pore water concentrations. Partitioning of the various PAHs between the PDMS and the pore water was found to be linear and characterized by a partition coefficient of K_f. The values for K_f correlated well with octanol-water partition coefficients (K_{ow}), consistent with the approach presented by Mayer et al. (2000b). Using K_{ow} values from MacKay et al. (1992), the best fit correlation for K_f versus K_{ow} was found to be:

$$\log K_f = 0.839 * \log K_{ow} + 0.117 \quad (5.1)$$

Equilibrium was attained within a day for lower molecular weight compounds but required up to a month for higher weight compounds ($\log K_{ow} > 5.8$).

For all PDMS analyses, the fiber was cleaned prior to deployment by sonication in hexane for a minimum of half an hour, followed by a rinse with acetone and then de-

ionized water. After equilibration of the fibers with the sediment, fibers were rinsed clean (to remove any particles) with deionized water and then placed into 100 µL HPLC inserts with 100 µL of acetonitrile. The acetonitrile was found to remove essentially 100% of the PAH mass from the fiber within 24 hours.

5.2.4 Field apparatus

To measure pore water concentration profiles of PAHs in sediment caps, a field-deployable PDMS profiling apparatus was developed. To protect the fibers in the sediment column, a stainless steel piezometer was used as a tool to insert and recover the PDMS fibers into the sediment environment. An approximately 2-mm wide rectangular groove was made in the inner rod of the piezometer to serve as a frame for the fragile PDMS fibers. Approximately 0.5-mm thick slits were cut into the outer part of the piezometer at ¼" spacing to allow equilibration of the fiber with the neighboring sediment. The bottom and top of the rods were sealed shut to prevent an inflow of pore water through the system. Figure 13 shows a schematic of the PDMS field sampling device.

5.2.5 Laboratory Microcosm Studies

To demonstrate the ability of the PDMS fibers to appropriately predict the transient migration of HOCs in sediment caps and the associated effects on benthic invertebrates, laboratory microcosms of PAH-contaminated sediments with sand caps of varying thicknesses (0, 2, 4, 6, and 10 cm) were set up and analyzed. While profiles were measured for many PAHs, two four-ring compounds (PYR and BAA) were selected for characterization of pore water profiles due to their relatively rapid equilibration time in

PDMS fibers (approximately a few days based on lab assessments), quantifiability, and expected short migration times in through the sand.

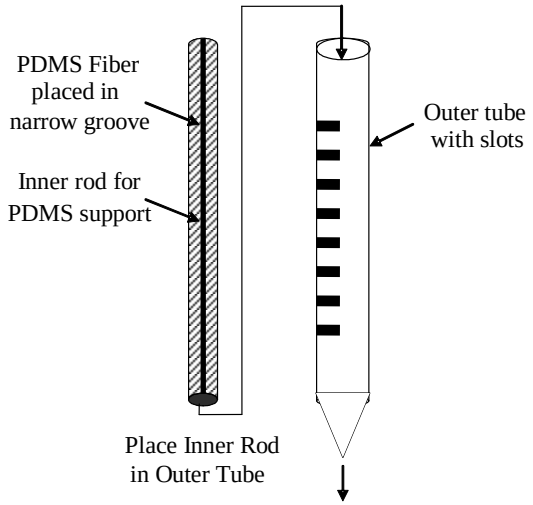

Figure 13. Field PDMS sampling device.
The PDMS-coated glass fiber is placed inside the narrow slit in the stainless steel piezometer. An outer stainless steel sheath with a series of cuts protects the fiber during deployment but still enables interaction between the pore water and the fiber.

Contaminated sediments used in these studies were taken from the Anacostia River in Washington DC. Anacostia sediment contains PAH levels of approximately 10-30 mg PAH/kg dry sediment (Reible et al. 2006). Artificial pond water consisting of 0.5 mM NaCl, 0.2 mM $NaHCO_3$, 0.05 mM KCl, and 0.4mM $CaCl_2$ dissolved in deionized water was passed over the sand cap at a velocity of approximately 5 cm/s to provide a clean sink for PAHs. Clean sediments taken from University Lake in Baton Rouge, LA were placed over sand caps to simulate the deposition of fresh (uncontaminated) sediment and to provide a suitable habitat for benthic invertebrates. A culture of the benthic organism *Ilyodrilus templetoni* was placed into this microcosm to encourage colonization

of the surface sediments and mimic the deposition commonly observed in sediment environments. PDMS fibers were placed into the microcosms, then sampled and analyzed in triplicate at 28 days to determine concentration profiles at 1-cm resolution.

5.2.6 Field Coring Studies

To evaluate the effectiveness of capping at decreasing the contaminant concentrations in surficial sediments, the concentration profiles of contaminants in the solid phase were evaluated through sediment cores. Undisturbed cap/sediment samples from all the caps except the coke breeze cap were collected by a vibrating coring or vibracore sampler. The vibracore sampler used was a 3.25-in diameter stainless-steel core barrel fitted with a 2-7/8-in clear plastic liner. After a core sample was retrieved, the overlying water was bled by cutting the core liner with a hacksaw. The core liner was then capped with watertight plastic caps, sealed with tape, labeled with its identification and orientation, and shipped back to the lab for processing. The cores were extruded in the lab, and samples were collected at 0.5-cm intervals. The outside edge of the samples was discarded due to concerns about edge effects during collection and extrusion. For each sample, the concentration of PAHs was determined and a sieve analysis performed to assess the percentage of the cap material and the sediment within the sample. All solid-phase concentrations were normalized on a dry weight basis using the percent moisture from the sample.

At the interface between the overlying cap layer and the underlying sediment, a region exists where the two materials are present. Chemical analyses of the region therefore exhibit concentrations between those in the sediment and in the cap. As a means of distinguishing between this intermixing effect and contaminant migration, a

sieve analysis of the samples was used to quantify the percentage of a sample composed of native sediment and the cap material. The cap materials generally possessed larger particle diameters and hence a smaller percentage of the cap materials would pass through the sieve. The samples were dried and then sieved using a U.S. number 80 (0.18 mm) sieve (preliminary analysis indicated that it provided the most efficient separation between the materials) and evaluated for percent passing. As a small part of the sediment (approximately 20% by mass) was retained on this sieve and a small part of the capping materials passed through the sieve (less than 10%), the actual percent native sediment was estimated by normalizing the scale to stretch from 0% to 100%.

5.2.7 Field Demonstration of PDMS Sampler for Assessment of Sediment Capping

The field apparatus was deployed at the Anacostia River in Washington DC to demonstrate the ability of the device to quantify *in situ* pore water concentration profiles of PAHs. This site contains a field-scale demonstration of the capping contaminated sediments, and is thoroughly described in a former paper (Reible et al. 2006). Rods were placed in triplicate into capped and uncapped areas using divers and left to equilibrate for 28 days. Upon retrieval, the PDMS fibers were immediately cleaned, processed into solvent in 5-cm intervals, and analyzed for PAHs.

5.3 Experimental Results and Discussion

5.3.1 Microcosm Experiments

One goal for the microcosm studies was to demonstrate the ability of PDMS fibers to measure pore water concentration profiles in sediment caps. To this end, pore water profiles using the PDMS technique were placed into the microcosms and analyzed after a 28-day period. Concentration profiles were assessed 28 days after placement at 1-

cm resolution. The flow of the overlying water maintained a near-zero concentration at the sediment-water interface throughout the experiments.

5.3.2 PDMS-Derived Profiles from Microcosm Experiments

Figure 14 shows the concentration profiles of PYR and BAA in the microcosms with cap thicknesses of 4 cm or less. There were no statistically significant differences in the concentration profiles in each of these experiments. These results were consistent with expectations as bioturbation (organism-related mixing of surficial sediments) compromises the upper portions of sediment caps (Palermo 1998). The bioturbation depth for *Ilyodrilus templetoni* was estimated from inspection of the various microcosms and found to be approximately 4 cm, which was consistent with expectations as organism lengths ranged from two to five cm and *Ilyodrilus templetoni* is a head-down feeder with a high bioturbation rate (Schaffner 1997). The profiles in Figure 14 show a linear trend from the underlying contaminated zone to the clean overlying water. The presence of bioturbation substantially increases the effective diffusion coefficient and was assumed to dominate this parameter relative to molecular diffusion (Boudreau 1997). The effective diffusion coefficient was modeled by the following (Boudreau 1997) expression:

$$D = D_{bio}\ \rho f_{oc} K_{oc} \tag{5.2}$$

Where D_{bio} represents the diffusion of particles by bioturbation and should be the same for all compounds. As bioturbation is a quasi-diffusive process, the observed linear profiles can be explained by a steady-state diffusion model.

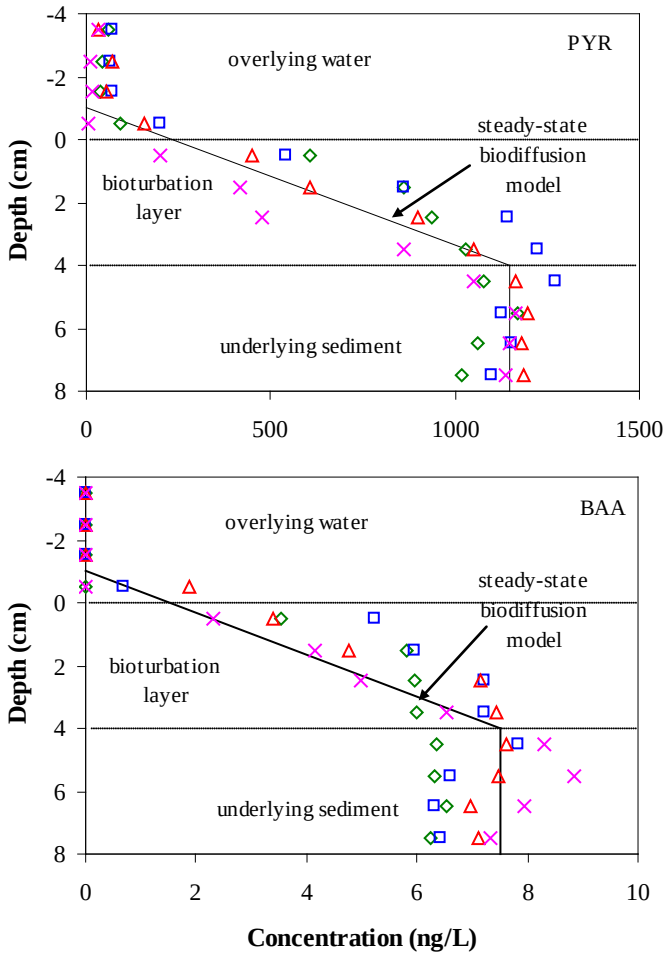

Figure 14. Laboratory microcosm PAH profiles for caps of 4 cm or less.[11]

Top: PYR, bottom: BAA. Because the bioturbation depth is less than the cap depth, contaminant migration is rapid and the concentration profiles can be described by a steady-state linear diffusion model between the underlying contaminated sediment and the clean overlying water.

Figure 15 shows the concentration profiles of PYR and BAA in the 6-cm cap microcosm. Unlike the cases for the thinner caps, the 6-cm sand layer was deeper than the nominal bioturbation depth of 4 cm, leaving a 2-cm isolation layer between the contaminated sediment and the organisms. Particle and pore water mixing in the

[11] Experimental data taken from Sarchet (2008)

biologically active layer enhanced the diffusion of contaminants, which created profiles that were linear in each individual layer but with different slopes because of the different diffusion rates.

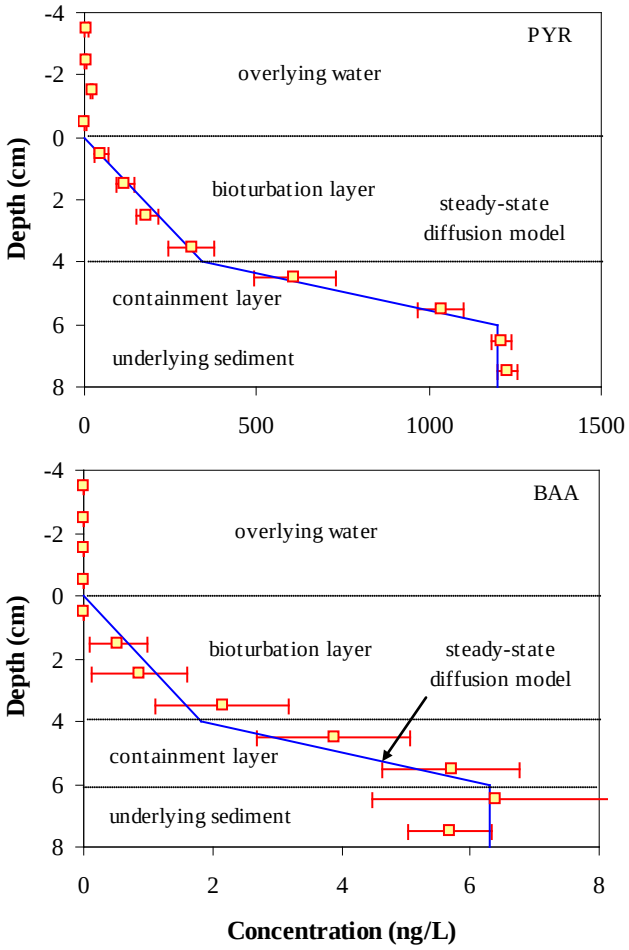

Figure 15. Laboratory microcosm PAH profiles for caps of 6 cm.[12]

Top: PYR, bottom: BAA. The top 4 cm of the cap is compromised by bioturbation, leaving the remaining 2 cm to isolate the organisms from the contamination. The two layer steady-state diffusion model of Lampert and Reible (2009) accurately predicts the concentration profiles based on a biodiffusion coefficient of 2E-5 cm^2/s.

[12] Experimental data taken from Sarchet (2008)

Lampert and Reible (2009) developed a two-layer steady state model capable of predicting concentrations and fluxes in the 2-cm isolation layer and the 4-cm bioturbation layer. To investigate the hypothesis of steady state conditions, the time to breakthrough of the 2-cm sand containment layer estimated using the method described in Chapter 3 (Equation 3.11). Retardation onto the sand was modeled assuming an effective fraction organic carbon of 0.0001 while the organic carbon partition coefficients were estimated from the correlations of Schwarzenbach et al. (2003). The molecular diffusion coefficients were estimated using the method described by Hayduk and Laudie (1974). The effective diffusion coefficient for each chemical in the 2-cm isolation layer was then estimated by correcting for porosity and tortuosity as described by Lampert and Reible (2009). The estimated times to breakthrough for this layer were 3.6 days for PYR and 9.8 days for BAA, which justified the assumption of steady state conditions after 28 days. The diffusion coefficient for the 4-cm bioturbation layer was fit to the data using the two-layer model. The results implied a value for D_{bio} of approximately five times the molecular diffusion coefficient in the sand layer. The predictions from the two-layer steady-state model are shown in Figure 15.

The results of the 10-cm thick sand cap microcosm are displayed in Figure 16. The 28-day period was sufficiently short that the contaminants were unable to diffuse through the containment part of the sand cap to the bioturbation zone. To interpret the results, a three-layer numerical model was developed using the approach described in Appendix B to predict the migration rates of the contaminants through the cap. The sediment, sand, and bioturbation layers were modeled explicitly. As no pressure gradient was present in the microcosms, the Darcy velocity was zero and thus transport through

the sand and sediment was assumed to be dominated by molecular diffusion. The diffusion coefficients and retardation factors estimated for the 6-cm microcosm were used to model the 10-cm microcosm. It should be noted that none of the parameters were fit; the predictions appear in Figure 16 and show a general agreement with the observed transport rates. Trace levels of contaminants were observed throughout the caps that did show some discrepancy between the model predictions and the experimental data; however, these data were small relative to the underlying sediment and may be associated with small amounts of intermixing of sediment layer and pore water during placement of the sediment and cap layers in the microcosm.

5.3.3 Microcosm Tissue Results

The worm tissues were analyzed for PAH levels and lipid content in each of the laboratory microcosms. The *n*-octanol-water partition coefficient K_{ow} has been suggested as a surrogate for the lipid-water partition coefficient in biological organisms (Chiou et al. 1977, Geyer et al. 1984, Mackay 1982, Isnard and Lambert 1988, Bintein et al. 1993). Using values for K_{ow} from MacKay (1992) and the average pore water concentration from the upper 5 cm of each cell (as this is where the worm exposure occurred), the concentration of PAHs in the tissues of the worms q_{lipid} was predicted for each of seven PAHs and compared to the lipid concentration predicted by the product of the pore water concentration C_w and K_{ow}. The results are shown in Figure 17.

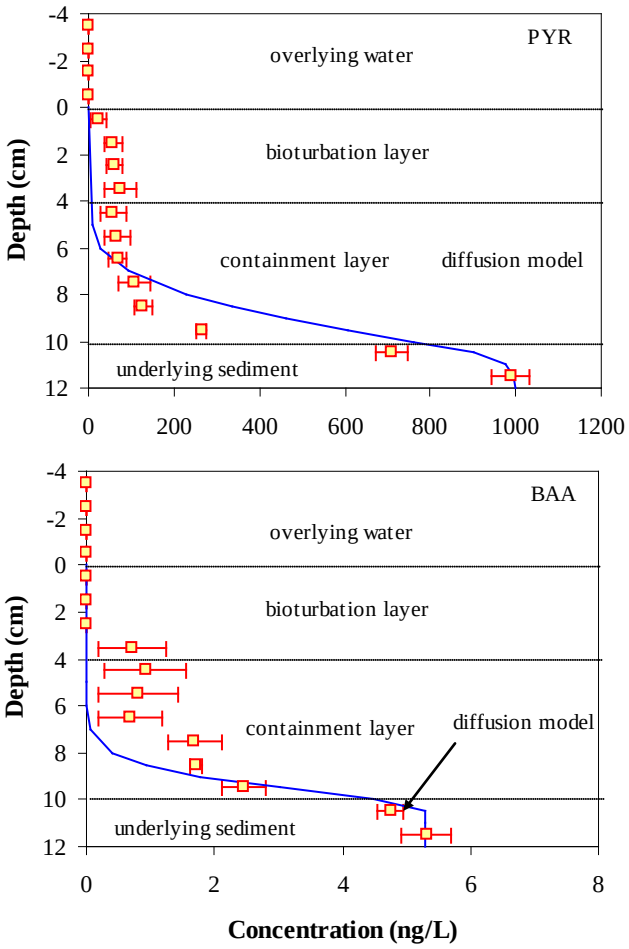

Figure 16. Laboratory microcosm PAH profiles for caps of 10 cm.[13]

Top: PYR, bottom: BAA. The 28-day period was sufficiently short to prevent significant migration of the contaminants from the underlying sediment to the biologically active zone. The model predictions agreed with the assumption of insufficient time to breakthrough of the sand for PYR, although for BAA migration was slightly under predicted.

[13] Experimental data taken from Sarchet (2008)

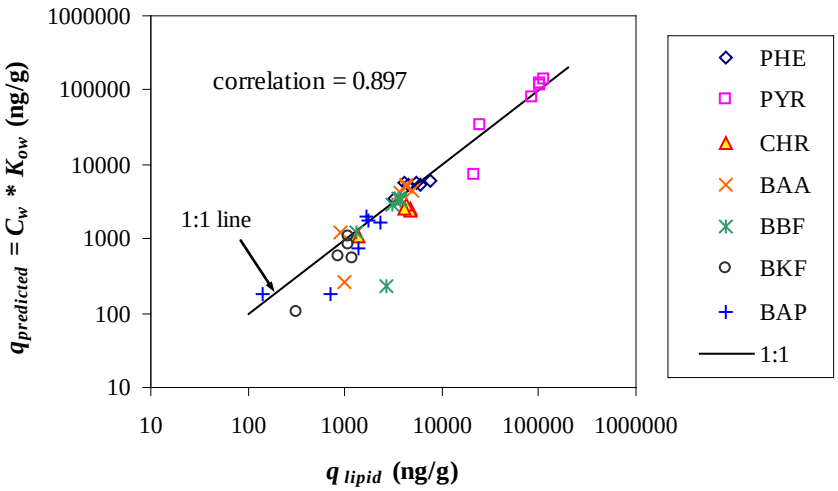

Figure 17. Laboratory microcosm predicted and measured tissue concentrations for *I. templetoni*.[14]

Tissue concentrations were predicted through the pore water bioaccumulation model. Bioaccumulation of the PAHs showed a strong correlation with the predictions based on the product of the pore water concentration and K_{ow} (correlation coefficient = 0.897).

Because of order-of-magnitude differences in absolute concentrations between various compounds, a logarithmic transform was applied to the data which were then used to compute the linear correlation coefficient. This method assumes the relative errors are the same for each sample, which is reasonable for as the relative standard deviation in the pore water concentrations were approximately the same for the various compounds. The correlation coefficient between measured and predicted bioaccumulation of the PAHs was 0.90, which indicates a strong positive trend.

To test the longer-term impacts of these results, worms from the 4-cm microcosm worm analyzed again after 56 days. The tissue concentrations after the 56-day period actually demonstrated lower PAH concentrations than were seen at 28 days (Table 2), which may have been the result of depletion of contaminant mass in the sediment or

metabolism of the compounds. The observed decrease in bioaccumulation over time lends credence to the concept of the steady state modeling approach for cap design. The decreases in organism tissue concentrations over time were consistent with other PAH bioaccumulation studies with oligochaetes (Lyytikainen 2007). These results provide a strong case for the applicability of the PDMS-fiber method for assessment of sediment quality and demonstrate the potential for even a relatively thin layer of sand to reduce ecological risks of PAHs.

Table 2: Comparison of 28 and 56-Day Tissue Concentrations in 4-cm Microcosm[15]

Compound	28-Day (ng/g) (Mean +/- Standard Deviation)	56-Day Concentration (ng/g) (Mean +/- Standard Deviation)
PHE	397 +/- 54	132 +/- 83
PYR	7491 +/- 1899	3877 +/- 1310
CHR	368 +/- 72	184 +/- 60
BAA	321 +/- 79	153 +/- 67
BBF	268 +/- 70	121 +/- 50
BKF	77 +/- 17	34 +/- 17
BAP	124 +/- 57	61 +/- 58

5.3.4 Microcosm Summary

The results of the thin layer sand cap microcosm experiments have several significant implications. First, the consistency of the PDMS pore water measurements demonstrates the ability of the method to assess concentration profiles in caps. It appears that this technique can be used to assess the effectiveness of capping as a sediment remediation technology. The consistency of the pore water profiles with theoretical model predictions validates the models to some extent as well as increases the confidence level that the observed profiles represent the real interstitial water concentrations of the

[14] Experimental data taken from Sarchet (2008)

contaminants. The decreased concentration levels in the bioturbation zones should translate into lower exposure doses and subsequently contaminant bioaccumulation. The results of these experiments also demonstrate the potential effectiveness of thin layer caps as a sediment remediation technology. The results imply that both contaminant transport and bioaccumulation can be assessed using PDMS-coated fibers. By using typical literature values for parameters and simple, well-established modeling approaches, the observed profiles were closely predicted. In addition, the sample replicates showed statistically significant differences across the various depths in the sediment environment.

5.3.5 Anacostia River Field Demonstration

The next step in the development of the PDMS passive sampling approach was application to a field site. The field apparatus described above was deployed for measurement of concentration profiles at the Anacostia River in Washington DC, the site of an extensive sediment capping demonstration described by Reible et al. (2006). As the concentration in the solid-phase is frequently used in sediment assessment (Doucette et al. 2003), sediment cores were taken from the site, analyzed, and compared to the PDMS field device.

5.3.6 Anacostia Coring Results

Figure 18 shows the solid-phase concentration profiles of each of the seven PAHs normalized by the concentration in the underlying sediment in a sand cap core. The percent native sediment in the sample as described in 5.2.6 is also plotted. The percent sediment in the sample provides a quantitative means of estimating the intermixing in the region at the interface of the sand cap and the underling contaminated sediment. Because

[15] Data taken from Sarchet (2008)

the normalized concentrations of all the contaminants fall essentially on top of the percent native sediment line, on the basis of solid-phase concentration there appears to be no significant contaminant migration. However, because of the differences in partitioning between the sand and underlying sediment, the concentrations may not be indicative of contaminant migration. The figure also shows the concentrations near the cap-water interface to be greater than zero. In a sediment capping environment where the contamination is completely capped and sources are cut off, it is expected that new sediment would be contaminant free. However, because the demonstration area caps only a small fraction of the total contaminated area, it is likely that the deposited sediments have similar levels to those underlying sediment. As a result, new sediment deposition levels were observed to be greater than zero.

5.3.7 Anacostia PDMS Profiler Results

The Anacostia demonstration has both a traditional sand cap and another sand cap with an underlying mat filled with coke breeze. The presence of the coke retards contaminant migration to the overlying water. This experiment was performed approximately 42 months after placement of the caps. The profilers were placed into both the sand and coke breeze caps and into the overlying water. The overlying water above the caps demonstrated concentrations of about half those in the sediment column, which helps to explain the relatively small gradients in the observed profiles. The presence of the contamination in the water column may be explained by several factors, including the presence of uncapped contaminated sediment in the vicinity of the demonstration and deposition of new contaminated sediment onto each of the caps.

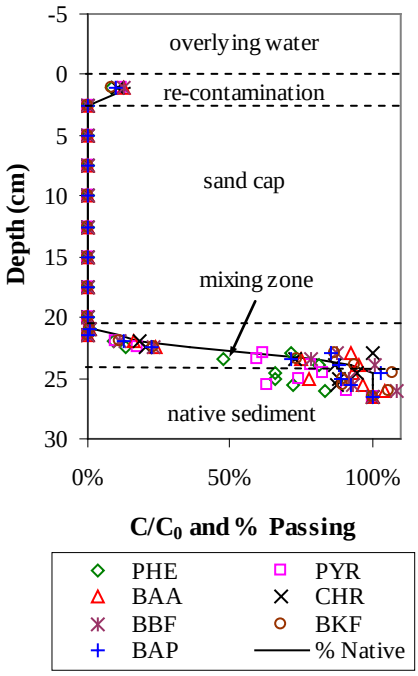

Figure 18. Sand cap dimensionless solid-phase PAH profiles and percent sediment. For each cross-section, the percentage native sediment mass out of the total mass was computed to quantify the effect of mixing (solid line). The concentration profiles for each PAH were normalized by the concentration in the underlying sediment (data points). The percent native sediment and the dimensionless profiles were essentially identical, which implies that no migration of the contaminants had occurred. The observed profiles represent the effect of intermixing and re-contamination of freshly deposited sediment.

Figure 19 shows the results of the PDMS pore water analysis in the sand and coke breeze caps during this deployment. The concentrations showed relatively modest profiles within the sand cap, likely as a result of attainment of a steady state condition. Unlike the laboratory-scale experiments, the newly-deposited sediment and overlying water in the Anacostia were not contaminant-free and thus the steady state condition in the caps is nearly identical to the pre-cap condition. The Anacostia pore water has previously been shown to flow both into and out of the capping materials (described in detail in Chapter 4). As a result of the rapid mixing, steady state conditions were

expected to be attained relatively rapidly. The profiles show high concentrations at depth, lower concentrations in the middle of the cap, and then high concentrations near the overlying water. These observations are consistent with the concept of mixing due to tidal effects from both an underlying and overlying contaminated layer.

The coke breeze cap, however, with its greater sorption capacity, did exhibit a slight linear pore water concentration gradient. The concentrations in the underlying sediment were higher than those in the overlying cap material as evidenced by the error bars (here representing the sample standard deviation). Because the thickness of the sand layer above the coke breeze mat was only six inches for this cap, the decreases in concentration observed in the sand cap were not observed.

In general, variability among the replicates was fairly small as characterized by the relative standard deviation (mean divided by sample standard deviation) in the cap material (below a depth of 30 cm). These values are displayed in Table 3 and were typically about 0.25. The higher degree of variability in the PDMS measurements in the underlying sediment is likely due to natural variability in the sediment environment.

While the concentration profiles did not show large decreases from the underlying sediment in the capped areas, the relative concentrations in the sand capped area were lower than values measured from the uncapped sediment. Table 4 shows the average concentrations and for each of the compounds that were above detection limits. The lighter compounds were nearly identical in the capped and uncapped areas, perhaps due to their high mobility. The concentrations of the heavier PAHs, however, were generally 50% lower in the sand caps than in the uncapped area. It appears that the new contamination had migrated about six inches into each of the caps. Despite the re-

contamination, the caps seem to provide a slight decrease in observed concentrations relative to the uncapped areas.

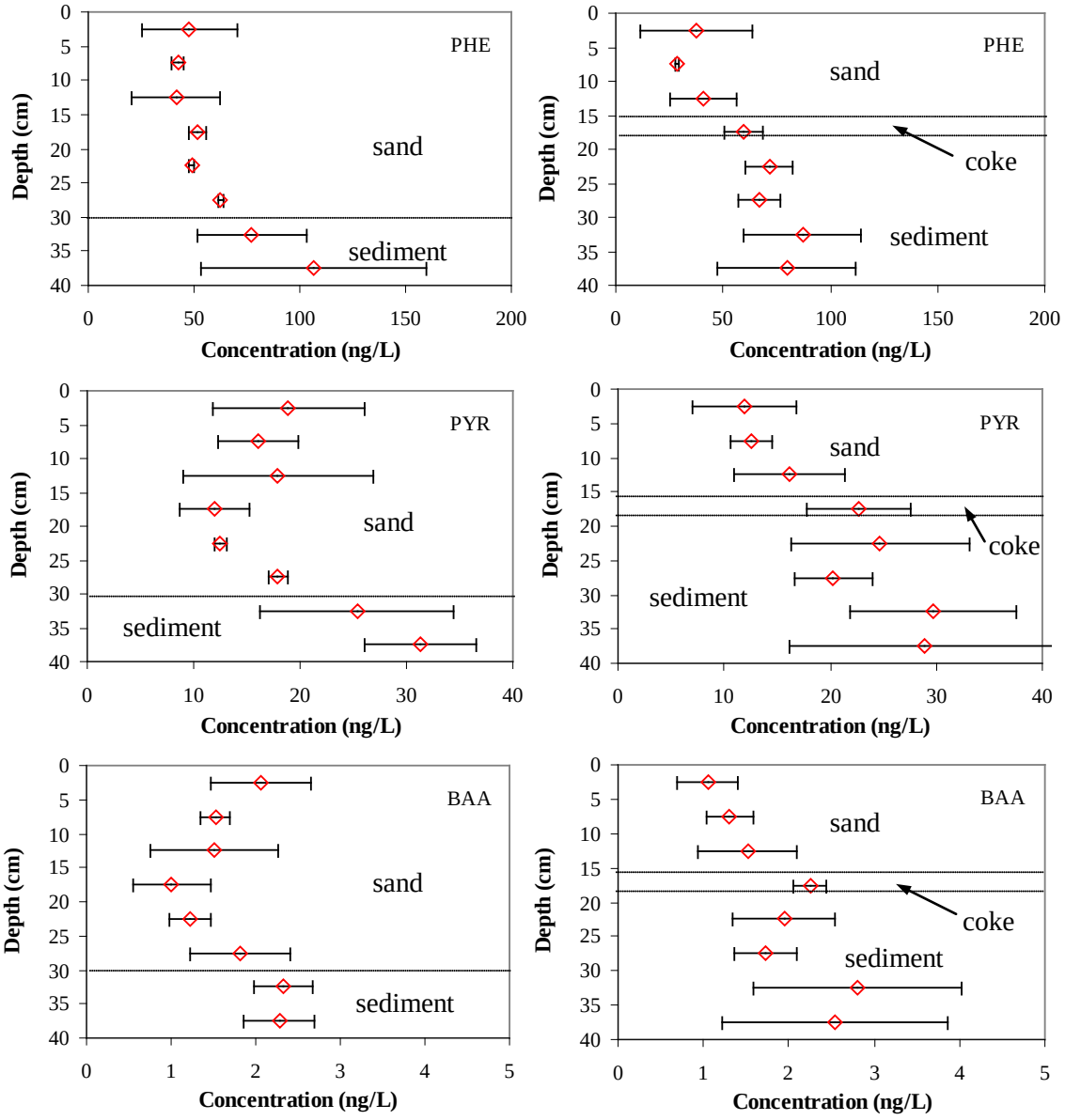

Figure 19. PAH pore water profiles in sand cap (left) and coke breeze cap (right).

The sand cap appeared to have achieved a steady state condition in 42 months, while a small gradient and slightly diminished concentrations were observed in the coke breeze. No trends were observed with hydrophobicity.

Table 3: Coefficients of Variation for Replicates in Coke Breeze Cap

Depth (cm)	PHE	PYR	BAA
2.5	0.22	0.24	0.29
7.5	0.02	0.16	0.21
12.5	0.38	0.32	0.38
17.5	0.15	0.22	0.09
22.5	0.16	0.34	0.31
27.5	0.15	0.18	0.21
Mean in cap	**0.18**	**0.24**	**0.25**
32.5*	0.31	0.26	0.43
37.5*	0.40	0.44	0.52

*Underyling sediment layer with greater variability

Table 4: Average Pore Water Concentrations at Anacostia Site

Compound	Uncapped	Sand	Percent Reduction
Naphthalene	2181	2046	94%
Fluorene	2645	2527	96%
Acenaphthene	889	506	57%
Phenanthrene	1471	738	50%
Anthracene	152	139	91%
Fluoranthene	464	211	45%
Pyrene	383	161	42%
Chrysene	41.7	22.6	54%
Benz[a]anthracene	29.0	15.2	52%
Benzo[b]fluoranthene	13.9	6.3	45%
Benzo[k]fluoranthene	4.0	1.8	44%
Benzo[a]pyrene	4.8	2.3	49%
Benzo[ghi]perylene	1.2	0.7	64%
Total	**8280**	**6376**	**77%**

5.3.8 Consistency of the coring and pore water concentrations

The results of the coring experiments apparently indicated no migration of contaminants through the sand cap. The PDMS profiler, however, showed a different result as significant concentrations appeared to have penetrated both the sand and coke breeze caps after 42 months. While these results seem contradictory, they can be explained on the difference in partitioning between the sand and the sediment. Using the

pore water concentrations measured by the PDMS profiler and a partition coefficient based on the percent sediment in each sample, the expected solid-phase concentrations at equilibrium were predicted in the sand cap. The results are shown in Figure 20 and show good consistency with the measured solid-phase concentration profiles. Because of the relatively small partitioning of the contaminants onto sand, the concentrations were below detection limits in this layer. By looking solely at concentrations in the solid-phase, it is impossible to determine whether contaminants have transported through the sediment caps. This is a significant result as it shows that solid-phase concentrations are inappropriate for assessing contaminant migration in caps.

5.3.9 Field Demonstration Summary

The results of the field demonstration were encouraging. On the basis of solid-phase concentration, it appeared that no significant migration had taken place in the caps. However, using the pore water profiling method, significant concentrations were measured throughout the cap due to migration from the contaminated sediment below and the re-contaminated layer above in both the sand and coke breeze caps. The differences can be explained by differences in equilibrium partitioning between the various phases. The PDMS profiler was found to be capable of measuring pore water concentrations in the field. It appears that the Anacostia caps have approached near-equilibrium levels in 42 months as a result of re-contamination and tidal pumping forces. While the caps may have reached steady state, the observed concentrations in the sand cap were lower than those in the uncapped areas. Thus it does appear that the caps have served to remediate the area to some extent.

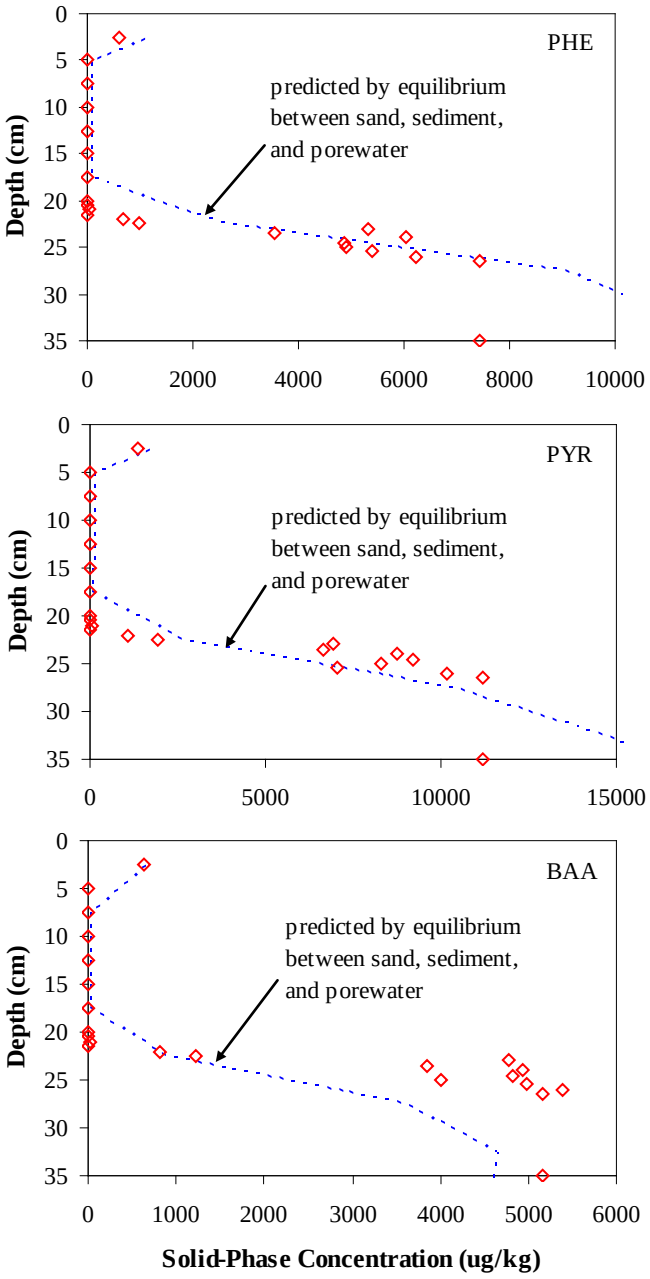

Figure 20. Consistency of pore water and solid phase concentrations.

The solid-phase concentrations indicated no migration while the pore water concentrations showed penetration through the cap. However, this apparent inconsistency can be explained by different partitioning in the sand and sediment. The solid-phase concentrations can be accurately predicted by using the appropriate partition coefficient and the pore water concentrations.

5.4 Conclusions

In this study, results have been presented that demonstrate the ability of a PDMS fiber approach to assess the impairment of sediments and the effectiveness of capping as a remediation technology. The PDMS sampling device is capable of measuring concentrations profiles in a sediment environment that agree well with model predictions. These results imply that observed concentration profiles are real and not the results of experiment artifacts. They also lend credibility to the theoretical model predictions that are frequently used in cap assessment and design. A field-deployable PDMS device was shown to measure concentration profiles in a capping system. In the future this method can be used to assess contaminant migration in cap monitoring.

There are several outstanding research needs for the PDMS profiler. The kinetics of uptake in fibers from sediments are not well understood. A thorough characterization of the diffusive uptake of contaminants by fibers of different geometries would provide insight into the time necessary to achieve steady state conditions for a variety of compounds. Future application of PDMS profiling to field studies can provide valuable insight into the efficacy of capping, particularly with layers of active materials. Finally, the ability of PDMS-coated fibers to predict bioaccumulation of other HOCs (in addition to PAHs) in field studies should be demonstrated.

5.5 Acknowledgements

The authors wish to thank the Environmental Security Technology Certification Program and the District of Columbia Appropriations Committee for funding this research. In addition, the authors wish to thank the United States Army Corps Engineer Research Development Center for tissue and sediment analysis.

5.6 References

1. Accardi-Dey, A. and Gschwend, P.M. 2002. "Assessing the combined roles of natural organic matter and black carbon as sorbents in sediments," Environmental Science & Technology, 36:21-29.
2. Bintein S, Devillers J, and Karcher W. 1993. "Nonlinear dependence of fish bioconcentration on n-octanol/water partition coefficient," SAR QSAR Environmental Research, 1:29–39.
3. Booij, K., Shiu, W.Y., Mackay, D. 1998. "Calibrating the uptake kinetics of semipermeable membrane devices using exposure standards," Environmental Toxicology and Chemistry. 17:1236–1345.
4. Boudreau, B. 1997. Diagenetic Models and Their Implementation: Modeling Transport Reactions in Aquatic Sediments. Springer-Verlag, New York.
5. Burton, G.A. 1991. "Assessing the toxicity of freshwater sediments," Environmental Toxicology and Chemistry, 10:1585-1627.
6. Burton, G.A., Greenberg, M.S., Rowland, C.D., Irvine, C.A., Lavoie, D.R., Brooker, J.A., Moore, L., Raymer, D.F.N., McWilliam, R.A. 2005. "In situ exposures using caged organisms: a multi-compartment approach to detect aquatic toxicity and bioaccumulation," Environmental Pollution, 134:133-144.
7. Carslaw, H.S. and Jaeger, J.C. 1959. Conduction of Heat in Solids.
8. Chiou, C.T., Freed, V.H., Schmedding, D.W., and Kohnert, R.L. 1977. "Partition Coefficient and Bioaccumulation of Selected Organic Chemicals," Environmental Science & Technology, 11(5):475-478.

9. Doucette, W.J., 2003. "Quantitative structure-activity relationships for predicting soil-sediment sorption coefficients for organic chemicals," Environmental Toxicology and Chemistry, 22:1771–1788.
10. Fredrickson, H.L., Furey, J., Talley, J.W., and Richmond, M. 2004. "Bioavailability of hydrophobic organic contaminants and quality of organic carbon," Environmental Chemistry Letters, 2:77-81.
11. Futoma, D.J, Smith, S.R., Smith, T.E., and Tanaka, J. 1981. Polycyclic Aromatic Hydrocarbons in Water Systems. CRC Press, Boca Raton, FL, USA.
12. Geyer, H., Politzki, G., and Freitag, D. 1984. "Prediction of Ecotoxicological Behaviour of Chemicals: Relationship between n-Octanol/Water Partition Coefficient and Bioaccumulation of Organic Chemicals by Alga," Chemosphere, 13(2):269-284.
13. Ghosh, U., Gillette, J.S., Luthy, R.G., and Zare, R.N. 2000. "Microscale location, characterization, and association of polycyclic aromatic hydrocarbons on harbor sediment particles," Environmental Science & Technology, 34:1729–1736
14. Harris D., Horwath, W., and van Kessel, C. 2001. "Acid fumigation of soils to remove carbonates prior to total organic carbon or CARBON-13 isotopic analysis," Soil Science Society of America Journal, 65:1853–1856.
15. Hayduk, W. and Laudie, H. 1974. "Predicting diffusion coefficients for nonelectrolytes in dilute aqueous solutions," AICheE Journal, 20:611.
16. Hedges, J.L., and Stern, J.H. 1984. "Carbon and nitrogen determination of carbonate-containing solids," Limnology and Oceanography, 29:657–663.
17. Isnard P, and Lambert S. 1988. "Estimating bioconcentration factors from octanol–water coefficient and aqueous solubility," Chemosphere, 17:21–34.

18. Jonker, M.T.O., Koelmans, A.A., 2001. “Polymethylene solid-phase extraction as a partitioning method for hydrophobic organic chemicals in sediment and soot,” Environmental Science & Technology, 35:3742–3749.
19. Kraaij R., Mayer P., Busser F.J.M., Bolscher M.V.H., Seinen W., Tolls J. 2003. “Measured pore-water concentrations make equilibrium partitioning work-a data analysis,” Environmental Science & Technology, 37:268-274.
20. Kan, A.T., Fu, G., Hunter, M.A., Tomson, M.B. 1997. “Irreversible sorption of naphthalene and tetrachlorobiphenyl to Lula and surrogate sediments,” Environmental Science & Technology, 31:2176-2185.
21. Lampert, D.J. and Reible, D.D. 2009. “An Analytical Modeling Approach for Evaluation of Capping of Contaminated Sediments,” Soil and Sediment Contamination: an International Journal, 18(4):470-488.
22. Lu, X., Reible, D.D., and Fleeger, J.W. 2006. “Bioavailability of polycyclic aromatic hydrocarbons in field-contaminated Anacostia River (Washington, DC) sediment,” Environmental Toxicology and Chemistry, 25:2869-2874.
23. Lyttikainen M., Pehkonen,, S., Akkanen, J., Leppanen, M., and Kukkonen, J. 2007. “Bioaccumulation and Biotransformation of Polycyclic Aromatic Hydrocarbons During Sediment Tests with Oligochaetes (*Lumbriculus variegatus*).” Environmental Toxicology and Chemistry, 26: 2660-2666.
24. Mayer, P., Vaes, W.H.J., Wijnker, F., Legierse, K.C.H.M., Kraaij, H., Tolls, J., Hermens, J.L.M., 2000a. “Sensing dissolved sediment porewater concentrations of persistent and bioaccumulative pollutants using disposable solid-phase microextraction fibers,” Environmental Science & Technology, 34:5177–5183.

25. Mayer, P., Vaes, W. H. J., and Hermens, J. L. M. 2000b. "Sensing dissolved sediment porewater concentrations of persistent and bioaccumulative pollutants using disposable solid-phase microextraction fibers," Analytical Chemistry, 72:459-464.
26. MacKay, D. 1982. "Correlation of bioconcentration factors," Environmental Science & Technology, 16:274–278.
27. MacKay, D.; Shiu, W. Y.; Ma, K. C. 1992. Illustrated Handbook of Physical-Chemical Properties and Environmental Fate for Organic Chemicals, Volume 3. Lewis Publishers: Chelsea, MI.
28. McDonough, K., Murphy, P., Olsta, J. Zhu, Y., Reible, D., Lowry, G. 2007. "Development of a Sorbent-Amended Thin Layer Sediment Cap in the Anacostia River," Soil & Sediment Contamination, 16(3):313-322.
29. McGroddy, S.E. and Farrington, J.W. 1995. "Sediment porewater partitioning of polycyclic aromatic hydrocarbons in three cores from Boston Harbor, Massachusetts," Environmental Science & Technology, 29:1542-1550.
30. Meloche, L.M, deBruyn, A.M.H., Otton, S.V., Ikonomou, M.G., and Gobas, F.A.P.C. 2009. "Assessing exposure of sediment biota to organic contaminants by thin-film solid phase microextraction," Environmental Toxicology and Chemistry, 28:247–253.
31. Murphy, P., Marquette, A., Reible, D., and Lowry G.V. 2006. "Predicting the Performance of Activated Carbon-, Coke-, and Soil-Amended Thin Layer Sediment Caps," Journal of Environmental Engineering, 132(7):787-794.
32. Palermo, M.R. 1998. "Design considerations for in-situ capping of contaminated sediments," Water Science and Technology, 37:315-321.

33. Reible, D.D., Lampert, D.J., Constant, D., Mutch, R., Zhu, Y. 2006. "Active capping demonstration in the Anacostia River in Washington DC," Remediation Journal, 17:39-53.

34. Sarchet, W.V. 2008. Effects of a Thin Layer Cap on Bioavailability and Bioaccumulation in Sediments. Master's Thesis, The University of Texas at Austin.

35. Schaffner, L.C., Dickhut, R.M., Mitra, S., Lay, P.W., and Brouwer-Riel, C. 1997. "Effects of Physical Chemistry and Bioturbation by Estuarine Macrofauna on the Transport of Hydrophobic Organic Contaminants in the Benthos," Environmental Science and Technology, 31:3120-3125.

36. Schwarzenbach, R.P., Gshwend, P.M., and Imboden, D.M. 2003. Environmental Organic Chemistry, 2nd Edition, Wiley & Sons, Hoboken, New Jersey.

37. Thibodeaux, L.J. and Bosworth, W.S. 1990. "A Theoretical Evaluation of the Effectiveness of Capping PCB Contaminated New Bedford Harbor Bed Sediment, Final Report," Hazardous Waste Research Center, Louisiana State University, Baton Rouge, LA.

38. Thoma, G.J., Reible, D.D., Valsaraj, K.T., and Thibodeaux, L.J. 1993. "Efficiency of Capping Contaminated Bed Sediments In Situ. 2. Mathematics of Diffusion-Adsorption in the Capping Layer," Environmental Science & Technology, 27:2412-2419.

39. Thoms, S.R., Matisoff, G., McCall, P.L., and Wang, X. 1995. Models for Alteration of Sediments by Benthic Organisms, Project 92-NPS-2, Water Environment Research Foundation, Alexandria Virginia.

40. US EPA. 1998. Contaminated Sediment Management Strategy (EPA 823-R-98-004). Accessed via website http://www.epa.gov/OST/cs/ stratefs.html.
41. Vinturella, A.E. Burgess, R.M., Coull, B.A., Thompson, K.M., and Shine, J.P. 2004. "Use of passive samplers to mimic uptake of polycyclic aromatic hydrocarbons by benthic polychaetes," Environmental Science & Technology, 38:1154-1160.
42. Wang, X.Q., Thibodeaux, L.J., Valsaraj, J.T., and Reible, D.D. 1981. "Efficiency of Capping Contaminated Bed Sediments In Situ. 1. Laboratory-Scale Experiments on Diffusion-Adsorption in the Capping Layer," Environmental Science & Technology, 18:395-403.
43. Zeman, A.J. and Patterson, T.S. 1997. "Preliminary Results of Demonstration Capping Project in Hamilton Harbour," Water Quality Research Journal of Canada, 32(2):439-452.

Chapter 6: An Assessment of the Significance of Internal and External Transport Processes for Predicting Contaminant Uptake Rates in Passive Samplers[16]

David J. Lampert[17] and Danny D. Reible[18]

6.0 Abstract

A critical element in the development of passive sampling devices such as polydimethylsiloxane-coated fibers, polyethylene strips, and polyoxymethylene pellets for estimating contaminant *in situ* pore water concentrations in sediments is to predict the rate of uptake within the device. Herein, by using literature values for passive sampling materials and existing diffusion models it is demonstrated that external mass transport processes control uptake in many passive samplers. As such uptake rates are closely related to the surface area to volume ratio of the sampling device. By calculating a single dimensionless parameter σ for a given sampler it is possible to assess the relative importance of internal to external mass transport. Exact solutions to the model problems with negligible internal transport are derived for both rectangular Cartesian coordinates (for sampler sheets) and cylindrical coordinates (for fibers). An initial comparison with field data suggests that contaminant uptake rates can be predicted using the model and that the release of contaminants from particles may be important for assessing transport.

---

[16] Manuscript in preparation for submission

[17] PhD Candidate, Department of Civil, Architectural, Environmental Engineering, The University of Texas at Austin, 1 University Station C1786, Austin, TX 78712-0273, djl@mail.utexas.edu

[18] Bettie Margaret Smith Professor of Environmental Health Engineering, Department of Civil, Architectural, Environmental Engineering, The University of Texas at Austin, 1 University Station C1786, Austin, TX 78712-0273, reible@mail.utexas.edu

6.1 Introduction

Sediments serve as the ultimate sink for many hydrophobic organic compounds (HOCs) such as polycyclic aromatic hydrocarbons (PAHs) and polychlorinated biphenyls (PCBs). As a result, the presence of HOCs in sediments often presents a residual environmental risk as a route of entry for contaminants into the food chain many years after sources of contamination are cut off. Because of poor understanding of the ecological risks associated with contaminated sediments and the ubiquitous nature of the problem, assessment and remediation of contaminated sediments presents a major research challenge for the environmental community (US EPA, 1998).

6.1.1 The Relationship between Solid-Phase and Pore Water Concentrations

The particle or bulk solid-phase concentration of sediment contaminants is often used to assess sediment quality because it is relatively easy to measure (Doucette 2003). However, solid-phase concentrations have been found to be a poor metric for assessing bioavailability (Burton 1991). *In situ* pore water concentrations are thought to be linked to bioaccumulation of HOCs in sediments (Kraaij et al. 2003, Lu et al. 2006, Meloche et al. 2009). However, direct measurement of HOC concentrations in the aqueous phase is often difficult due to analytical limitations.

Critical to understanding pore water concentrations in sediments is the relationship between the bulk solid phase concentration and the neighboring pore water concentration. This relationship has traditionally been modeled using the approach of linear sorption onto the organic carbon fraction presented by Karickhoff et al. (1979):

$$q = f_{oc} K_{oc} C \tag{6.1}$$

Where:

q = solid phase concentration (M M^{-1})

C = pore water concentration (M L^{-3})

f_{oc} = fraction organic carbon (M M^{-1})

K_{oc} = organic carbon partition coefficient (L^{-3} M)

The value of K_{oc} is is often estimated for a particular class of compounds using the octanol-water partition coefficient K_{ow} (Karickhoff 1981, Baker et al. 1997). In a recent literature survey, Arp et al. (2009) found a trend of under prediction in the values of K_{oc} using these literature correlations compared to calculated field measurements based on q, C, and f_{oc}. The reported field values were found to vary by as much as a factor of 30 from site to site. The authors concluded that due to the heterogeneity of the organic carbon phases, prediction of pore water concentrations from sediment phase concentrations is an inappropriate means for assessing sediment quality.

6.1.2 Passive Sampling for Estimating Pore Water Concentrations

As direct measurement of pore water concentrations is often difficult or impossible, passive sampling methods are a current research focus (Mayer et al. 2000, Jonker and Koelmans 2001, Namiesnik et al. 2005, Adams et al. 2007). Such methods have been shown to correlate well with bioaccumulation in the field (You et al. 2006, Jonker et al. 2007, Trimble et al. 2008, Van der Heijden and Jonker 2009). Various passive sampling approaches have been tested for estimation of *in situ* HOC pore water concentrations, including semi-permeable membrane devices (SPMDs, Booij et al. 1998), polyoxymethylene (POM) sheets (Jonker and Koelmens 2001), polyethylene (PE) sheets (Vinturella et al. 2004), and polydimethylsiloxane (PDMS)-coated glass fibers (Mayer et

al. 2000). For each of these methods, the sampler is placed *in situ* followed by a contaminant uptake period within the device. The pore water concentration is then back-calculated from a pre-established partitioning relationship.

The PDMS-coated fibers can be manufactured to very small sizes (e.g., 110 µm glass diameter with 30-µm PDMS coating, Mayer et al. 2000). Because of this relatively small size, the method should not significantly deplete the contaminant mass in the neighboring sediment particles, and hence should not affect the equilibrium chemistry. In addition, equilibrium is thought to be attained relatively rapidly (Mayer et al. 2000).

6.1.3 Passive Sampler Kinetics

Studies on passive samplers in sediments, however, have revealed that equilibrium can take a significant amount of time to achieve. Huckins et al. (2006) present an approach for modeling uptake in SPMDs. Resistance to mass transport was assumed to be dominated by the SPMD and that the neighboring sediment pore water concentration remained constant. The authors presented an "overall conductivity" approach based on mass transfer coefficients and a simple first order kinetic model for transport within the SPMD device to model contaminant uptake. This method provided an initial means of assessing transport but suffered many limitations from the numerous simplifying assumptions used in its development. To follow on to this approach, Huckins et al. (2002) described the use of impregnated performance reference compounds during field deployments to estimate the extent of equilibrium attained within the device. The SPMD device is initially equilibrated with an innocuous species that is not native to the site. The mass of the performance reference compound is then measured after the deployment in an effort to determine the extent of equilibrium.

To speed equilibrium in passive sampling devices, the thickness of the materials has become much less than that originally used in the development of the SPMD method. As such, the equilibrium time for transport within passive sampling devices has dropped rapidly to the point that it may be negligible relative to the transport time of the contaminants from the neighboring sediment environment. Despite the rapid decrease in transport times within these devices, modeling has generally focused on diffusion within the sampler with little focus on transport from the neighboring sediment to the sampler. A characteristic time scale for internal diffusion within a passive sampling sheet with a characteristic length of L and diffusivity of D can be determined by:

$$t_{internal} \approx \frac{L^2}{D} \tag{6.2}$$

The characteristic length must account for diffusion from both sides of the sampler and in the case of a sheet is thus half the thickness; for a cylindrical fiber, L is the magnitude of the PDMS coating thickness. For observed equilibration periods significantly longer than $t_{internal}$, transport in the sediment matrix controls the overall uptake in the POM sampler.

Ahn et al. (2005) measured diffusivities for polycyclic aromatic hydrocarbons (PAHs) in POM sheets. Hong and Luthy (2008) extended this work and found that for PAHs with log K_{ow} less than 5.8 L/kg, mass transport was controlled by the aqueous phase. These authors reported that POM diffusivities scale with molecular weight to the negative third power.

Fernandez et al. (2009) developed the first diffusion-based model to predict mass transport in PE sheets that explicitly modeled external transport to the device. Mass

transport was assumed to be dominated by molecular diffusion through the passive sampling device and the neighboring pore water. While this model does account for diffusion in the sediment matrix, it assumes instantaneous equilibrium between the sediment particles and pore water and thus fails to account for transport resistance to and from the sediment particles, which may be quite significant (Weber and Miller 1988, Ball and Roberts 1991, Pignatello and Xing 1996, Werth and Reinhardt 1997, Weber et al. 2001). Jonker et al. (2007) observed uptake rates in PDMS fibers in soils and various classes and found the kinetics to be substantially different, which they attributed to release rates from the particles. Ignoring slow release from these phases within the sediment matrix may result in inappropriate equilibrium corrections.

Rusina et al. (2007) measured the diffusion and partition coefficients of different passive sampling materials for several PAHs in PDMS. Figure 21 shows the characteristic diffusion times versus log K_{ow} for a variety of PAHs calculated from Equation (6.1) for a 20, 50 and 500-µm POM, PE, and PDMS sheets using values for POM reported by Hong and Luthy (2008) for POM, correlations for PE from Fernandez et al. (2009), and PDMS values from Rusina et al. (2007). As these studies have found that equilibration times for passive samplers are weeks to months, it appears that when characteristic internal diffusion times are less than a day, internal diffusion becomes negligible compared to contaminant transport from the sediment environment to the device. The results in Figure 21 show that for PDMS, internal diffusion is negligible even for a characteristic length of 250 µm. For PE and POM, internal diffusion appears to be negligible when the sampler thickness is less than about 50 µm; however, for thicker POM and PE (e.g., 500 µm) it may be important depending on the corresponding

external transport rates. As many compounds of concern fall into the range of hydrophobicity in Figure 21, a model that accounts for transport within the sediment bed seems necessary for estimate equilibrium time.

Cornelissen et al. (2008) studied equilibrium time in POM and PDMS fibers in the field. The authors reported that equilibrium in a 55-µm POM sheet was reached in between 23 and 60 days for 5 and 6-ring PAHs (log K_{ow} < 7). However, the characteristic diffusion time for such compounds would imply equilibrium in under a day; thus it would appear that external diffusive forces dominate the overall transport resistance. In the same study, the authors concluded that equilibrium had not been established in a 500-µm thick (characteristic length of 250 µm) POM sheet or a 100-µm (characteristic length of 50 µm) PE sheet for 5 and 6-ring PAHs even after 119 days; they attributed the slow kinetics to external mass transport resistances. These experimental results coupled to the example characteristic diffusion times in Figure 21 imply that more effort should be made to incorporate external mass transfer resistances into passive sampler uptake kinetics modeling.

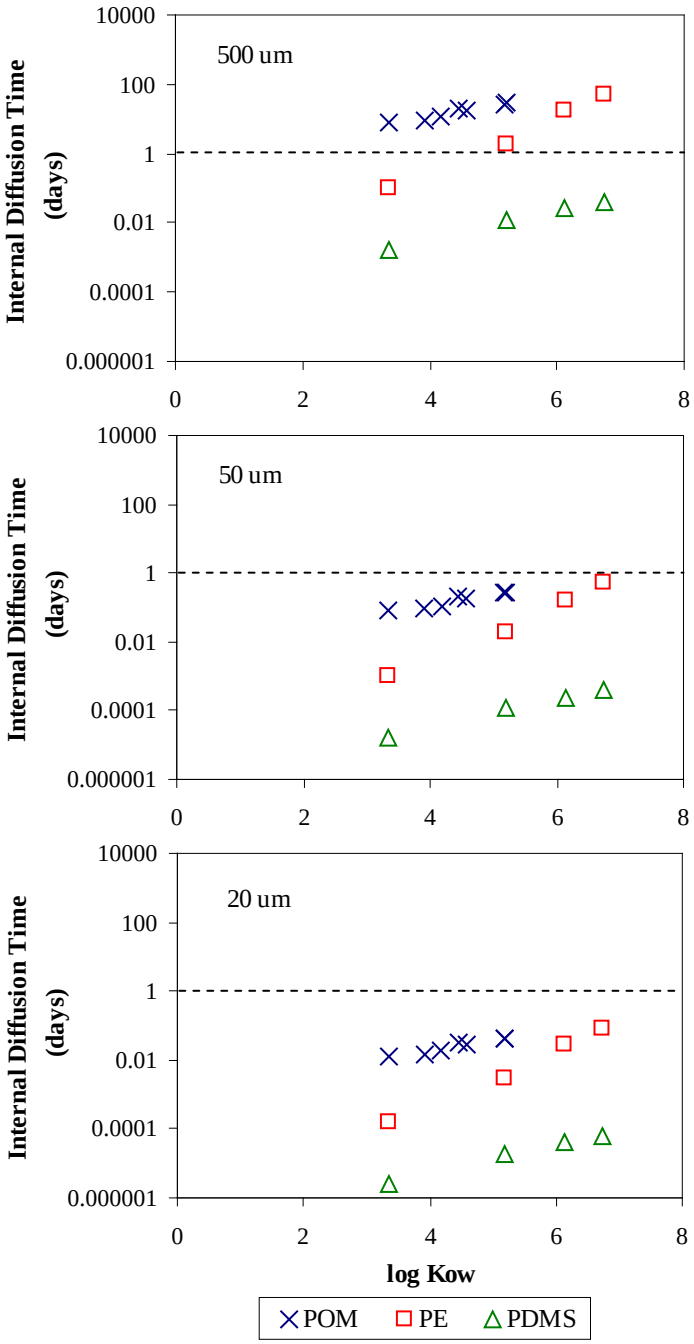

Figure 21. Characteristic diffusion times for (a) 500-µm, (b) 50-µm, and (c) 20-µm thick for POM, PE, and PDMS.

Diffusivities based for POM, PE, and PDMS from Hong and Luthy (2008), Fernandez et al. (2009), and Rusina et al. (2007), respectively. Diffusion times less than a day are proposed to be relatively negligible in controlling overall transport rates to passive sampling devices.

6.1.4 Research Objectives

Herein, the model of Fernandez et al. (2009) is used to infer the relative significance of internal and external mass transport on passive sampler uptake. In many instances, external transport controls overall kinetics. A modeling approach is developed for estimating contaminant uptake in passive sampling devices that incorporates sorption onto both LC and HC, and considers external fiber transport resistances including slow contaminant release from sediment particles. Semi-analytical and exact solutions are then developed for both a radial coordinate geometry consistent with the design of PDMS fibers and also to a rectangular Cartesian coordinate system applicable for POM and PE sheets. A discussion is made of the various parameters, which with the exception of the sediment release rate are relatively well-characterized. The model behavior and consistency with field measurements is then presented.

6.2 Polyethylene Diffusion Model in Rectangular Cartesian Coordinates (from Fernandez et al. 2009)

6.2.1 Model Description

The model presented by Fernandez et al. (2009) explicitly accounts for diffusion within the passive sampling device of thickness 2*L*, but ignores transport resistances from within the sediment particles. The governing equations, auxiliary conditions, and a brief summary of the solution technique are presented here for comparison with the other models derived herein. For the passive sampler with concentration C_{PE} and at point x and time t with diffusivity D_{PE}, the transport equation is:

$$\frac{\partial C_{PE}(x,t)}{\partial t} = D_{PE}\frac{\partial^2 C_{PE}(x,t)}{\partial x^2} \tag{6.3}$$

For the sediment, instantaneous equilibrium is assumed between the pore water and particles. The transport equation for the pore water concentration C at point x and time t is:

$$(\varepsilon + \rho f_{oc} K_{oc}) \frac{\partial C(x,t)}{\partial t} = D \frac{\partial^2 C(x,t)}{\partial x^2} \tag{6.4}$$

Where:

ε = porosity ($L^3\ L^{-3}$)

ρ = particle bulk density ($M\ L^{-3}$)

D = effective diffusion coefficient ($L^2\ T^{-1}$)

The value of D represents the molecular diffusivity D_w after a correction for tortuosity and porosity such as described by Boudreau (1997):

$$D = \frac{\varepsilon D_w}{1 - \ln \varepsilon^2} \tag{6.5}$$

At the interface between the sampling device and the sediment (x=L), equilibrium between the pore water and PE governed by the partition coefficient K_{PEW} and continuity of flux is assumed. There is no flux across the center of the PE due to symmetry. The PE is assumed to be initially clean, and the sediment initially uniformly saturated at concentration C_0. The following boundary and initial conditions reflect these assumptions:

$$D_{PE} \frac{\partial C_{PE}(x = L,t)}{\partial x} = D \frac{\partial C(x = L,t)}{\partial x} \tag{6.6}$$

$$C_{PE}(x = L,t) = K_{PEW} C(x = L,t) \tag{6.7}$$

$$\frac{\partial C_{PE}(x=0,t)}{\partial x} = 0 \tag{6.8}$$

$$C_{PE}(x,t=0) = 0 \tag{6.9}$$

$$C(x,t=0) = C_0 \tag{6.10}$$

The authors non-dimensionalized the governing equations and then solved them by numerical inversion of the Laplace transform. Using this method, the mass M in the PE at dimensionless time $\frac{D_{PE}t}{L^2}$ can be determined from numerically inverting the dimensionless auxiliary equation:

$$\overline{M}(s) = \frac{1}{s^{3/2}\left(\sigma + \coth\sqrt{s}\right)} 2LK_{PEW}C_0 \tag{6.11}$$

Where s is the auxiliary dimensionless time variable and the parameter σ is defined as:

$$\sigma = \sqrt{\frac{D_{PE}}{D(\varepsilon + f_{oc}K_{oc})}} K_{PEW} \tag{6.12}$$

Thus, the percent of equilibrium as a function of the dimensionless time has only one parameter, σ.

6.2.2 Model Behavior

To illustrate the behavior of the model, a series of simulations were performed. Uptake in PE was simulated for two PAHs, pyrene (PYR) and beno[a]pyrene (BAP). The values for f_{oc}, K_{oc}, K_{PEW}, and L were taken from a field study of Oslo Harbor performed by Cornelissen et al. (2008). The bulk density and porosity were assumed to be typical sediment values of 0.8 kg/L and 0.6, respectively. The values of D_{PE} were estimated as described by Fernandez et al. (2009), while the value of D_w was estimated

using the correlation of Hayduk and Laudie (1974). The resulting values for σ were 27.0 for PYR and 48.0 for BAP. Table 5 summarizes the parameter values used in the simulations.

Table 5: Parameters Used in Simulating Uptake in PDMS and PE

Parameter	Units	PYR	BAP
Sediment and Contaminant Properties			
ε		0.7	0.7
ρ	kg/L	0.8	0.8
f_{oc}[19]		0.03	0.03
f_{lc}[19]		0.0275	0.0275
f_{bc}[19]		0.0025	0.0025
K_{ow}[20]	log(L/L)	5.18	6.13
K_{lc}[21]	log(L/kg)	4.75	5.69
K_{bc}	log(L/kg)	6.45	7.38
K_{oc}[22]	log(L/L)	5.46	6.39
D_w[23]	cm^2/s	4.9E-6	4.3E-6
Polyethylene Strip Properties			
K_{PEW}[19]	log(L/L)	5.02	6.22
D_{PE}[24]	cm^2/s	1.15E-9	1.08E-10
L[19]	µm	100	100
$\sigma = \sqrt{D_{PE} / D /(\varepsilon + \rho f_{oc} K_{oc})} K_{PEW}$		27.0	48.0
PDMS Fiber Properties			
r_1[19]	µm	50	50
r_2[19]	µm	78.5	78.5
K_f[19]	log(L/L)	4.61	5.39

[19] Cornelissen et al (2008)
[20] MacKay et al. (1992)
[21] Zimmerman et al. (2004)
[22] Estimated from correlation provided by Schwarzenbach et al. (2003)
[23] Estimated using method described by Hayduk and Laudie (1974)
[24] Fernandez et al. (2009)

Figure 22 shows the dimensionless concentration profiles for the PYR and BAP using the model of Fernandez et al. (2009). The profiles at early times showed a gradient at the sampler-sediment interface, which quickly diminished to a uniform profile consistent with an external-diffusion controlled problem. Equation (6.11) depends only on σ and the dimensionless time. The parameter σ is the ratio of the transport rate in the PE to that in the sediment. In both cases σ was much larger than one, which would indicate that internal mass transport resistances were negligible for estimating uptake rates.

To further examine this point, additional model simulations were performed with all parameters the same other than the diffusion coefficient, which was increased by six orders of magnitude to produce a value of σ of 0.048. The results are shown in Figure 23 and show steep gradients within the PE and negligible gradients within the sediment-pore water matrix. Thus it appears that when $\sigma << 1$, internal mass transfer controls.

These results imply that the relative importance of internal to external diffusion decreases as hydrophobicity increases. PYR is more mobile than BAP based on their octanol-water partition coefficients (log K_{ow}=5.18 and 6.13 for PYR and BAP, respectively). For compounds with more mobility than PYR, equilibrium conditions will be relatively fast and thus there is little need for any kinetic correction to measured pore water concentrations. For compounds with less mobility, the value of σ increases which correspondingly increases the relative significance of external mass transport processes. A quick calculation of the value of σ for a problem can reveal whether internal mass transport is significant.

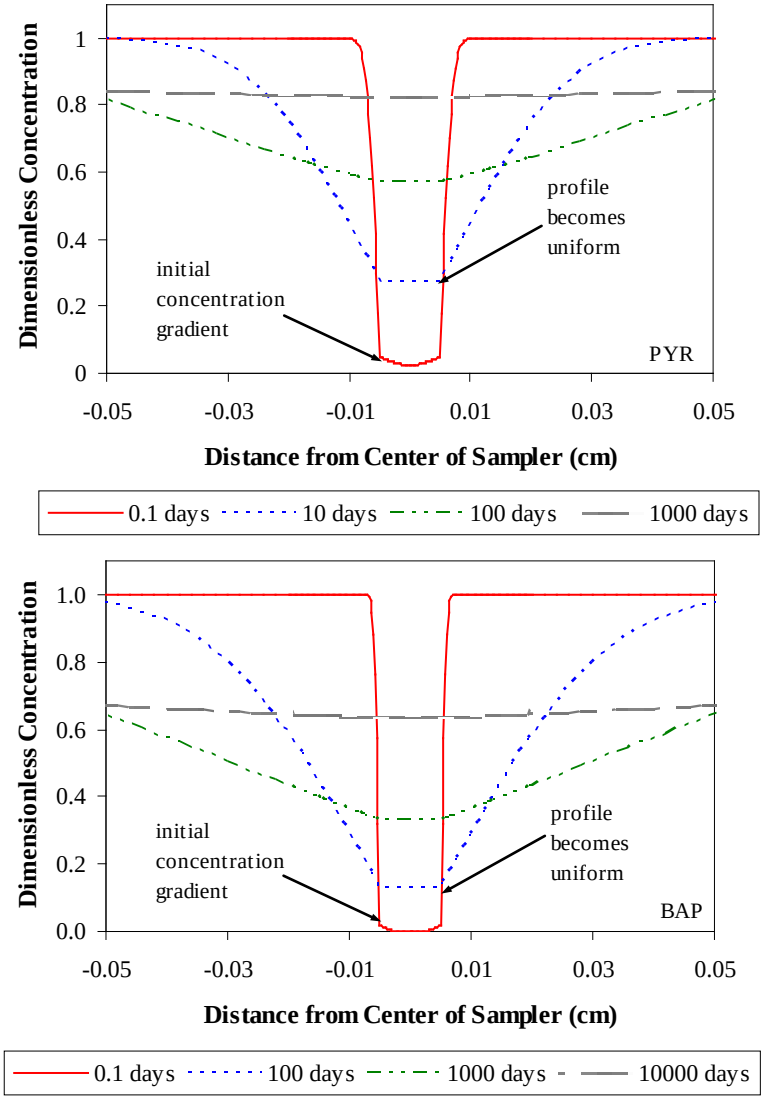

Figure 22. Dimensionless concentration profiles at various times for the model of Fernandez et al. (2009) for pyrene (top) and benzo[a]pyrene (bottom).

Values used in simulations were from Table 5. The concentration profiles in the PE were nearly uniform after a brief period of time as the value of σ was significantly larger than unity in both cases. These results imply that when σ is larger than one, internal diffusion within passive sampling devices is negligible.

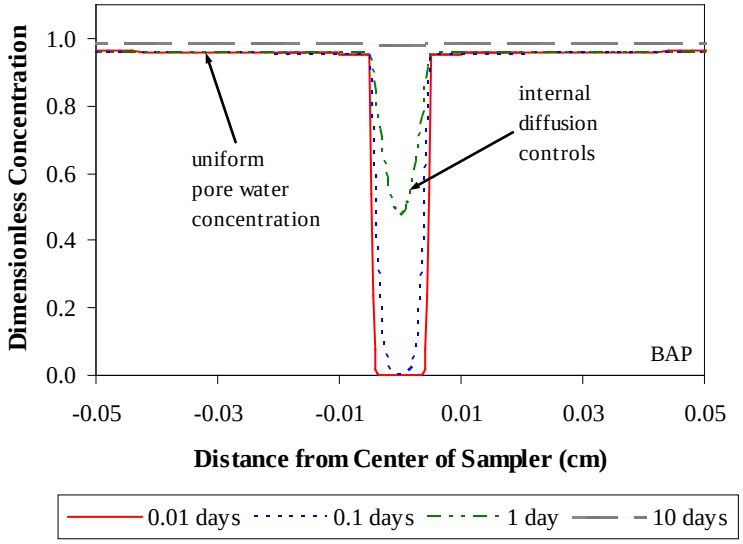

Figure 23. Dimensionless concentration profiles for external diffusion controlled problem.

Values used were from Table 5 (BAP) with the exception of D_w, which was increased to demonstrate an internal mass transport-controlled system.

6.3 Kinetically-Limited Release Passive Sampler Model

In this section, a model that ignores internal diffusion but considers a third transport mechanism, the release rate of the contaminants from the sediment particles is developed.

6.3.1 HOC Sediment-Water Equilibrium

To predict the kinetics of passive samplers requires some assumptions about long-term equilibrium behavior. The classical approach of linear sorption onto the organic carbon fraction (6.1) is commonly used to estimate equilibrium sediment-phase concentrations. More recently it has become apparent that the classic model predicts short-term sorption accurately, but over predicts desorption over environmentally-relevant concentration ranges (Kan et al. 1997, Cornelissen et al. 2008, Arp et al. 2009).

Recent research (Gustafsson et al. 1997, Accardi-Dey and Gschwend 2002, Lohmann et al. 2005) has focused on the sorption and desorption characteristics of sediments and soils onto "black" or "hard" carbon (HC), which is the carbon that remains after 24 hours of combustion at 375°C and removal of inorganic carbon fraction by acidification. The results of these studies indicate that the HC fraction exhibits very strong and slow sorption and appears to be partly responsible for over prediction of classic linear partitioning in soils and sediments. The effects of HC are obscured over the high concentration ranges where many of the measured values of K_{oc} used to develop the correlations with K_{ow} were performed (Accardi-Dey and Gschwend 2002, Cornelissen and Gustafsson 2004).

Gustaffson et al. (1997) characterized sorption of HOCs onto HC using activated carbon sorption data from Walters and Luthy (1984) and sorption of the labile organic carbon (LC) using Equation (6.1) with values for K_{ow} from Miller et al. (1985) and correlation parameters from Karickhoff (1981). The results of the analysis matched observed field concentrations closely. Herein, it assumed that equilibrium sediment particle concentration q and pore water concentration C can be modeled using a similar approach:

$$q = q_{lc} + q_{hc} = f_{lc}K_{lc}C + f_{hc}K_{hc}C = f_{oc}K_{oc}C \tag{6.13}$$

Where:

q_{lc} = labile organic carbon concentration (M M^{-1})

q_{hc} = hard organic carbon concentration (M M^{-1})

f_{lc} = fraction labile organic carbon (M M^{-1})

f_{hc} = fraction hard organic carbon ($M\ M^{-1}$)

K_{lc} = labile organic carbon partition coefficient ($L^{-3}\ M$)

K_{hc} = hard organic carbon partition coefficient ($L^{-3}\ M$)

For high concentrations, the assumption of linearity in the HC fails and the value of q_{hc} reaches a plateau (Accardi-Dey and Gschwend 2002, Cornelissen and Gustafsson 2004). However, over environmentally relevant (low) concentration ranges it may dominate the overall partitioning (Accardi-Dey and Gschwend 2002, Cornelissen and Gustafsson 2004). Zimmerman et al. (2004) found PCB K_{hc} values in Hunters Point Naval Shipyard, San Francisco, CA sediment to be two orders of magnitude larger than those predicted using octanol-water partition coefficient correlations such as Schwarzenbach et al. (2003). The authors attributed the difference to the sediment organic matter at Hunters Point, which had previously been shown to contain 5-7% HC (Ghosh et al. 2003). The value of K_{lc} can be estimated using octanol-water partition coefficient correlations such as those in Schwarzenbach et al. (2003). Relatively large values of K_{hc} explain why the values of K_{oc} (the weighted average of K_{lc} and K_{hc}) observed in the field are larger than those predicted by the traditional methods.

6.3.2 Conceptual Model

Conceptually, the model assumes an initial state of equilibrium exists amongst the contaminant concentrations in the sediment pore water and particle phases. The equilibrium state is perturbed when the initially contaminant-free fiber is inserted into the sediment environment, thereby creating a sink for contaminant mass present in the other phases. Over time, the fiber and surrounding environment re-equilibrate to the initial conditions. The model assumes molecular diffusion of the contaminants dominates

transport from the neighboring pore water to the PDMS fiber. Local equilibrium is assumed to exist between the pore water and LC phases, while kinetically-limited sorption is assumed on the HC.

6.3.3 Governing Equations and Assumptions

To predict transport of contaminants in the sediment environment based on the conceptual model, mathematical relationships describing the three dependent variables, the pore water concentration C, the LC concentration q_{lc}, and the HC concentration q_{hc}, are required. Because the LC is assumed to be in equilibrium with the neighboring pore water, the concentration in the LC phase can be explicitly determined by:

$$q_{lc} = f_{lc} K_{lc} C \tag{6.14}$$

To account for slow adsorption and desorption from the HC fraction, sorption and desorption between the HC and the neighboring pore water is assumed to be governed by a mass transfer relationship:

$$\frac{\partial q_{hc}}{\partial t} = k_h \left(f_{hc} K_{hc} C - q_{hc} \right) \tag{6.15}$$

Where:

k_h = sediment-water mass transfer coefficient ($L\ T^{-1}$)

f_{hc} = fraction hard carbon ($M\ M^{-1}$)

K_{hc} = hard organic carbon equilibrium partition coefficient ($L^{-3}\ M$)

The parameter k_h represents the intrinsic velocity of contaminants through the sediment particles; clearly this parameter varies from particle to particle and site to site. However, this methodology does provide a mechanism for exploring the importance of sediment-side mass transfer resistances in passive sampler uptake kinetics, and for

molecules of similar size and class (e.g., PCBs or PAHs) should be relatively compound independent.

The governing transport equation in the sediment-pore water matrix is:

$$\varepsilon \frac{\partial C}{\partial t} + \rho \frac{\partial q_{lc}}{\partial t} + \rho \frac{\partial q_{hc}}{\partial t} = R \frac{\partial C}{\partial t} + \rho \frac{\partial q_{hc}}{\partial t} = D \nabla^2 C \tag{6.16}$$

Where:

R = retardation factor for pore water concentrations with the LC = $\varepsilon + \rho\ f_{lc} K_{lc}$

∇^2 = the Laplacian operator (coordinate dependent)

The parameter D is the product of the molecular diffusivity times the porosity and divided by the tortuosity as in Equation (6.5).

The initial conditions for C and q_h and the conditions far away from the sampler are assumed to be at the initial values of C_0 and $f_{hc}K_{hc}C_0$, respectively, until restoration of equilibrium. The concentration in the passive sampling device is initially zero. When internal diffusion within the device is negligible, transport within the device can be modeled by a mass balance on the sampling device, which is assumed to be well-mixed. The sampling devices are assumed to be "long;" that is, that the length of the device is significantly greater than the characteristic diffusion length scale so that edge effects are negligible. This assumption allows a one-dimensional approach.

6.4 Kinetically-Limited Release Passive Sampler Model in Rectangular Cartesian Coordinate System for POM and PE Sheets

For the case of POM and PE sheets of thickness 2L (characteristic length L), the geometry is most appropriately modeled in a one-dimensional rectangular Cartesian

coordinate system with the distance from the sheet of *x*. For the case when internal diffusion in the sheet is negligible, the transport equations and auxiliary conditions are:

$$R\frac{\partial C(x,t)}{\partial t}+\rho\frac{\partial q_{hc}(x,t)}{\partial t}=D\frac{\partial^2 C(x,t)}{\partial x^2} \tag{6.17}$$

$$\frac{\partial q_{hc}(x,t)}{\partial t}=k_h\left(f_{hc}K_{hc}C(x,t)-q_{hc}(x,t)\right) \tag{6.18}$$

$$C(t=0)=\begin{cases}C_0 & x>0\\ 0 & x=0\end{cases} \tag{6.19}$$

$$q_{hc}(x>0,t=0)=f_{hc}K_{hc}C_0 \tag{6.20}$$

$$C(x\to\infty,t)=C_0 \tag{6.21}$$

$$K_{PEW}L\frac{\partial C(x=0,t)}{\partial t}=D\frac{\partial C(x=0,t)}{\partial x} \tag{6.22}$$

For further insight and solution of this model, it is convenient to convert the system (6.17-6.22) into dimensionless form. The following dimensionless variables and parameters are introduced:

$$u=\frac{C_0-C}{C_0} \tag{6.23}$$

$$v=\frac{f_{hc}K_{hc}C_0-q}{f_{hc}K_{hc}C_0} \tag{6.24}$$

$$\tau=\frac{Dt}{L^2} \tag{6.25}$$

$$\xi=\frac{x}{L} \tag{6.26}$$

$$Bi = \text{Biot number} = \frac{k_h L^2}{D} = \frac{\text{rate of transport in sediment particles}}{\text{rate of diffision though sediment pore water}} \tag{6.27}$$

Thus the system (6.17-6.22) can be re-written:

$$R\frac{\partial u}{\partial \tau} + \rho\, f_{hc} K_{hc} \frac{\partial v}{\partial \tau} = \frac{\partial^2 u}{\partial \xi^2} \tag{6.28}$$

$$\frac{\partial v}{\partial \tau} = Bi(u - v) \tag{6.29}$$

$$u(\tau = 0) = \begin{cases} 0 & \xi > 0 \\ 1 & \xi \le 0 \end{cases} \tag{6.30}$$

$$v(\xi > 0, \tau = 0) = 0 \tag{6.31}$$

$$u(\xi \to \infty, \tau) = 0 \tag{6.32}$$

$$K_{PEW} \frac{\partial u(\xi = 0, \tau)}{\partial \tau} = \frac{\partial u(\xi = 0, \tau)}{\partial \xi} \tag{6.33}$$

To solve the dimensionless system (6.28-6.33), the Laplace Transform is applied:

$$\overline{f}(s) = L\{f(t)\} = \int_0^\infty e^{-st} f(t) dt \tag{6.34}$$

The auxiliary problem in the Laplace transformed domain is:

$$R s\bar{u} + \rho\, f_{hc} K_{hc}\, s\bar{v} = \frac{d^2 \bar{u}}{d\xi^2} \tag{6.35}$$

$$s\bar{v} = Bi(\bar{u} - \bar{v}) \tag{6.36}$$

$$\bar{u}(\xi \to \infty) = 0 \tag{6.37}$$

$$s\bar{u}(\xi = 0) - 1 = \frac{1}{K_{PEW}} \frac{d\bar{u}(\xi = 0)}{d\xi} \tag{6.38}$$

The over bars refer to the value of the variable in the Laplace transformed domain. The solution to auxiliary problem is:

$$\bar{u} = \frac{K_{PEW}}{\beta + K_{PEW} s} \exp\left[-\beta\xi\right] \tag{6.39}$$

$$\bar{v} = \frac{Bi\, K_{PEW}}{\left(\beta + K_{PEW} s\right)\left(s + Bi\right)} \exp\left[-\beta\xi\right] \tag{6.40}$$

Where:

$$\beta = \sqrt{\frac{Rs^2 + (R + \rho f_{hc} K_{hc}) Bi\, s}{s + Bi}} \tag{6.41}$$

The definition of the inverse Laplace transform is:

$$f(t) = L^{-1}\left\{\bar{f}(s)\right\} = \frac{1}{2\pi i} \lim_{T\to\infty} \int_{\gamma - iT}^{\gamma + iT} e^{st}\, \bar{f}(s) ds \tag{6.42}$$

Thus for this case:

$$u(\xi,\tau) = \frac{1}{2\pi i} \lim_{T\to\infty} \int_{\gamma - iT}^{\gamma + iT} \frac{K_{PEW}}{\beta + K_{PEW} s} \exp\left[s\tau - \beta\xi\right] ds \tag{6.43}$$

$$v(\xi,\tau) = \frac{1}{2\pi i} \lim_{T\to\infty} \int_{\gamma - iT}^{\gamma + iT} \frac{Bi\, K_p}{\left(\beta + K_{PEW} s\right)\left(s + Bi\right)} \exp\left[s\tau - \beta\xi\right] ds \tag{6.44}$$

While there are no apparent exact solutions to these complex contour integrals, it is possible to perform the inversions numerically. This method provides numerous advantages over discretization methods for solving differential equations; there are no issues with stability; the model applies to infinite and semi-infinite domains; the inversion can be performed at specific points in space and time without the need for a lengthy simulation. A script was developed in the Python programming language using

the Scientific Python package (Jones et al. 2001) to perform the inversion. The algorithm for the inversion is based on Talbot's method as described by Trefethen et al. (2006). A code developed by Nieuwveldt (2010) was used to implement the algorithm into Python and was subsequently modified to numerically solve Equations (6.43) and (6.44).

The value of the pore water concentration C and the total sediment concentration q (M M^{-1}) at any point in space or time can be determined by the following:

$$C(x,t) = \left[1 - u\left(\xi = \frac{x}{L}, \tau = \frac{Dt}{L^2}\right)\right] C_0 \tag{6.45}$$

$$q(x,t) = \left[1 - u\left(\xi = \frac{x}{L}, \tau = \frac{Dt}{L^2}\right)\right] f_{lc} K_{lc} C_0 + \left[1 - v\left(\xi = \frac{x}{L}, \tau = \frac{Dt}{L^2}\right)\right] f_{hc} K_{hc} C_0 \tag{6.46}$$

Finally, the value of the contaminant mass, M, on the sampler over time can be determined by the following:

$$M(t) = \left[1 - u\left(\xi = 0, \tau = \frac{Dt}{L^2}\right)\right] 2LK_{PEW} C_0 \tag{6.47}$$

For the case of instantaneous release of contaminant mass from the sediment particles, Bi approaches infinity and the values of u and v are equal. Carslaw and Jaeger (1959) presented an exact solution for the analogous heat conduction problem. By adapting this solution to the mass transport problem presented herein, the following expression is obtained for the mass in the instantaneous release case:

$$M(t) = \left[1 - \exp\left(\frac{D(R + \rho f_{hc} K_{hc})t}{L^2 K_{PEW}^2}\right) \operatorname{erfc}\left(\frac{\sqrt{D(R + \rho f_{hc} K_{hc})t}}{LK_{PEW}}\right)\right] 2LK_{PEW} C_0 \tag{6.48}$$

Equation (6.48) can also be applied to the case of no release from the HC by setting K_{hc} = 0 and/or no release from the LC using K_{lc} = 0.

6.5 Comparison of Polyethylene Diffusion and Instant Release Models

To demonstrate the validity of the model developed in 7.4, simulations were performed under the fast release case (Equation 7.48) and compared to the model of Fernandez et al. (2009) for BAP. The values of f_{hc}, f_{lc}, K_{PEW}, and L were taken from the study done by Cornelissen et al. (2008) on Oslo Harbor sediment. The values of K_{lc} were estimated using the traditional correlations from Schwarzenbach et al. (2003) based on octanol-water partition coefficients (K_{ow}) from MacKay et al. (1992). As Cornelissen et al. (2008) provided values of all the other equilibrium parameters, the value of K_{hc} was estimated using Equation (6.13). A simulation of the sampler uptake was performed using the values summarized in Table 5 for both of the models. The results of this simulation showed identical uptake at all times, which is unsurprising as the value of σ was much larger than one. The uptake rates for the two models were compared and found to be virtually identical for both cases.

To further investigate this point, the simulations were repeated with smaller values of K_{PEW} (and hence, σ) to observe behavior when the two models might diverge. The results are shown in Figure 24 and demonstrate that as the parameter σ grows significantly larger than unity, internal mass transport resistance is negligible and the model (6.48) and that of Fernandez et al. (2009) converge. This is a significant result, as Equation (6.48) is more easily applied than the numerical modeling approach presented in that study.

The results in Figure 24 show that the two models have the same behavior for large σ and long times. To estimate the error associated with ignoring internal diffusion, both models were run for a variety of dimensionless times (based on D_{PE}) and values of

σ. The results are plotted in Figure 25. By calculating the dimensionless time $D_{PE}t/L^2$ and σ and plotting the values on this graph, the percentage error can be estimated. For values of $\sigma > 3$, the models converged rapidly.

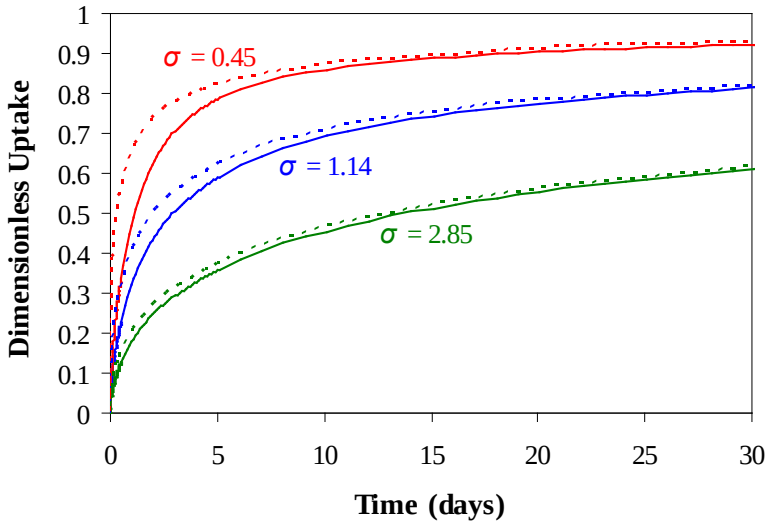

Figure 24: Dimensionless uptake rates $M/(2LK_{PEW}C_0)$ at various values of σ.
Solid lines: no internal resistance (proposed) model. Dashed lines: internal and external resistance (Fernandez et al. 2009) model. As σ grows larger than unity, the mass transport resistance within the passive sampling device becomes negligible and Equation (6.48) may be safely applied.

In addition, it should be noted that Equation (6.48) is a limiting case of the kinetically-limited release model. It is possible to use Equation (6.48) under the limits of instantaneous and no release from the different phases for inference of the influence of additional transport processes (i.e., the release rate from the sediments). A similar approach can be taken for cylindrical PDMS fibers or POM sheets. Due to the relatively rapid diffusion rates in PDMS shown in Figure 21, the assumption of negligible mass transport in the sampling device will be justified in general for PDMS fibers.

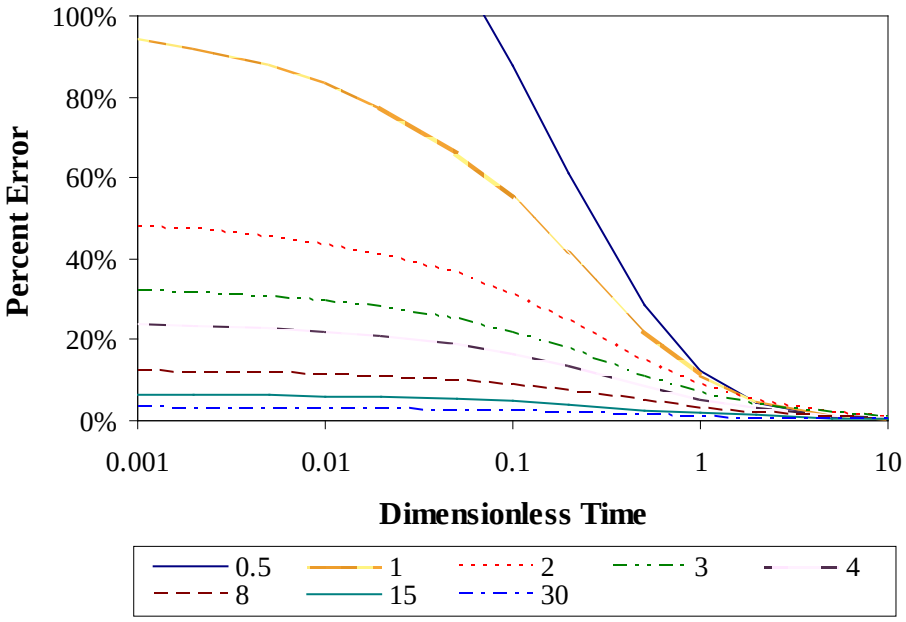

Figure 25: Percent Error Associated with Neglecting Internal Diffusion in Equilibrium Predictions.

The percent error in the equilibrium predictions associated with neglecting internal diffusion was calculated for a variety of dimensionless times $D_{PE}t/L^2$ and values of σ. This graph can be used to determine whether internal diffusion can be ignored for a given passive sampler after a given period of time.

6.6 Kinetically-Limited Release Passive Sampler Model in Cylindrical Coordinate System for PDMS Fibers

For cylindrical PDMS fibers, a cylindrical coordinate system is most appropriate for assessing contaminant transport. The transport equations in this case are:

$$\left(\varepsilon + \rho\ f_{lc}K_{lc}\right)\frac{\partial C(r,t)}{\partial t} + \rho\frac{\partial q_{hc}(r,t)}{\partial t} = D\frac{\partial^2 C(r,t)}{\partial r^2} + \frac{D}{r}\frac{\partial C(r,t)}{\partial r} \tag{6.49}$$

$$\frac{\partial q_{hc}(r,t)}{\partial t} = k_h\left(f_{hc}K_{hc}C(r,t) - q_{hc}(r,t)\right) \tag{6.50}$$

Where:

r = radial distance from the center of the fiber (L)

t = time (T)

The initial and boundary conditions for C and q_{hc} are:

$$C(t=0) = \begin{cases} C_0 & r > r_2 \\ 0 & r \le r_2 \end{cases} \tag{6.51}$$

$$q_{hc}(r > r_2, t = 0) = f_{hc} K_{hc} C_0 \tag{6.52}$$

$$C(r \to \infty, t) = C_0 \tag{6.53}$$

$$K_f \pi (r_2^2 - r_1^2) \frac{\partial C(r = r_2, t)}{\partial t} = 2\pi r_2 D \frac{\partial C(r = r_2, t)}{\partial r} \tag{6.54}$$

Where:

r_1 = radius of inner glass fiber core (L)

r_2 = radius of inner glass fiber core + PDMS coating (L)

K_f = the fiber-water partition coefficient for the compound ($L^3\ L^{-3}$)

As before, it is convenient to convert the system (6.49-6.54) into dimensionless form. The following dimensionless variables and parameters are introduced:

$$u = \frac{C_0 - C}{C_0} \tag{6.55}$$

$$v = \frac{f_{hc} K_{hc} C_0 - q}{f_{hc} K_{hc} C_0} \tag{6.56}$$

$$\tau = \frac{Dt}{r_2^2} \tag{6.57}$$

$$\xi = \frac{r}{r_2} \tag{6.58}$$

$$Bi = \frac{k_h r_2^2}{D} \tag{6.59}$$

$$\alpha = \frac{2Dr_2}{K_f (r_2^2 - r_1^2)} \tag{6.60}$$

Thus the system (6.49-6.54) can be re-written:

$$R\frac{\partial u}{\partial \tau} + \rho\, f_{hc} K_{hc} \frac{\partial v}{\partial \tau} = \frac{\partial^2 u}{\partial \xi^2} + \frac{1}{\xi}\frac{\partial u}{\partial \xi} \tag{6.61}$$

$$\frac{\partial v}{\partial \tau} = Bi(u - v) \tag{6.62}$$

$$u(\tau = 0) = \begin{cases} 0 & \xi > 1 \\ 1 & \xi \le 1 \end{cases} \tag{6.63}$$

$$v(\xi > 1, \tau = 0) = 0 \tag{6.64}$$

$$u(\xi \to \infty, \tau) = 0 \tag{6.65}$$

$$\frac{\partial u(\xi = 1, \tau)}{\partial \tau} = \alpha \frac{\partial u(\xi = 1, \tau)}{\partial \xi} \tag{6.66}$$

To solve the system (6.61-6.66), the Laplace Transform method was again applied. The auxiliary problem in the Laplace transformed domain is:

$$Rs\bar{u} + \rho\, f_{hc} K_{hc}\, s\bar{v} = \frac{d^2\bar{u}}{d\xi^2} + \frac{1}{\xi}\frac{d\bar{u}}{d\xi} \tag{6.67}$$

$$s\bar{v} = Bi(\bar{u} - \bar{v}) \tag{6.68}$$

$$\bar{u}(\xi \to \infty) = 0 \tag{6.69}$$

$$s\bar{u}(\xi = 1) - 1 = \alpha \frac{d\bar{u}}{d\xi} \tag{6.70}$$

The over bars again refer to the value of the variable in the Laplace transformed domain. The solution to auxiliary problem is:

$$\bar{u}(\xi, s) = \frac{K_0(\beta\xi)}{sK_0(\beta) + \alpha\beta K_1(\beta)} \tag{6.71}$$

$$\bar{v}(\xi, s) = \frac{BiK_0(\beta\xi)}{\left(sK_0(\beta) + \alpha\beta K_1(\beta)\right)\left(s + Bi\right)} \tag{6.72}$$

Where as before:

$$\beta = \sqrt{\frac{Rs^2 + (R + \rho f_{hc} K_{hc})Bi\, s}{s + Bi}} \tag{6.73}$$

$K_n(x)$ = The modified Bessel function of the second kind of order *n*.

As before there are no apparent exact expressions for the inverse of these functions, but the inversions can be performed numerically. A script was developed in the Python programming language using the Scientific Python package (Jones et al. 2001) to perform the inversion including a graphical-user interface for rapid model assessment.

The value of the pore water concentration *C* and the total sediment concentration *q* (M M^{-1}) at any point in space or time can be determined by the following:

$$C(r,t) = \left[1 - u\left(\xi = \frac{r}{r_2}, \tau = \frac{Dt}{r_2^2}\right)\right] C_0 \tag{6.74}$$

$$q(r,t) = \left[1 - u\left(\xi = \frac{r}{r_2}, \tau = \frac{Dt}{r_2^2}\right)\right] f_{lc} K_{lc} C_0 + \left[1 - v\left(\xi = \frac{r}{r_2}, \tau = \frac{Dt}{r_2^2}\right)\right] f_{hc} K_{hc} C_0 \tag{6.75}$$

Finally, the value of the contaminant mass, *M*, on the sampler over time can be determined by the following:

$$M(t) = \left[1 - u\left(\xi = 1, \tau = \frac{Dt}{r_2^2}\right)\right]\pi\left(r_2^2 - r_1^2\right)K_f C_0 \tag{6.76}$$

For the case of instantaneous release of contaminant mass from the sediment particles, *Bi* approaches infinity and the values of *u* and *v* are the same. Carslaw and Jaeger (1959) presented an exact solution for the analogous heat conduction problem. By adapting this solution to the mass transport problem presented herein, the following expression is obtained for the mass in the instantaneous release case:

$$M(t) = \left\{1 - \frac{4\alpha}{\pi^2}\int_0^\infty \frac{\exp\left(-\dfrac{z^2 Dt}{(R + \rho\, f_{hc} K_{hc}) r_2^2}\right)}{z\left(z J_0(z) - \alpha J_1(z)\right)^2 + z\left(z Y_0(z) - \alpha Y_1(z)\right)^2}\, dz\right\}\pi\left(r_2^2 - r_1^2\right)K_f C_0 \tag{6.77}$$

Equation (6.77) can also be applied to the case of no release from the HC by setting K_{hc} = 0 and/or no release from the LC using K_{lc} = 0. These cases represent the limiting extents of the model; for situations where both sediment-side mass transfer resistance and pore water diffusion are important, the numerical inversion technique is necessary.

6.7 PDMS Model Behavior

To illustrate the behavior of the model, a series of simulations were performed. Uptake in PDMS for PYR and BAP were simulated using the parameters in Table 5 from the study of Cornelissen et al. (2008) as described previously. The field study was performed in Oslo Harbor at temperatures of 2 to 10°C with water currents in the range of 2 to 4 cm/s. The values for the PDMS parameters K_f, r_1 and r_2 were provided as the study was a comparison of different passive sampling techniques.

Figure 26 shows the results of the simulations and the field estimates by Cornelissen et al. (2008) of the percent equilibrium. The authors determined that equilibrium was attained by 63 days in the field for 4-ring PAHs such as pyrene; this result is in line with model predictions which indicate equilibrium in 50-100 days. In the case of 5-ring PAHs such as benzo[a]pyrene, the authors indicated equilibrium was not achieved over the 63-day period. The estimates fall near the model predictions for instant release from the LC and no release from the HC; these results appear to indicate that mass transport resistance in the sediment is a significant factor to consider when modeling uptake with passive samplers.

6.8 Limitations

The models presented herein assume no advective contaminant transport. This assumption is valid in stagnant laboratory settings and may applicable in the field under low seepage conditions. The diffusion rate within the sampling device is also ignored. For environments where either significant advection occurs (e.g., tidal zones, near surface sediments, and high upwelling areas) or where the value of σ is less than one, the model assumptions may break down. The use of the model is reserved for scenarios where little to no significant advection within the region of influence of the device is expected.

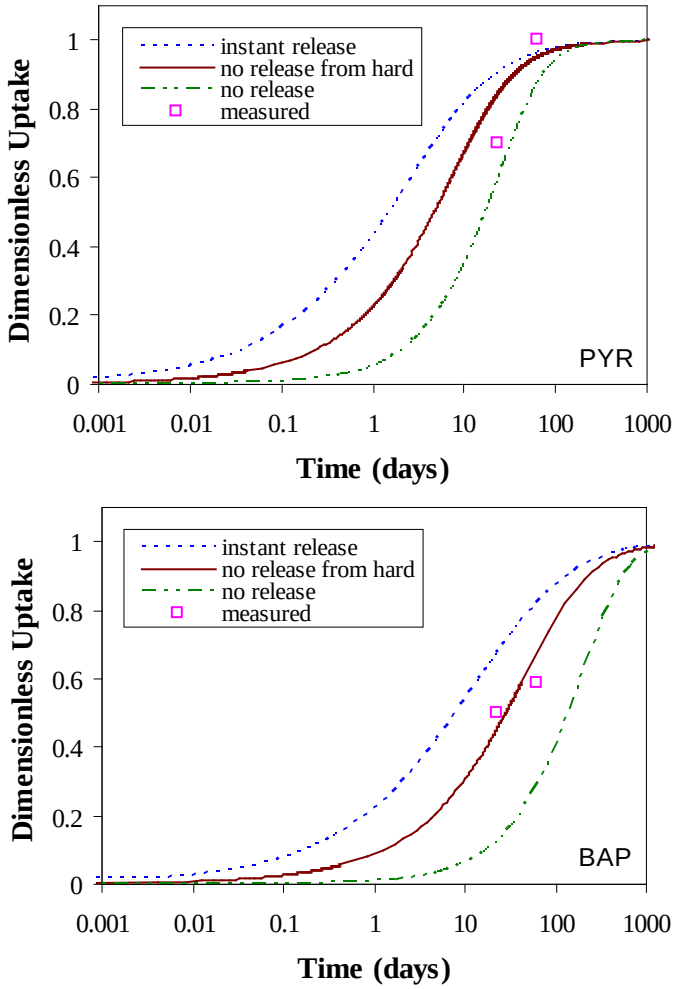

Figure 26: Dimensionless uptake rates in PDMS fibers under different sediment release rates for pyrene (top) and benzo[a]pyrene (bottom).

The dimensionless uptake rate $M/\left(\pi(r_2^2 - r_1^2)K_f C_0\right)$ is shown along with experimental observations from Cornelissen et al. (2008). The no release case and instant release cases represent the extremes of the model derived herein, and bracketed the data. Thus it is concluded that sediment-side mass transfer resistances may be a significant factor in passive sampler uptake kinetics.

6.9 Summary and Conclusions

In this study, a model for assessing uptake or HOCs from sediments into passive sampling devices has been presented. Based on the results herein, it appears that

transport within passive sampling devices can be neglected in many cases. To verify the validity of this assumption, one must simply determine the value of the parameter σ and see that it is larger than one. The model presented herein allows for mass transport resistances within the sediment matrix to be considered, which may control the overall rate of uptake. Model predictions matched field predictions from Cornelissen et al. (2008). Under the extreme cases of no release of transport or instant release from the particles, an analytical solution exists. In between these extremes, a code has been written that may be applied to determine the mass transfer release rate k_h from the sediment particles. Future studies should attempt to quantify this parameter under a variety of conditions to determine the overall importance of sediment-side mass transfer resistances in passive sampler uptake kinetics.

6.10 References

1. Accardi-Dey, A. and Gschwend, P.M. 2002. "Assessing the Combined Roles of Natural Organic Matter and Black Carbon as Sorbents in Sediments," Environmental Science & Technology, 36:21-29.
2. Adams, R.G., Lohman, R., Fernandez, L.A., MacFarlane, J.K., and Gschwend, P.M. 2007. "Polyethylene Devices: Passive Samplers for Measuring Dissolved Hydrophobic Organic Compounds in Aquatic Environments," Environmental Science & Technology, 41(4):1317-1323.
3. Ahn, S., Werner, D., Karapanagioti, H.K., McGlothlin, D.R., Zare, R.N., and Luthy, R.G. 2005. "Phenanthrene and Pyrene Sorption and Intraparticle Diffusion in Polyoxymethylene, Coke, and Activated Carbon," Environmental Science & Technology, 39:6516-6526.

4. Arp, H.P., Breedveld, G.D., Cornelissen, G.E. 2009. "Estimating the in situ sediment-porewater distribution of PAHs and chlorinated aromatic hydrocarbons in anthropogenic impacted sediments," Environmental Science & Technology, 43(15): 5576-5585.
5. Baker, J.R., Mihelcic, J.R., Luehrs, D.C., and Hickey, J.P. 1997. "Evaluation of Estimation Methods for Organic Carbon Normalized Sorption Coefficients," Water Environment Federation, 69(2):136-145.
6. Ball, W.P. and Roberts, P.V. 1991. "Long-Term Sorption of Halogenated Organic Chemicals by Aquifer Material. 2. Intraparticle Diffusion," Environmental Science & Technology, 25:1237-1249.
7. Boudreau, B. 1997. Diagenetic Models and Their Implementation: Modeling Transport Reactions in Aquatic Sediments. Springer-Verlag, New York.
8. Burton, G.A. 1991. "Assessing the toxicity of freshwater sediments," Environmental Toxicology and Chemistry, 10:1585-1627.
9. Carslaw, H.S. and Jaeger, J.C. 1959. Conduction of Heat in Solids, 2nd Edition. Oxford University Press, London, UK.
10. Cornelissen, G. and Gustafsson, O. 2004. "Sorption of Phenanthrene to Environmental Black Carbon in Sediment with and without Organic Matter and Native Sorbates," Environmental Science & Technology, 38:148-155.
11. Cornelissen, G., Petterson, A., Broman, D., Mayer, P., and Breedveld, D. 2008. "Field Testing of Equilibrium Passive Samplers to Determine Freely Dissolved Native Polycyclic Aromatic Hydrocarbon Concentrations," Environmental Toxicology and Chemistry, 27(3):499-508.

12. Doucette, W.J., 2003. "Quantitative structure-activity relationships for predicting soil-sediment sorption coefficients for organic chemicals," Environmental Toxicology and Chemistry, 22:1771–1788.
13. Fernandez, L.A., Harvey, C.F., and Gschwend, P.M. 2009. "Using Performance Reference Compounds in Polyethylene Passive Samplers to Deduce Sediment Porewater Concentrations for Numerous Target Chemicals," Environmental Science & Technology, 43:8888-8894.
14. Ghosh, U., Zimmerman, J.R., and Luthy, R.G. 2003. "PCB and PAH Speciation amound Particle Types in Contaminated Harbor Sediments and Effects on PAH Bioavailability," Environmental Science & Technology, 37:2209-2217.
15. Gustaffson, O., Haghseta, F., Chan, C., Macfarlane, J., Gschwend, P.M. 1997. "Quantification of the Dilute Sedimentary Soot Phase: Implications for PAH speciation and Bioavailability," Environmental Science & Technology, 31:203-209.
16. Hayduk, W. and Laudie, H. 1974. "Predicting diffusion coefficients for nonelectrolytes in dilute aqueous solutions," AICheE Journal, 20:611.
17. Hong, L. and Luthy, R.G. 2008. "Uptake of PAHs into polyoxymethylene and application to oil-soot (lampblack)-impacted soil samples," Chemosphere, 72(2):272-281.
18. Huckins, J. N.; Petty, J. D.; Lebo, J. A.; Almeida, F. V.; Booij, K., Alvarez, D. A., Cranor, W. L., Clark, R. C., and Mogensen, B. B. 2002. "Development of the permeability/performance reference compound approach for in situ calibration of semipermeable membrane devices," Environmental Science & Technology, 36(1):85-91.

19. Huckins, J.N., Petty. J.D., and Booij, K. 2006. Monitors of Organic Chemicals in the Environment, Semipermeable Membrane Devices. Springer, New York, NY.
20. Jones, E., Oliphant, T., and Peterson, P. 2001. SciPy: Open Source Scientific Tools for Python. http://www.scipy.org.
21. Jonker, M.T. and Koelmans, A.A. 2001. "Polyoxymethylene solid phase extraction as a partitioning method for hydrophobic organic chemicals in sediment and soot," Environmental Science & Technology, 35:3742-3748.
22. Jonker, M.T., van der Heijden, S.A., Kreitinger, J.P., and Hawthorne, S.B. 2007. "Predicting PAH Bioaccumulation and Toxicity in Earthworms Exposed to Manufactured Gas Plant Soils with Solid-Phase Microextraction," Environmental Science & Technology, 41:7472-7478.
23. Kan, A.T., Fu, G., Hunter, M.A., Tomson, M.B. 1997. "Irreversible sorption of naphthalene and tetrachlorobiphenyl to Lula and surrogate sediments," Environmental Science & Technology, 31:2176-2185.
24. Karickhoff, S.W., Brown, D.S., and Scott, T.A. 1979. "Sorption of Hydrophobic Pollutants in Natural Sediments," Water Research, 13, 241-248.
25. Karickhoff, S.W. 1981. "Semi-Empirical Estimation of Sorption of Hydrophobic Pollutants on Soils and Sediments," Chemosphere, 10:833-846.
26. Kraaij R., Mayer P., Busser F.J.M., Bolscher M.V.H., Seinen W., Tolls J. 2003. "Measured pore-water concentrations make equilibrium partitioning work-a data analysis," Environmental Science & Technology 37:268-274.

27. Lohmann, R., MacFarlane, J.K., Gschwend, P.M. 2005. "Importance of Black Carbon to Sorption of Native PAHs, PCBs, and PCDDs in Boston and New York Harbor Sediments," Environmental Science & Technology, 39:141-148.
28. Lu, X., Reible, D.D., Fleeger, J.W. 2006. "Bioavailability of Polycyclic Aromatic Hydrocarbons in Field-Contaminated Anacostia River (Washington, DC) Sediment," Environmental Toxicology and Chemistry, 25(11):2869-2874.
29. Mayer, P., Vaes, W., Wijnker, F., Legierse, K., Kraaij, R., Tolls, J., and Hermans, J. 2000. "Sensing Dissolved Sediment Porewater Concentrations of Persistent and Bioaccumulative Pollutants Using Disposable Solid-Phase Microextraction Fibers," Environmental Science & Technology, 34:5177-5183.
30. Mackay, D.; Shiu, W. Y.; Ma, K. C. 1992. Illustrated Handbook of Physical-Chemical Properties and Environmental Fate for Organic Chemicals, Volume 3. Lewis Publishers: Chelsea, MI.
31. Meloche, L.M, deBruyn, A.M.H., Otton, S.V., Ikonomou, M.G., and Gobas, F.A.P.C. 2009. "Assessing exposure of sediment biota to organic contaminants by thin-film solid phase microextraction," Environmental Toxicology and Chemistry, 28:247–253.
32. Miller, M.M., Wassik, S.P., Huang, G.L., Shiu, W.Y., MacKay, D. 1985. "Relationships between Octanol-Water Partition Coefficient and Aqueous Solubility," Environmental Science & Technology, 19:522-529.
33. Namiesnik, J., Zabiegala, B., Kot-Wasik, A., Partyka, M., and Wasik, A. 2005. "Passive sampling and/or extraction techniques in environmental analysis: a review." Analytical and Bioanalytical Chemistry, 381(2):279-301.

34. Nieuwveldt, F. 2009. Recipe 576934: Numerical Inversion of the Laplace Transform using the Talbot method. (Python). http://code.activestate.com/recipes/576934/.
35. Pignatello, J.J. and Xing, B. 1996. "Mechanisms of Slow Sorption of Organic Chemicals to Natural Particles," Environmental Science & Technology, 30:1-11.
36. Rusina, T.P., Smedes, F., Klanova, J., Booij, K.S., and Holoubek, I. 2007. "Polymer selection for passive sampling: A comparison of critical properties," Chemosphere, 68:1344-1351.
37. Schwarzenbach, R.P., Gshwend, P.M., Imboden, D.M. 2003. "Chapter 9: Sorption I: Introduction and Sorption Processes Involving Organic Matter" and "Chapter 11: Sorption III: Sorption Processes Involving Inorganic Surfaces," Environmental Organic Chemistry, 2nd Edition, Wiley & Sons, Hoboken, New Jersey, 275-330 and 387-458.
38. Trefethen, L.N., Weideman, J.A.C., and Schmelzer, T. 2006. Talbot quadratures and rational approximations. BIT. Numerical Mathematics, 46(3):653-670.
39. Trimble, T.A., You, J., Lydy, M.J. 2008. "Bioavailability of PCBs from field-collected sediments: Application of Tenax extraction and matrix-SPME techniques," Chemosphere, 71(2):337-344.
40. US EPA. 1998. Contaminated Sediment Management Strategy (EPA 823-R-98-004). Accessed via website http://www.epa.gov/OST/cs/ stratefs.html.
41. Van der Heijden, S.A. and Jonker, M.T. 2009. "PAH Bioavailability in Field Sediments: Comparing Different Methods for Predicting in Situ Bioaccumulation," Environmental Science & Technology, 43:3757-3763.

42. Vinturella, A.E. Burgess, R.M., Coull, B.A., Thompson, K.M., and Shine, J.P. 2004. "Use of passive samplers to mimic uptake of polycyclic aromatic hydrocarbons by benthic polychaetes," Environmental Science & Technology, 38:1154-1160.
43. Walters, R.W. and Luthy, R.G. 1984. "Equilibrium Adsorption of Polycyclic Aromatic Hydrocarbons from Water onto Activated Carbon," Environmental Science & Technology, 25:1578-1584.
44. Weber, W.J. and Miller, C.T. 1988. "Modeling the sorption of hydrophobic contaminants by aquifer materials—I. Rates and equilibria," Water Research, 22(4):457-464.
45. Weber W.J., LeBouf, E.J., Young, T.M., and Huang, W. 2001. "Contaminant Interactions with Geosorbent Organic Matter: Insights Drawn from Polymer Sciences," Water Research, 35, 853-868.
46. Werth, C.J. and Reinhard, M. 1997. "Effects of temperature on trichloroethylene desorption from silica gel and natural sediments. Kinetics." Environmental Science & Technology, 31:697–703.
47. You, J., Landrum, P.F., Lydy, M.J. 2006. "Comparison of Chemical Approaches for Assessing Bioavailability of Sediment-Associated Contaminants," Environmental Science & Technology, 40:6348-6353.
48. Zimmerman, J.R., Ghosh, U., Millward, R.N., Bridges, T.S., Luthy, R.G. 2004. "Addition of Carbon Sorbents to Reduce PCB and PAH Bioavailability in Marine Sediments: Physicochemical Tests," Environmental Science & Technology, 38(20):5458-5464.

Chapter 7: Interpreting Uptake Rates in Passive Samplers for Contaminated Sediment through a Diffusion Model[25]

David J. Lampert[26], Alison E. Skwarski[27], Xiaoxia Lu[26], and Danny D. Reible[26]

7.0 Abstract

A current research focus for contaminated sediment management is the development of passive sampling devices such as polydimethylsiloxane (PDMS)-coated fibers for estimating contaminant *in situ* pore water concentrations. Herein, uptake of polycyclic aromatic hydrocarbons (PAHs) in PDMS fibers is assessed in batch laboratory experiments and interpreted using an external mass transfer resistance-controlled radial diffusion model. The results suggest the importance of explicitly modeling transport to the passive sampler rather than focusing on internal diffusion. The model was then used to interpret uptake rates of polychlorinated biphenyls (PCBs) in the field.

[25] Manuscript in preparation for submission

[26] Department of Civil, Architectural, Environmental Engineering, The University of Texas, Austin, TX

[27]Alison E. Skwarski, Environmental Designer 1, ARCADIS U.S., Inc., 10559 Citation Drive, Suite 100, Brighton, MI, 48116, alison.skwarski@arcadis-us.com

7.1 Introduction

The persistence of hydrophobic organic compounds (HOCs) such as polycyclic aromatic hydrocarbons (PAHs) and polychlorinated biphenyls (PCBs) in sediments presents a residual environmental risk as a route of entry for these contaminants into the food chain many years after sources of contamination are cut off. Because of poor understanding of the ecological risks associated with contaminated sediments and the ubiquitous nature of the problem, assessment and remediation of contaminated sediments presents a major research challenge for the environmental community (US EPA, 1998).

The particle or bulk solid-phase concentration of sediment contaminants is often used to assess sediment quality because it is relatively easy to measure (Doucette 2003). However, studies have found that solid-phase concentrations are often a poor metric for assessing bioavailability (Burton 1991). *In situ* pore water concentrations are thought to be linked to bioaccumulation of HOCs in sediments (Kraaij et al. 2003, Lu et al. 2006, Meloche et al. 2009). However, direct measurement of HOC concentrations in the aqueous phase is often difficult due to analytical limitations.

Critical to understanding pore water concentrations in sediments is the relationship between the bulk solid phase concentration and the neighboring pore water concentration. The pore water is often assumed to be in an instantaneous equilibrium with the sediment organic carbon that is governed by the linear partitioning proposed by Karickhoff et al. (1979):

$$q = f_{oc} K_{oc} C \tag{7.1}$$

Where:

q = solid phase concentration (M M^{-1})

C = pore water concentration (M L^{-3})

f_{oc} = fraction organic carbon (M M^{-1})

K_{oc} = organic carbon partition coefficient (L^{-3} M)

The value of K_{oc} is often estimated for a particular class of compounds using the octanol-water partition coefficient K_{ow} (Karickhoff 1981, Baker et al. 1997). In a recent literature survey, Arp et al. (2009) found a trend of under prediction in the values of K_{oc} using these literature correlations compared to calculated field measurements based on q, C, and f_{oc}. The reported field values were found to vary by as much as a factor of 30 from site to site. The authors concluded that due to the heterogeneity of the organic carbon phases, prediction of pore water concentrations from sediment phase concentrations is an inappropriate means for assessing sediment quality.

As direct measurement of pore water concentrations is often difficult or impossible, passive sampling with sorbent materials such as with polydimethylsiloxane (PDMS)-coated glass fibers are a current research focus (Mayer et al. 2000, Adams et al. 2007). Passive sampling methods have been shown to correlate well with bioaccumulation in the field (You et al. 2006, Jonker et al. 2007, Trimble et al. 2008, Van der Heijden and Jonker 2009). For each of these methods, the sampler is placed *in situ* followed by a contaminant uptake period within the device. The pore water concentration is then back-calculated from a pre-established partitioning relationship.

The PDMS-coated fibers can be manufactured to very small sizes (e.g., 110-µm glass diameter with 30-µm PDMS coating, Mayer et al. 2000). Because of this relatively small size, the method should not significantly deplete the contaminant mass in the

neighboring sediment particles, and hence should not affect the equilibrium chemistry. In addition, equilibrium is thought to be attained relatively rapidly (Mayer et al. 2000).

Studies on passive samplers in sediments, however, have revealed that equilibrium can take a significant amount of time to achieve. To speed equilibrium, thin (e.g., 100 μm) sorbent materials are being manufactured for passive sampling. As such, the equilibrium time for transport within passive sampling devices has dropped rapidly to the point that it may be negligible. However, studies have revealed that even for these thin materials equilibrium may not be attained for months (Cornelissen et al. 2008, Fernandez et al. 2009). Thus may be due to the transport time of the contaminants from the neighboring sediment environment to the sampling device (Hong and Luthy 2008, Cornelissen et al. 2008, Fernandez et al. 2009). The studies and the results from Chapter 7 would support a model that examines the rate of release of contaminants from the sediment to the pore water and the associated diffusion of contaminants to the sampling device for estimating passive sampler kinetics.

Herein, the modeling approach developed in Chapter 7 for estimating contaminant uptake in PDMS-coated fibers is applied to experimental data to assess the applicability of the model to laboratory and field data. The underlying model assumptions and parameters are presented briefly first. Next, the results of laboratory batch kinetics experiments on PAH and PCB-contaminated sediment from the Anacostia River are presented. The application of the model to a field study of the uptake of PCB at Hunters Point Naval Shipyard, San Francisco, CA is then discussed. Through these results, the applicability of the model to estimating equilibrium times is demonstrated. This

methodology can be used to correct measured values when it is infeasible to wait for equilibrium conditions.

7.2 PDMS Fiber Radial Diffusion Model

To predict the uptake kinetics of PDMS fibers, some assumptions about long-term equilibrium behavior are required. Recently it has become apparent that the approach of linear sorption onto the organic carbon fraction (Equation 8.1) over predicts the release of HOCs from sediments (Cornelissen et al. 2008, Arp et al. 2009). This behavior has been linked to "black" or "hard" carbon (HC), which is the carbon that remains after 24 hours of combustion at 375°C and removal of inorganic carbon fraction by acidification (Gustafsson et al. 1997, Accardi-Dey and Gschwend 2002, Lohmann et al. 2005). Herein, it assumed that equilibrium sediment particle concentration q and pore water concentration C can be modeled using the following approach:

$$q = q_{lc} + q_{hc} = f_{lc}K_{lc}C + f_{hc}K_{hc}C = f_{oc}K_{oc}C \tag{7.2}$$

Where:

q_{lc} = labile organic carbon concentration (M M^{-1})

q_{hc} = hard organic carbon concentration (M M^{-1})

f_{lc} = fraction labile organic carbon (M M^{-1})

f_{hc} = fraction hard organic carbon (M M^{-1})

K_{lc} = labile organic carbon partition coefficient (L^{-3} M)

K_{hc} = hard organic carbon partition coefficient (L^{-3} M)

For high concentrations, the assumption of linearity in the HC fails and the value of q_{hc} reaches a plateau (Accardi-Dey and Gschwend 2002, Cornelissen and Gustafsson

2004). However, over environmentally relevant (low) concentration ranges it may dominate the overall partitioning (Accardi-Dey and Gschwend 2002, Cornelissen and Gustafsson 2004). Zimmerman et al. (2004) found PCB K_{hc} values in Hunters Point Naval Shipyard, San Francisco, CA sediment to be two orders of magnitude larger than those predicted using octanol-water partition coefficient correlations such as Schwarzenbach et al. (2003). The authors attributed the difference to the sediment organic matter at Hunters Point, which had previously been shown to contain 5-7% HC (Ghosh et al. 2003). The value of K_{lc} can be estimated using octanol-water partition coefficient correlations such as those in Schwarzenbach et al. (2003). Relatively large values of K_{hc} explain why the values of K_{oc} (the weighted average of K_{lc} and K_{hc}) observed in the field are larger than those predicted by the traditional methods.

To predict contaminant uptake, transport through the sediment is assumed to be dominated by molecular diffusion. To account for slow adsorption and desorption from the HC fraction, sorption and desorption between the HC and the neighboring pore water is assumed to be governed by a mass transfer relationship. The initial conditions for C and q_{hc} and the conditions far away from the sampler are assumed to be at the initial values of C_0 and $f_{hc}K_{hc}C_0$, respectively, until restoration of equilibrium. The concentration in the passive sampling device is initially zero. The device is assumed to be well-mixed.

Thus for a cylindrical PDMS fiber the governing transport equations and auxiliary conditions are:

$$\left(\varepsilon + \rho\ f_{lc}K_{lc}\right)\frac{\partial C(r,t)}{\partial t} + \rho\frac{\partial q_{hc}(r,t)}{\partial t} = D\frac{\partial^2 C(r,t)}{\partial r^2} + \frac{D}{r}\frac{\partial C(r,t)}{\partial r} \tag{7.3}$$

$$\frac{\partial q_{hc}(r,t)}{\partial t} = k_h\left(f_{hc}K_{hc}C(r,t) - q_{hc}(r,t)\right) \tag{7.4}$$

$$C(t=0) = \begin{cases} C_0 & r > r_2 \\ 0 & r \le r_2 \end{cases} \tag{7.5}$$

$$q_{hc}(r > r_2, t = 0) = f_{hc}K_{hc}C_0 \tag{7.6}$$

$$C(r \to \infty, t) = C_0 \tag{7.7}$$

$$K_f \pi (r_2^2 - r_1^2)\frac{\partial C(r = r_2, t)}{\partial t} = 2\pi r_2 D \frac{\partial C(r = r_2, t)}{\partial r} \tag{7.8}$$

Where:

r = radial distance from the center of the fiber (L)

t = time (T)

ε = porosity ($L^3\ L^{-3}$)

ρ = particle bulk density ($M\ L^{-3}$)

D = effective diffusion coefficient ($L^2\ T^{-1}$)

k_h = sediment-water mass transfer coefficient ($L\ T^{-1}$)

r_1 = radius of inner glass fiber core (L)

r_2 = radius of inner glass fiber core + PDMS coating (L)

K_f = the fiber-water partition coefficient for the compound ($L^3\ L^{-3}$)

The parameter D is the product of the molecular diffusivity D_w times the porosity and divided by the tortuosity (Boudreau 1997):

$$D = \frac{\varepsilon\, D_w}{1 - \ln \varepsilon^2} \tag{7.9}$$

The parameter k_h represents the intrinsic velocity of contaminants through the sediment particles, which is a site-specific parameter that should be relatively compound independent for molecules of similar size and class (e.g., PCBs or PAHs).

The LC is assumed to be in equilibrium with the neighboring pore water, so the concentration in the LC phase can be explicitly determined by:

$$q_{lc} = f_{lc} K_{lc} C \tag{7.10}$$

The Biot number is a useful representation of the rate of transport through the sediment particles relative to that in the sediment pore water:

$$Bi = \frac{k_h r_2^2}{D} \tag{7.11}$$

The value of the contaminant mass, *M*, on the sampler over time can be determined by the following:

$$M(t) = \pi\left(r_2^2 - r_1^2\right) K_f C\left(r = r_2, t\right) \tag{7.12}$$

To determine the uptake rate of the fibers, the problem was converted into dimensionless form and solved by numerically inverting the Laplace-transformed solution. For the case of instantaneous release of contaminant mass from the sediment particles, *Bi* approaches infinity which simplifies the mathematics sufficiently to enable an exact solution (Carslaw and Jaeger 1959):

$$M(t) = \left\{1 - \frac{4\alpha}{\pi^2} \int_0^\infty \frac{\exp\left(-\dfrac{z^2 Dt}{(R + \rho\, f_{hc} K_{hc}) r_2^2}\right)}{z\left(z J_0(z) - \alpha J_1(z)\right)^2 + z\left(z Y_0(z) - \alpha Y_1(z)\right)^2} dz \right\} \pi\left(r_2^2 - r_1^2\right) K_f C_0 \tag{7.13}$$

Where:

$$\alpha = \frac{2Dr_2}{K_f (r_2^2 - r_1^2)} \tag{7.14}$$

$$R = \varepsilon + \rho\, f_{lc} K_{lc} \tag{7.15}$$

Equation (7.13) can also be applied to the case of no release from the HC by setting K_{hc} = 0 and/or no release from the LC using K_{lc} = 0. These cases represent the limiting extents of the model; for situations where both sediment-side mass transfer resistance and pore water diffusion are important, the numerical inversion or other suitable technique is necessary to solve the problem.

The attainment of equilibrium could be enhanced in the presence of advective transport mechanisms (i.e., tides, waves, or pore water upwelling). However, the characteristic length scales of transport for these compounds are similar to the thickness of the PDMS coating as $K_f \sim f_{oc}K_{oc}$. Over these length scales (10-100 μm) diffusive transport mechanisms tend to dominate.

7.3 Experimental Materials and Methods

7.3.1 Analytical Methods

PAH analysis was performed using high performance liquid chromatography for separation with fluorescence detection (HPLC/FD) for quantification. All analyses were performed in accordance with EPA Method 8310: Polynuclear Aromatic Hydrocarbons using a Waters 2795 Separations Module. An isocratic flow rate of 1.0 mL/min composed of 3:7 water:acetonitrile (v:v) was used for separation of the target analytes. Detection was achieved using a Waters 2475 multiwavelength fluorescence detector. The optimal excitation and emission wavelengths used for quantification of each of the PAHs were taken from Futoma et al. (1981). All analyses utilized linear calibration curves with

a minimum of five points. Check standards and blanks were used with every sample set to ensure performance. Seven PAHs were analyzed in all of these studies: phenanthrene (PHE), pyrene (PYR), benz[a]anthracene (BAA), chrysene (CHR), benzo[b]fluoranthene (BBF), benzo[k]fluoranthene (BKF), and benzo[a]pyrene (BAP).

PCB analysis was performed using gas chromatography for separation with electron capture detection (GC/ECD) for analyte quantification using a modified Environmental Protection Agency (EPA) method 8082. Analyses were performed at both the University of Texas (UT) and Stanford University. Analyses at UT were performed using an Agilent Technologies, Inc. (Santa Clara, CA) model 6890 gas chromatograph with a ^{63}Ni micro-electron capture detector. Hydrogen was used as the carrier gas and nitrogen as the make-up gas. Separation was achieved using a 60-m long, 250-µm diameter fused-silica model HP-5 capillary column from Agilent Technologies (Santa Clara, CA). Standards were developed using a known PCB mixture from the EPA's National Health and Environmental Effects Research Laboratory 1 in Grosse Ile, MI (EPA, 1997). The method simulates Aroclor 1242 using a 75:54:54 mixture of Aroclors 1232, 1248, and 1262, respectively. All analyses utilized linear calibration curves with a minimum of five points. PCB congener number 209 (decachlorobiphenyl) was used as an internal standard. Check standards and blanks were used with every sample set to ensure performance.

The total organic carbon of sediment samples was determined by elemental analysis on a Carlo-Erba 1108 according to Hedges and Stern (1984) modified according to Harris et al. (2001) (i.e., overnight vapor acidification with a hydrochloric acid atmosphere to remove inorganic carbon from samples). The oxidation column was run at

1020°C, while the reduction column was run at 650°C. The oven temperature was maintained at 60°C. Each sample was measured in triplicate and the results averaged to obtain the final values used for analysis.

7.3.2 PDMS Fibers

Three different PDMS fibers were used in these studies. The first two fibers (hereafter referred to as PM 170/110) were obtained from Poly Micro Industries (Phoenix, AZ). The first had a 110-µm core with a 30-µm PDMS coating or outer diameter of 170 µm, which equates to a specific volume of 13.55 µL/m fiber. The second fiber (hereafter referred to as PM 1060/1000) had a 1-mm (1000-µm) core with a 30-µm coating, which equates to a specific volume of 123.6 µL/m fiber. The third fiber (hereafter referred to as FG 230/210) was obtained from Fiber Guide Industries (Stirling, NJ) and had a 210-µm core with a 10-µm PDMS coating or outer diameter of 230-µm, which equates to a specific volume of 6.91 µL/m fiber. The fibers were very thin, brittle, and nearly transparent.

Each of the PDMS fibers was tested in the laboratory to verify its ability to quantify sediment pore water concentrations. Partitioning of PAHs between the PDMS and the pore water was found to be linear and consistent with linear partition coefficients estimated using the correlation presented by Mayer et al. (2000b). For PAHs, partitioning was measured for individual compounds, with the best fit determined to be:

$$\log K_f = 0.839 * \log K_{ow} + 0.117 \qquad (7.16)$$

Where K_f is the partition coefficient between the pore water and the PDMS coating and K_{ow} is the *n*-octanol-water partition coefficient. Equilibrium was attained within a day for

lower molecular weight compounds but required up to a month for higher weight compounds. For PCBs, values for K_{ow} were taken from Hawker and Connell (1988). Using both values from Mayer et al. (2000b) and others measured specifically for these experiments, the best fit for PCBs was determined to be:

$$\log K_f = 1.03 * \log K_{ow} - 0.938 \quad (7.17)$$

For all PDMS fiber analyses, the fiber was cleaned prior to deployment by sonication in hexane for a minimum of half an hour, followed by a rinse with acetone and then de-ionized water. After equilibration of the fibers with the sediment, fibers were rinsed clean (to remove any particles) with deionized water and then placed into 100 µL HPLC inserts with either 100 µL of acetonitrile (for PAHs) or 100 µL of hexane (for PCBs). The solvents were found to remove essentially 100% of the PAH mass from the fiber within 24 hours. Some interference was observed in the method blanks; congeners with mean values of less than three times the value observed in the blank were removed from the dataset.

7.3.3 Laboratory Assessment of PAH Uptake Kinetics

The uptake of PAHs and in PDMS fibers were assessed in a series of laboratory experiments. Data were taken from Skwarski (2008). Sediment was taken from the Anacostia site described previously, sieved through a No. 8 (2.35 mm) sieve and homogenized. Contaminant mass in PDMS fibers was monitored over time in a series of experiments using Anacostia River sediment in sealed glass vials with Teflon-coated caps. The PM 170/110 fiber was analyzed for PAHs in quadruplicate after 1, 2, 5, 10, and 20 days. Sodium azide was added to all reactors to prevent microbial degradation.

7.3.4 Hunters Point Field Assessment of PCB Pore Water Concentrations

Hunters Point Naval Shipyard is the site of an extensive field demonstration of the ability to reduce contaminant bioavailability using *in situ* stabilization with activated carbon as described in Chapter 2, section 2.5.3. Further details of this site are described by Cho et al. (2009). For this study, sediment from the site was sieved through a No. 8 (2.35 mm) sieve and homogenized. The sediment was placed into a cage along with three 5-cm length pieces of the FG 230/210 and three 2-cm length pieces of the PM 1000/1060 fiber. Cages were then placed into the Hunters Point tidal mudflat and then retrieved after 14 and 42 days. The PCB concentrations of the congeners in both fibers were then analyzed.

7.4 Results and Discussion

7.4.1 Laboratory-Scale Reactors from Anacostia

The uptake rates of PAHs in the PM 170/110 fibers were studied in a series of batch kinetics experiments. Samples were taken at 1, 2, 5, 10, and 20 days and averaged. To predict contaminant uptake rates from the sediment, estimates were made for the parameters in the radial diffusion model. The bulk density and porosity were assumed to be typical sediment values of 1.0 kg/L and 0.6, respectively. The fraction organic carbon was analyzed and determined to be about 1%. As no HC analysis had been performed on the Anacostia sediment, for an initial assumption interactions with HC were assumed to be irrelevant; thus f_{hc} was assumed to be zero, $f_{lc} = f_{oc}$, and $k_h = \infty$. The values of D_w were estimated using the correlation of Hayduk and Laudie (1974). The values for K_{lc} were estimated using the correlation with the octanol-water partition coefficient presented by Schwarzenbach et al. (2003). No assumption was necessary for K_{hc} as f_{hc} was assumed to

be zero. Finally, the values of K_f were estimated from Equation (7.16). Table 6 summarizes the parameters for the sediment and each of the PAHs.

Table 6: Parameters from Anacostia Sediment, PDMS Fiber, and PAHs

Sediment and Fiber Parameters

Parameter	Value	Units
bulk density, ρ	1.0	kg/L
porosity, ε	0.6	
fraction organic carbon, f_{oc}	0.01	
fraction HC, f_{hc}	0	
fraction LC, f_{lc}	0.01	
Sediment mass transfer rate, k_h	∞	
inner fiber radius, r_1	55	μm
outer fiber radius, r_2	85	μm

Compound Properties and Results

Compound	log K_{ow}[28] (L/kg)	log K_{oc}[29] (L/kg)	log K_f (L/kg)	D_w[30] (cm^2/s)	% Steady State (20 days)	Estimated C_0 (ng/L)
PHE	4.57	4.2	3.8	4.8E-6	98.8	400
PYR	5.18	4.8	4.4	4.9 E-6	93.4	7000
CHR	5.81	5.4	5.0	4.6 E-6	70.5	270
BAA	5.61	5.2	4.8	4.6 E-6	80.1	280
BBF	6.10	5.7	5.3	4.3 E-6	54.9	550
BKF	6.11	5.7	5.4	4.3 E-6	54.4	320
BAP	6.13	5.7	5.4	4.3 E-6	53.3	500

The only unknown parameter for each compound was the initial concentration. To illustrate the behavior of the model for the various PAHs, Figure 27 shows the dimensionless concentration profiles for the seven compounds. The graphs demonstrate that even under the assumption of instantaneous release of contaminants from the

[28] MacKay et al. (1992)
[29] Estimated using correlation provided by Schwarzenbach et al. (2003)
[30] Estimated using correlation provided by Hayduk and Laudie (1974)

particles, steady state conditions can take weeks to months to occur depending on the hydrophobicity of the compounds.

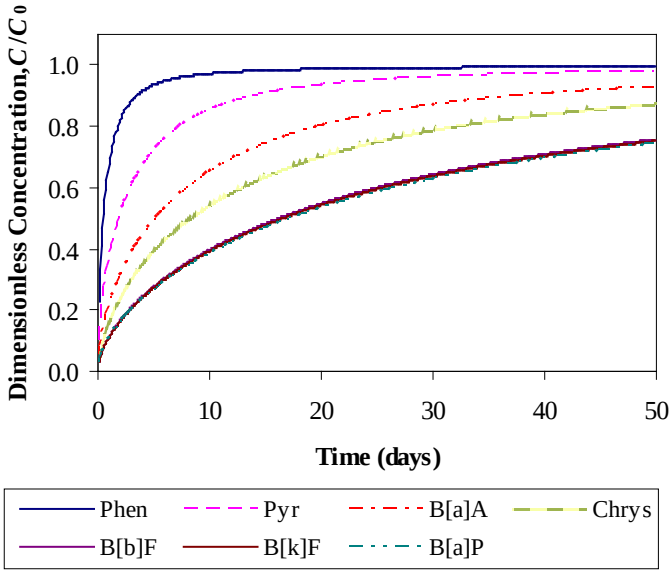

Figure 27. Dimensionless uptake rates in PDMS fibers under different sediment release rates for PAHs.

The dimensionless uptake rate $M/\left(\pi(r_2^2 - r_1^2)K_f C_0\right)$ is shown for the parameters from Table 6.

Figure 28 shows the experimental results for PHE, CHR, and BKF (one 3-ring, one 4-ring, and one 5-ring PAH). The error bars represent one sample standard deviation from the set of four. The models were fit to the data using only the value of C_0, which serves only to scale the results. The fit appears to be quite consistent with uptake kinetics predictions. Fits for the other compounds showed similar results. From the model it is possible to infer the pore water concentrations in the sediment despite non-attainment of equilibrium. The estimated values of C_0 after correction for non-equilibrium and the percent steady state at 20 days are shown for each compound in Table 6.

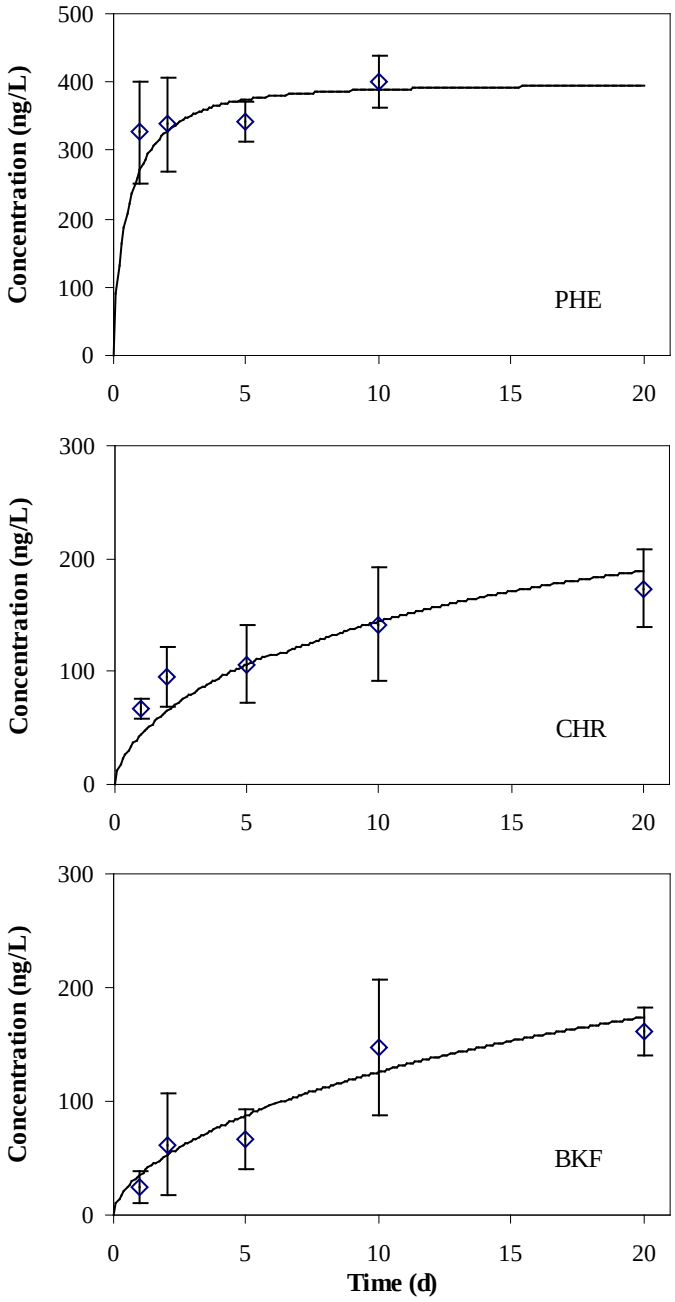

Figure 28. Batch uptake experimental results and model predictions.[31]

Mean concentrations (n = 4) and model predictions, error bars represent one sample standard deviation for PHE, CHR, and BKF.

[31] Experimental data taken from Skwarski (2008)

In these simulations, the release rate from the sediments was assumed to be instantaneous from all carbon phases. Since the data fit the model well, it can be inferred that there was little HC present in the Anacostia sediment or that its presence did not significantly affect equilibration time in the fibers. The actual field K_{oc} was likely larger than that estimated using the correlation, but because of slow kinetics the HC may have little impact on the uptake. Without the actual HC value it is difficult to ascertain. However, as these results have demonstrated, the assumption of fast release provides a reasonable first-cut approach for estimating the concentrations in pore water in systems where equilibrium may not be attained. It should be noted that the corrections were made without fitting any parameters other than the scaling factor C_0; as a result, this approach can be applied provided the values of the parameters listed in Table 6 are known.

7.4.2 Model Application to Field Data from Hunters Point

To test the application of the model to field data, a study was performed at Hunters Point comparing the concentrations derived from two PDMS fibers, PM 1060/1000 fiber and the FG 230/210 fiber (believed to have different kinetic properties due to different surface area to volume ratios) to those in worm tissues. Fibers were sampled at 14 and 42 days. A total of 39 congeners were present at levels distinguishable from method blanks. For both the small and large fiber in both treated and untreated sediment, the concentrations at 42 days were larger than for 14 days for almost all congeners, which suggests equilibrium was not attained for many of the compounds within the 14-day period.

To assess uptake kinetics, the radial diffusion model was applied to each of the individual congeners to assess contaminant uptake rates. Previous work at Hunters Point

had characterized HC to be 5-7% (Ghosh et al. 2003). The f_{oc} was measured and found to be between 0.007 and 0.011; a value of 0.01 was taken for simplicity. Bulk density and porosity were again assumed to be 1.0 kg/L and 0.6 for simplicity. The values of D_w for each congener were estimated using the correlation of Hayduk and Laudie (1974). The values for K_{lc} were estimated using the correlation with the octanol-water partition coefficient presented by Baker et al. (1997). Octanol-water partition coefficients were taken from Hawker and Connell (1988). Sorption onto HC was assumed to be two orders of magnitude greater than LC as discussed by Zimmerman et al. (2004) for Hunters Point sediment. For an initial assessment, release of contaminants from HC was assumed to be either instantaneous or negligible. Fiber-water partition coefficients were estimated using Equation (7.17). The parameters used are summarized in Table 7.

Table 7: Parameters from Hunters Point Sediment

Parameter	Value	Units
bulk density, ρ	1.0	kg/L
porosity, ε	0.6	
fraction organic carbon, f_{oc}	0.01	
fraction HC, f_{hc}	0	
fraction LC, f_{lc}	0.01	
Sediment mass transfer rate, k_h	∞	s^{-1}

Concentrations were measured at two points in time using two fibers, which when coupled with the kinetics model provides four independent estimates of C_0. Table 8 presents a summary of the data, including the 14-day and 42-day concentrations for both fibers in the sediment. For an initial comparison, the values of C_0 at 14 days assuming equilibrium had been attained were plotted as shown in Figure 29. The values obtained

from the larger fiber were consistently smaller as shown in the figure, which was attributed to slower kinetics. For an initial assessment of kinetic effects, the concentrations of each compound were corrected using model predictions with instant release from the particles for the 14-day data. These results are displayed in Figure 29 and showed a dramatic improvement of the consistency of the two datasets.

To assess the best method for modeling the release rate from the sediment particles, model predictions were developed under three extreme cases: instantaneous release from the sediment, no release from the HC, and no release from any carbon. The ratio of the 14-day to 42-day concentrations for both fibers and the ratio of the measured 14-day and 42-day concentrations were then plotted for the sediment as shown in Figure 30. The PM 1060/1000 showed high and relatively constant ratio for all compounds. The similarities amongst most the congeners were the result of the long time from equilibrium, which made model predictions similar. In addition, the influence of the hard carbon release rate likely affected some parameters more than others. For the smaller FG 230/210 fiber, mass accumulated in the fiber more quickly and thus differences in behavior were observed for some of the lighter molecular weight congeners. From visual inspection, it appears that the smaller FG 230/210 fiber is better approximated than the PM 1060/1000 fiber using the model predictions. Since the 14-day data demonstrated lower relative standard deviations, the values from this dataset were corrected for equilibrium using the no release from HC model. The estimations of the fraction of steady state using the no release from HC are presented in Table 9.

Table 8: 14-Day and 42-Day Concentrations in Hunters Point Sediment

Congener	log K_{ow}[32]	PM 1060/1000 14-Day	PM1060/1000 42-Day	FG 230/210 14-Day	FG 230/210 42-Day
51	5.63	1114	2564	1264	2789
52	5.84	5247	8612	6992	8560
47	5.85	1138	3226	1650	2216
41	5.69	810	2336	1257	2073
40	5.66	1275	1879	1840	2518
81	6.36	267	773	570	1209
77	6.36	846	2413	1762	2993
95	6.13	3767	9550	7917	14279
91	6.13	257	512	362	602
92	6.35	738	338	1242	2316
101	6.38	1079	1828	2284	4570
99	6.39	471	1290	749	2596
83	6.26	63	334	147	158
85	6.30	110	366	229	490
107	6.71	48	68	111	202
123	6.74	1018	2788	2363	4737
118	6.74	145	424	305	723
105	6.65	421	1227	927	2358
136	6.22	427	1198	1234	2243
134	6.55	62	152	128	277
146	6.89	150	424	346	848
153	6.92	982	2658	2196	5130
141	6.82	115	343	279	671
163	6.99	750	2004	1614	3665
158	7.02	78	192	154	354
178	7.14	49	140	100	224
187	7.17	161	419	366	840
183	7.20	202	602	435	1080
185	7.11	17	41	39	86
174	7.11	139	366	303	736
177	7.08	91	237	191	418
172	7.33	29	45	37	73
180	7.36	158	425	225	682
191	7.55	4	10	8	17
170	7.27	40	107	75	146
201	7.62	16	43	36	70
203	7.65	20	51	39	79
195	7.56	10	25	21	42
194	7.80	6	16	11	22

[32] Hawker and Connell (1988)

Table 9: Fraction of Steady State Predicted by PDMS Diffusion Model

Congener	log K_{ow}[33]	PM 1060/1000 14-Day	PM1060/1000 42-Day	FG 230/210 14-Day	FG 230/210 42-Day
51	5.63	0.36	0.56	0.83	0.95
52	5.84	0.29	0.47	0.75	0.91
47	5.85	0.29	0.47	0.75	0.91
41	5.69	0.36	0.56	0.83	0.95
40	5.66	0.36	0.56	0.83	0.95
81	6.36	0.15	0.27	0.49	0.73
77	6.36	0.15	0.27	0.49	0.73
95	6.13	0.19	0.33	0.59	0.82
91	6.13	0.19	0.33	0.59	0.82
92	6.35	0.15	0.27	0.49	0.73
101	6.38	0.17	0.28	0.51	0.74
99	6.39	0.17	0.28	0.51	0.74
83	6.26	0.17	0.30	0.54	0.77
85	6.30	0.15	0.27	0.49	0.73
107	6.71	0.10	0.17	0.32	0.53
123	6.74	0.10	0.17	0.32	0.53
118	6.74	0.10	0.17	0.32	0.53
105	6.65	0.11	0.19	0.36	0.58
136	6.22	0.17	0.30	0.54	0.77
134	6.55	0.12	0.21	0.40	0.63
146	6.89	0.07	0.12	0.24	0.41
153	6.92	0.07	0.12	0.24	0.41
141	6.82	0.09	0.15	0.29	0.48
163	6.99	0.06	0.11	0.21	0.37
158	7.02	0.06	0.11	0.21	0.37
178	7.14	0.05	0.10	0.19	0.33
187	7.17	0.06	0.10	0.20	0.35
183	7.20	0.05	0.08	0.16	0.29
185	7.11	0.05	0.10	0.19	0.33
174	7.11	0.05	0.10	0.19	0.33
177	7.08	0.05	0.10	0.19	0.33
172	7.33	0.04	0.08	0.15	0.26
180	7.36	0.04	0.08	0.15	0.26
191	7.55	0.03	0.06	0.11	0.20
170	7.27	0.04	0.08	0.15	0.26
201	7.62	0.03	0.05	0.10	0.18
203	7.65	0.03	0.05	0.10	0.18
195	7.56	0.03	0.06	0.11	0.20
194	7.80	0.02	0.04	0.07	0.13

[33] Hawker and Connell (1988)

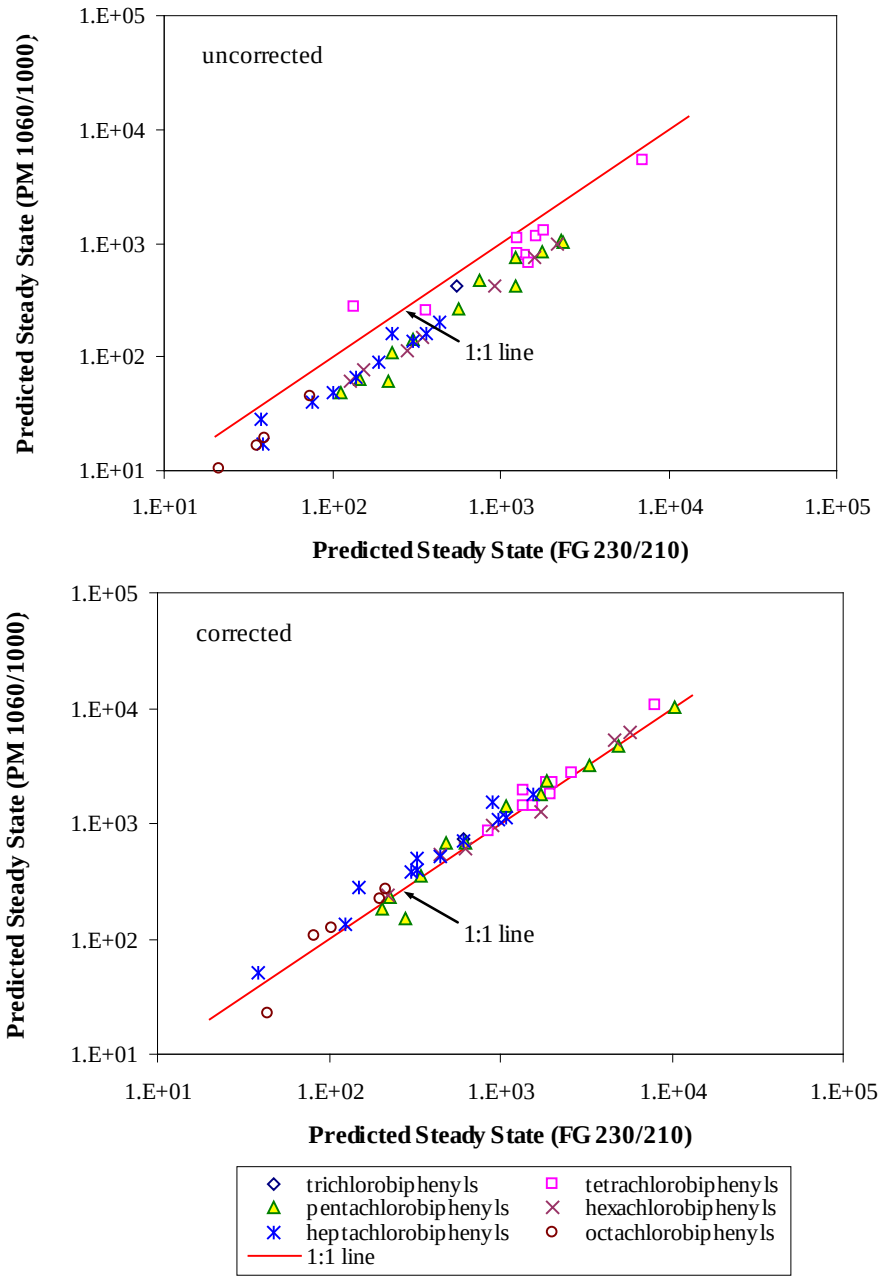

Figure 29. Comparison of 14-day PM 1060/1000 fiber predictions to FG 230/210 before (top) and after (bottom) applying a correction for kinetics.

The 14-day predictions from the larger fiber were lower than the smaller fiber because of failure to attain equilibrium corrections. Assuming instant release of particles from the sediment phase, the concentrations were corrected for kinetics which dramatically improved the consistency of the predicted pore water concentrations.

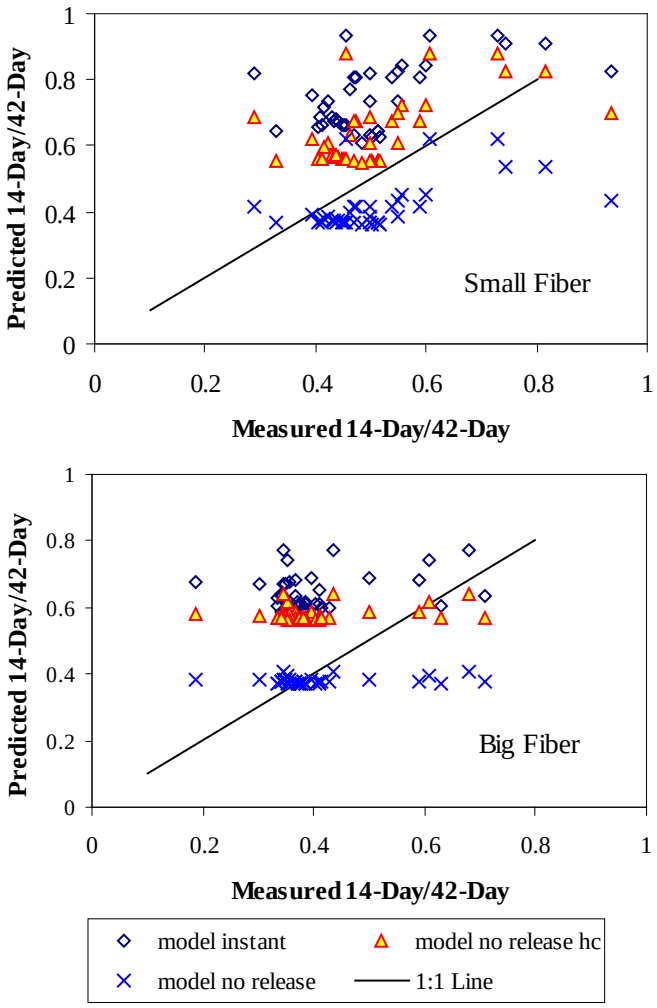

Figure 30. Comparison of release rate kinetics models to experimental data.

Three release rate extremes were considered to compare with experimental data. It appears that the no release from HC is the closest fit to the data for both fibers and that the small fiber with no release from HC provides the best fit to the predictions.

7.5 Summary and Conclusions

In this study, a radial diffusion model was used to interpret experimental results of uptake of HOCs in PDMS fibers. In a laboratory setting, the model was found to predict the equilibrium of PAHs quite accurately by fitting only the sediment release rate (assumed to be infinite). The model predictions from this approach can be used to

estimate the equilibrium concentration when it is infeasible to wait for equilibrium. The modeling approach was applied to PCBs from Hunters Point sediment to correct measured field values. The sediment release rate was determined to be fast for Anacostia sediment and slower for Hunters Point. This may be the result of the high fraction of HC present at Hunters Point. Future experiments are needed to gain further insight into the sediment release rate, which could be important for calibration of the model in the future.

7.6 References

1. Accardi-Dey, A. and Gschwend, P.M. 2002. "Assessing the Combined Roles of Natural Organic Matter and Black Carbon as Sorbents in Sediments," Environmental Science & Technology, 36:21-29.
2. Adams, R.G., Lohman, R., Fernandez, L.A., MacFarlane, J.K., and Gschwend, P.M. 2007. "Polyethylene Devices: Passive Samplers for Measuring Dissolved Hydrophobic Organic Compounds in Aquatic Environments," Environmental Science & Technology, 41(4):1317-1323.
3. Arp, H.P., Breedveld, G.D., Cornelissen, G.E. 2009. "Estimating the in situ sediment-porewater distribution of PAHs and chlorinated aromatic hydrocarbons in anthropogenic impacted sediments," Environmental Science & Technology, 43(15): 5576-5585.
4. Baker, J.R., Mihelcic, J.R., Luehrs, D.C., and Hickey, J.P. 1997. "Evaluation of Estimation Methods for Organic Carbon Normalized Sorption Coefficients," Water Environment Federation, 69(2):136-145.
5. Cho Y.M., Ghosh U., Kennedy A.J., Grossman A., Ray G., Tomaszewski J.E., Smithenry D.W., Bridges T.S., Luthy R.G. 2009. "Field application of activated

carbon amendment for in-situ stabilization of polychlorinated biphenyls in marine sediment," Environmental Science & Technology, 43(10):3815-3823.

6. Cornelissen, G. and Gustafsson, O. 2004. "Sorption of Phenanthrene to Environmental Black Carbon in Sediment with and without Organic Matter and Native Sorbates," Environmental Science & Technology, 38:148-155.
7. Cornelissen, G., Petterson, A., Broman, D., Mayer, P., and Breedveld, D. 2008. "Field Testing of Equilibrium Passive Samplers to Determine Freely Dissolved Native Polycyclic Aromatic Hydrocarbon Concentrations," Environmental Toxicology and Chemistry, 27(3):499-508.
8. Doucette, W.J., 2003. "Quantitative structure-activity relationships for predicting soil-sediment sorption coefficients for organic chemicals," Environmental Toxicology and Chemistry, 22:1771–1788.
9. EPA. 1997. Lake Michigan Mass Balance Study (LMMB) Methods Compendium, Volume 3: Metals, Conventionals, Radiochemistry, and Biomonitoring Sample Analysis Techniques; EPA-905/R-97-012c; U.S. Environmental Protection Agency, Great Lakes National Program Office: Chicago, IL, 1997.
10. Fernandez, L.A., Harvey, C.F., and Gschwend, P.M. 2009. "Using Performance Reference Compounds in Polyethylene Passive Samplers to Deduce Sediment Porewater Concentrations for Numerous Target Chemicals," Environmental Science & Technology, 43:8888-8894.
11. Ghosh, U., Zimmerman, J.R., and Luthy, R.G. 2003. "PCB and PAH Speciation amound Particle Types in Contaminated Harbor Sediments and Effects on PAH Bioavailability," Environmental Science & Technology, 37:2209-2217.

12. Gustaffson, O., Haghseta, F., Chan, C., Macfarlane, J., Gschwend, P.M. 1997. "Quantification of the Dilute Sedimentary Soot Phase: Implications for PAH speciation and Bioavailability," Environmental Science & Technology, 31:203-209.
13. Hawker, D.W. and Connell, D.W. 1988. "Octanol water partition-coefficients of polychlorinated biphenyl congeners," Environmental Science & Technology, 22(4):382-287.
14. Hayduk, W. and Laudie, H. 1974. "Predicting diffusion coefficients for nonelectrolytes in dilute aqueous solutions," AICheE Journal, 20:611.
15. Hedges, J.L., and Stern, J.H. 1984. "Carbon and Nitrogen Determination of Carbonate-Containing Solids," Limnology and Oceanography, 29:657–663.
16. Herbes, S.E. and Allen, C.P. 1983. "Lipid Quantification of Freshwater Invertebrates: Method Modification for Microquantification," Canadian Journal of Fisheries and Aquatic Sciences, 40:1315-1317.
17. Hong, L. and Luthy, R.G. 2008. "Uptake of PAHs into polyoxymethylene and application to oil-soot (lampblack)-impacted soil samples," Chemosphere, 72(2):272-281.
18. Jonker, M.T. and Koelmans, A.A. 2001. "Polyoxymethylene solid phase extraction as a partitioning method for hydrophobic organic chemicals in sediment and soot," Environmental Science & Technology, 35:3742-3748.
19. Karickhoff, S.W., Brown, D.S., and Scott, T.A. 1979. "Sorption of Hydrophobic Pollutants in Natural Sediments," Water Research, 13, 241-248.
20. Karickhoff, S.W. 1981. "Semi-Empirical Estimation of Sorption of Hydrophobic Pollutants on Soils and Sediments," Chemosphere, 10:833-846.

21. Kraaij R., Mayer P., Busser F.J.M., Bolscher M.V.H., Seinen W., Tolls J. 2003. “Measured pore-water concentrations make equilibrium partitioning work-a data analysis,” Environmental Science & Technology 37:268-274.
22. Lu, X., Reible, D.D., Fleeger, J.W. 2006. “Bioavailability of Polycyclic Aromatic Hydrocarbons in Field-Contaminated Anacostia River (Washington, DC) Sediment,” Environmental Toxicology and Chemistry, 25(11):2869-2874.
23. Mayer, P., Vaes, W., Wijnker, F., Legierse, K., Kraaij, R., Tolls, J., and Hermans, J. 2000. “Sensing Dissolved Sediment Porewater Concentrations of Persistent and Bioaccumulative Pollutants Using Disposable Solid-Phase Microextraction Fibers,” Environmental Science & Technology, 34:5177-5183.
24. Meloche, L.M, deBruyn, A.M.H., Otton, S.V., Ikonomou, M.G., and Gobas, F.A.P.C. 2009. “Assessing exposure of sediment biota to organic contaminants by thin-film solid phase microextraction,” Environmental Toxicology and Chemistry, 28:247–253.
25. Namiesnik, J., Zabiegala, B., Kot-Wasik, A., Partyka, M., and Wasik, A. 2005. "Passive sampling and/or extraction techniques in environmental analysis: a review." Analytical and Bioanalytical Chemistry, 381(2):279-301.
26. Schwarzenbach, R.P., Gshwend, P.M., Imboden, D.M. 2003. “Chapter 9: Sorption I: Introduction and Sorption Processes Involving Organic Matter” and “Chapter 11: Sorption III: Sorption Processes Involving Inorganic Surfaces,” Environmental Organic Chemistry, 2nd Edition, Wiley & Sons, Hoboken, New Jersey, 275-330 and 387-458.

27. Skwarski, A.E. 2008. Demonstration and Evaluation of Solid-Phase Microextraction for Assessment of Contaminant Mobility and Bioavailability, Master's Thesis, The University of Texas at Austin.
28. US EPA. 1998. Contaminated Sediment Management Strategy (EPA 823-R-98-004). Accessed via website http://www.epa.gov/OST/cs/ stratefs.html.
29. Zimmerman, J.R., Ghosh, U., Millward, R.N., Bridges, T.S., Luthy, R.G. 2004. "Addition of Carbon Sorbents to Reduce PCB and PAH Bioavailability in Marine Sediments: Physicochemical Tests," Environmental Science & Technology, 38(20):5458-5464.

Chapter 8: Application of a PDMS Passive Sampler for Assessing Bioaccumulation of Hydrophobic Organic Compounds from Sediments[34]

David J. Lampert[35], Xiaoxia Lu[36], and Danny D. Reible[37]

8.0 Abstract

Sediments frequently present a residual environmental risk as a route of entry for hydrophobic organic contaminants (HOCs) into the food chain. Passive sampling with a sorbent phase such as polydimethylsiloxane (PDMS) for measuring pore water concentrations is a promising technique for assessing availability of HOCs in contaminated sediments. In this paper, a method for measuring *in situ* pore water concentrations using a field-deployable PDMS sampling device is presented. The predicted pore water concentrations using the device are demonstrated to correlate well with bioaccumulation in the field. Similar results were seen in untreated sediment, sediment caps, and sediment undergoing *in situ* stabilization with activated carbon. By applying a correction for slow uptake kinetics, correlations between bioaccumulation and observed pore water concentrations were improved. As a result, it appears that the PDMS sampling device is an appropriate means of assessing both sediment quality and the effectiveness of *in situ* treatment technologies.

---

[34] Manuscript in preparation for submission

[35]PhD Candidate, Department of Civil, Architectural, Environmental Engineering, The University of Texas at Austin, 1 University Station C1786, Austin, TX 78712-0273, djl@mail.utexas.edu

[36]Research Associate, Department of Civil, Architectural, Environmental Engineering, The University of Texas at Austin, 1 University Station C1786, Austin, TX 78712-0273,

[37] Bettie Margaret Smith Professor of Environmental Health Engineering, Department of Civil, Architectural, Environmental Engineering, The University of Texas at Austin, 1 University Station C1786, Austin, TX 78712-0273, reible@mail.utexas.edu

8.1 Introduction

Sediments serve as the ultimate sink for many hydrophobic organic compounds (HOCs) such as polycyclic aromatic hydrocarbons (PAHs) and polychlorinated biphenyls (PCBs). As a result, the presence of HOCs in sediments often presents a residual environmental risk many years after sources of contamination are cut off. Because of poor understanding of the ecological risks associated with contaminated sediments and the ubiquitous nature of the problem, assessment and remediation of contaminated sediments presents a major research challenge for the environmental community (US EPA, 1998).

A common method for interpreting the bioaccumulation of contaminants from sediments is equilibrium partitioning theory. This concept assumes that a contaminant will distribute among the sediment, pore water, and organisms according to a predictable partitioning relationship. The biota-sediment accumulation factor (BSAF) is frequently used to interpret the bioaccumulation of HOCs from sediments (McFarland 1984, Bierman 1990, Lu et al. 2006):

$$\mathrm{BSAF} = \frac{q_{lipid}}{q_{oc}} = \frac{q_{organism} / f_{lipid}}{q_{sediment} / f_{oc}} \tag{8.1}$$

Where q_{lipid} represents the contaminant lipid-phase concentration of the organism, q_{oc} is the contaminant concentration in the sediment organic matter, $q_{organism}$ is the contaminant concentration in the organism, $q_{sediment}$ is the contaminant concentration in sediment, f_{lipid} is the lipid fraction of the organism, and f_{oc} is the organic carbon fraction in sediment. In equilibrium partitioning theory, the BSAF is theoretically the same for a particular

contaminant in different sediments because bioaccumulation of a contaminant is dictated by the contaminant concentration in the organic carbon. This approach thus assumes equilibrium conditions between sediment organic matter and organism tissue. Recent studies have shown that contaminant release from sediment organic carbon can vary significantly from site to site (McGroddy and Farrington 1995, Ghosh et al. 2003, Accardi-Dey and Gschwend 2002) and may be very slow due to the presence of "black" or "hard" carbon phases. As a result, the bulk solid-phase concentration often correlates poorly with bioavailability (Burton 1991).

The difficulties with the traditional BSAF approach for predicting bioaccumulation of contaminants has led researchers to search for an alternative means of predicting uptake (i.e., the pore water concentration C_w). Assuming that a lipid-water equilibrium partition coefficient K_{lw} exists, the lipid-normalized tissue concentration q_{lipid} can be predicted by:

$$q_{lipid} = K_{lw} C_w \tag{8.2}$$

The *n*-octanol-water partition coefficient K_{ow} is often used as a surrogate for K_{lw} (Mackay 1982, Isnard and Lambert 1988, Bintein et al. 1993).

Measurements of *in situ* pore water concentrations using this concept have been linked to bioaccumulation of HOCs in sediments (Kraaij et al. 2003, Lu et al. 2006, Meloche et al. 2009). However, direct measurement of HOC concentrations in the aqueous phase is often difficult due to analytical limitations; thus the much more readily quantified solid-phase concentration is often used for assessment of sediment quality (Doucette 2003) despite its poor correlation with bioavailability (Burton 1991). As a

result, a current research topic is the use of passive sampling devices for assessing pore water concentrations of HOCs in sediments.

Various passive sampling approaches have been tested for estimation of *in situ* HOC pore water concentrations, including semi-permeable membrane devices (SPMDs) (Booij et al. 1998), polyoxymethylene (POM) sheets (Jonker and Koelmens 2001), polyethylene (PE) sheets (Vinturella et al. 2004), and polydimethyl siloxane (PDMS) coated glass fibers (Mayer et al. 2000a). Each of these techniques "passively" samples the pore water concentration using a pre-established relationship between the mass sorbed onto the sampling device and the sediment.

The PDMS-coated fibers can be manufactured to very small sizes (e.g., 200 µm glass diameter with 15-µm PDMS coating, Mayer et al. 2000a). Because of this relatively small size, the method does not significantly deplete the neighboring sediment particles, and hence should not affect the equilibrium chemistry. The small thickness also equates to more rapid equilibration times.

Pore water concentrations measured using the PDMS fiber technique have been linked to bioaccumulation in laboratory studies. You et al. (2006) performed a comparison of various methods for predicting bioaccumulation of PAHs in laboratory-spiked and field-contaminated sediments using oligochaetes and found that PDMS fibers to be an excellent predictor of bioaccumulation. Trimble et al. (2008) assessed the bioaccumulation of PCBs to oligochaetes from field-contaminated sediments in the laboratory with PDMS fibers and found the technique to be a suitable substitute for traditional bioassays.

Based on the success of these studies and the laboratory analysis described in Chapter 5, it appears that PDMS fibers can be used as a biomimetic for assessing sediment quality. The next step in developing this technique is proof of concept at the field level. The purpose of this paper is to document the application of the PDMS sampler to various contaminated sites to demonstrate that PDMS-derived pore water concentrations correlate well with bioaccumulation from contaminated sediments *in situ*. A field-deployable apparatus was developed for *in situ* sampling with the PDMS fibers for characterization of HOC concentrations. The PDMS sampling method was applied at three locations, Naval Station San Diego, San Diego, CA, the Anacostia River in Washington DC, and Hunters Point Naval Station, San Francisco, CA. Through these results, it is demonstrated that PDMS-derived pore water concentrations provide an appropriate means of assessing the impairment of sediment site as opposed to a costly and highly variable bioaccumulation study or an inappropriate measure such as the bulk solid-phase concentration.

8.2 Materials and Methods

8.2.1 Analytical Methods

PAHs and PCBs were chosen as target analytes in the study due to their ubiquitous nature and relative sensitivity. PAH analysis was performed at the University of Texas at Austin (UT) using high performance liquid chromatography for separation with fluorescence detection (HPLC/FD) for quantification and at the United States Army Corps of Engineers Research and Development Center (ERDC) by gas chromatography with mass spectrometry (GC-MS). Analyses at UT were performed in accordance with EPA Method 8310: Polynuclear Aromatic Hydrocarbons using a Waters 2795

Separations Module. An isocratic flow rate of 1.0 mL/min composed of 3:7 water:acetonitrile (v:v) was used for separation of the target analytes. Detection was achieved using a Waters 2475 multiwavelength fluorescence detector. The optimal excitation and emission wavelengths used for quantification of each of the PAHs were taken from Futoma et al. (1981). PAH analysis performed by ERDC utilized by gas chromatography with mass spectrometry (GC-MS) in accordance with EPA Methods 3550b and 8271. All analyses utilized linear calibration curves with a minimum of five points. Check standards and blanks were used with every sample set to ensure performance. The method was optimized for quantification of seven PAHs: phenanthrene (PHE), pyrene (PYR), benz[a]anthracene (BAA), chrysene (CHR), benzo[b]fluoranthene (BBF), benzo[k]fluoranthene (BKF), and benzo[a]pyrene (BAP).

PCB analysis was performed using gas chromatography for separation with electron capture detection (GC/ECD) for analyte quantification using a modified Environmental Protection Agency (EPA) method 8082. Analyses were performed by both UT and Stanford University. Analyses at UT were performed using an Agilent Technologies, Inc. (Santa Clara, CA) model 6890 gas chromatograph with a ^{63}Ni micro-electron capture detector. Hydrogen was used as the carrier gas and nitrogen as the make-up gas. Separation was achieved using a 60 m long, 250 μm diameter fused-silica model HP-5 capillary column from Agilent Technologies (Santa Clara, CA). Standards were developed using a known PCB mixture from the EPA's National Health and Environmental Effects Research Laboratory 1 in Grosse Ile, MI (EPA, 1997). The method simulates Aroclor 1242 using a 75:54:54 mixture of Aroclors 1232, 1248, and 1262, respectively. All analyses utilized linear calibration curves with a minimum of five

points. PCB congener number 209 (decachlorobiphenyl) was used as an internal standard. Check standards and blanks were used with every sample set to ensure performance.

The total organic carbon (f_{oc}) of sediment samples was determined by elemental analysis on a Carlo-Erba 1108 according to Hedges and Stern (1984) modified according to Harris et al. (2001) (i.e., overnight vapor acidification with a hydrochloric acid atmosphere to remove inorganic carbon from samples). The oxidation column was run at 1020°C, while the reduction column was run at 650°C. The oven temperature was maintained at 60°C. Each sample was measured in triplicate and the results averaged to obtain the final values used for analysis.

Lipid content was assessed using the method first described by Herbes and Allen (1983) to convert wet worm tissue loadings to lipid-phase concentrations. Twenty worms (~100 mg wet weight) were transferred to pre-weighed 15-mL centrifuge tubes and then re-weighed to assess worm mass. Five mL of a 1:1 (v:v) solution of reagent grade methanol and reagent grade chloroform (Fisher Scientific, Waltham, MA) were added to each tube for lipid extraction. The samples were then sonicated for 30 seconds and allowed to equilibrate for four hours. The tubes were centrifuged, and the supernatant was transferred to a new tube. An addition five mL of the methanol-chloroform solution were added to the original tube to remove any remaining extract. The extract was then equilibrated with two mL of water to remove tissue protein, dried at 50°C, and weighed to assess the lipid mass in the original sample. Method blanks were evaluated and showed no solvent residuals.

8.2.2 PDMS Fibers

Three different PDMS fibers were used in these studies. The first two fibers (hereafter referred to as PM 170/110) were obtained from Poly Micro Industries (Phoenix, AZ). The first had a 110-µm core with a 30-µm PDMS coating or outer diameter of 170 µm, which equates to a specific volume of 13.55 µL/m fiber. The second fiber (hereafter referred to as PM 1060/1000) had a 1-mm (1000-µm) core with a 30-µm coating, which equates to a specific volume of 123.6 µL/m fiber. The third fiber (hereafter referred to as FG 230/210) was obtained from Fiber Guide Industries (Stirling, NJ) and had a 210-µm core with a 10-µm PDMS coating or outer diameter of 230 µm, which equates to a specific volume of 6.91 µL/m fiber. The fibers were very thin, brittle, and nearly transparent.

8.2.3 Laboratory Characterization of PDMS Fibers

Each of the PDMS fibers was tested in the laboratory to verify its ability to quantify sediment pore water concentrations. Partitioning of PAHs between the PDMS and the pore water was found to be linear and consistent with linear partition coefficients estimated using the correlation presented by Mayer et al. (2000b). For PAHs, partitioning was measured for individual compounds, with the best fit determined to be:

$$\log K_f = 0.839 * \log K_{ow} + 0.117 \qquad (8.3)$$

Where K_f is the partition coefficient between the pore water and the PDMS coating and K_{ow} is the *n*-octanol-water partition coefficient. Equilibrium was attained within a day for lower molecular weight compounds but required up to a month for higher weight compounds. For PCBs, values for K_{ow} were taken from Hawker and Connell (1988).

Using the experimental values of K_f from Mayer et al. (2000b) and the values for K_{ow}, the best fit for PCBs was determined to be:

$$\log K_f = 1.03 * \log K_{ow} - 0.938 \quad (8.4)$$

For all PDMS fiber analyses, the fiber was cleaned prior to deployment by sonication in hexane for a minimum of half an hour, followed by a rinse with acetone and then de-ionized water. After equilibration of the fibers with the sediment, fibers were rinsed clean (to remove any particles) with deionized water and then placed into 100 µL HPLC inserts with either 100 µL of acetonitrile (for PAHs) or 100 µL of hexane (for PCBs). The solvents were found to remove essentially 100% of the PAH mass from the fiber within 24 hours.

8.2.4 Field PDMS sampling device

To measure concentrations of PAHs and PCBs in the field, an *in situ* apparatus for deploying the PDMS fibers was developed. To protect the fibers in the sediment column, a stainless steel piezometer was used as a tool to insert and recover the PDMS fibers into the sediment environment. An approximately 2-mm wide rectangular groove was made in the inner rod of the piezometer to serve as a frame for the fragile PDMS fibers. Approximately 0.5-mm thick slits were cut into the outer part of the piezometer at ¼" spacing to allow equilibration of the fiber with the neighboring sediment. The bottom and top of the rods were sealed shut to prevent an inflow of pore water through the system. Figure 31 shows a schematic of the PDMS field sampling device.

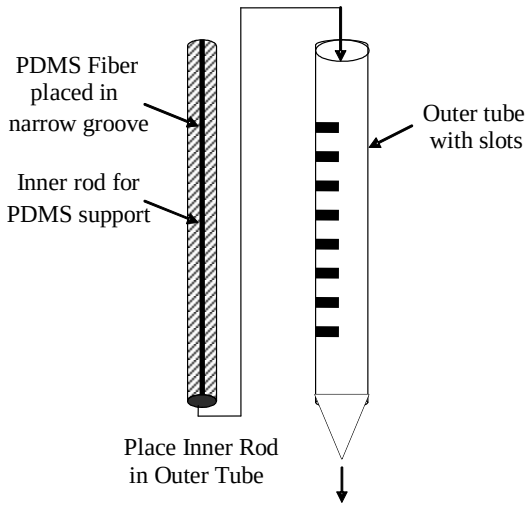

Figure 31. Field PDMS sampling device.

8.2.5 Test Organisms

Oligochaetes and polychaetes are benthic organisms that are responsible for intense sediment re-working and are often present in high densities in contaminated sediments (Reible et al. 1996). Due to their ability to tolerate significant environmental stresses, they make excellent test organisms for contaminant uptake in heavily contaminated environments. The freshwater deposit feeding oligochaetes *Ilyodrilus templetoni*, *Tubifex tubifex*, and *Lumbriculus variegatus* were used in Anacostia freshwater bioavailability experiments. For studies in marine environments, the polychaete *Neanthes arenaceodenta* and the bivalve mytilida *Musculista senhousia* (Asian date mussel) were used to assess bioaccumulation. In previous studies, these species have shown ability to handle stress, to be easily cultured, and to withstand a variety of sediment characteristics and exposures (Brinkhurst and Cook 1980, Lu 2003, Burton et al. 2005).

8.2.6 Field Worm Cages

To assess field bioaccumulation of HOCs in benthic invertebrates, worm cages were constructed based on the model described by Burton et al. (2005). The worm cages provide a means of inserting suitable test organisms with a known initial condition into a sediment site for evaluation of contaminant uptake. The standard *in situ* chamber was a cylinder constructed of transparent core tubing of cellulose acetate butyrate with a 6.67-cm inner diameter, 6.98-cm outer diameter, 0.16-cm wall thickness, and cut to a length of 12.7 cm. Polyethylene closures were used to cap each end. Two 4-cm by 8-cm rectangular windows were cut on each core tube opposite each other and covered with nylon mesh.

8.2.7 Naval Station San Diego Demonstration for Predicting PAH Bioaccumulation

To demonstrate the ability of the PDMS pore water sampling method to predict *in situ* bioaccumulation potential and thus serve as a surrogate to bioaccumulation studies, the PDMS sampler containing the FG 230/210 fiber was deployed at a variety of sediment sites of different contamination levels at Naval Station San Diego in San Diego Bay, CA. The PDMS samplers were placed in triplicate at four sites of differing contamination levels and co-located with caged organisms for *in situ* toxicity testing such as described by Burton et al. (2005). The bivalve mytilida *Musculista senhousia* was chosen as a test organism for 21-day bioaccumulation experiments in accordance with previous experimental work (Burton et al. 2005). At each location, the sediment-phase concentration, f_{oc}, 21-day PDMS concentration, centrifuged pore water concentration, and tissue concentration were assessed after the 21-day experiment. All PDMS analysis

was performed at UT, while centrifugation, tissue, and sediment analyses were performed at ERDC.

8.2.8 Anacostia River Field Demonstration for Predicting PAH Bioaccumulation in Caps

The field apparatus was deployed at the Anacostia River in Washington DC to demonstrate the ability of the device to quantify *in situ* PAH pore water concentrations. This site contains a field-scale demonstration of the capping contaminated sediments, and is thoroughly described in a former paper (Reible et al. 2006). PDMS samplers containing the FG 230/210 fiber were placed into capped and uncapped areas in triplicate using divers. The organism *Lumbriculus variegatus* was used for assessing bioaccumulation. Sediment from the test location was placed into cages along with organisms. The cages were then co-located with the PDMS samplers *in situ* at various locations throughout the demonstration area. Upon retrieval at 28 days, the PDMS fibers were immediately cleaned, processed into solvent in 5-cm intervals, and analyzed for PAHs. Organisms from the cages were separated from the sediment and allowed to depurate for 24 hours before tissue and lipid extractions. Worm tissue and fiber extracts were analyzed at UT as described in 8.2.1.

8.2.9 Hunters Point Naval Shipyard Demonstration for Predicting PCB Bioaccumulation

Hunters Point Naval Shipyard is the site of an extensive field demonstration of the ability to reduce contaminant bioavailability using *in situ* stabilization with activated carbon as described in Chapter 2, section 2.5.3. Further details of this study are described by Cho et al. (2009). For this study, sediment from the site was sieved through a No. 8 (2.35 mm) sieve and homogenized. A portion of homogeneous sediment was amended with 3.4% activated carbon (TOG-NDS 50 × 200, Calgon Carbon, Catlettsburg, KY) and

mixed for 28 days in accordance with the procedure described by Zimmermann et al. (20) Treated and untreated Hunters Point sediment was placed into each worm cage along with the 15 of the marine polychaete *Neanthes arenaceodenta*, three 5-cm length pieces of the FG 230/210, and three 2-cm length pieces of the PM 1000/1060 fiber. Cages were then placed into the Hunters Point tidal mudflat and then retrieved after 14 and 42 days. The PCB concentrations and lipid contents of the worms and the concentrations of the congeners in both fibers were then analyzed. Some interference was observed in the method blanks; congeners with mean values of less than three times the value observed in the blank were removed from the dataset.

8.3 Experimental Results and Discussion

After successfully demonstrating the ability to quantify trace-level HOC pore water concentrations in the field with the PDMS sampler and the correlation between these concentrations and bioaccumulation in laboratory settings, the next major step in the development of this method for assessment and remediation of contaminated sediment was predicting bioaccumulation. The following sections describe the experimental results from the three test studies.

8.3.1 Naval Station San Diego

The PDMS samplers were deployed along with caged organisms in San Diego Bay at Naval Station San Diego for characterization of PAH bioaccumulation from sediments into benthic invertebrates. This site was not undergoing any active *in situ* remediation. However, the four test locations were believed to have differing contamination levels and thus bioaccumulation was assumed to reflect these differences.

Figure 32 shows a plot of the measured PDMS pore water concentrations for three of the PAHs (BBF, BKF, and BAP) versus the organic carbon-normalized solid-phase concentrations, pore water concentrations from the PDMS sampler, and concentrations derived from centrifugation along with linear fits to the data. The concentrations of other PAHs were below detection limits. The values of r^2 for the linear correlation between q_{lipid} and both C_w and q_{oc} are summarized in Table 10. Because the values of Kow are similar for each of these compounds, the data for each of the individual compounds can be combined for analysis.

The slope of the regressed line of q_{lipid} versus C_w represents the lipid-water partition coefficient K_{lw}. The values of K_{lw} were about half a log unit below those of K_{ow}, which implies an over prediction of bioaccumulation by the model. There are several possible explanations for this result. First, it is possible that the organisms had not yet achieved steady-state conditions. Second, it is possible that the PAHs were metabolized to some degree by the organism (Lyttikainen et al. 2007). Finally, the organism activity levels may have been diminished due to other stressors in the system and as a result not accumulated contaminants to the same degree as in a normal environment.

The correlations between bioaccumulation and concentration were much higher for PDMS-derived pore water concentrations than bulk solid-phase concentrations or centrifuged pore water concentrations for each of the compounds. This is a significant result as sediment quality criteria are often based on the solid-phase concentrations, which appear to be a weaker indicator of bioaccumulation potential than pore water

concentrations. The lack of correlation between the centrifuged data and bioaccumulation is attributed to analytical difficulties.

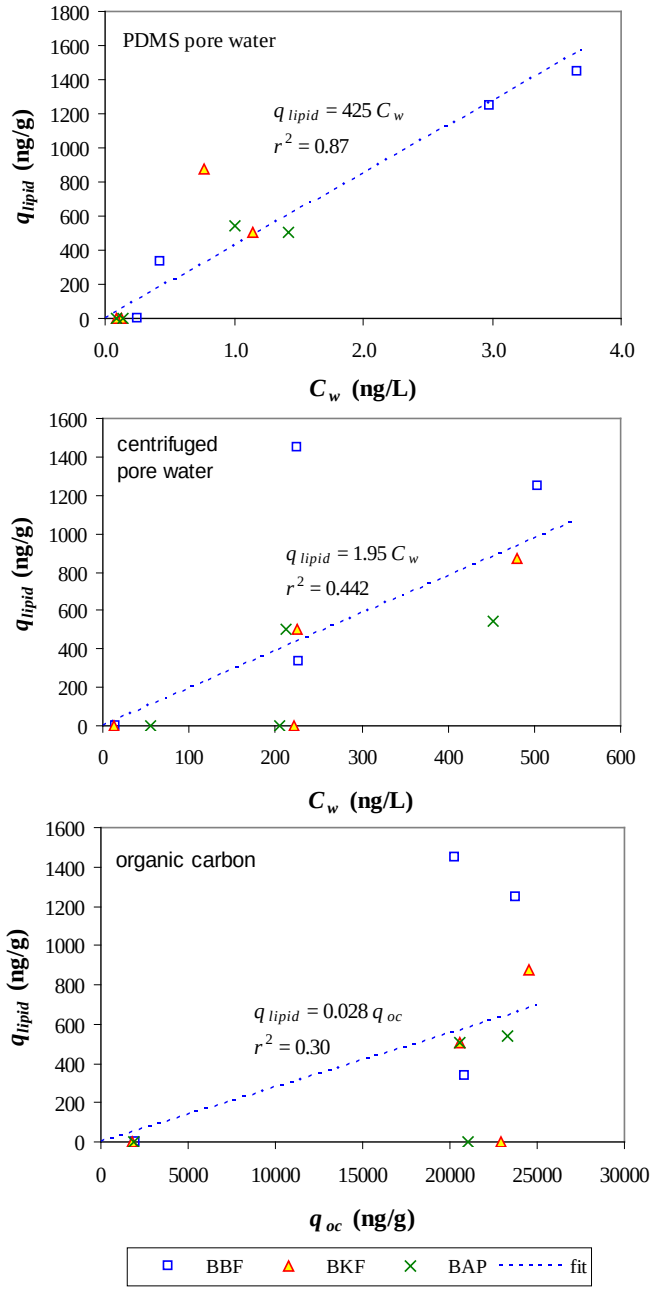

Figure 32. Correlation of *M. senhousia* tissue concentrations with PDMS pore water concentrations (top), centrifuged pore water concentrations (middle) and organic carbon concentrations (bottom).

PDMS-derived pore water concentrations were better correlated to the data than organic carbon phase concentrations or those from centrifugation. The slope of the lines in the top graphs represents the estimated lipid-water partition coefficient, while the slope of the line in the bottom graph is the BSAF.

Table 10: Correlation between Tissue, Solid-Phase, and PDMS-derived Pore Water Concentrations

Compound	log K_{ow}, log (L/kg)[38]	q_{lipid} vs. C_w (PDMS)		q_{lipid} vs. C_w (Centrifuged)	q_{lipid} vs. q_{oc}
		log K_{lw}	r^2	r^2	r^2
BAA	5.91	5.13	0.72	-0.23	0.16
BBF	6.1	5.61	0.97	0.52	0.53
BKF	6.11	5.81	0.61	0.54	0.32
BAP	6.13	5.61	0.90	0.51	0.37

To examine the relationship between the predicted and measured values of q_{lipid}, the data for each of the compounds and a linear, forced-origin fit were plotted as shown in Figure 33. If no variability existed in the data or the values of K_{ow} and the model assumptions were perfect, then the predicted values and the observed values would be the same. To quantify the relationship between bioaccumulation and pore water concentrations, the correlation coefficient was computed after a logarithmic transformation of the data. This method assumes that relative errors in predicted tissue concentrations are the same for each sample, which was deemed to be appropriate since the relative standard deviations of the sample pore water concentrations were similar. The value of the correlation coefficient of the log-transformed data was determined to be 0.814. This parameter indicates the positive trend in the values of the tissue concentrations versus those in the pore water and thus it is concluded that pore water

[38] MacKay et al. (1992)

concentrations predict bioaccumulation. The under predictions of the model versus the observed values are likely a reflection of the combined effects of overestimation of the actual lipid-water partition coefficient by K_{ow}, elimination effects, organism stress, and insufficient time for the organisms to reach equilibrium conditions. In addition to these model errors, other sources of variability in the data include measured pore water concentrations, variability in the fiber geometry, variability in the tissue concentrations, and variability in the worm lipid content. With so many potential sources of variability, it seems a significant result that such a simple model (based solely on K_{ow} and C_w) explains the majority of the observed variation in the data.

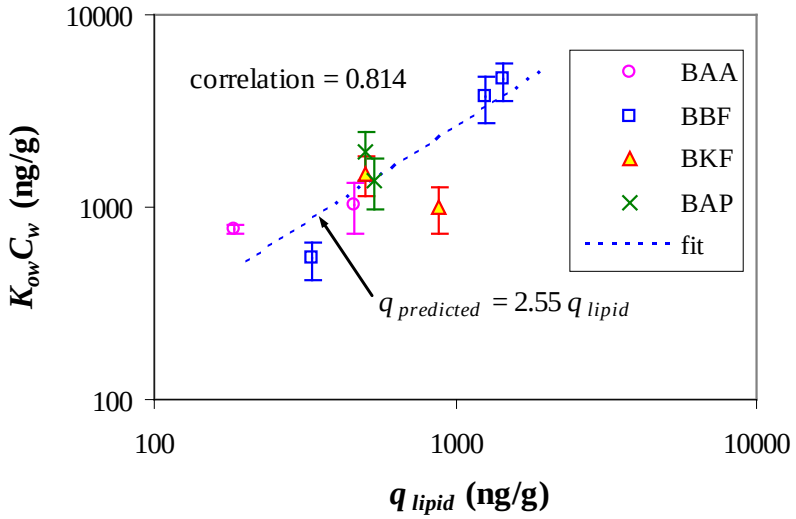

Figure 33. Predicted versus measured tissue concentrations for *M. senhousia* at Naval Station San Diego.

Bioaccumulation predicted by the simple linear uptake model was highly correlated to the experimental data. The over prediction by the model is attributed to error in the assumption of K_{ow} for K_{lw} and inadequate field equilibration time.

8.3.2 Anacostia River Capping Demonstration

PDMS samplers were placed into the sand cap, coke breeze cap, and uncapped areas at the Anacostia River along with caged organisms. Following retrieval, the organisms were analyzed to determine the lipid-phase concentrations of the contaminants and pore water concentrations were measured using the PDMS sampling approach at each location. Using Equation (8.2) and values of K_{ow} from MacKay et al. (1992), the lipid-phase concentrations q_{lipid} for each of the contaminants was predicted.

Following the methodology used at San Diego, to examine the relationship between the predicted and measured values of q_{lipid}, the data for each of the compounds and a linear, forced origin fit were plotted as shown in Figure 34. As before, if no variability existed in the data or the values of K_{ow} and the model assumptions were perfect, then the data and predictions would be equal. The value of the correlation coefficient of the log-transformed data was determined to be 0.840. This parameter indicates the positive trend in the values of the tissue concentrations versus those in the pore water and thus it is concluded that pore water concentrations represent an appropriate indicator for bioaccumulation. Unlike the San Diego Bay data, the model predictions for the Anacostia data showed slight under prediction of bioaccumulation with measured values approximately 30% less than those predicted by the model. The differences between the results are likely related to differences between the two organisms, behavior, and exposure duration. The San Diego Bay study utilized mussels as opposed to worms, which may have different uptake mechanisms and lipid-water partitioning. It is significant that these results were observed at a capping demonstration. Due to the consistency of the result (higher pore water concentrations = higher

bioaccumulation), it is concluded that the traditional bioaccumulation model can be used in assessing the performance of caps and not just for assessing the untreated sediments.

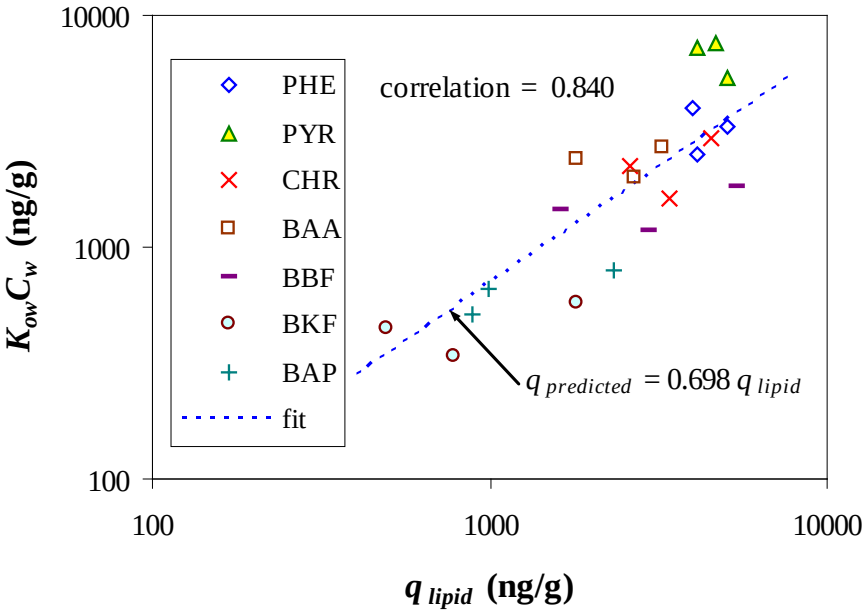

Figure 34. Predicted versus measured PAH tissue concentrations for *L. variegatus* at field demonstration of capped sediments.

Measured bioaccumulation compared favorably to predictions from K_{ow} and measured pore water concentrations using the PDMS sampling method at the Anacostia River capping demonstration.

8.3.3 Hunters Point *In Situ* Stabilization with Activated Carbon Demonstration

To study the correlation of PCB bioaccumulation with the PDMS pore water sampling method, PDMS fibers were placed with caged organisms into treated and untreated sediment at the Hunters Point field demonstration of *in situ* stabilization. Deployments were made using both the FG 230/210 and PM 1060/1000 fibers at 14 and 42 days in both treated and untreated sediment. A large number of congeners (39 for untreated and 29 for treated) were quantified at levels distinguishable from blanks in both worms and fibers in these deployments. The two deployment times were used in an

attempt to determine the effects of kinetics on fiber uptake. There were thus a total of four measurements, two fibers and two times. The 14-day data from the small FG 230/210 demonstrated the lowest average relative standard deviations, and was chosen for assessment of bioaccumulation.

To study the pore water bioaccumulation model, values for log K_{ow} were taken from Hawker and Connell (1988). Figure 35 shows the data from both the treated and untreated sediments, the regression fit, and linear, forced-origin fits to the data. The data were analyzed as before with the log-log transformation. As before, the relative standard deviations of the data showed no trend with absolute concentration, which suggests the appropriateness of the logarithmic transformation. The observed bioaccumulation was significantly less than the pore water predictions in both the treated and untreated sediment, which as in the case of the San Diego data is attributed to diminished organism activity and failure to reach equilibrium conditions. The treated sediment demonstrated more inconsistency with the model than the untreated. This difference may reflect differences in equilibrium time for both the sampler and the organism in the treated sediment. The presence of the activated carbon could have slowed down the transport rates in both the organisms and the sampling device.

Because PCB congeners are more hydrophobic than many of the PAHs that had been examined to date, there was concern that slow uptake kinetics would distort experimental results. A kinetics model based on diffusion in a cylindrical coordinate system was used to correct for kinetic effects in PDMS samplers. The model is discussed in more detail in Chapters 6 and 7. The correlation coefficients were 0.921 and 0.568 for the untreated and treated sediments after applying the correction, respectively. The

improvement in predictions lends credence to both the pore water bioaccumulation model and demonstrates the importance of passive sampler kinetics for more hydrophobic compounds. As in the case of the Anacostia data, it is significant that the results were consistent for both treated and untreated sediments, which implies that the PDMS-based approach can be used to assess the effectiveness of remediation using this technology.

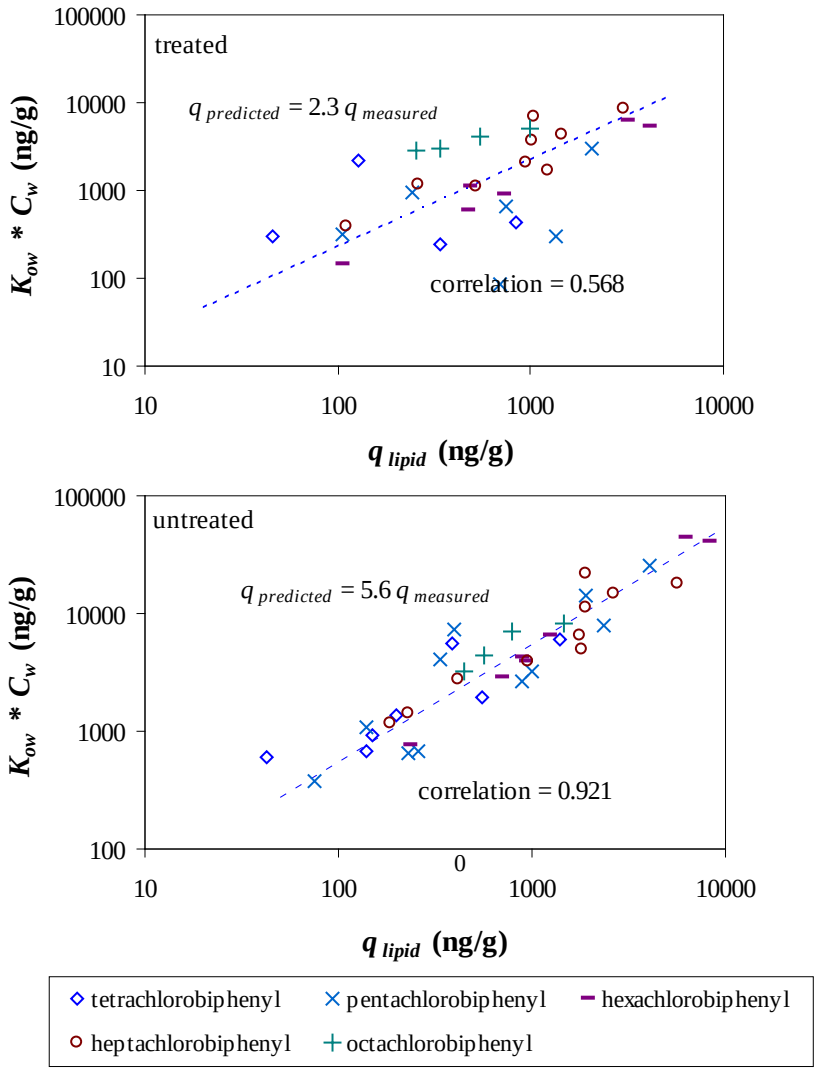

Figure 35. Predicted versus measured tissue concentrations for *N. arenaceodenta* at field demonstration of *in situ* stabilization with activated carbon.

Measured field tissue concentrations correlate well with predictions from K_{ow} and measured pore water concentrations using the PDMS sampling method at Hunters Point, San Francisco, CA. The data were corrected for kinetics due to slow equilibration times for PCB congeners. Top: sediment treated by *in situ* stabilization with activated carbon, bottom: untreated sediment.

8.4 Conclusions

In this study, results have been presented that demonstrate the ability of a PDMS sampler to assess both the impairment of sediments and the effectiveness of remediation technologies. The field-deployable apparatus was shown to predict bioaccumulation of PAHs accurately through the pore water bioaccumulation model. Similar results were seen in untreated sediment, sediment caps, and sediment undergoing *in situ* stabilization with activated carbon. For contaminants that are extremely hydrophobic, it may be infeasible to wait for the attainment of equilibrium conditions in the field. Using an uptake kinetics model, the data for PCB congeners in Hunters Point sediment were corrected. The model corrections improved bioaccumulation correlations substantially. More experimental work is needed to further demonstrate the validity of this approach.

8.5 Acknowledgements

The authors wish to thank the Environmental Security Technology Certification Program and the District of Columbia Appropriations Committee for funding this research. In addition, the authors wish to thank the United States Army Corps Engineer Research Development Center and for tissue and sediment analysis for San Diego Bay data and Professor Richard Luthy's research group at Stanford University for lipid and tissue analysis at Hunters Point.

8.6 References

1. Accardi-Dey, A. and Gschwend, P.M. 2002. "Assessing the combined roles of natural organic matter and black carbon as sorbents in sediments," Environmental Science & Technology, 36:21-29.
2. Bierman, V.J. 1990. "Equilibrium Partitioning and Biomagnification of Organic Chemicals in Benthic Animals," Environmental Science & Technology, 24:1407-1412.
3. Bintein S, Devillers J, and Karcher W. 1993. "Nonlinear dependence of fish bioconcentration on n-octanol/water partition coefficient," SAR QSAR Environmental Research, 1:29–39.
4. Booij, K., Shiu, W.Y., Mackay, D. 1998. "Calibrating the uptake kinetics of semipermeable membrane devices using exposure standards," Environmental Toxicology and Chemistry. 17:1236–1345.
5. Boudreau, B. 1997. Diagenetic Models and Their Implementation: Modeling Transport Reactions in Aquatic Sediments. Springer-Verlag, New York.
6. Brinkhurst R.O., and Cook, D.G. 1980. Aquatic Oligochaete Biology. Plenum Press, New York, NY.
7. Burton, G.A. 1991. "Assessing the toxicity of freshwater sediments," Environmental Toxicology and Chemistry, 10:1585-1627.
8. Burton, G.A., Greenberg, M.S., Rowland, C.D., Irvine, C.A., Lavoie, D.R., Brooker, J.A., Moore, L., Raymer, D.F.N., McWilliam, R.A. 2005. "*In situ* exposures using caged organisms: a multi-compartment approach to detect aquatic toxicity and bioaccumulation," Environmental Pollution, 134:133-144.

9. Cho Y.M., Ghosh U., Kennedy A.J., Grossman A., Ray G., Tomaszewski J.E., Smithenry D.W., Bridges T.S., Luthy R.G. 2009. "Field application of activated carbon amendment for in-situ stabilization of polychlorinated biphenyls in marine sediment," Environmental Science & Technology, 43(10):3815-3823.
10. Doucette, W.J., 2003. "Quantitative structure-activity relationships for predicting soil-sediment sorption coefficients for organic chemicals," Environmental Toxicology and Chemistry, 22:1771–1788.
11. EPA. 1997. Lake Michigan Mass Balance Study (LMMB) Methods Compendium, Volume 3: Metals, Conventionals, Radiochemistry, and Biomonitoring Sample Analysis Techniques; EPA-905/R-97-012c; U.S. Environmental Protection Agency, Great Lakes National Program Office: Chicago, IL, 1997.
12. Fredrickson, H.L., Furey, J., Talley, J.W., and Richmond, M. 2004. "Bioavailability of hydrophobic organic contaminants and quality of organic carbon," Environmental Chemistry Letters, 2:77-81.
13. Futoma, D.J, Smith, S.R., Smith, T.E., and Tanaka, J. 1981. Polycyclic Aromatic Hydrocarbons in Water Systems. CRC Press, Boca Raton, FL, USA.
14. Ghosh, U., Gillette, J.S., Luthy, R.G., and Zare, R.N. 2000. "Microscale location, characterization, and association of polycyclic aromatic hydrocarbons on harbor sediment particles," Environmental Science & Technology, 34:1729–1736
15. Harris D., Horwath, W., and van Kessel, C. 2001. "Acid fumigation of soils to remove carbonates prior to total organic carbon or CARBON-13 isotopic analysis," Soil Science Society of America Journal, 65:1853–1856.

16. Hawker, D.W. and Connell, D.W. 1988. “Octanol water partition-coefficients of polychlorinated biphenyl congeners,” Environmental Science & Technology, 22(4):382-287.
17. Hedges, J.L., and Stern, J.H. 1984. “Carbon and nitrogen determination of carbonate-containing solids,” Limnology and Oceanography, 29:657–663.
18. Herbes, S.E. and Allen, C.P. 1983. “Lipid Quantification of Freshwater Invertebrates: Method Modification for Microquantification,” Canadian Journal of Fisheries and Aquatic Sciences, 40:1315-1317.
19. Isnard P, and Lambert S. 1988. “Estimating bioconcentration factors from octanol–water coefficient and aqueous solubility,” Chemosphere, 17:21–34.
20. Kraaij R., Mayer P., Busser F.J.M., Bolscher M.V.H., Seinen W., Tolls J. 2003. “Measured pore-water concentrations make equilibrium partitioning work-a data analysis,” Environmental Science & Technology, 37:268-274.
21. Kan, A.T., Fu, G., Hunter, M.A., Tomson, M.B. 1997. “Irreversible sorption of naphthalene and tetrachlorobiphenyl to Lula and surrogate sediments,” Environmental Science & Technology, 31:2176-2185.
22. Lu X., Reible, D.D., Fleeger, J.W., and Chai, Y. 2003. “Bioavailability of Desorption-Resistant Phenanthrene to the Oligochaete *Ilyodrilus templetoni*.” Environmental Toxicology and Chemistry, 22:153-160.
23. Lu, X., Reible, D.D., and Fleeger, J.W. 2006. “Bioavailability of polycyclic aromatic hydrocarbons in field-contaminated Anacostia River (Washington, DC) sediment,” Environmental Toxicology and Chemistry, 25:2869-2874.

24. Lyttikainen M., Pehkonen,, S., Akkanen, J., Leppanen, M., and Kukkonen, J. 2007. "Bioaccumulation and Biotransformation of Polycyclic Aromatic Hydrocarbons During Sediment Tests with Oligochaetes (*Lumbriculus variegatus*)." Environmental Toxicology and Chemistry, 26: 2660-2666.

25. Mayer, P., Vaes, W.H.J., Wijnker, F., Legierse, K.C.H.M., Kraaij, H., Tolls, J., Hermens, J.L.M., 2000a. "Sensing dissolved sediment porewater concentrations of persistent and bioaccumulative pollutants using disposable solid-phase microextraction fibers," Environmental Science & Technology, 34:5177–5183.

26. Mayer, P., Vaes, W. H. J., and Hermens, J. L. M. 2000b. "Sensing dissolved sediment porewater concentrations of persistent and bioaccumulative pollutants using disposable solid-phase microextraction fibers," Analytical Chemistry, 72:459-464.

27. Mackay, D. 1982. "Correlation of bioconcentration factors," Environmental Science & Technology, 16:274–278.

28. MacKay, D.; Shiu, W. Y.; Ma, K. C. 1992. Illustrated Handbook of Physical-Chemical Properties and Environmental Fate for Organic Chemicals, Volume 3. Lewis Publishers: Chelsea, MI.

29. McFarland V.A. 1984. "Activity-Based Evaluation of Potential Bioaccumulation from Sediments," Montgomery RL, Leach JL (eds) Dredging and Dredged Material Disposal, American Society of Civil Engineers, New York, 1:461-467.

30. McGroddy, S.E. and Farrington, J.W. 1995. "Sediment porewater partitioning of polycyclic aromatic hydrocarbons in three cores from Boston Harbor, Massachusetts," Environmental Science & Technology, 29:1542-1550.

31. Meloche, L.M, deBruyn, A.M.H., Otton, S.V., Ikonomou, M.G., and Gobas, F.A.P.C. 2009. "Assessing exposure of sediment biota to organic contaminants by thin-film solid phase microextraction," Environmental Toxicology and Chemistry, 28:247–253.
32. Reible, D.D., Lampert, D.J., Constant, D., Mutch, R., Zhu, Y. 2006. "Active capping demonstration in the Anacostia River in Washington DC," Remediation Journal, 17:39-53.
33. Schwarzenbach, R.P., Gshwend, P.M., and Imboden, D.M. 2003. Environmental Organic Chemistry, 2nd Edition, Wiley & Sons, Hoboken, New Jersey.
34. Thoms, S.R., Matisoff, G., McCall, P.L., and Wang, X. 1995. Models for Alteration of Sediments by Benthic Organisms, Project 92-NPS-2, Water Environment Research Foundation, Alexandria Virginia.
35. Trimble, T.A., You, J., Lydy, M.J. 2008. "Bioavailability of PCBs from field-collected sediments: Application of Tenax extraction and matrix-SPME techniques," Chemosphere, 71(2):337-344.
36. US EPA. 1998. Contaminated Sediment Management Strategy (EPA 823-R-98-004). Accessed via website http://www.epa.gov/OST/cs/ stratefs.html.
37. Vinturella, A.E. Burgess, R.M., Coull, B.A., Thompson, K.M., and Shine, J.P. 2004. "Use of passive samplers to mimic uptake of polycyclic aromatic hydrocarbons by benthic polychaetes," Environmental Science & Technology, 38:1154-1160.
38. You, J., Landrum, P.F., Lydy, M.J. 2006. "Comparison of Chemical Approaches for Assessing Bioavailability of Sediment-Associated Contaminants," Environmental Science & Technology, 40:6348-6353.

Chapter 9: Summary and Conclusions

9.1 Research Objectives

The present work has developed tools for assessing the effectiveness of *in situ* management of sediments contaminated with hydrophobic organic compounds (HOCs) such as polycyclic aromatic hydrocarbons (PAHs) and polychlorinated biphenyls (PCBs). *In situ* management techniques such as capping provide many benefits over other sediment remediation strategies, including cost, restoration of benthic habitats, and isolation of contaminants from biological receptors. This dissertation had the following purposes regarding the current state of the practice of contaminated sediment management:

1. to demonstrate that pore water concentrations are the most appropriate metric for assessing performance of *in situ* remediation technologies
2. to determine the significant mechanisms of contaminant transport in sediment caps
3. to develop models based on relevant transport mechanisms for design and assessment of in situ management (i.e. capping)

To achieve these objectives, a number of laboratory, field, and modeling exercises were performed including field assessments at the Anacostia River in Washington DC, Naval Station San Diego and Hunters Point in San Francisco.

9.2 Research Accomplishments

The key conclusion of this dissertation is that pore water concentrations must be quantified for assessment and remediation of contaminated sediments. Pore water

concentrations represent the most appropriate metric for the assessment of contaminant transport and bioaccumulation in sediments. A summary of the individual conclusions that can be drawn from each chapter are:

1. Chapter 3: An Analytical Modeling Approach for Evaluation of Capping of Contaminated Sediments
    a. A transient model based on advection, diffusion, and reaction processes can predict the transient migration rates through the containment layer of a sediment cap
    b. For a sediment cap with a thickness h, retardation factor R, net advective velocity U and the effective diffusion coefficient D, the characteristic time scale for contaminant migration is:

$$t = \frac{Rh^2}{16D + Uh} \tag{9.1}$$

    c. A steady state model based on advection, diffusion, reaction, and bioturbation processes can predict the long-term behavior of a sediment cap
2. Chapter 4: Active Capping Demonstration in the Anacostia River, Washington DC
    a. Even with high resolution solid-phase cores it is impossible to use solid-phase concentration to assess cap performance
    b. Solid phase cores can be used to assess re-contamination and source control

3. Chapter 5: Demonstration of PDMS Passive Sampling for Measuring Contaminant Pore Water Concentration Profiles in Sediment Caps: Implications for Remediation
    a. Based on laboratory-scale analysis, thin layer capping of post-dredged sediments reduces pore water concentrations and subsequently bioaccumulation risks
    b. Thin layer caps must be sufficiently thick to provide separation of the bioturbation layer from benthos
    c. The dilution of surficial sediment concentrations with inert sands by organism mixing does not reduce bioaccumulation
    d. The steady state design model of Chapter 3 accurately predicts long-term observed pore water concentration profiles in sand caps
    e. The transient design model of Chapter 3 predicts chemical isolation layer breakthrough time in sand caps
    f. A field-deployable passive sampler with a polydimethylsiloxane (PDMS) sorbent layer can predict field pore water concentration profiles
    g. Field-measured solid-phase concentration profiles do not accurately reflect contaminant migration within caps
    h. Tidal forces significantly decrease the design life of caps
4. Chapter 6: An Assessment of the Significance of Internal and External Transport Processes for Predicting Contaminant Uptake Rates in Passive Samplers
    a. For a passive sampling sheet with internal diffusivity D_{PE} and material-water partition coefficient K_{PEW} in a sediment with effective diffusion

coefficient D, porosity ε, fraction organic carbon f_{oc}, and organic carbon partition coefficient K_{oc}, by calculating the dimensionless parameter:

$$\sigma = \sqrt{\frac{D_{PE}}{D(\varepsilon + f_{oc}K_{oc})}}K_{PEW} \tag{9.2}$$

it is possible to assess the importance of internal to external transport in the device

b. Using literature values for the sampler materials, it appears that external transport processes control uptake for many compounds in sediment environments

c. Models for predicting passive sampler uptake based on diffusion through the sediment and release from the particles were developed for both rectangular Cartesian coordinate and cylindrical geometries

d. Exact solutions to transport equations for both coordinate systems were derived for cases of instant release of contaminants from particles

e. Initial comparisons to field measurements indicates release of contaminants from particles may be an important transport mechanism

5. Chapter 7: Interpreting Uptake Rates in Passive Samplers for Contaminated Sediment through a Diffusion Model

    a. Uptake rates in PDMS fibers can be predicted using an external mass transport-dominated diffusion approach

    b. The accuracy of field pore water concentration measurements can be improved by correcting for uptake kinetics

6. Chapter 8: Application of a PDMS Passive Sampler for Assessing Bioaccumulation of Hydrophobic Organic Compounds from Sediments
    a. Bioaccumulation of organisms in sediments of varying degrees of contamination can be estimated by the PDMS-derived pore water concentration model
    b. Bioaccumulation of organisms on caps of contaminated sediments is accurately predicted by the PDMS-derived pore water concentrations
    c. Bioaccumulation of organisms from sediments treated by *in situ* stabilization can be estimated by the PDMS-derived pore water concentrations
    d. By correcting PDMS-derived pore water concentrations for kinetics, bioaccumulation predictions are improved

9.3 Outstanding Research Needs

In situ management of contaminated sediments through capping remains a relatively new technology and as such there are many outstanding issues to address. The results of this study have significant implications in the future for contaminated sediment management. However, the following is a list of outstanding questions about capping and potential future research topics in this area:

1. *Long term monitoring of cap performance*—The Anacostia caps attained steady state conditions within a few years due to tidal forces and lack of source control. Thus the results were inconclusive as to the long-term efficacy of both sand and active caps.

2. *Field demonstration of reduction of surficial pore water concentrations through active capping with PDMS samplers*—The results of this dissertation show the need to measure field pore water concentration in caps and the ability to measure profiles in simple lab studies. However, the ability to measure significant reductions in surficial pore water concentration was not demonstrated because the transient migration period in the caps occurred prior to the development of the pore water concentration profiling technique and because steady state levels were near those in uncapped sediments due to tides and re-contamination.
3. *Effects of natural organic matter on the effectiveness of active capping*—Activated carbon theoretically has the ability to sequester contaminants for thousands of years, although the practical design life is likely much less due to the competition of contaminants with natural organic matter. Both laboratory and field scale assessment of the effectiveness of activated carbon mats would be helpful in understanding the relationship between natural organic matter and design life.
4. *Effects of biological degradation on in situ management*—Biological decay may significantly enhance the performance of capping techniques. It may be possible to enhance the decay of contaminants through capping materials and thus radically improve cap design life.
5. *Funnel-and-gate assessment of capping using AquaBlok™*—The results of the modeling assessments showed the significance of even a small (1 m/yr) Darcy velocity on cap design lifetime, and the ability to alter pore water flow paths using AquaBlok™ was demonstrated in the Anacostia study. However, clearly it is

impossible to completely prevent the infiltration/exfiltration of groundwater. However, it may be possible to divert flow to active treatment systems such as activated carbon mats or materials that can enhance biodegradation.

6. *Assessment of sediment release dynamics on passive sampler uptake*—passive sampler uptake kinetics appear to be controlled by external mass transfer resistances (characterized by the surface area to volume ratio of the device). A long-term assessment of the kinetics of uptake in fibers in sediments with differing levels of hard and labile carbon with a variety of compounds is necessary to answer this question.
7. *Assessment of passive sampler kinetics for in situ stabilization with activated carbon*—By adding activated carbon to sediments, pore water concentrations and subsequently bioaccumulation are thought to decrease. Because of the extreme retardation of mass transport by the carbon, assessments using passive samplers over short time periods may not accurately reflect the long-term effectiveness of this technology.
8. *Field assessment of the effectiveness of capping on metals*—Initially this study had a significant focus on performance of capping for control of metals. However, due to time and budgetary constraints it was infeasible to address both hydrophobic organic compounds and metals. The interaction of metals with sorbent materials is well documented, thus active capping with materials like apatite has potential.

Appendix A: Experimental Materials and Methods

In this appendix, the experimental methods specifically used for this dissertation (not described elsewhere) are presented in detail. The analytical methods, including the quality assurance and control, are discussed first, followed by the experimental work on desorption resistance. The experimental work on the Anacostia, including core analysis and pore water concentration measurements using the polydimethylsiloxane (PDMS)-coated glass fiber passive sampling device are then presented.

A.1 Analytical Methods

The following section discusses the analytical techniques used to quantify various parameters germane to this dissertation, including quality assurance and control. These include PAH and metals concentrations in the bulk solid phase, PAH concentrations in pore water, and total organic carbon. PCBs, while present at the Anacostia site, were not analyzed as their behavior was assumed to be similar to that of the PAHs (as both are hydrophobic organic compounds).

A.1.1 PAH Extraction from Solid Matrices

PAHs were extracted from the solid phase (sediments as well as cap materials) using EPA Method 3550B: Ultrasonic Extraction. This technique is used for extracting nonvolatile and semivolatile compounds from solid matrices. Approximately two grams of sample were mixed with anhydrous sodium sulfate in thoroughly pre-cleaned glassware until a free-flowing powder was formed. Next, 60 mL of a 1:1 (v:v) hexane:acetone solution were then added to the jar. The samples were then placed into a water bath in a Branson (Danbury, CT) Model 2200 Ultrasonicator for 30 minutes to

dismember the particles. Samples were equilibrated overnight, after which an aliquot of the extract was separated, blown down with nitrogen gas using a Labconco (Kansas City, MO) Model 79100 RapidVap N2 Evaporation System, and finally reconstituted with acetonitrile for final analysis. The solid-phase concentrations were determined by back-calculation using mass, which was measured at each step in the extraction. Method blanks were used to check for contamination with every set of samples. A sample was periodically spiked as a check on extraction efficiency.

A.1.2 Metals Extraction from Solid Matrices

Metals were extracted from the solid phase (sediments as well as cap materials) using digestion in accordance with EPA Method SW 846-3051a: Microwave Assisted Acid Digestion of Sediments, Sludges, and Soils. All digestions were performed using a CEM (Matthews, NC) Model MDS-2000 Microwave. Approximately 0.5 g of sample were placed in CEM teflon microwave vessels along with approximately 10 mL of concentrated trace-metal grade nitric acid (70% by weight). Samples were then sealed and heated to 175°C (corresponding to a pressure of 70 psi, which was monitored instead of temperature) for 4.5 minutes. Samples were then filtered and transferred to plastic vials for storage until final analysis. Method blanks and check standards were used for quality assurance.

A.1.3 High Performance Liquid Chromatography with Fluorescence Detection (HPLC/FD) for PAH Quantification

PAH analysis was performed using high performance liquid chromatography for separation with fluorescence detection (HPLC/FD) for quantification. All analyses were performed in accordance with EPA Method 8310: Polynuclear Aromatic Hydrocarbons

using a Waters 2795 Separations Module. An isocratic flow rate of 1.0 mL/min composed of 3:7 water:acetonitrile (v:v) was used for separation of the target analytes. The PAHs quantified in these experiments were phenanthrene, pyrene, chrysene, benz[a]anthracene, benzo[b]fluoranthene, benzo[k]fluoranthene, and benzo[a]pyrene. Detection was achieved using a Waters 2475 multiwavelength fluorescence detector. The excitation and emission wavelengths used for quantification of phenanthrene and pyrene were 244 nm and 360 nm, respectively. For the remaining compounds, excitation and emission wavelengths of 255 and 420 nm, respectively, were used. All analyses utilized linear calibration curves with a minimum of five points. Check standards and blanks were used with every sample set to ensure performance.

A.1.4 Gas Chromatograph with Electron Capture Detection (GC/ECD) for PCB Quantification

PCB analysis was performed using gas chromatography for separation with electron capture detection (GC/ECD) for analyte quantification using a modified Environmental Protection Agency (EPA) method 8082. Analyses were performed using an Agilent Technologies, Inc. (Santa Clara, CA) model 6890 gas chromatograph with a ^{63}Ni micro-electron capture detector. Hydrogen was used as the carrier gas and nitrogen as the make-up gas. Separation was achieved using a 60 m long, 250 μm diameter fused-silica model HP-5 capillary column from Agilent Technologies (Santa Clara, CA). Standards were developed using a known PCB mixture from the EPA's National Health and Environmental Effects Research Laboratory 1 in Grosse Ile, MI (EPA, 1997). The method simulates Aroclor 1242 using a 75:54:54 mixture of Aroclors 1232, 1248, and 1262, respectively. All analyses utilized linear calibration curves with a minimum of five

points. PCB congener number 209 (decachlorobiphenyl) was used as an internal standard. Check standards and blanks were used with every sample set to ensure performance.

A.1.5 Inductively Coupled Plasma Atomic Emission Spectroscopy (ICP/AES) for Metals Quantification

Metal concentrations were determined using inductively coupled plasma atomic emission spectroscopy (ICP/AES). All analyses were performed on a Spectro Ciros (Mawhah, NJ) ICP/AES in accordance with EPA Method 6010B: Inductively Coupled Plasma Atomic Emission Spectroscopy. Five-point calibrations were used to develop standard curves. Standards were prepared by diluting 1,000 mg/L commercial stock solutions (Fisher Scientific, Waltham, MA) with Millipore (Billerica, MA) water to the desired concentration range. All the available emission wavelengths for the individual metals from the library in the instrument's database were scanned, and the wavelength with the best fit (as measured by the correlation coefficients from the linear calibration curves) was selected for quantifying the target analyte. Scandium was used as the internal standard for quality assurance.

A.1.6 Total Organic Carbon

The total or fractional organic carbon (f_{oc}) of each of the soils was determined by elemental analysis on a Carlo-Erba 1108 according to Hedges and Stern (1984) modified according to Harris et al. (2001) (i.e., overnight vapor acidification with a hydrochloric acid atmosphere to remove inorganic carbon from samples). The oxidation column was run at 1020°C, while the reduction column was run at 650°C. The oven temperature was

maintained at 60°C. Each sample was measured in triplicate and the results averaged to obtain the final values used for analysis of adsorption and desorption behavior.

A.1.7 Worm Tissue Concentration Analysis

Worm tissue extraction was performed using EPA method 3550b: Ultrasonic Extraction for Solid Matrices. Worm tissues were placed in amber glass vials and weighed. Anhydrous sodium sulfate was then used to absorb excess water. Reagent grade dichloromethane (Fisher Scientific, Waltham, MA) was used to extract analytes. Samples were sonicated in a Branson (Danbury, CT) Model 2200 Ultrasonicator for thirty minutes to enhance desorption. An aliquot of the extract was then exchanged to reagent grade acetonitrile (Fisher Scientific, Waltham, MA) and analyzed.

A.1.8 Worm Lipid Analysis

Lipid content was assessed using the method first described by Herbes et al. (1983) to convert wet worm tissue loadings to lipid-phase concentrations. Twenty worms (~100 mg wet weight) were transferred to pre-weighed 15 mL centrifuge tubes and then re-weighed to assess worm mass. Five mL of a 1:1 (v:v) solution of reagent grade methanol and reagent grade chloroform (Fisher Scientific, Waltham, MA) were added to each tube for lipid extraction. The samples were then sonicated for 30 seconds and allowed to equilibrate for four hours. The tubes were centrifuged, and the supernatant was transferred to a new tube. An addition five mL of the methanol-chloroform solution were added to the original tube to remove any remaining extract. The extract was then equilibrated with two mL of water to remove tissue protein. The extract was then dried at 50°C and weighed to assess the lipid mass in the original sample. Method blanks were evaluated and showed no solvent residuals.

A.2 Core Experiments

To evaluate the effectiveness of capping at decreasing the contaminant concentrations in surficial sediments, the concentration profiles of contaminants in the solid phase were evaluated through sediment cores. Undisturbed cap/sediment samples from all the caps except the coke breeze cap were collected by a vibrate core sampler. The vibrate core sampler used was a 3.25-in diameter stainless-steel core barrel fitted with a 2-7/8-in clear plastic liner. After a core sample was retrieved, the overlying water was bled by cutting the core liner with a hacksaw. The core liner was then capped with watertight plastic caps, sealed with tape, labeled with its identification and orientation, and shipped back to the lab for processing. The cores were extruded in the lab, and samples were collected at 0.5 cm intervals. The outside edge of the samples was discarded due to concerns about edge effects during collection and extrusion. Samples were then analyzed for metals, PAHs, and sieve analysis (described below) in triplicate and averaged. All solid-phase concentrations were normalized on a dry weight basis using the percent moisture from the sample.

At the interface between the overlying cap layer and the underlying sediment, a region exists where the two materials are present. Chemical analyses of the region therefore exhibit concentrations between those in the sediment and in the cap. As a means of distinguishing between this intermixing effect and contaminant migration, a sieve analysis of the samples was used to quantify the percentage of a sample composed of sediment and the cap material. The cap materials generally possessed larger particle diameters and hence a smaller percentage of the cap materials would pass through the sieve. The samples were dried and then sieved using a #80 (0.18-mm) sieve (preliminary analysis indicated that it provided the most efficient separation between the materials) and evaluated for percent passing. As a small part of the sediment (approximately 20%

by mass) was retained on this sieve and a small part of the capping materials passed through the sieve (less than 10%), the actual percent sediment was estimated by normalizing the scale to stretch from 0% to 100%.

Samples from the coke breeze cap were collected by divers, including samples from the mat and the overlying sand layer. The sand layer samples were collected by pushing plastic tubing into the sand layer. The coke breeze samples were cut from the mats using a knife. The sample mats were rolled to avoid the loss of coke breeze materials. The sand and coke were then analyzed in the lab for PAHs.

A.3 Field PDMS Profiling Experiments

To measure pore water concentration profiles of PAHs, *in situ* experiments with the PDMS profiling device were performed. To protect the fibers in the sediment column, a stainless steel piezometer was used as a tool to insert and recover the PDMS fibers into the sediment/cap column. An approximately 2-mm wide rectangular groove was made in the inner rod of the piezometer to serve as a frame for the fragile PDMS fibers. Approximately 0.5-mm thick slits were cut into the outer part of the piezometer at ¼" spacing. Figure 36 shows a schematic of the piezometer/PDMS device.

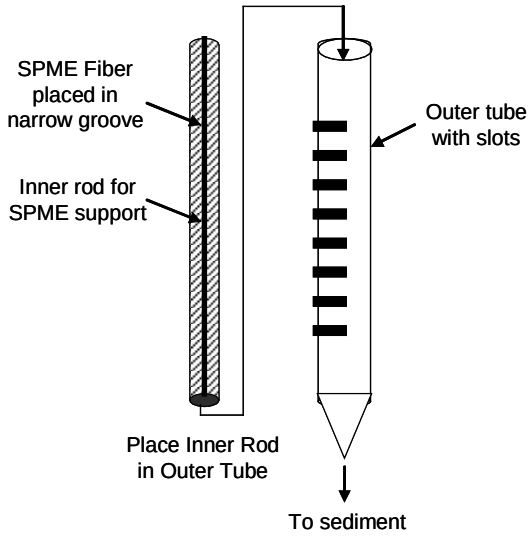

Figure 36. Field PDMS passive sampling device

Before deployment, all PDMS sampling devices were cleaned with Alconox detergent, distilled water, and a hexane solvent rinse. PDMS fibers were cleaned before by sonicating with a Branson (Danbury, CT) 2200 sonicator in hexane for 10-15 minutes first, then again in acetonitrile for 10-15 minutes. The fibers were then placed in to the groove in the field sampling device. Silicon grease (vacuum grease) was used to hold the fiber in place within the groove. The rods were placed by divers into the sediment column and allowed to equilibrate. The rods were removed from the river bottom by a diver, packaged in plastic wrap and plastic garbage bags, taped, and shipped in ice chests cold to the lab, and stored in plastic bags at 4°C until analysis.

After deployment and equilibration, the fibers were processed in the lab. Fibers were cut at 1 to 4-cm intervals (the interval length being a trade-off between accuracy and resolution), then placed into HPLC vial inserts. A volume of approximately 100 µL of HPLC grade acetonitrile (Fisher Scientific, Waltham, MA) was then added to each of the vials to extract the PAHs. The samples were then analyzed by HPLC/FD.

The PDMS field sampling devices were deployed three times at the Anacostia River site, first in May 2007, then again in December 2007, and then in August 2008. On the first deployment, the fibers were shipped back and processed over the course of four days and the PM 170/110 fiber was used. The results later showed that significant loss may have occurred during the processing time; as a result, during the second deployment the fibers were processed in the field. To enhance contaminant uptake, the FG 230/210 fiber was used as it has a smaller PDMS coating which should theoretically control the uptake rate.

A.4 Field Worm Cage Experiments

In an attempt to evaluate the effects of the caps assess the importance of pore water concentrations on biological uptake, field worm cage experiments of contaminant bioaccumulation were performed with the PDMS sampler field studies. The experiments followed the procedures outlined by Burton et al. (2005). The standard *in situ* chamber was a cylinder constructed of transparent core tubing of cellulose acetate butyrate or Eastman Tenite Butyrate with a 6.67-cm inner diameter, 6.98-cm outer diameter, 0.16-cm wall thickness, and cut to a length of 12.7 cm. Polyethylene closures were used to cap each end. Two 4 X 8 cm rectangular windows were cut on each core tube opposite each other and covered with nylon mesh (usually 74–80 mm). Figure 37 shows a schematic of the worm cages.

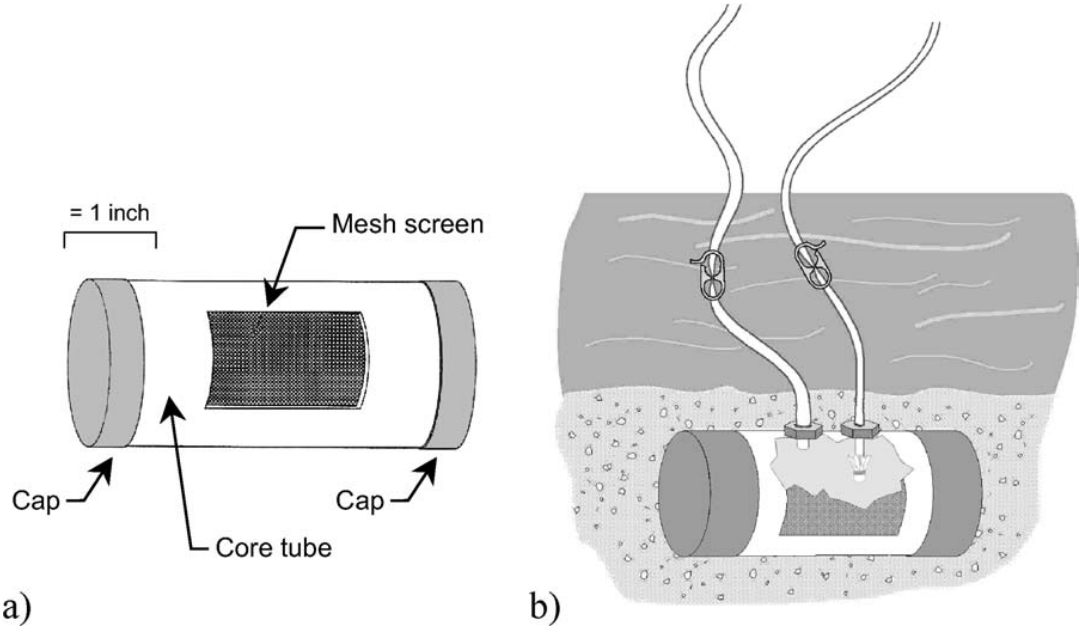

Figure 37. Worm cage design (from Burton et al. 2005 with permission)

For the bioaccumulation experiments, tubificid oligochaetes were cultivated in the laboratory. Tubificid oligochaetes provide a suitable choice organism for accumulation experiments as they have sufficient mass for tissue analysis, demonstrate PAH accumulation, and achieve a steady state concentration in a relatively rapid period of time (Reible and Lu 2000). For these bioaccumulation experiments, the species *Lumbriculus variegatus* were used. The test organisms were placed into the cages, which were then shipped to the Anacostia site, inserted into the sediment control area, sand cap, and coke breeze cap by divers. The cages were allowed to equilibrate and later removed by the divers. The worm tissues were then analyzed as described in A.2.6 and A.2.7 to determine lipid-phase contaminant concentrations.

Appendix B: A Numerical Modeling Approach for Simulating Contaminant Transport in Sediment Caps

B.1 Introduction

In this appendix, a more general modeling approach for design and evaluation of sediment caps systems is developed. An essential part of the design of sediment caps is reduction of surficial pore water concentrations, sediment particle concentrations, and contaminant fluxes; therefore any modeling approach should provide a method for evaluating the cap's effect on these parameters. A basic framework for contaminant transport modeling in sediment caps is first presented. The various contaminant transport processes in sediments and their relationships to the governing equations are then discussed. A methodology for non-dimensionalizing the equations is then presented. After that, an algorithm is developed to solve the dimensionless system of equations for a three-layer cap over a finite sediment mass. To perform the calculations using this approach, a code was written in MATLAB. The code is presented in Appendix C.

B.2 Model Framework

To develop sediment capping models, the sediment-cap-water column is divided into: the underlying sediment, the containment layer (subdivided into active and passive layers), the bioturbation layer, and the overlying water column. The cap layer consists of both the chemical isolation layer and the bioturbation layer. The underlying sediment layer also includes the zone in which cap and sediment have intermixed during placement because it will typically exhibit pore water concentrations essentially indistinguishable from the underlying sediment. In transient calculations any portion of the cap compromised by chemical migration due to consolidation (typically much less than the

portion penetrated by expressed pore water due to sorption-related retardation) should also be considered part of the underlying sediment. The positive *z*-axis is assumed down (associated with depth). Figure 38 shows the conceptual model of the sediment cap system.

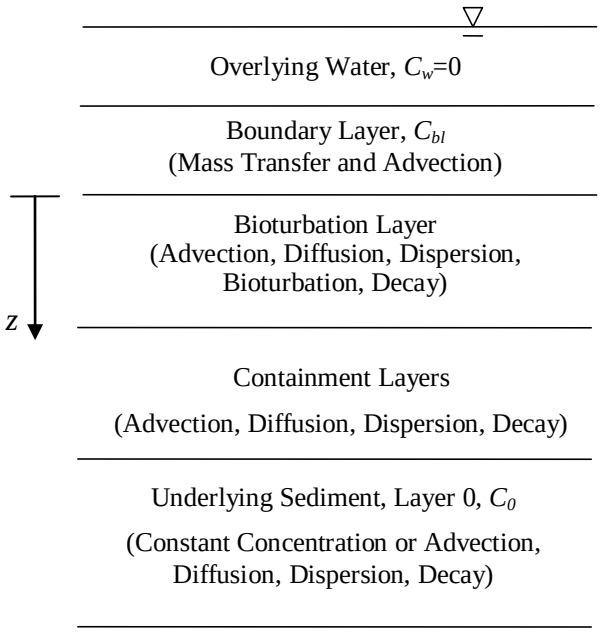

Figure 38. Conceptual model of sediment cap system

Due to the low solubility of most sediment contaminants, the bulk sediment loading, *W*, (mass of contaminant on solid phase per mass of solid phase) is the parameter that is often used for quantifying contaminant levels in sediments instead of the pore water (mobile phase) concentration. Under the assumption of linear partitioning, the bulk sediment loading at depth *z* and time *t* can be related to the pore water concentration, *C*, through the following relationship, assuming local equilibrium:

$$W(z,t) = K_d C(z,t) \tag{B.1}$$

Where K_d represents the effective sediment-water partition coefficient. Although chemical diffusion within the sediment particle can be slow, it is generally reasonable to assume local equilibrium with the pore water at some effective (measured) partition coefficient due to the relatively slow contaminant migration rates within the sediment bed.

For organic contaminants, the contaminant partition coefficient is often estimated as the product of the fraction organic carbon f_{oc} and the organic carbon partition coefficient, K_{oc} (Equation 2.1). This is likely a crude assumption in the underlying sediment which may contain significant contamination in strongly sorbing phases (e.g., hard carbon) but may be a good assumption for the cap material. For typical sand, the organic carbon fraction tends to be less than 0.1%. At these low organic carbon contents, mineral sorption tends to become important even for organic compounds; so, the assumption of 0.01%-0.1% organic carbon is likely a lower bound to the effective sorption of organic contaminants on cap materials (Schwarzenbach et al. 2003).

The approach presented here is developed using pore water concentrations, which represent the mobile contaminant phase in a stable cap. The solid-phase loading can be different within a cap system if the partition coefficient is different in different parts of a cap (e.g., the underlying sediment, cap material, and the newly deposited sediment). The pore water concentration predictions of the model can be converted to sediment loadings using the appropriate partitioning relationship. The decay of the contaminant is assumed to be first-order and to occur only in the pore water.

Transport through the aqueous boundary layer at the cap-water interface is dictated by the benthic boundary layer mass transfer coefficient (Boudreau and Jorgensen

2001). For the overlying water, the concentration is assumed to be zero. This assumption is easily justified for rivers where advection rapidly sweeps away the effluent pore water.

B.3 Governing Equations and Auxiliary Conditions

B.3.1 Underlying Sediment

The simplest approach for modeling the underlying sediment is to assume the concentration remains constant. For sediment with a concentration of C_0 at a depth of h_{cap}:

$$C\ (z = h_{cap},\ t > 0) = C_0 \tag{B.2}$$

A model that considers a finite contaminant mass in sediment requires a governing equation for the sediment column (Layer 0). The equation for a retardation factor R_0, effective diffusion coefficient D_0, net advective velocity U, porosity ε_0, and decay rate λ_0 is:

$$R_0 \frac{\partial C}{\partial t} = D_0 \frac{\partial^2 C}{\partial z^2} + U \frac{\partial C}{\partial z} - \varepsilon_0 \lambda_0 C \tag{B.3}$$

This equation requires an initial condition for the concentration, which is assumed to be uniformly C_0 across the sediment with a thickness h_{sed} (with $h_{tot} = h_{sed} + h_{cap}$):

$$C(h_{cap} < z < h_{tot}, t = 0) = C_0 \tag{B.4}$$

The sediment column requires an additional boundary condition at the bottom (depth $h_{cap} + h_{sed}$). Unfortunately, the proper boundary condition depends on the physics of the problem. For an advectively-dominated system the correct condition is zero-concentration to prevent influx of mass from the underlying clean sediments. This boundary condition creates an artificial gradient that actually increases flux out of the

bottom of the sediment column in a diffusion-dominated system, however. For a diffusion-dominated problem, a no flux boundary at the bottom of the sediment column requires a zero slope boundary condition. For an advection-dominated problem this eventually becomes a constant concentration boundary condition when the concentration in the cap becomes sufficiently large. Therefore, neither condition is perfect. The zero-slope boundary provides a conservative estimate of surficial sediment pore water concentrations and is recommended here.

$$\frac{\partial C_0(z = h_{tot}, t > 0)}{\partial z} = 0 \tag{B.5}$$

B.3.2 Containment and Bioturbation Layers

The transport processes in the layers are sorption, advection, diffusion/dispersion, and decay. For the bioturbation layer, bioturbation-induced movement of particles and pore water are also considered. Bioturbation-related processes are considered quasi-diffusive and hence are assumed to increase the effective diffusion/dispersion coefficient in that layer. For predicting chemical concentrations in the j^{th} layer, the governing transport equation is:

$$R_j \frac{\partial C}{\partial t} = D_j \frac{\partial^2 C}{\partial z^2} + U \frac{\partial C}{\partial z} - \varepsilon_j \lambda_j C \tag{B.6}$$

Where C is the pore water concentration, z is the depth downward from the cap-water interface, t is the time, R_j is the retardation factor in the layer (defined here as the ratio of the total concentration to that in the mobile phase), D_j is the diffusion/dispersion coefficient in the containment layer, U is the net advective velocity (assumed to be directed upward), λ_j is the decay rate constant, and ε_j is the porosity in the layer.

Boundary conditions are required at the interfaces between each of the layers. The appropriate boundary conditions for the interface between the j^{th} and $(j - 1)^{th}$ layers (depth h_j) are continuity of concentration and flux. Continuity of concentration is satisfied trivially. Because the advective fluxes in each layer are equivalent, to satisfy continuity the diffusive fluxes must also be equal. The following boundary condition represents this concept mathematically:

$$D_j \frac{\partial C(z = h_j, t > 0)}{\partial z} = D_{j-1} \frac{\partial C(z = h_j, t > 0)}{\partial z} \tag{B.7}$$

The boundary condition at the cap-water interface is the most complex, as it essentially requires the effluent boundary condition from a porous medium, which has a long history and is the subject of many papers (Hulbert 1944, Danckwerts 1953, Wehner and Wilhelm 1956). The concept of a diffuse benthic boundary layer above the sediment-water interface has long been used for modeling mass transport from surficial sediments and is widely accepted in soil and marine science kind (Boudreau and Jorgensen, 2001). The following represents such a boundary condition for the uppermost layer in the system with an effective diffusion coefficient of D_j:

$$D_j \frac{\partial C(z = 0, t > 0)}{\partial z} = k_{bl} C(z = 0, t > 0) \tag{B.8}$$

Initial conditions are required for the concentration in each of the layers. Assuming the cap materials are initially clean provides the following initial condition for the j^{th} layer:

$$C(t = 0, z) = 0 \tag{B.9}$$

B.3.3 Summary

The basic concept of the cap system is clean overlying water that interacts with the bioturbation layer through the benthic boundary layer, which overlays the cap layers, which overlays the sediment layers, which is assumed to have an impermeable bottom. Thus, each layer has its own governing transport equation. The top boundary condition is a third-type to account for the benthic boundary layer, the bottom is a zero-slope (for conservatism), although it can be altered as needed to simulate the particular problem of interest, and the interfaces between each layer require constant flux boundary conditions. The initial conditions can theoretically be arbitrary, but herein are assumed to be zero in the cap layers and constant concentration in the contaminated sediment. With this approach, it is possible to simulate quite complex capping systems.

B.4 Parameter Estimation

The models described previously contain numerous parameters. In this section relationships for calculating the values of these parameters are listed.

B.4.1 Retardation Factors

The factor R_j, in the j^{th} layer as defined here is the ratios of the total concentration in an elementary sediment volume (stationary and mobile phases) to that in the pore water (mobile phase only) for the cap layers. A significant proportion of the total concentration in the pore water may be present in colloidal organic matter (Baker et al. 1985, Chin and Gschwend 1992). A simple model to account for this relationship is to assume linear partitioning onto the total organic carbon in the pore water, ρ_{doc}, with a colloidal organic carbon partition coefficient, K_{doc}. Coupling this assumption with the linear partitioning onto solid-phase produces the following relationships for the

retardation factor in the j^{th} layer R_j, terms of the colloidal organic carbon concentration ρ_{doc}, K_{doc}, the porosity in the j^{th} layer ε_j, the bulk density of the j^{th} layer ρ_j, and partition coefficient of the j^{th} layer $(K_d)_j$:

$$R_j = \frac{\varepsilon_j + \varepsilon_j \rho_{doc} K_{doc} + \rho_j (K_d)_j}{1 + \rho_{doc} K_{doc}} \tag{B.10}$$

If a nonlinear sorption isotherm is to be used for modeling the relationship between the pore water and the sediment/cap material (such as in an active cap layer or a nonlinear sediment-water partitioning relationship) the retardation factor becomes a function of the concentration and the system becomes a nonlinear system of partial differential equations. In these situations, the rate of change of mass in an elementary volume in the j^{th} layer can be written as:

$$R_j(z,t)\frac{\partial C}{\partial t} = \frac{\varepsilon_j + \varepsilon_j \rho_{doc} K_{doc} + \rho_j \dfrac{\partial q}{\partial C}}{1 + \rho_{doc} K_{doc}} \frac{\partial C}{\partial t} \tag{B.11}$$

For example, using a Freundlich isotherm with coefficients K_{fr} and N to model adsorption in Layer 1 would produce the following equation for the retardation factor:

$$R_1(z,t)\frac{\partial C}{\partial t} = \frac{\varepsilon_1 + \varepsilon_1 \rho_{doc} K_{doc} + \rho_1 N K_{fr} C^{N-1}}{1 + \rho_{doc} K_{doc}} \tag{B.12}$$

A numerical solution to a nonlinear system requires an increased level of complexity as the finite difference equations create a nonlinear system at each time step. As a relatively simple alternative, the retardation factor can be assumed constant over a given time period and then updated after each time step. This approximation is discussed later in this section.

B.4.2 Advection

The Darcy velocity, *U*, here accounts for both groundwater upwelling and the effect of erosion/deposition. In a coordinate system fixed relative to the cap-water interface, deposition or erosion changes the net effective advective flux. Because particle deposition effectively buries both pore water and solid associated contaminants, the effective advective flux also encompasses both. The effective advective velocity associated with both the Darcy pore water upwelling, *V*, the velocity of sediment deposition, V_{dep}, and the retardation factor for the deposited sediment, *R*, is:

$$U = V - RV_{dep} \tag{B.13}$$

Note that although new sediment is typically deposited at the cap–water interface, the mixing in this region is rapid and governed by bioturbation, or particle mixing processes that are not subject to retardation by pore water transport. Transient migration in the underlying cap containment layer is delayed by burial with new sediment and the apparent shifting of the cap-water interface. In the event of net erosion rather than deposition the value of V_{dep} will be negative.

The advective flow is perhaps the most important parameter in this analysis, as it will dominate the analysis in many natural systems. In the absence of direct measurements, the flow may be modeled using Darcy's Law. The local effective hydraulic conductivity for the sediment-cap system is dictated by the layer with the lowest hydraulic conductivity. Because of the high permeability of most capping materials (e.g., sand), the hydraulic conductivity of the system is generally unaffected by the presence of the cap.

B.4.3 Diffusion/Dispersion

The value of D_j is the diffusion/dispersion coefficient for the j^{th} layer. In all layers excluding the bioturbation layer, D_j accounts for the transport processes of molecular diffusion and mechanical dispersion. Diffusion through granular porous media is often characterized by an effective diffusion coefficient given by the molecular diffusivity times the porosity (the available diffusion area) and divided by a hindrance parameter (the lengthening of the diffusion path by the media). The model of Millington and Quirk (1961), where the hindrance parameter is taken to be the porosity to the negative one-third power, is widely used for diffusion in granular porous media such as a typical sand cap. Boudreau (1997), however, suggests an alternative that may be more applicable for fine-grained sediments where the tortuosity is modeled as one minus the natural logarithm of the porosity squared. The molecular diffusivity, D_w, is a function of temperature and molecular weight and can be estimated (e.g., Lyman et al. 1990). Chapter 3 presents the equations for estimating an effective diffusion coefficient based on these assumptions.

Mechanical dispersion of the contaminant through the cap is modeled as a Fickian diffusion-like process. The dispersion coefficient can be modeled as the product of the velocity through the cap and some length scale defined as the dispersivity, α. This parameter tends to be fairly site and material specific, although Neumann (1990) presented an argument that the length scale should increase with the size of the domain. Chapter 3 presents the equations for estimating an effective dispersion coefficient based on these assumptions

After placement of a sediment cap, new sediment is deposited at the cap surface. As this deposition occurs, the top of the sediment cap is re-colonized by benthic organisms (worms and other macro invertebrates). These organisms blend the sediments at the top of cap, resulting in relatively rapid transport of contaminants from the bottom of the layer to the overlying water. Provided that the movement of particles and pore water by these organisms is essentially random, the length scale of the movement of the particles is smaller than that being studied (i.e., the cap thickness), and time scale between mixing events is smaller relative to other processes, the transport processes can be taken as quasi-diffusive (Boudreau 1986). The diffusion of particles is known as bioturbation, while the diffusion of pore water is bioirrigation. These processes increase diffusion/dispersion coefficient in the bioturbation layer. In Chapter 3, the equations are presented for estimating a dispersion coefficient for bioturbation layers.

B.4.4 Degradation Rates

Contaminant degradation is a function of numerous parameters; it is possible to study this process in the laboratory although these studies can be costly both in terms of money and time. The model taken here is based on first-order kinetics, which may not be appropriate as the degradation may depend on many factors other than the contaminant concentration but provides a relatively simple way of incorporating this important mechanism into a mathematical model. The model here is capable of using a different first-order rate constant in each layer. In the absence of a study, the literature may be used to estimate a degradation rate.

B.4.5 Benthic Boundary Layer

Transport at the cap-water interface is dictated by the benthic boundary layer mass transfer coefficient, which is a function of the turbulence and shear of the overlying water column. Boudreau and Jorgensen (2001) and Thibodeaux (1996) present empirical correlations based on an extensive body of research to estimate this parameter. The following equation can be used to estimate the benthic boundary layer mass transfer coefficient in a river:

$$k_{bl} = \frac{0.114 v_x n \sqrt{g h_{channel}}}{r_H^{2/3} Sc^{2/3}} \tag{B.14}$$

Where k_{bl} is in m/s, v_x is the velocity of the river (m/s), n is Manning's n (from Manning's equation for open-channel flow in metric units), g is the acceleration due to gravity (m/s^2), $h_{channel}$ is the depth of the channel (m), r_H is the hydraulic radius (ratio of the channel cross-sectional area to the wetted perimeter, m), and Sc is the Schmidt number, which can be defined in terms of the kinematic viscosity of water, ν_w, and the molecular diffusion coefficient as:

$$Sc = \frac{\text{momentum diffusion}}{\text{mass diffusion}} = \frac{\nu_w}{D_w} \tag{B.15}$$

For low-velocity systems, wind-driven circulation of water drives the mass transport. Thibodeaux (1996) presents the following relationship for the mass transfer coefficient:

$$k_{bl} = \left(\frac{0.031\,\text{cm}^2}{\text{s}} \right) \frac{\rho_a}{\rho_w} \frac{v_a^2 h_{channel}^2}{M_w^{1/2} L_{lake}} \tag{B.16}$$

Where ρ_a and ρ_w are the density of air and water, respectively, v_a is the wind velocity, M_w is the molecular weight of the contaminant, and L_{lake} is the fetch of lake or water body in the direction of wind.

B.5 Dimensionless Equations and Parameters

It is useful to introduce a number of dimensionless parameters, including the dimensionless concentration, depth, and time, u, ζ, and τ; the Peclet, Damkohler and Sherwood numbers, Pe, Da, and Sh; the ratio of the retardation factor in the j^{th} layer to that in the bottom layer, ψ_j; the ratio of the diffusion/dispersion coefficient in the j^{th} layer to that in the bottom layer, δ_j; and the ratio of the product of the porosity and decay rate to in the j^{th} layer to that in the bottom layer, l_j:

$$u(z,t) = C(z,t)/C_0 \tag{B.17}$$

$$\zeta = \frac{z}{h_{tot}} \tag{B.18}$$

$$\tau = \frac{D_0 t}{R_0 h_{tot}^2} \tag{B.19}$$

$$Pe = \frac{U h_{tot}}{D_0} \tag{B.20}$$

$$Da = \frac{\varepsilon_0 \lambda_0 h_{tot}^2}{D_0} \tag{B.21}$$

$$Sh = \frac{k_{bl} h_{tot}}{D_0} \tag{B.22}$$

$$\psi_j = \frac{R_j}{R_0} \tag{B.23}$$

$$\delta_j = \frac{D_j}{D_0} \tag{B.24}$$

$$l_j = \frac{\varepsilon_j \lambda_j}{\varepsilon_0 \lambda_0} \tag{B.25}$$

The governing equations (B.3) and (B.6) can be re-written in dimensionless form:

$$\frac{\partial u_0}{\partial \tau} = \frac{\partial^2 u_0}{\partial \zeta^2} + Pe \frac{\partial u_0}{\partial \zeta} - Da\ u_0 \tag{B.26}$$

$$\frac{\partial u}{\partial \tau} = \frac{\delta_j}{\psi_j} \frac{\partial^2 u}{\partial \zeta^2} + \frac{Pe}{\psi_j} \frac{\partial u}{\partial \zeta} - \frac{l_j Da}{\psi_j} u \tag{B.27}$$

Similarly, the boundary conditions (B.5), (B.7), and (B.8) can be re-written in dimensionless form:

$$\frac{\partial u(\zeta = 1, \tau > 0)}{\partial \zeta} = 0 \tag{B.28}$$

$$\delta_j \frac{\partial u\left(\zeta = \frac{h_j}{h_{tot}}, \tau > 0\right)}{\partial \zeta} = \delta_{j-1} \frac{\partial u\left(\zeta = \frac{h_j}{h_{tot}}, \tau > 0\right)}{\partial \zeta} \tag{B.29}$$

$$\frac{\partial u(\zeta = 0, \tau > 0)}{\partial \zeta} = Sh \delta_j u(\zeta = 0, \tau > 0) \tag{B.30}$$

The initial conditions (B.4) and (B.9) can also be re-written:

$$u\left(\tau = 0, 0 < \zeta < \frac{h_{cap}}{h_{tot}}\right) = 0 \tag{B.31}$$

$$u\left(\tau = 0, \frac{h_j}{h_{tot}} < \zeta < 1\right) = 1 \tag{B.32}$$

The governing equations (B.26) and (B.27) for as many layers as necessary subject to the auxiliary conditions (B.28-B.32) can be solved numerically to determine transient concentration profiles.

B.6 Solution Method

A numerical model was developed in MATLAB to solve these equations for an active capping system with depletion. The code is set up to simulate 4 layers (sediment, active, sand, and bioturbation layers), although the model could easily be altered for a different number of layers or different boundary and initial conditions. The governing equations were solved using the finite difference method. The finite differencing scheme utilized the Crank-Nicolson method with a two-point upwind and one-point downwind difference scheme for the advection term and a central difference scheme for the diffusion term. The programs were designed to give the user flexibility in choosing grid spacing to maximize the tradeoff between truncation error and run time. The time step size is increased periodically to optimize run time and truncation error.

B.6.1 Overview of Algorithm and Finite Difference Approximations

The grid is divided into a total number of points, p, with the bottom of the j^{th} layer corresponding to the point p_j. The spatial domain of the model is divided into a grid with spacing $\Delta\zeta = 1/(p\text{-}1)$, while the temporal domain is divided into a grid with time step size $\Delta\tau$. The grid number is subscripted i, while the time step number is superscripted n. Table B.1 provides a summary of the spacing.

Table 11: Finite Difference Spacing Scheme

Layer	Layer	Depth	Grid Points
Bioturbation	3	h_3	i=1:p_3
Sand	2	h_2	i=p_3:p_2
Active	1	h_1	i=p_2:p_1
Contaminated Sediment	0	h_{sed}	i=p_1:p

The second derivative of the dimensionless pore water concentration, u, may be approximated with the following finite difference equation:

$$\frac{\partial^2 u}{\partial \zeta^2} \approx \frac{u_{i-1} - 2u_i + u_{i+1}}{\Delta \zeta^2} \tag{B.33}$$

The finite differencing for the first derivative is more complicated, since a centered difference is unstable in advection-diffusion problems. It is possible to use forward differencing to solve the equations, but a better scheme is a two-point upwind centered difference that uses two upwind points, the value of the function at the point, and one downwind point. This scheme provides truncation error of $O(\Delta\zeta^3)$ as opposed to $O(\Delta\zeta)$ for a two-point forward difference. Note that "upwind" means from the source, which is at $\zeta = 1$ rather than 0; this means the four points in the difference approximation are i-1, i, i+1, and i+2. Therefore, the following finite difference equation can be used to approximate the first derivative:

$$\frac{\partial u}{\partial \zeta} \approx \frac{-2u_{i-1} - 3u_i + 6u_{i+1} - u_{i+2}}{6\Delta \zeta} \tag{B.34}$$

At the last points before the boundaries (i.e., p_1-1, p_2-1, p_3-1, and p-1), a different differencing scheme must be used for the first derivative that does not incorporate values

from the underlying layers into the finite difference equations. A two-point forward difference is taken for the first derivative to account for this:

$$\frac{\partial u}{\partial \zeta} \approx \frac{u_{i+1} - u_i}{\Delta \zeta} \qquad i = p_1 - 1, p_2 - 1, p_3 - 1 \tag{B.35}$$

Three-point forward or backward differences are taken to approximate the spatial first derivative to prevent values from the adjoining layer being used and provide lower truncation error than the two-point approximation for the boundary conditions. The three-point forward difference approximation is:

$$\frac{\partial u}{\partial \zeta} \approx \frac{-3u_i + 4u_{i+1} - u_{i+2}}{2\Delta \zeta} \qquad i = p_1, p_2, p_3 \tag{B.36}$$

The three-point backward difference approximation is:

$$\frac{\partial u}{\partial \zeta} \approx \frac{u_{i-2} - 4u_{i-1} + 3u_i}{2\Delta \zeta} \qquad i = p_1, p_2, p_3 \tag{B.37}$$

The Crank-Nicolson method (Crank and Nicolson 1947) provides the good stability and small truncation error for solving advection-diffusion problems. The method approximates the temporal derivative using the arithmetic average of the forward and backward difference.

B.6.2 Governing Equations

Using the assumptions stated above, the following finite difference equation can be used to approximate Equation (B.26):

$$\frac{u_i^{n+1} - u_i^n}{\Delta \tau} = \frac{1}{2}\left\{ \begin{array}{l} \dfrac{u_{i-1}^n - 2u_i^n + u_{i+1}^n}{\Delta \zeta^2} + Pe\dfrac{-2u_{i-1}^n - 3u_i^n + 6u_{i+1}^n - u_{i+2}^n}{6\Delta \zeta} - Da\ u_i^n + \\ \dfrac{u_{i-1}^{n+1} - 2u_i^{n+1} + u_{i+1}^{n+1}}{\Delta \zeta^2} + Pe\dfrac{-2u_{i-1}^{n+1} - 3u_i^{n+1} + 6u_{i+1}^{n+1} - u_{i+2}^{n+1}}{6\Delta \zeta} - Da\ u_i^{n+1} \end{array} \right\} \tag{B.38}$$

Similarly, for the governing equation for the j^{th} layer (B.27):

$$\frac{u_i^{n+1}-u_i^n}{\Delta\tau}=\frac{1}{2}\left\{\begin{array}{l}\dfrac{\delta_j}{\rho_j}\dfrac{u_{i-1}^n-2u_i^n+u_{i+1}^n}{\Delta\zeta^2}+\dfrac{Pe}{\rho_j}\dfrac{-2u_{i-1}^n-3u_i^n+6u_{i+1}^n-u_{i+2}^n}{6\Delta\zeta}-\dfrac{l_jDa}{\rho_j}\,u_i^n+\\ \dfrac{\delta_j}{\rho_j}\dfrac{u_{i-1}^{n+1}-2u_i^{n+1}+u_{i+1}^{n+1}}{\Delta\zeta^2}+\dfrac{Pe}{\rho_j}\dfrac{-2u_{i-1}^{n+1}-3u_i^{n+1}+6u_{i+1}^{n+1}-u_{i+2}^{n+1}}{6\Delta\zeta}-\dfrac{l_jDa}{\rho_j}\,u_i^{n+1}\end{array}\right\} \quad \text{(B.39)}$$

The values q_0, r_0, and s_0 are now defined as:

$$q_0=\frac{\Delta\tau}{2\Delta\zeta^2} \quad \text{(B.40)}$$

$$r_0=\frac{Pe\Delta\tau}{12\Delta\zeta} \quad \text{(B.41)}$$

$$s_0=\frac{Da\Delta\tau}{2} \quad \text{(B.42)}$$

The values q_j, r_j, and s_j (where the subscript j again refers to the layer number are also defined as:

$$q_j=\frac{\delta_j}{\psi_j}\frac{\Delta\tau}{2\Delta\zeta^2} \quad \text{(B.43)}$$

$$r_j=\frac{1}{\psi_j}\frac{Pe\Delta\tau}{12\Delta\zeta} \quad \text{(B.44)}$$

$$s_j=\frac{l_j}{\psi_j}\frac{Da\Delta\tau}{2} \quad \text{(B.45)}$$

After some simplification, Equation (B.39) can be re-written for the j^{th} layer as follows:

$$\begin{array}{l}\left[-q_j+2r_j\right]u_{i-1}^{n+1}+\left[1+2q_j+3r_j+s_j\right]u_i^{n+1}+\left[-q_j-6r_j\right]u_{i+1}^{n+1}+\left[r_j\right]u_{i+2}^{n+1}=\\ \left[q_j-2r_j\right]u_{i-1}^{n}+\left[1-2q_j-3r_j-s_j\right]u_i^{n}+\left[q_j+6r_j\right]u_{i+1}^{n}+\left[-r_j\right]u_{i+2}^{n}\end{array} \quad \text{(B.46)}$$

The simplified version of the finite difference equation (using the two-point forward difference for the first derivative) at the points before the boundaries ($i = p_1$-1, p_2-1, p_3-1, and p-1) for the j^{th} layer (j = 0, 1, 2, 3) is:

$$\begin{aligned}&\left[-q_j\right]u_{i-1}^{n+1}+\left[1+2q_j+6r_j+s_j\right]u_i^{n+1}+\left[-q_j-6r_j\right]u_{i+1}^{n+1}=\\&\left[q_j\right]u_{i-1}^{n}+\left[1-2q_j-6r_j-s_j\right]u_i^{n}+\left[q_j+6r_j\right]u_{i+1}^{n}\end{aligned} \tag{B.47}$$

B.6.3 Boundary Conditions

The boundary conditions (B.28-B.30) are all independent of time. Equation (B.28) for the zero slope boundary can be approximated by the following difference equation for all n:

$$\frac{u_p^n-u_{p-1}^n}{\Delta\zeta}=0 \tag{B.48}$$

Equation (B.48) can be re-written:

$$\left[1\right]u_{p-1}^n+\left[-1\right]u_p^n=0 \tag{B.49}$$

Equation (B.29) for the continuity of flux at the interface of the j^{th} layer and j-1^{th} layer can be approximated by the following difference equations for all n:

$$\delta_j\frac{u_{p_j-2}^n-4u_{p_j-1}^n+3u_{p_j}^n}{2\Delta\zeta}=\delta_{j-1}\frac{-3u_{p_j}^n+4u_{p_j+1}^n-u_{p_j+2}^n}{2\Delta\zeta}\qquad j=1,2,3 \tag{B.50}$$

Equation (B.50) can be re-written:

$$\left[1\right]u_{p_j-2}^n+\left[-4\right]u_{p_j-1}^n+\left[3+3\frac{\delta_{j-1}}{\delta_j}\right]u_{p_j}^n+\left[-4\right]u_{p_j+1}^n\left[\frac{\delta_{j-1}}{\delta_j}\right]u_{p_j+2}^n=0 \tag{B.51}$$

Equation (B.30) can be approximated by the following difference equation for all n:

$$\frac{-3u_1^n + 4u_2^n - u_3^n}{2\Delta\zeta} = Sh\ u_1^n \tag{B.52}$$

Equation (B.52) can be re-written:

$$\left[2Sh\Delta\zeta + 3\right]u_1^n + \left[-4\right]u_2^n + \left[1\right]u_3^n = 0 \tag{B.53}$$

B.6.4 Nonlinear Sorption

For an active capping system and for sediment desorption, the assumption of linear partitioning may be poor. A better assumption may a Freundlich isotherm for the active layer or another model for the sediment layer. An implicit technique such as the Crank-Nicolson method with nonlinear sorption creates a system of nonlinear equations. While it is possible to solve these nonlinear equations with a technique such as the Newton-Raphson method, it is much easier and only slightly less accurate to use an explicit finite difference approximation for the sorption term. Only the value of the retardation factor must be updated at each time step in this approach, and the system remains linear.

B.6.5 Numerical Solution to Governing Equation and Auxiliary Conditions

The numerical solution of the system for a total number of time steps N can be stored in a (p x n) matrix, $\boldsymbol{u}$. The initial conditions are given in (B.31) and (B.32) and can immediately be written into the first column of $\boldsymbol{u}$:

$$u(1: p_1 - 1,1) = 0 \tag{B.54}$$

$$u(p_1 : p_0,1) = 1 \tag{B.55}$$

$$u(p_0 : p,1) = 0 \tag{B.56}$$

The finite difference equations (B.46), (B.47), (B.49), (B.51), and (B.53) can be used to solve for the values of $u(1{:}p,n{+}1)$ at the second ($n = 1$) and subsequent time step. The values in brackets on the left hand ($n + 1$) side in (B.46), (B.47), (B.49), (B.51), and (B.53) can be placed into a matrix **A**, while the values on the right hand side can be placed into a matrix **B**. The **A** and **B** matrices can be used to find the unknown values of $u(1{:}\ p,\ n+1)$ according to the following:

$$\mathbf{A}\,u(1{:}\ p,n+1) = \mathbf{B}\,u(1{:}\ p,n) \tag{B.59}$$

Note that changing the value of the time step size or using a variable retardation factor (in the nonlinear sorption case) changes the coefficients of **A** and **B**. The system can be solved very efficiently using a MATLAB subroutine called "linsolve." The method uses LU factorization with partial pivoting when the matrix is square or QR factorization with column pivoting otherwise. For more information see Horne and Johnson (1985). Alternatively, if the coefficients of **A** and **B** do not change (i.e., the linear sorption and constant step size case), it may be more computationally efficient to invert **A** to determine the values of u at the next time step:

$$u(1{:}\ p,n+1) = \mathbf{A}^{-1}\mathbf{B}u(1{:}\ p,n) \tag{B.28}$$

To improve computational efficiency, the time step size should be increased periodically. The MATLAB files used to generate this program use three step sizes for the sand and active capping models and four step sizes for the depletion model.

B.7 Summary

An approach for numerically solving the model is presented here based on finite differencing with the Crank-Nicolson method. The values of the parameters must be

determined first using the methods discussed in B.4, followed by their dimensionless representations (Peclet, Damkohler, Sherwood number, etc.). Based on the grid and step sizes, the values of q_j, r_j and s_j can be determined for each layer and used to fill in the coefficients of matrices **A** and **B**. If nonlinear sorption is used in the system or if the time step size is changed, the values in the **A** and **B** matrices must be updated accordingly. Starting with the initial conditions, the u solution matrix can then be calculated at the next time step until reaching the desired endpoint. The dimensionless depth, ζ; time, τ; and concentration, u, can then be re-converted to the appropriate dimensions for analysis. Appendix C contains the MATLAB code that can be used to model cap transport behavior in sand caps, active caps, and active caps with depletion. This algorithm can easily be extended to include more layers with different transport properties.

Appendix C: MATLAB Source Code for Simulating Contaminant Transport in Sediment Caps

In this appendix, the source code for a MATLAB file that is capable of simulating more general conditions for active caps is presented. The model assumes four layers are present, a sediment layer, an active layer with Freundlich sorption parameters, a sand layer, and a bioturbation layer. The details of the model are presented in Appendix B. The source code begins on the next page. The interested reader is encouraged to contact the author for the source code and instructions on applying the model.

```
%Active Capping Transport Model
%By David Lampert and Danny Reible
%djl@mail.utexas.edu and reible@mail.utexas.edu
%Department of Civil, Architectural, and Environmental Engineering
%The University of Texas at Austin
%Last Updated: 4/02/2008

%Purpose: This model calculates contaminant transport through a
%sediment cap assuming advection, diffusion/dispersion, reaction,
%bioturbation, deposition and retardation with local equilibrium
%between particle, pore water, and dissolved organic matter.  This
%model can be used for cap design.

%The active layer is assumed to maintain a Freundlich partitioning
%relationship with the pore water.  The governing equations are solved
%using a two-point upwind centered differencing scheme in space and the
%Crank-Nicolson method.  The time step is increased four times to
%provide a more efficient calculation of contaminant transport.

%Instructions:  Copy this program into the Matlab directory.  Then
%change the "Inputs" to view the transient concentration profiles for
%the model.  Users familiar may change the number of grid points, p,
%although using too few may result in model failure.  More grid points
%can be used to improve the accuracy.

%The initial depth of contamination and an optional underlying clean
%layer may also be specified by the user.  The appropriate bottom
%boundary condition varies with the specifics of the problem and may be
%changed by the user.  The default is a zero-slope boundary, which
%reduces to a constant concentration for an advectively-dominated
%system and a zero-%flux for a diffusion-dominated system.  The
%sediment can also be %assumed an infinte source (constant
%concentration).  For more details %see lines 337-347 and 373-380.  For
%a sand cap, use the same %properties in the %sand and active layers,
%set the Freundlich "n" %equal to 1, and the %Freundlich "Kf" equal to
%the product of Kocsand %and focsand.

%The program calculates the steady state values of Cbio, the
%concentration at the interface of the bioturbation and sand layers,
%and Cbl, the concentration at the sediment-water interface, and the
%numerical %values for comparison.  The theoretical times to
%breakthrough for the active, sand, and bioturbation layers, t1, t2,
%and t3, are used as the basis for the time spacing and plotting.  The
%dimensionless depth, actual depth, the dimensionless time, the actual
%time, and the dimensionless concentration profiles are then exported
%to an Excel file for further manipulation (for more information see
%lines 877-887).

%-------------------------Begin User Inputs----------------------------

%Inputs.  These are divided into Contaminant Properties, Sediment
%Properties, and Cap Properties.
```

```
%Contaminant Properties (Contaminant Specific)

logKoc=4.3;         %Organic Carbon Partition Coefficient, log (L/kg)
logKdoc=4;          %Colloidal Matter Partition Coefficient, log (L/kg)
Dw=6e-6;            %Molecular Diffusivity in Water, cm2/s

%Sediment Properties (Site Specific)

hcontaminated=20;   %Depth of Contamination, cm
hclean=20;           %Depth of Clean Sediment, cm
esed=0.5;           %Sediment Porosity
rhosed=2.6;         %Sediment Particle Density, g/cm3
focsed=.05;        %Sediment Fraction Organic Carbon
lambda0=0;          %Sediment Decay Rate, yr-1
C0=1;               %Contaminant Underlying Pore Water Concentration,
ug/L
rhodoc=10;          %Colloidal Matter Concentration, mg/L
Vdar=100;            %Darcy Velocity, cm/yr
Vdep=0.1;           %Depositional Velocity, cm/yr

%Bioturbation Layer Properties (Site Specific)

h3=10;              %Bioturbation Layer Thickness, cm
focbio=focsed;      %Bioturbation Layer Fraction Organic Carbon
lambda3=9.461;      %Bioturbation Decay Rate, yr-1
Dbiopw=315;         %Pore Water Biodiffusion Coefficient, cm2/yr
Dbiop=4;            %Particle Biodiffusion Coefficient, cm2/yr
kbl=1;              %Boundary Layer Mass Transfer Coefficient, cm/hr

%Active Cap Properties (Design Parameters)

h1=2.5;             %Active Layer Thickness, cm
eactive=0.5;        %Active Layer Porosity
rhoactive=2.6;      %Active Layer Particle Density, g/cm3
Kf=10^(logKoc);     %Active Layer Freundlich Coefficient
nf=.5;              %Active Layer Freundlich n
lambda1=0.9461;     %Active Layer Decay Rate, yr-1


%Sand Cap Properties (Design Parameters)

hsand=57.5;         %Total Sand Cap Thickness, cm
esand=eactive;      %Sand Layer Porosity
rhosand=2.6;        %Sand Layer Particle Density, g/cm3
focsand=.001;       %Sand Layer Fraction Organic Carbon
lambda2=lambda1;    %Sand Layer Decay Rate, yr-1

%Simulation Properties

p=251;              %Number of Grid Points

%--------------------------END USER INPUTS----------------------------
```

```
%Parameter Calculations

h=hcontaminated+hclean+h1+hsand;   %total domain thickness
h0=hcontaminated+hclean;           %total sediment thickness, cm
h2=hsand-h3;                       %effective cap layer thickness, cm
alpha=1.69*((hsand+h1)/100)^1.53;  %dispersivity, cm

D0=Dw*86400*365/(1-log(esed^2))+...
    alpha*Vdar;                    %sediment diff/disp coeff, cm2/yr
D1=Dw*86400*365*esand^(4/3)+...
    alpha*Vdar;                    %active layer diff/disp coeff,
cm2/yr
D2=Dw*86400*365*eactive^(4/3)+...
    alpha*Vdar;                    %sand diff/disp coeff, cm2/yr
D3=D1+Dbiop*(1-esand)*rhosand*focbio*10^...
    logKoc+Dbiopw;                 %bioturbation diff/disp coef,cm2/yr

R0=(esed+esed*rhodoc*10^(logKdoc-6)+(1-...
    esed)*rhosed*focsed*10^logKoc)/(1+...
    rhodoc*10^(logKdoc-6));        %sediment layer retardation factor
R1=(eactive+eactive*rhodoc*10^(logKdoc-6)+(1-...
    eactive)*rhoactive*Kf)/(1+...
    rhodoc*10^(logKdoc-6));        %active layer retardation factor
R2=(esand+esand*rhodoc*10^(logKdoc-6)+(1-esand)*...
    rhosand*focsand*10^logKoc)/(1+...
    rhodoc*10^(logKdoc-6));        %effective cap retardation factor
R3=(esand+esand*rhodoc*10^(logKdoc-6)+(1-...
    esand)*rhosand*focbio*10^logKoc)/(1+...
    rhodoc*10^(logKdoc-6));        %bioturbation retardation factor
Ract=0;                            %active layer retardation factors

U=Vdar-R2*Vdep;                    %effective advective velocity, cm/yr

if Vdar == 0
    U=0.00001;
end

%Dimensionless Calculations

Pe=U*h/D0;                  %Peclet Number
Da=esed*lambda0*h^2/D0;     %Damkohler Number
Sh=kbl*h*24*365/D3;         %Sherwood Number
del=0;                      %cap diffusivity vector
del(1)=D1/D0;
del(2)=D2/D0;
del(3)=D3/D0;
v=0;                        %cap retardation vector
v(1)=R1/R0;
v(2)=R2/R0;
v(3)=R3/R0;
zeta=0;                     %cap depth vector
zeta(1)=h1/h;
zeta(2)=h2/h;
```

```
zeta(3)=h3/h;

%Breakthrough Times (for finite differencing)

tadv=0;                     %layer characteristic advection times
tdiff=0;                    %layer characteristic diffusion times
tchar=0;                    %layer characteristic transport times
tauchar=0;                  %dimensionless transport times
tadv=R0*h/U.*v.*zeta;
tdiff=R0*h^2/D0/16.*v.*zeta.^2./del;
tchar=1./(1./tadv+1./tdiff);
tauchar=tchar.*D0./R0./h^2;

%Transient Solution.  The solution is split up into three pieces with
%different time steps based on the characteristic times, tau1, tau2,
%and tau3.  The different time steps ensure a more rapid run time
%without compromising accuracy.  The finite difference equations must
%be updated when the time step size changes.  The details of the finite
%differencing appear only in the first piece.  The equations are solved
%in dimensionless form: tau=t*D0/R0/h^2; zeta=z/h, u=C/C0.  The number
%of grid points can be changed to either decrease run time or increase
%accuracy.  The time steps can be changed in all of the pieces below.

p=p;                            %number of grid points
delz=1/(p-1);                   %grid spacing
p3=uint16(h3/h*(p-1)+1);        %point at the bottom of bioturbation
layer
p2=uint16((h2+h3)/h*(p-1)+1);   %point at the bottom of sand layer
p1=uint16((h1+h2+h3)/h*(p-1)+1);%point at the bottom of active layer
p0=uint16((h1+h2+h3+hcontaminated)/h*(p-1)+1);
                                %point at the bottom of contamination
q=0;                            %intermediate calculation
r=0;                            %intermediate calculation
s=0;                            %intermediate calculation
A=0;                            %intermediate calculation
k=0;                            %intermediate calculation

delt1=0.005*tauchar(1);             %time step size 1
delt2=0.01*(tauchar(1)+tauchar(2)); %time step size 2
delt3=0.1*sum(tauchar);             %time step size 3
delt4=sum(tauchar);                 %time step size 3

%solution variables

u=0;                        %solution matrix (rows follow points in
time,
                            %columns are profiles at one point in time)
uplot=0;                    %stores a condensed form of the solution
for
                            %graphing and exporting to Excel
time=0;                     %stores the time  and dimensionless time
for
                            %the values in wplot
```

```
%start with the initial conditions; these are arbitrary and can be
%changed by the user.  The default is constant concentration.

n=1;                        %time step count
t=0;                        %dimensionless time

%containment layers

u(1:p1-1,1)=0;
Ract(p2:p1)=R1;

%contaminated layer

u(p1:p0,1)=1;

%clean sediment layer

u(p0+1:p,1)=0;

time(1,1)=0;
time(1,2)=0;
uplot(1:p,1)=u(1:p,n);

%step forward in time

%Time Period 1

delt=delt1;               %Piece one dimensionless time step size

q0=delt/2/delz^2;
r0=Pe*delt/12/delz;
s0=Da*delt/2;
q=q0.*del;
r(1:3)=r0;
s(1)=eactive*lambda1*h^2/D0*delt/2;
s(2)=esand*lambda2*h^2/D0*delt/2;
s(3)=esand*lambda3*h^2/D0*delt/2;

%start with the top boundary condition

A(1,1)=2*delz*Sh+3;
A(1,2)=-4;
A(1,3)=1;

%fill in the difference equations for the bioturbation layer (j=3)

j=3;

for i=2:p3-2
    A(i,i-1)=-1*q(j)+2*r(j);
    A(i,i)=v(j)+2*q(j)+3*r(j)+s(j);
    A(i,i+1)=-1*q(j)-6*r(j);
```

```
    A(i,i+2)=r(j);
    k(i,i-1)=q(j)-2*r(j);
    k(i,i)=v(j)-2*q(j)-3*r(j)-s(j);
    k(i,i+1)=q(j)+6*r(j);
    k(i,i+2)=-1*r(j);
end

%must use a lower-order difference near the interface

A(p3-1,p3-2)=-1*q(j);
A(p3-1,p3-1)=v(j)+2*q(j)+6*r(j)+s(j);
A(p3-1,p3)=-1*q(j)-6*r(j);
k(p3-1,p3-2)=q(j);
k(p3-1,p3-1)=v(j)-2*q(j)-6*r(j)-s(j);
k(p3-1,p3)=q(j)+6*r(j);

%now the flux boundary condition

A(p3,p3-2)=1;
A(p3,p3-1)=-4;
A(p3,p3)=3+3*del(j-1)/del(j);
A(p3,p3+1)=-4*del(j-1)/del(j);
A(p3,p3+2)=del(j-1)/del(j);

%fill in the difference equations for the sand layer (j=2)

j=2;

for i=p3+1:p2-2
    A(i,i-1)=-1*q(j)+2*r(j);
    A(i,i)=v(j)+2*q(j)+3*r(j)+s(j);
    A(i,i+1)=-1*q(j)-6*r(j);
    A(i,i+2)=r(j);
    k(i,i-1)=q(j)-2*r(j);
    k(i,i)=v(j)-2*q(j)-3*r(j)-s(j);
    k(i,i+1)=q(j)+6*r(j);
    k(i,i+2)=-1*r(j);
end

%must use a lower-order difference near the interface

A(p2-1,p2-2)=-1*q(j);
A(p2-1,p2-1)=v(j)+2*q(j)+6*r(j)+s(j);
A(p2-1,p2)=-1*q(j)-6*r(j);
k(p2-1,p2-2)=q(j);
k(p2-1,p2-1)=v(j)-2*q(j)-6*r(j)-s(j);
k(p2-1,p2)=q(j)+6*r(j);

%now the flux boundary condition

A(p2,p2-2)=1;
A(p2,p2-1)=-4;
A(p2,p2)=3+3*del(j-1)/del(j);
```

```
A(p2,p2+1)=-4*del(j-1)/del(j);
A(p2,p2+2)=del(j-1)/del(j);

%fill in the difference equations for the active layer (j=1)

j=1;
for i=p2+1:p1-2
    A(i,i-1)=-1*q(j)+2*r(j);
    A(i,i)=v(j)+2*q(j)+3*r(j)+s(j);
    A(i,i+1)=-1*q(j)-6*r(j);
    A(i,i+2)=r(j);
    k(i,i-1)=q(j)-2*r(j);
    k(i,i)=v(j)-2*q(j)-3*r(j)-s(j);
    k(i,i+1)=q(j)+6*r(j);
    k(i,i+2)=-1*r(j);
end

%must use a lower-order difference near the interface

A(p1-1,p1-2)=-1*q(j);
A(p1-1,p1-1)=v(j)+2*q(j)+6*r(j)+s(j);
A(p1-1,p1)=-1*q(j)-6*r(j);
k(p1-1,p1-2)=q(j);
k(p1-1,p1-1)=v(j)-2*q(j)-6*r(j)-s(j);
k(p1-1,p1)=q(j)+6*r(j);

%now the flux boundary condition; for an infinite source case use the
%commented out version, comment out the next 5 lines and use hclean=0.

%A(p1,p1)=1;
%k(p1,p1)=1;

A(p1,p1-2)=1;
A(p1,p1-1)=-4;
A(p1,p1)=3+3/del(1);
A(p1,p1+1)=-4/del(1);
A(p1,p1+2)=1/del(1);

%fill in the difference equations for the contaminated layer (j=0)

j=0;

for i=p1+1:p-2
    A(i,i-1)=-1*q0+2*r0;
    A(i,i)=1+2*q0+3*r0+s0;
    A(i,i+1)=-1*q0-6*r0;
    A(i,i+2)=r0;
    k(i,i-1)=q0-2*r0;
    k(i,i)=1-2*q0-3*r0-s0;
    k(i,i+1)=q0+6*r0;
    k(i,i+2)=-1*r0;
end
```

```
%must use a lower-order difference near the interface

A(p-1,p-2)=-1*q0;
A(p-1,p-1)=1+2*q0+6*r0+s0;
A(p-1,p)=-1*q0-6*r0;
k(p-1,p-2)=q0;
k(p-1,p-1)=1-2*q0-6*r0-s0;
k(p-1,p)=q0+6*r0;

%now the flux boundary condition- infinite layer of contamination
%for finite layer of contamination and fixed concentration at bottom
%(such as in an advectively-dominated system)comment out A(p,p-1), and
%set k(p,p) to desired concentration (e.g. 0 or 1)

A(p,p-1)=-1;
A(p,p)=1;
k(p,p)=0;

while t < 0.5*tauchar(1)
    t=t+delt;
    u(1:p,n+1)=linsolve(A,k*u(1:p,n));
    n=n+1;

    %update the retardation factors in the active layer

    for i=p2+1:p1-1
        if (u(i,n) > 0.01)
            Ract(i)=(eactive*(1+rhodoc*10^(logKdoc-6))+(1-eactive)*...
                rhoactive*Kf*(u(i,n)*C0)^(nf-1))/(1+rhodoc*...
                10^(logKdoc6));
        end
        A(i,i)=Ract(i)/R1*v(1)+2*q(1)+3*r(1)+s(1);
        k(i,i)=Ract(i)/R1*v(1)-2*q(1)-3*r(1)-s(1);
    end
    A(p1-1,p1-1)=Ract(p1-1)/R1*v(1)+2*q(1)+6*r(1)+s(1);
    k(p1-1,p1-1)=Ract(p1-1)/R1*v(1)-2*q(1)-6*r(1)-s(1);
end

time(2,1)=t;
time(2,2)=t*R0/D0*h^2;
uplot(1:p,2)=u(1:p,n);

while t < tauchar(1)
    t=t+delt;
    u(1:p,n+1)=linsolve(A,k*u(1:p,n));
    n=n+1;
    for i=p2+1:p1-1
        if (u(i,n) > 0.01)
            Ract(i)=(eactive*(1+rhodoc*10^(logKdoc-6))+(1-eactive)*...
            rhoactive*Kf*(u(i,n)*C0)^(nf-1))/(1+rhodoc*10^(logKdoc-6));
        end
        A(i,i)=Ract(i)/R1*v(1)+2*q(1)+3*r(1)+s(1);
        k(i,i)=Ract(i)/R1*v(1)-2*q(1)-3*r(1)-s(1);
```

```
    end
    A(p1-1,p1-1)=Ract(p1-1)/R1*v(1)+2*q(1)+6*r(1)+s(1);
    k(p1-1,p1-1)=Ract(p1-1)/R1*v(1)-2*q(1)-6*r(1)-s(1);
end

time(3,1)=t;
time(3,2)=t*R0/D0*h^2;
uplot(1:p,3)=u(1:p,n);

%Time Period 2

delt=delt2;                %Piece two dimensionless time step size

q0=delt/2/delz^2;
r0=Pe*delt/12/delz;
s0=Da*delt/2;
q=q0.*del;
r(1:3)=r0;
s(1)=eactive*lambda1*h^2/D0*delt/2;
s(2)=esand*lambda2*h^2/D0*delt/2;
s(3)=esand*lambda3*h^2/D0*delt/2;

j=3;
for i=2:p3-2
    A(i,i-1)=-1*q(j)+2*r(j);
    A(i,i)=v(j)+2*q(j)+3*r(j)+s(j);
    A(i,i+1)=-1*q(j)-6*r(j);
    A(i,i+2)=r(j);
    k(i,i-1)=q(j)-2*r(j);
    k(i,i)=v(j)-2*q(j)-3*r(j)-s(j);
    k(i,i+1)=q(j)+6*r(j);
    k(i,i+2)=-1*r(j);
end

A(p3-1,p3-2)=-1*q(j);
A(p3-1,p3-1)=v(j)+2*q(j)+6*r(j)+s(j);
A(p3-1,p3)=-1*q(j)-6*r(j);
k(p3-1,p3-2)=q(j);
k(p3-1,p3-1)=v(j)-2*q(j)-6*r(j)-s(j);
k(p3-1,p3)=q(j)+6*r(j);

j=2;
for i=p3+1:p2-2
    A(i,i-1)=-1*q(j)+2*r(j);
    A(i,i)=v(j)+2*q(j)+3*r(j)+s(j);
    A(i,i+1)=-1*q(j)-6*r(j);
    A(i,i+2)=r(j);
    k(i,i-1)=q(j)-2*r(j);
    k(i,i)=v(j)-2*q(j)-3*r(j)-s(j);
    k(i,i+1)=q(j)+6*r(j);
    k(i,i+2)=-1*r(j);
end
```

```
A(p2-1,p2-2)=-1*q(j);
A(p2-1,p2-1)=v(j)+2*q(j)+6*r(j)+s(j);
A(p2-1,p2)=-1*q(j)-6*r(j);
k(p2-1,p2-2)=q(j);
k(p2-1,p2-1)=v(j)-2*q(j)-6*r(j)-s(j);
k(p2-1,p2)=q(j)+6*r(j);

j=1;
for i=p2+1:p1-2
    A(i,i-1)=-1*q(j)+2*r(j);
    A(i,i)=Ract(i)/R1*v(j)+2*q(j)+3*r(j)+s(j);
    A(i,i+1)=-1*q(j)-6*r(j);
    A(i,i+2)=r(j);
    k(i,i-1)=q(j)-2*r(j);
    k(i,i)=Ract(i)/R1*v(j)-2*q(j)-3*r(j)-s(j);
    k(i,i+1)=q(j)+6*r(j);
    k(i,i+2)=-1*r(j);
end

A(p1-1,p1-2)=-1*q(j);
A(p1-1,p1-1)=Ract(p1-1)/R1*v(j)+2*q(j)+6*r(j)+s(j);
A(p1-1,p1)=-1*q(j)-6*r(j);
k(p1-1,p1-2)=q(j);
k(p1-1,p1-1)=Ract(p1-1)/R1*v(j)-2*q(j)-6*r(j)-s(j);
k(p1-1,p1)=q(j)+6*r(j);

j=0;
for i=p1+1:p-2
    A(i,i-1)=-1*q0+2*r0;
    A(i,i)=1+2*q0+3*r0+s0;
    A(i,i+1)=-1*q0-6*r0;
    A(i,i+2)=r0;
    k(i,i-1)=q0-2*r0;
    k(i,i)=1-2*q0-3*r0-s0;
    k(i,i+1)=q0+6*r0;
    k(i,i+2)=-1*r0;
end

A(p-1,p-2)=-1*q0;
A(p-1,p-1)=1+2*q0+6*r0+s0;
A(p-1,p)=-1*q0-6*r0;
k(p-1,p-2)=q0;
k(p-1,p-1)=1-2*q0-6*r0-s0;
k(p-1,p)=q0+6*r0;

while t < tauchar(1)+tauchar(2)
    t=t+delt;
    u(1:p,n+1)=linsolve(A,k*u(1:p,n));
    n=n+1;
    for i=p2+1:p1-1
        if (u(i,n) > 0.01)
            Ract(i)=(eactive*(1+rhodoc*10^(logKdoc-6))+(1-eactive)*...
            rhoactive*Kf*(u(i,n)*C0)^(nf-1))/(1+rhodoc*10^(logKdoc-6));
```

```
        end
        A(i,i)=Ract(i)/R1*v(1)+2*q(1)+3*r(1)+s(1);
        k(i,i)=Ract(i)/R1*v(1)-2*q(1)-3*r(1)-s(1);
    end
    A(p1-1,p1-1)=Ract(p1-1)/R1*v(1)+2*q(1)+6*r(1)+s(1);
    k(p1-1,p1-1)=Ract(p1-1)/R1*v(1)-2*q(1)-6*r(1)-s(1);
end

time(4,1)=t;
time(4,2)=t*R0/D0*h^2;
uplot(1:p,4)=u(1:p,n);

while t < sum(tauchar)
    t=t+delt;
    u(1:p,n+1)=linsolve(A,k*u(1:p,n));
    n=n+1;
    for i=p2+1:p1-1
        if (u(i,n) > 0.01)
            Ract(i)=(eactive*(1+rhodoc*10^(logKdoc-6))+(1-eactive)*...
            rhoactive*Kf*(u(i,n)*C0)^(nf-1))/(1+rhodoc*10^(logKdoc-6));
        end
        A(i,i)=Ract(i)/R1*v(1)+2*q(1)+3*r(1)+s(1);
        k(i,i)=Ract(i)/R1*v(1)-2*q(1)-3*r(1)-s(1);
    end
    A(p1-1,p1-1)=Ract(p1-1)/R1*v(1)+2*q(1)+6*r(1)+s(1);
    k(p1-1,p1-1)=Ract(p1-1)/R1*v(1)-2*q(1)-6*r(1)-s(1);
end

time(5,1)=t;
time(5,2)=t*R0/D0*h^2;
uplot(1:p,5)=u(1:p,n);

while t < 2*sum(tauchar)
    t=t+delt;
    u(1:p,n+1)=linsolve(A,k*u(1:p,n));
    n=n+1;
    for i=p2+1:p1-1
        if (u(i,n) > 0.01)
            Ract(i)=(eactive*(1+rhodoc*10^(logKdoc-6))+(1-eactive)*...
            rhoactive*Kf*(u(i,n)*C0)^(nf-1))/(1+rhodoc*10^(logKdoc-6));
        end
        A(i,i)=Ract(i)/R1*v(1)+2*q(1)+3*r(1)+s(1);
        k(i,i)=Ract(i)/R1*v(1)-2*q(1)-3*r(1)-s(1);
    end
    A(p1-1,p1-1)=Ract(p1-1)/R1*v(1)+2*q(1)+6*r(1)+s(1);
    k(p1-1,p1-1)=Ract(p1-1)/R1*v(1)-2*q(1)-6*r(1)-s(1);
end

time(6,1)=t;
time(6,2)=t*R0/D0*h^2;
uplot(1:p,6)=u(1:p,n);

%Time Period 3
```

```
delt=delt3;                %Piece three dimensionless time step size

q0=delt/2/delz^2;
r0=Pe*delt/12/delz;
s0=Da*delt/2;
q=q0.*del;
r(1:3)=r0;
s(1)=eactive*lambda1*h^2/D0*delt/2;
s(2)=esand*lambda2*h^2/D0*delt/2;
s(3)=esand*lambda3*h^2/D0*delt/2;

j=3;
for i=2:p3-2
    A(i,i-1)=-1*q(j)+2*r(j);
    A(i,i)=v(j)+2*q(j)+3*r(j)+s(j);
    A(i,i+1)=-1*q(j)-6*r(j);
    A(i,i+2)=r(j);
    k(i,i-1)=q(j)-2*r(j);
    k(i,i)=v(j)-2*q(j)-3*r(j)-s(j);
    k(i,i+1)=q(j)+6*r(j);
    k(i,i+2)=-1*r(j);
end

A(p3-1,p3-2)=-1*q(j);
A(p3-1,p3-1)=v(j)+2*q(j)+6*r(j)+s(j);
A(p3-1,p3)=-1*q(j)-6*r(j);
k(p3-1,p3-2)=q(j);
k(p3-1,p3-1)=v(j)-2*q(j)-6*r(j)-s(j);
k(p3-1,p3)=q(j)+6*r(j);

j=2;
for i=p3+1:p2-2
    A(i,i-1)=-1*q(j)+2*r(j);
    A(i,i)=v(j)+2*q(j)+3*r(j)+s(j);
    A(i,i+1)=-1*q(j)-6*r(j);
    A(i,i+2)=r(j);
    k(i,i-1)=q(j)-2*r(j);
    k(i,i)=v(j)-2*q(j)-3*r(j)-s(j);
    k(i,i+1)=q(j)+6*r(j);
    k(i,i+2)=-1*r(j);
end

A(p2-1,p2-2)=-1*q(j);
A(p2-1,p2-1)=v(j)+2*q(j)+6*r(j)+s(j);
A(p2-1,p2)=-1*q(j)-6*r(j);
k(p2-1,p2-2)=q(j);
k(p2-1,p2-1)=v(j)-2*q(j)-6*r(j)-s(j);
k(p2-1,p2)=q(j)+6*r(j);

j=1;
for i=p2+1:p1-2
    A(i,i-1)=-1*q(j)+2*r(j);
```

```
    A(i,i)=Ract(i)/R1*v(j)+2*q(j)+3*r(j)+s(j);
    A(i,i+1)=-1*q(j)-6*r(j);
    A(i,i+2)=r(j);
    k(i,i-1)=q(j)-2*r(j);
    k(i,i)=Ract(i)/R1*v(j)-2*q(j)-3*r(j)-s(j);
    k(i,i+1)=q(j)+6*r(j);
    k(i,i+2)=-1*r(j);
end

A(p1-1,p1-2)=-1*q(j);
A(p1-1,p1-1)=Ract(p1-1)/R1*v(j)+2*q(j)+6*r(j)+s(j);
A(p1-1,p1)=-1*q(j)-6*r(j);
k(p1-1,p1-2)=q(j);
k(p1-1,p1-1)=Ract(p1-1)/R1*v(j)-2*q(j)-6*r(j)-s(j);
k(p1-1,p1)=q(j)+6*r(j);

j=0;
for i=p1+1:p-2
    A(i,i-1)=-1*q0+2*r0;
    A(i,i)=1+2*q0+3*r0+s0;
    A(i,i+1)=-1*q0-6*r0;
    A(i,i+2)=r0;
    k(i,i-1)=q0-2*r0;
    k(i,i)=1-2*q0-3*r0-s0;
    k(i,i+1)=q0+6*r0;
    k(i,i+2)=-1*r0;
end

A(p-1,p-2)=-1*q0;
A(p-1,p-1)=1+2*q0+6*r0+s0;
A(p-1,p)=-1*q0-6*r0;
k(p-1,p-2)=q0;
k(p-1,p-1)=1-2*q0-6*r0-s0;
k(p-1,p)=q0+6*r0;

while t < 5*sum(tauchar)
    t=t+delt;
    u(1:p,n+1)=linsolve(A,k*u(1:p,n));
    n=n+1;
    for i=p2+1:p1-1
        if (u(i,n) > 0.01)
            Ract(i)=(eactive*(1+rhodoc*10^(logKdoc-6))+(1-eactive)*...
            rhoactive*Kf*(u(i,n)*C0)^(nf-1))/(1+rhodoc*10^(logKdoc-6));
        end
        A(i,i)=Ract(i)/R1*v(1)+2*q(1)+3*r(1)+s(1);
        k(i,i)=Ract(i)/R1*v(1)-2*q(1)-3*r(1)-s(1);
    end
    A(p1-1,p1-1)=Ract(p1-1)/R1*v(1)+2*q(1)+6*r(1)+s(1);
    k(p1-1,p1-1)=Ract(p1-1)/R1*v(1)-2*q(1)-6*r(1)-s(1);
end

time(7,1)=t;
time(7,2)=t*R0/D0*h^2;
```

```
uplot(1:p,7)=u(1:p,n);

delt=delt4;                %Piece four dimensionless time step size

q0=delt/2/delz^2;
r0=Pe*delt/12/delz;
s0=Da*delt/2;
q=q0.*del;
r(1:3)=r0;
s(1)=eactive*lambda1*h^2/D0*delt/2;
s(2)=esand*lambda2*h^2/D0*delt/2;
s(3)=esand*lambda3*h^2/D0*delt/2;

j=3;
for i=2:p3-2
    A(i,i-1)=-1*q(j)+2*r(j);
    A(i,i)=v(j)+2*q(j)+3*r(j)+s(j);
    A(i,i+1)=-1*q(j)-6*r(j);
    A(i,i+2)=r(j);
    k(i,i-1)=q(j)-2*r(j);
    k(i,i)=v(j)-2*q(j)-3*r(j)-s(j);
    k(i,i+1)=q(j)+6*r(j);
    k(i,i+2)=-1*r(j);
end

A(p3-1,p3-2)=-1*q(j);
A(p3-1,p3-1)=v(j)+2*q(j)+6*r(j)+s(j);
A(p3-1,p3)=-1*q(j)-6*r(j);
k(p3-1,p3-2)=q(j);
k(p3-1,p3-1)=v(j)-2*q(j)-6*r(j)-s(j);
k(p3-1,p3)=q(j)+6*r(j);

j=2;
for i=p3+1:p2-2
    A(i,i-1)=-1*q(j)+2*r(j);
    A(i,i)=v(j)+2*q(j)+3*r(j)+s(j);
    A(i,i+1)=-1*q(j)-6*r(j);
    A(i,i+2)=r(j);
    k(i,i-1)=q(j)-2*r(j);
    k(i,i)=v(j)-2*q(j)-3*r(j)-s(j);
    k(i,i+1)=q(j)+6*r(j);
    k(i,i+2)=-1*r(j);
end

A(p2-1,p2-2)=-1*q(j);
A(p2-1,p2-1)=v(j)+2*q(j)+6*r(j)+s(j);
A(p2-1,p2)=-1*q(j)-6*r(j);
k(p2-1,p2-2)=q(j);
k(p2-1,p2-1)=v(j)-2*q(j)-6*r(j)-s(j);
k(p2-1,p2)=q(j)+6*r(j);

j=1;
for i=p2+1:p1-2
```

```
    A(i,i-1)=-1*q(j)+2*r(j);
    A(i,i)=Ract(i)/R1*v(j)+2*q(j)+3*r(j)+s(j);
    A(i,i+1)=-1*q(j)-6*r(j);
    A(i,i+2)=r(j);
    k(i,i-1)=q(j)-2*r(j);
    k(i,i)=Ract(i)/R1*v(j)-2*q(j)-3*r(j)-s(j);
    k(i,i+1)=q(j)+6*r(j);
    k(i,i+2)=-1*r(j);
end

A(p1-1,p1-2)=-1*q(j);
A(p1-1,p1-1)=Ract(p1-1)/R1*v(j)+2*q(j)+6*r(j)+s(j);
A(p1-1,p1)=-1*q(j)-6*r(j);
k(p1-1,p1-2)=q(j);
k(p1-1,p1-1)=Ract(p1-1)/R1*v(j)-2*q(j)-6*r(j)-s(j);
k(p1-1,p1)=q(j)+6*r(j);

j=0;
for i=p1+1:p-2
    A(i,i-1)=-1*q0+2*r0;
    A(i,i)=1+2*q0+3*r0+s0;
    A(i,i+1)=-1*q0-6*r0;
    A(i,i+2)=r0;
    k(i,i-1)=q0-2*r0;
    k(i,i)=1-2*q0-3*r0-s0;
    k(i,i+1)=q0+6*r0;
    k(i,i+2)=-1*r0;
end

A(p-1,p-2)=-1*q0;
A(p-1,p-1)=1+2*q0+6*r0+s0;
A(p-1,p)=-1*q0-6*r0;
k(p-1,p-2)=q0;
k(p-1,p-1)=1-2*q0-6*r0-s0;
k(p-1,p)=q0+6*r0;

while t < 10*sum(tauchar)
    t=t+delt;
    u(1:p,n+1)=linsolve(A,k*u(1:p,n));
    n=n+1;
    for i=p2+1:p1-1
        if (u(i,n) > 0.01)
            Ract(i)=(eactive*(1+rhodoc*10^(logKdoc-6))+(1-eactive)*...
            rhoactive*Kf*(u(i,n)*C0)^(nf-1))/(1+rhodoc*10^(logKdoc-6));
        end
        A(i,i)=Ract(i)/R1*v(1)+2*q(1)+3*r(1)+s(1);
        k(i,i)=Ract(i)/R1*v(1)-2*q(1)-3*r(1)-s(1);
    end
    A(p1-1,p1-1)=Ract(p1-1)/R1*v(1)+2*q(1)+6*r(1)+s(1);
    k(p1-1,p1-1)=Ract(p1-1)/R1*v(1)-2*q(1)-6*r(1)-s(1);
end

time(8,1)=t;
```

```
time(8,2)=t*R0/D0*h^2;
uplot(1:p,8)=u(1:p,n);

while t < 25*sum(tauchar)
    t=t+delt;
    u(1:p,n+1)=linsolve(A,k*u(1:p,n));
    n=n+1;
    for i=p2+1:p1-1
        if (u(i,n) > 0.01)
            Ract(i)=(eactive*(1+rhodoc*10^(logKdoc-6))+(1-eactive)*...
            rhoactive*Kf*(u(i,n)*C0)^(nf-1))/(1+rhodoc*10^(logKdoc-6));
        end
        A(i,i)=Ract(i)/R1*v(1)+2*q(1)+3*r(1)+s(1);
        k(i,i)=Ract(i)/R1*v(1)-2*q(1)-3*r(1)-s(1);
    end
    A(p1-1,p1-1)=Ract(p1-1)/R1*v(1)+2*q(1)+6*r(1)+s(1);
    k(p1-1,p1-1)=Ract(p1-1)/R1*v(1)-2*q(1)-6*r(1)-s(1);
end

time(9,1)=t;
time(9,2)=t*R0/D0*h^2;
uplot(1:p,9)=u(1:p,n);

while t < 60*sum(tauchar)
    t=t+delt;
    u(1:p,n+1)=linsolve(A,k*u(1:p,n));
    n=n+1;
    for i=p2+1:p1-1
        if (u(i,n) > 0.01)
            Ract(i)=(eactive*(1+rhodoc*10^(logKdoc-6))+(1-eactive)*...
            rhoactive*Kf*(u(i,n)*C0)^(nf-1))/(1+rhodoc*10^(logKdoc-6));
        end
        A(i,i)=Ract(i)/R1*v(1)+2*q(1)+3*r(1)+s(1);
        k(i,i)=Ract(i)/R1*v(1)-2*q(1)-3*r(1)-s(1);
    end
    A(p1-1,p1-1)=Ract(p1-1)/R1*v(1)+2*q(1)+6*r(1)+s(1);
    k(p1-1,p1-1)=Ract(p1-1)/R1*v(1)-2*q(1)-6*r(1)-s(1);
end

time(10,1)=t;
time(10,2)=t*R0/D0*h^2;
uplot(1:p,10)=u(1:p,n);

while t < 250*sum(tauchar)
    t=t+delt;
    u(1:p,n+1)=linsolve(A,k*u(1:p,n));
    n=n+1;
    for i=p2+1:p1-1
        if (u(i,n) > 0.01)
            Ract(i)=(eactive*(1+rhodoc*10^(logKdoc-6))+(1-eactive)*...
            rhoactive*Kf*(u(i,n)*C0)^(nf-1))/(1+rhodoc*10^(logKdoc-6));
        end
        A(i,i)=Ract(i)/R1*v(1)+2*q(1)+3*r(1)+s(1);
```

```
        k(i,i)=Ract(i)/R1*v(1)-2*q(1)-3*r(1)-s(1);
    end
    A(p1-1,p1-1)=Ract(p1-1)/R1*v(1)+2*q(1)+6*r(1)+s(1);
    k(p1-1,p1-1)=Ract(p1-1)/R1*v(1)-2*q(1)-6*r(1)-s(1);
end

time(11,1)=t;
time(11,2)=t*R0/D0*h^2;
uplot(1:p,11)=u(1:p,n);

%Now reduce and plot the data

Cplot=uplot.*C0;
depth=(0:delz:1).*h;
Cbionumerical=uplot(p3,11)
Cblnumerical=uplot(1,11)

%Steady State Solution; note that this will not compare favorably with
%the numerical simulation if the decay rates are different in the
%active and passive layers

Pe1=U*(h1+h2)/D1;               %effective cap Peclet number
Da1=esand*lambda1*(h1+h2)^2/D1; %effective cap Damkohler number
Pe3=U*h3/D3;                    %bioturbation Peclet number
Da3=esand*lambda3*h3^2/D3;      %biotubation Damkohler number
Sh=kbl*24*365*h3/D3;            %Sherwood Number at cap/water interface
beta=(Pe1^2/4+Da1)^0.5;         %intermediate calculation
gamma=(Pe3^2/4+Da3)^0.5;        %intermediate calculation

Cbio=beta*Pe3/Pe1*exp(Pe1/2)*sinh(gamma)/(beta*sinh(gamma)*...
    cosh(beta)*Pe3/Pe1+gamma*cosh(gamma)*sinh(beta)-gamma^2*...
    sinh(beta)/((Sh+Pe3/2)*sinh(gamma)+gamma*cosh(gamma)))

Cbl=exp(Pe1/2+Pe3/2)/((Pe1/2+Sh*Pe1/Pe3)*sinh(beta)*cosh(gamma)/...
      beta+(Pe3/2+Sh)*cosh(beta)*sinh(gamma)/gamma+Pe1/Pe3*gamma*...
      sinh(gamma)*sinh(beta)/beta+cosh(beta)*cosh(gamma))

%The "output" vector here stores the time in row 1, the dimensionless
depth
%in Column 1, the actual depth in Column 2, and the dimensionless
%concentration profiles in the rest of the matrix.

output=0;
output(1,3:13)=transpose(time(1:11,2));
output(2:p+1,1)=0:delz:1;
output(2:p+1,2)=(0:delz:1).*h;
output(2:p+1,3:13)=Cplot;

xlswrite('capsimulation',output);

leg=0;
leg=num2str(time(1:11,2),3);
plot(depth,Cplot)
```

```
xlabel('Depth, cm')
ylabel('Concentration, ug/L')
title('Concentration Profiles within a Sediment Cap (Time in Years)')
legend(leg,'Location','EastOutside','Orientation','vertical')
```

Appendix D: Python Programs for Solving Passive Sampler Diffusion Models

The time to equilibrium in PDMS fibers can be extensive; therefore, it is important to be able to predict the time to reach equilibrium for experimental design, or, if complete equilibration is impossible, to predict the percentage of equilibrium attained in a given time period. In this appendix, the source code for a mathematical model for mass transport is presented. The derivation of the model approach is presented in Chapter 6. The method is based on the numerical inversion of the dimensionless Laplace-transformed solution. The source begins on the next page, including an example using the model to calculate the percentage of steady state for the default conditions with a different porosity. The interested reader is encouraged to contact the author for information on using the script.

```
#! /usr/bin/env python
#
#a script for numerical inversion of Laplace Transform using the Talbot method
#
#Instructions: The "Inputs" class type is developed with the model input
#parameters.  This file serves as the input to the "System" class type, which
#essentially converts the parameters into dimensionless form to be used as
#an input to the "SolveU" and "SolveV" routines.  SolveU provides the pore
#water concentration at dimensionless time t and dimensionless distance x for
#the system (i.e. fiber and sediment) developed previously.  The dimensionless
#uptake in the fiber can be quantified by looking at the value of "SolveU" at
#x = 1.  An example is shown in the last lines.

from cmath import *
from math  import log

import scipy.special as sp

class Inputs:
    """Holds the input parameters for the system."""

    def __init__(self):

        self.C0  = 1.       #initial porewater concentration    (ng/L)
        self.e   = 0.5      #porosity                           (-)
        self.rho = 1.5      #bulk density                       (g/cm3)
        self.flc = 0.01     #fraction labile organic carbon     (-)
        self.fhc = 0.0006   #fraction hard organic carbon
        self.Klc = 4.       #labile carbon partition coeff      (log(L/kg))
        self.Khc = 4.       #hard carbon partition coeff        (log(L/kg))
        self.Dw  = 1.e-5    #molecular diffusivity in water     (cm2/s)
        self.kh  = 1.       #sediment-water sorption mtc        (s-1)
        self.Kf  = 4.       #fiber-water partition coefficient  (L/L)
        self.D1  = 0.1      #fiber inner diameter               (cm)
        self.D2  = 0.106    #fiber outer diameter               (cm)
        self.rf  = 0.159    #outermost radius to compute        (cm)
        self.nr  = 100      #number of radial grid points
        self.nt  = 1        #number of time graphs to create
        self.tf  = 1.       #final time to plot                 (hr)
        self.np  = 100      #number of time points
        self.opt = 0        #plot option
        self.name = 'input' #input file name
        self.t   = []       #times to plot

class System:
    """Holds the system parameters for the simulation."""

    def __init__(self, inputs):

        self.C0     = inputs.C0
        self.e      = inputs.e
        self.rho    = inputs.rho
        self.D      = self.e * inputs.Dw / (1 - log(self.e**2))
        self.D2     = inputs.D2
        self.Kd     = inputs.fhc * 10**inputs.Khc
        self.Kl     = inputs.flc * 10**inputs.Klc
        self.R      = self.e + self.rho * inputs.flc * 10**inputs.Klc
        self.Bi     = inputs.kh * self.D2**2 / 4 / self.D
        self.Dr     = 2 * self.D2**2 / (self.D2**2 - inputs.D1**2) / \
```

```
                    10**inputs.Kf
        self.xis    = []
        self.taus   = []

def cot(phi): return 1. / tan(phi)
def csc(phi): return 1. / sin(phi)

def solveU(t, x, system, N = 10):
    """Used for numerical inversion of the 'U' function given below using the
    Talbot method."""

    R   = system.R
    rho = system.rho
    Kd  = system.Kd
    Bi  = system.Bi
    Dr  = system.Dr

    def U(s):
        """Defines the Laplace transformed solution."""

        a = sqrt((R * s**2 + (R + rho * Kd) * Bi * s) / (s + Bi))
        return (sp.kv(0, a * x) / (s * sp.kv(0, a) + Dr * a * sp.kv(1, a)))

    #Initiate the stepsize

    h = 2 * pi / N;

    #Shift contour to the right in case there is a pole on the positive
    #real axis: Note the contour will not be optimal since it was
    #originally devoloped for function with singularities on the negative
    #real axis.

    #For example take F(s) = 1/(s-1), it has a pole at s = 1, the contour
    #needs to be shifted with one unit, i.e shift  = 1. But in the test
    #example no shifting is necessary.

    shift = 0.0;
    ans =   0.0;

    if t == 0:
        print "ERROR:   Inverse transform can not be calculated for t = 0"
        return ("Error");

    #The for loop is evaluating the Laplace inversion at each point theta which
    #is based on the trapezoidal rule

    for k in range(0, N):
        theta = -pi + (k + 1. / 2) * h
        z = shift + N / t * (0.5017 * theta * cot(0.6407 * theta) - 0.6122 \
                                + 0.2645j * theta)
        dz = N / t * (-0.5017 * 0.6407 * theta * (csc(0.6407 * theta)**2) +\
                           0.5017 * cot(0.6407 * theta) + 0.2645j)
        ans = ans + exp(z * t) * U(z) * dz

    return ((h/(2j * pi)) * ans).real

def solveV(t, x, system, N = 10):
    """Used for numerical inversion of the 'V' function given below using the
    Talbot method."""
```

```
    R   = system.R
    rho = system.rho
    Kd  = system.Kd
    Bi  = system.Bi
    Dr  = system.Dr

    def V(s):
        """Defines the Laplace transformed solution."""

        a = sqrt((R * s**2 + (R + rho * Kd) * Bi * s) / (s + Bi))
        return (Bi / (s + Bi) * sp.kv(0, a * x) / (s * sp.kv(0, a) +
                                                   Dr * a * sp.kv(1, a)))

    #Initiate the stepsize

    h = 2 * pi / N;

    #Shift contour to the right in case there is a pole on the positive
    #real axis: Note the contour will not be optimal since it was
    #originally devoloped for function with singularities on the negative
    #real axis.

    #For example take F(s) = 1/(s-1), it has a pole at s = 1, the contour
    #needs to be shifted with one unit, i.e shift  = 1. But in the test
    #example no shifting is necessary.

    shift = 0.0;
    ans =   0.0;

    if t == 0:
        print "ERROR:   Inverse transform can not be calculated for t = 0"
        return ("Error");

    #The for loop is evaluating the Laplace inversion at each point theta which
    #is based on the trapezoidal rule

    for k in range(0, N):
        theta = -pi + (k + 1. / 2) * h
        z = shift + N / t * (0.5017 * theta * cot(0.6407 * theta) - 0.6122 \
                             + 0.2645j * theta)
        dz = N / t * (-0.5017 * 0.6407 * theta * (csc(0.6407 * theta)**2) +\
                      0.5017 * cot(0.6407 * theta) + 0.2645j)
        ans = ans + exp(z * t) * V(z) * dz

    return ((h/(2j * pi)) * ans).real



#Example using default input values other than porosity for uptake at t = 1.

exampleinput   = Inputs()        #Create an input file with the defaults

exampleinput.e = 0.4             #Change the porosity to 0.4; any other
                                 #parameters can be changed in the same way

system = System(exampleinput)    #Use the input file to make a system
print solveU(1., 1., system)     #Solve for "U" at t = 1, x = 1
```

Appendix E: Experimental Data Used in Figures

This appendix contains experimental data that were collected for this dissertation. Data previously published in other sources are not re-printed here.

E.1 Anacostia Coring Data

Table 12: Anacostia Sand Cap Mean Solid-Phase Concentrations versus Depth

Depth (cm)	PHE (µg/kg)	PYR (µg/kg)	CHR (µg/kg)	BAA (µg/kg)	BBF (µg/kg)	BKF (µg/kg)	BAP (µg/kg)	Fraction Native
26.5	7450	11179	5159	4648	5877	2566	4902	1.000
26	6225	10186	5386	5173	6399	2718	5627	1.000
25.5	5390	7030	4987	4077	5481	2294	4540	1.000
25	4896	8292	4016	4108	5395	2297	4352	1.000
24.5	4884	9230	4817	4381	6945	2755	5055	0.999
24	6032	8744	4927	4031	5918	2413	4312	0.923
23.5	3537	6671	3852	3397	4618	1882	3506	0.798
23	5313	6915	4777	4666	5135	2227	4193	0.578
22.5	989	1948	1217	937	1371	602	1098	0.356
22	667	1075	824	854	639	280	625	0.176
21.5	11	17	9	8	14	6	10	0.000
21	27	54	30	32	37	18	33	0.022
20	3	<1	<1	<1	<1	<1	<1	0.000
17.5	4	1	<1	<1	1	<1	<1	0.000
15	<1	<1	<1	<1	<1	<1	<1	0.000
12.5	<1	<1	<1	<1	<1	<1	<1	0.000
10	<1	<1	<1	<1	<1	<1	<1	0.000
7.5	<1	<1	<1	<1	<1	<1	<1	0.000
5	<1	<1	<1	<1	<1	<1	<1	0.000
2.5	<1	<1	<1	<1	<1	<1	<1	0.000
1	1095	1726	651	586	483	101	133	0.150

Table 13: Anacostia Sand Cap Standard Deviations in Solid-Phase Concentrations

Depth (cm)	PHE (µg/kg)	PYR (µg/kg)	CHR (µg/kg)	BAA (µg/kg)	BBF (µg/kg)	BKF (µg/kg)	BAP (µg/kg)
26.5	7450	11179	5159	4648	5877	2566	4902
26	6225	10186	5386	5173	6399	2718	5627
25.5	5390	7030	4987	4077	5481	2294	4540
25	4896	8292	4016	4108	5395	2297	4352
24.5	4884	9230	4817	4381	6945	2755	5055
24	6032	8744	4927	4031	5918	2413	4312
23.5	3537	6671	3852	3397	4618	1882	3506
23	5313	6915	4777	4666	5135	2227	4193
22.5	989	1948	1217	937	1371	602	1098
22	667	1075	824	854	639	280	625
21.5	11	17	9	8	14	6	10
21	27	54	30	32	37	18	33
20	3	<1	<1	<1	<1	<1	<1
17.5	4	1	<1	<1	1	<1	<1
15	<1	<1	<1	<1	<1	<1	<1
12.5	<1	<1	<1	<1	<1	<1	<1
10	<1	<1	<1	<1	<1	<1	<1
7.5	<1	<1	<1	<1	<1	<1	<1
5	<1	<1	<1	<1	<1	<1	<1
2.5	<1	<1	<1	<1	<1	<1	<1
1	246	318	186	141	126	20	39

E.2 Anacostia Pore Water Concentrations

Table 14: Anacostia Sand Cap Mean Pore Water Concentrations at Different Depths

Depth (cm)	PHE (ng/L)	PYR (ng/L)	BAA (ng/L)	BBF (ng/L)	BKF (ng/L)	BAP (ng/L)
2.5	48	19	2.1	1.5	0.32	0.42
7.5	42	16	1.5	1.4	0.28	0.36
12.5	41	18	1.5	5.3	0.19	0.19
17.5	52	12	1.0	0.9	0.21	0.29
22.5	49	13	1.2	0.8	0.23	0.37
27.5	63	18	1.8	1.1	0.23	0.33
32.5	77	25	2.3	1.5	0.26	0.30
37.5	106	31	2.3	1.4	0.27	0.33

Table 15: Anacostia Sand Cap Pore Water Concentration Sample Standard Deviations at Different Depths

Depth (cm)	PHE (ng/L)	PYR (ng/L)	BAA (ng/L)	BBF (ng/L)	BKF (ng/L)	BAP (ng/L)
2.5	23	7	0.6	0.4	0.06	0.01
7.5	3	4	0.2	0.1	0.03	0.12
12.5	21	9	0.8	6.0	0.06	0.07
17.5	4	3	0.5	0.2	0.01	0.11
22.5	2	1	0.2	0.1	0.11	0.28
27.5	1	1	0.6	0.3	0.04	0.11
32.5	26	9	0.4	0.4	0.05	0.04
37.5	53	5	0.4	0.2	0.00	0.06

Table 16: Anacostia Coke Cap Mean Pore Water Concentrations at Different Depths

Depth (cm)	PHE (ng/L)	PYR (ng/L)	BAA (ng/L)	BBF (ng/L)	BKF (ng/L)	BAP (ng/L)
2.5	38	12	1.0	1.0	0.21	0.18
7.5	28	13	1.3	1.2	0.24	0.29
12.5	41	16	1.5	1.1	0.25	0.35
17.5	59	23	2.3	2.1	0.35	0.55
22.5	72	25	1.9	1.7	0.35	0.43
27.5	67	20	1.7	1.4	0.29	0.36
32.5	87	30	2.8	2.2	0.47	0.65
37.5	80	29	2.5	2.0	0.42	0.54
42.5	57	23	3.9	2.3	0.52	0.70

Table 17: Anacostia Coke Cap Pore Water Concentrations Standard Deviations at Different Depths

Depth (cm)	PHE (ng/L)	PYR (ng/L)	BAA (ng/L)	BBF (ng/L)	BKF (ng/L)	BAP (ng/L)
2.5	26	5	0.4	0.2	0.03	0.04
7.5	1	2	0.3	0.2	0.05	0.12
12.5	15	5	0.6	0.9	0.15	0.22
17.5	9	5	0.2	0.6	0.18	0.13
22.5	11	8	0.6	0.4	0.07	0.08
27.5	10	4	0.4	0.5	0.09	0.14
32.5	27	8	1.2	0.4	0.12	0.25
37.5	32	13	1.3	1.5	0.30	0.40
42.5	51	20	4.2	2.3	0.54	0.70

Table 18: Anacostia AquaBlok™ Cap Pore Water Concentrations at Different Depths

Depth (cm)	PHE (ng/L)	PYR (ng/L)	BAA (ng/L)	BBF (ng/L)	BKF (ng/L)	BAP (ng/L)
2.5	46	21	1.5	1.2	0.18	0.21
7.5	47	18	1.8	1.2	0.25	0.31
12.5	56	19	1.7	1.2	0.21	0.24
17.5	58	20	1.8	1.0	0.21	0.25
22.5	62	20	1.7	1.0	0.18	0.22
27.5	62	20	1.9	1.3	0.26	0.32
32.5	69	22	2.1	1.4	0.25	0.30
37.5	63	17	1.5	1.1	0.19	0.23
42.5	60	16	1.3	1.0	0.18	0.18

Table 19: Anacostia AquaBlok™ Cap Pore Water Concentrations Standard Deviation at Different Depths

Depth (cm)	PHE (ng/L)	PYR (ng/L)	BAA (ng/L)	BBF (ng/L)	BKF (ng/L)	BAP (ng/L)
2.5	30	9	0.5	0.0	0.01	0.02
7.5	26	10	0.2	0.2	0.05	0.09
12.5	29	10	0.7	0.6	0.08	0.08
17.5	31	10	0.8	0.6	0.09	0.12
22.5	28	10	0.7	0.4	0.06	0.08
27.5	30	11	0.9	0.6	0.12	0.13
32.5	35	15	1.0	0.8	0.11	0.16
37.5	36	9	0.6	0.4	0.08	0.11
42.5	49	10	0.8	0.4	0.05	0.09

E.3 Passive Sampler Internal Diffusion Coefficient Data

Table 20: Passive Sampler Internal Diffusion Coefficients and Hydrophobicity

Compound	log K_{ow}[39] log (L/L)	D_{PE}[40] -log(m^2/s)	D_{PDMS}[41] -log(m^2/s)	D_{POM}[42] -log(m^2/s)
Naphthalene	3.35	11.7	10.0	13.6
Acenaphthene	3.92	12.7		13.7
Fluorene	4.18	12.4		13.8
Phenanthrene	4.57	13.2		14
Anthracene	4.45	12.5		14.0
Fluoranthene	5.20	13.0	10.8	14.2
Pyrene	5.18	12.9		14.2
Benzo[a]pyrene	6.13	14.0	11.1	
Dibenz[a,h]anthracene	6.75	14.5	11.4	

E.4 Passive Sampler Field Bioaccumulation Studies Data

PHE = phenanthrene
PYR = pyrene
CHR = chrysene
BAA = benz[a]anthracene
BBF = benzo[b]fluoranthene
BKF = benzo[k]fluoranthene
BAP = benzo[a]pyrene
C_w = pore water concentration
q_{lipid} = lipid-phase concentration
q_{oc} = organic carbon phase concentration
Cl = number of chlorine atoms

[39] MacKay (1992)
[40] Fernandez et al. (2009)
[41] Rusina et al. (2007)
[42] Hong and Luthy (2008)

Table 21: San Diego Bay Data

Compound	log K_{ow}[43]	q_{oc}	C_w (centrifuged)	C_w (PDMS) Mean	C_w (PDMS) Standard Deviation	q_{lipid}
	log (L/L)	ng/g	ng/L	ng/L	ng/L	ng/g
BAA	5.61	13866	190	2.54	0.74	460
BAA	5.61	8466	12	1.86	0.10	185
BBF	6.10	23743	504	2.98	0.80	1250
BBF	6.10	20807	226	0.43	0.10	335
BBF	6.10	20249	225	3.65	0.80	1448
BBF	6.10	1982	15	0.26	0.25	<10
BKF	6.11	24484	480	0.77	0.21	875
BKF	6.11	22939	222	0.12	0.04	<10
BKF	6.11	20595	225	1.15	0.27	503
BKF	6.11	1807	12	0.09	0.08	<10
BAP	6.13	23295	453	1.01	0.30	542
BAP	6.13	21056	206	0.14	0.06	<10
BAP	6.13	20599	212	1.42	0.39	503
BAP	6.13	1875	55	0.08	0.08	<10

Table 22: Anacostia Control Area PAH concentrations

Compound	log K_{ow}[43]	C_w (PDMS)	q_{lipid}
	log (L/L)	ng/L	ng/g
PHE	4.57	89.2	5.04
PYR	5.18	50.4	4.66
CHR	5.86	3.11	2.59
BAA	5.91	2.96	1.82
BBF	6.10	1.43	1.62
BKF	6.11	0.45	0.49
BAP	6.13	0.61	0.99

[43] MacKay et al. (1992)

Table 23: Anacostia Sand Cap PAH concentrations

Compound	log K_{ow}[44] log (L/L)	C_w (PDMS) ng/L	q_{lipid} ng/g
PHE	4.57	67.1	4.13
PYR	5.18	35.8	5.07
CHR	5.86	2.26	3.40
BAA	5.91	2.45	2.70
BBF	6.10	1.18	2.97
BKF	6.11	0.34	0.78
BAP	6.13	0.46	0.89

Table 24: Anacostia Coke Cap PAH concentrations

Compound	log K_{ow}[44] log (L/L)	C_w (PDMS) ng/L	q_{lipid} ng/g
PHE	4.57	107.7	3.99
PYR	5.18	47.9	4.14
CHR	5.86	4.10	4.53
BAA	5.91	3.31	3.26
BBF	6.10	1.81	5.38
BKF	6.11	0.58	1.81
BAP	6.13	0.72	2.34

[44] MacKay et al. (1992)

Table 25: Hunters Point Untreated Sediment Data (No Kinetics Corrections)

Congener Number	log K_{ow}[45] log (L/L)	Cl	q_{oc} ng/g	q_{lipid} ng/g	14-Day Small C_w ng/L	14-Day Large C_w ng/L	42-Day Small C_w ng/L	42-Day Large C_w ng/L
51	5.63	4	60	43	1264	1114	2789	2564
52	5.84	4	120	389	6992	5247	8560	8612
47	5.85	4	75	201	1650	1138	2216	3226
41	5.69	4	70	140	1257	810	2073	2336
40	5.66	4	37	149	1840	1275	2518	1879
81	6.36	4	356	551	570	267	1209	773
77	6.36	4	1263	1388	1762	846	2993	2413
95	6.13	5	1881	1895	7917	3767	14279	9550
91	6.13	5	78	227	362	257	602	512
92	6.35	5	171	336	1242	738	2316	338
101	6.38	5	1962	2351	2284	1079	4570	1828
99	6.39	5	508	881	749	471	2596	1290
83	6.26	5	20	76	147	63	158	334
85	6.30	5	120	257	229	110	490	366
107	6.71	5	111	140	111	48	202	68
123	6.74	5	5423	4038	2363	1018	4737	2788
118	6.74	5	754	1005	305	145	723	424
105	6.65	5	382	400	927	421	2358	1227
136	6.22	6	1005	696	1234	427	2243	1198
134	6.55	6	262	235	128	62	277	152
146	6.89	6	1544	1251	346	150	848	424
153	6.92	6	7356	6149	2196	982	5130	2658
141	6.82	6	1740	936	279	115	671	343
163	6.99	6	10214	8187	1614	750	3665	2004
158	7.02	6	1061	892	154	78	354	192
178	7.14	7	982	950	100	49	224	140
187	7.17	7	4842	2639	366	161	840	419
183	7.20	7	3186	1896	435	202	1080	602
185	7.11	7	535	231	39	17	86	41
174	7.11	7	4736	1896	303	139	736	366
177	7.08	7	3237	1748	191	91	418	237
172	7.33	7	1409	416	37	29	73	45
180	7.36	7	12309	5626	225	158	682	425
191	7.55	7	449	185	7.9	4.2	16.8	9.8
170	7.27	7	5237	1802	75.2	39.8	146.3	106.8
201	7.62	8	3912	789	36.1	16.4	69.9	43.1
203	7.65	8	5001	1458	39.4	19.6	78.6	51.2
195	7.56	8	1198	443	21.1	10.2	42.5	24.7
194	7.80	8	2528	564	10.9	5.6	22.4	16.4

[45] Hawker and Connell (1988)

Table 26: Hunters Point Treated Sediment Data (No Kinetics Corrections)

Congener Number	log K_{ow}[46] log (L/L)	Cl	q_{lipid} ng/g	14-Day small C_w ng/L	14-Day Small C_w ng/L	14-Day Large C_w ng/L	42-Day Small C_w ng/L
52	5.84	4	127	2677	1988	1508	771
40	5.66	4	46	599	439	477	359
81	6.36	4	340	72	506	60	51
77	6.36	4	847	125	283	117	126
95	6.13	5	744	365	846	466	568
101	6.38	5	1365	85	263	123	143
107	6.71	5	107	32	48	12	13
123	6.74	5	2088	286	855	166	259
118	6.74	5	693	8	65	29	24
105	6.65	5	244	118	274	68	112
134	6.55	6	107	24	30	13	11
146	6.89	6	735	48	127	28	45
153	6.92	6	3150	313	898	183	291
141	6.82	6	490	81	242	23	73
163	6.99	6	4161	206	607	160	222
158	7.02	6	471	21	52	18	20
178	7.14	7	526	28	105	13	36
187	7.17	7	1439	112	369	49	163
183	7.20	7	1033	138	445	62	163
185	7.11	7	111	11	37	7	12
174	7.11	7	1022	101	309	47	112
177	7.08	7	942	61	208	35	66
172	7.33	7	260	15	41	10	16
180	7.36	7	3030	109	322	51	122
170	7.27	7	1220	25.6	61.8	13.8	32.1
201	7.62	8	552	21.2	116.1	9.2	20.2
203	7.65	8	981	24.6	55.3	10.7	24.1
195	7.56	8	252	18.1	28.5	5.9	12.7
194	7.80	8	337	7.4	13.1	3.1	7.2

[46] Hawker and Connell (1988)

References

Accardi-Dey, A. and Gschwend, P.M. 2002. "Assessing the Combined Roles of Natural Organic Matter and Black Carbon as Sorbents in Sediments," Environmental Science & Technology, 36:21-29.

Adams, R.G., Lohman, R., Fernandez, L.A., MacFarlane, J.K., and Gscwend, P.M. 2007. "Polyethylene Devices: Passive Samplers for Measuring Dissolved Hydrophobic Organic Compounds in Aquatic Environments," Environmental Science & Technology, 41(4):1317-1323.

Adriano, D.C. 2001. Trace Elements in Terrestrial Environments: Biogeochemistry, Bioavailability, and Risks of Metals, 2nd Edition. Springer-Verlag, New York.

Ahn, S., Werner, D., Karapanagioti, H.K., McGlothlin, D.R., Zare, R.N., and Luthy, R.G. 2005. "Phenanthrene and Pyrene Sorption and Intraparticle Diffusion in Polyoxymethylene, Coke, and Activated Carbon," Environmental Science & Technology, 39:6516-6526.

The Anacostia Watershed Toxics Alliance (AWTA). 2002. Chartering a Course toward Restoration: A Toxic Chemical Management Strategy for the Anacostia River. Draft Report, Washington, D.C.

Andelman, J.B. and Suess, M.J. 1970. "Polynuclear Aromatic Hydrocarbons in the Water Environment," Bulletin of the World Health Organization, 43:479-508

Ankley, G.T. and Schubauer-Berigan, M.K. 1994. "Comparison of Techniques for the Isolation of Sediment Pore Water for Toxicity Testing," Archives of Environmental Contamination and Toxicology, 27(4):507-512.

Araya M., McGoldrick M.C., Klevay L.M., Strain, J.J., Robson, P., Nielsen, F., Olivares, M., Pizarro, F., Johnson, L., Poirier, K.A. 2001. "Determination of an Acute No-Observed-Adverse Effect Level," Regulatory Toxicology and Pharmacology, 34(2):137-148.

Araya M., Chen, B., Klevay L.M., Strain, J.J., Johnson, L., Robson, P., Shi, W., Nielsen, F., Zhu, H., Olivares, M., Pizarro, F., Haber, L.T. 2003. "Confirmation of an Acute No-Observed-Adverse-Effect and Low-Observed-Adverse-Effect Level for Copper in Bottled Drinking Water in a Multi-Site International Study," Regulatory Toxicology and Pharmacology, 34(2):137-148.

Arp, H.P., Breedveld, G.D., Cornelissen, G.E. 2009. "Estimating the in situ sediment-porewater distribution of PAHs and chlorinated aromatic hydrocarbons in

anthropogenic impacted sediments," Environmental Science & Technology, 43(15): 5576-5585.

Augenfeld J.M., Anderson J.W., Riley R.G., Thomas B.L. 1982. "The fate of polyaromatic hydrocarbons in an intertidal sediment exposure system: bioavailability to Maeoma inquinata (Mollusca: Pelecypoda) and Abarenicola pac~ca (Annelida:Polychaeta)," Marine Environmental Research, 7:31-50.

Baker, J.E., Capel, P.D., Eisenreich, S.J. 1985. "Influence of Colloids on Sediment-Water Partition Coefficients of Polychlorobiphenyl Congeners in Natural Waters," Environmental Science & Technology, 20:1136-1143.

Baker, J.R., Mihelcic, J.R., Luehrs, D.C., and Hickey, J.P. 1997. "Evaluation of Estimation Methods for Organic Carbon Normalized Sorption Coefficients," Water Environment Federation, 69(2):136-145.

Ball, W.P. and Roberts, P.V. 1991. "Long-Term Sorption of Halogenated Organic Chemicals by Aquifer Material. 2. Intraparticle Diffusion," Environmental Science & Technology, 25:1237-1249.

Bauer, J.E. and Capone, D.G. 1985. "Degradation and Mineralization of the Polycyclic Aromatic Hydrocarbons Anthracene and Naphthalene in Intertidal Marine Sediments," Applied and Environmental Microbiology, 50(1):81-90.

Bear, J. 1972. Dynamics of Fluids in Porous Media. Elsevier, New York.

Beckles, D., Chen, W., Hughes, J. 2007. "Bioavailability of Polycyclic Aromatic Hydrocarbons Sequestered in Sediment: Microbial Study and Model Prediction," Environmental Toxicology and Chemistry, 26(5):878-883.

Bedard, D.L., Wagner, R.E., Brennan, M.J., Haberl, M.L., and Brown, J.F. 19987. "Extensive Degradation of Aroclors and Environmentally Transformed Polychlorinated Biphenyls by Alcaligenes Eutrophus H850," Applied and Environmental Microbiology, 53(5):1094-1102.

Bentley, S. 2004. Radiochemical Analysis of Anacostia Sediment. Draft Report, January 2004.

Berner, R.A. 1980. Early Diagenesis: A Theoretical Approach. Princeton University Press.

Bierman, V.J. 1990. "Equilibrium Partitioning and Biomagnification of Organic Chemicals in Benthic Animals," Environmental Science & Technology, 24:1407-1412.

Bintein S, Devillers J, and Karcher W. 1993. "Nonlinear dependence of fish bioconcentration on n-octanol/water partition coefficient," SAR QSAR Environmental Research, 1:29–39.

Booij, K., Shiu, W.Y., Mackay, D. 1998. "Calibrating the uptake kinetics of semipermeable membrane devices using exposure standards," Environmental Toxicology and Chemistry. 17:1236–1345.

Bopp, R.F., Gross, M.L., Tong, H., Simpson, H.J., Monson, S.J., Deck, B.L., and Moser, F.C. 1991. "A Major Incident of Dioxin Contamination," Environmental Science & Technology, 25:951-956.

Boudreau, B. 1986. "Mathematics of Tracer Mixing in Sediments: I. Spatially-Dependent, Diffusive Mixing," American Journal of Science, 286(3):161-198.

Boudreau, B. 1997. Diagenetic Models and Their Implementation: Modeling Transport Reactions in Aquatic Sediments. Springer-Verlag, New York.

Boudreau, B. and Jorgensen, B. 2001. The Benthic Boundary Layer. Oxford University Press, New York.

Brinkhurst R.O., and Cook, D.G. 1980. Aquatic Oligochaete Biology. Plenum Press, New York, NY.

Burton, G.A. 1991. "Assessing the Toxicity of Freshwater Sediments," Environmental Toxicology and Chemistry, 10:1585-1627.

Burton, G.A., Greenberg, M.S., Rowland, C.D., Irvine, C.A., Lavoie, D.R., Brooker, J.A., Moore, L., Raymer, D.F.N., and McWilliam, R.A. 2005. "In Situ Exposures Using Caged Organisms: A Multi-Compartment Approach to Detect Aquatic Toxicity and Bioaccumulation," Environmental Pollution, 134:133-144.

Carslaw, H.S. and Jaeger, J.C. 1959. Conduction of Heat in Solids, 332-334.

Carson, R. 1962. Silent Spring. Houghton Mifflin, Boston.

Cerniglia, C.E. 1992. "Biodegradation of Polycyclic Aromatic Hydrocarbons," Biodegradation, 3:351–358.

Chadwick D., Katz, C., Groves, J., Carlson, A., Smith, C., Paulsen, R., O'Rourke, D. and Gahr, N. 2001. Anacostia River Seepage & Porewater Survey Report-Draft. February 27, 2001. Marine Environmental Quality Branch, SPAWAR Systems Center, San Diego, CA 92152.

Chatwin, P.C. 1975. "On the Longitudinal Dispersion of Passive Contaminant in Oscillatory Flows in Tubes," Journal of Fluid Mechanics, 71:513-527.

Chen, X., Wright, J.V., Conca, J.L., Peurreng, L.M. 1997. "Effects of pH on Heavy Metal Sorption on Apatite," Environmental Science & Technology, 31(3):624-631.

Chen, W., Kan, A.T., Tomson, M.B. 2000. "Irreversible Adsorption of Chlorinated Benzenes to Sediments: Implications for Sediment Quality Criteria," Environmental Science & Technology, 34:385-392.

Chen, W., Lakshmanan, K., Kan, A.T., Tomson, M.B. (2002) "A Program for Evaluating Dual-Equilibrium Desorption Effects on Remediation," Ground Water, 42(4):620-624.

Chin, YP, Gschwend, P.M. 1992. "Partitioning of Polycyclic Aromatic Hydrocarbons to Marine Pore Water Organic Colloids," Environmental Science & Technology, 26:1621-1626.

Chiou, C.T., Porter, P.E., Schmedding, D.W. 1983. "Partition Equilibria of Nonionic Organic Compounds Soil Organic Matter and Water," Environmental Science & Technology, 17:227-231.

Cho, Y., Smithenry, D.W., Ghosh, U., Kennedy, A.J., Millward, R.N., Bridges, T.S., Luthy, R.G. 2007. "Field Methods for Amending Marine Sediment with Activated Carbon and Assessing Treatment Effectiveness," Marine Environmental Research, 64(5):541-555.

Cho Y.M., Ghosh U., Kennedy A.J., Grossman A., Ray G., Tomaszewski J.E., Smithenry D.W., Bridges T.S., Luthy R.G. 2009. "Field application of activated carbon amendment for in-situ stabilization of polychlorinated biphenyls in marine sediment," Environmental Science & Technology, 43(10):3815-3823.

Cook, J.W. 1932. "The Production of Cancer by Pure Hydrocarbons," Proceedings of the Royal Society of London. Series B, Containing Papers of a Biological Nature, 111(773):485-496.

Cook, P.G., Favreau, G., Dighton, J.C., Tickell, S. 2003. "Determining Natural Groundwater Influx to a Tropical River Using Radon, Chlorofluorocarbons, and Ionic Environmental Tracers," Journal of Hydrology, 277:74-88.

Cornelissen, G. and Gustafson, O. 2004. "Sorption of Phenanthrene to Black Carbon in Sediment with and without Organic Matter and Native Sorbates," Environmental Science & Technology, 38:148-155.

Cornelissen, G., Petterson, A., Broman, D., Mayer, P., and Breedveld, D. 2008. "Field Testing of Equilibrium Passive Samplers to Determine Freely Dissolved Native Polycyclic Aromatic Hydrocarbon Concentrations," Environmental Toxicology and Chemistry, 27(3):499-508.

Cornett, R.J., Risto, B.A., and Lee, D.R. 1989. "Measuring Groundwater Transport through Lake Sediments by Advection and Diffusion," Water Resources Research, 25(8):1815-1823.

Crank J. 1975. The Mathematics of Diffusion. Oxford University Press, London.

Crank, J. and Nicolson, P. 1947. "A Practical Method for Numerical Evaluation of Solutions of Partial Differential Equations of the Heat Conduction Type," Proceedings of the Cambridge Philosophical Society, 43:50-64.

Crannell, B.S., Eighmy, T.T., Hall, G., Willson, C., Reible, D.D., Ming, Y. 2004. "Pilot-Scale Reactive Barrier Technologies for Containment of Metal-Contaminated Sediments and Dredged Materials," NOAA/UNH Cooperative Institute for Coastal and Estuarine Environmental Technology (CICEET), Final Report.

Danckwerts, P.V. 1953. "Continuous Flow Systems," Chemical Engineering Science, 2:1-13.

Davis, J.A. 1982. "Adsorption of natural dissolved organic matter at the oxide/water interface," Geochimica et Cosmochimica Acta, 46:2381-2393.

Denkhaus, E. and Salnikow, K. 2002. "Nickel Essentiality, Toxicity, and Carcinogenicity," Critical Reviews in Oncology/Hemotology, 42(1):35-56.

Di Toro, D.M., Zarba, C.S., Hansen, D.J., Berry, W.J., Swartz, R.C., Cowan, C.E., Pavlou, S.P., Allen, H.E., Thomas, N.A., and Paquin, P.R. 1991. "Technical Basis for Establishing Sediment Quality Criteria for Nonionic Organic Chemicals Using Equilibrium Partitioning," Environmental Toxicology and Chemistry, 10:1541-1583.

Doucette, W.J., 2003. "Quantitative structure-activity relationships for predicting soil-sediment sorption coefficients for organic chemicals," Environmental Toxicology and Chemistry, 22:1771–1788.

Drake, B.E. 2007. "Bioavailability and trophic transfer of PAHs and PCBs," University of Texas at Austin, Master's Thesis.

Durant, N.D., Wilson, L.P., and Bouwer, E.J. 1995. "Microcosm Studies of Subsurface PAH-degrading Bacteria from a Former Manufactured Gas Plant," Journal of Contaminant Hydrology, 17(3):213-237

EPA. 1994. Assessment and Remediation of Contaminated Sediments (ARCS) Program Assessment Guidance Document, EPA-905-B94-002. Great Lakes National Program Office, Chicago, IL.

EPA. 1997. Lake Michigan Mass Balance Study (LMMB) Methods Compendium, Volume 3: Metals, Conventionals, Radiochemistry, and Biomonitoring Sample Analysis Techniques; EPA-905/R-97-012c; U.S. Environmental Protection Agency, Great Lakes National Program Office: Chicago, IL, 1997.

EPA. 1998. Contaminated Sediment Management Strategy, EPA 823-R-97-006, EPA 823-R-97-007, and EPA 823-R-97-008. Access via website http://www.epa.gov/OST/cs/ stratefs.html.

EPA. 2004. What You Need to Know About Mercury in Fish and Shellfish. EPA and FDA Advice For: Women Who Might Become Pregnant Women Who are Pregnant Nursing Mothers Young Children. EPA-823-R-04-005.

EPA. 2008. US EPA human health risk and exposure website: http://www.epa.gov/ebtpages/humaexposure.html.

Fairey, J.L, Speitel, G.E., Katz, L.E. 2006. "Impact of Natural Organic Matter on Monochloramine Reduction by Granular Activated Carbon: The Role of Porosity and Electrostatic Surface Properties," Environmental Science & Technology, 40(13):4268-4273.

Farrington, J.W., Loehr, R.C., Anderson, E.L., Bohlen, W.F., Cohen, Y., Farley, K.J., Giesy, J.P., Henshel, D.S., Lester, S.U., Liegel, K.J., McCarty, P.L., O'Donoghue, J.L., Opaluch, J.J, Reible, D.D. 2001. A Risk-Management Strategy for PCB-Contaminated Sediments. National Acadamies Press, Washington, DC.

Fernandez, L.A., Harvey, C.F., and Gschwend, P.M. 2009. "Using Performance Reference Compounds in Polyethylene Passive Samplers to Deduce Sediment Porewater Concentrations for Numerous Target Chemicals," Environmental Science & Technology, 43:8888-8894.

Fredrickson, H.L., Furey, J., Talley, J.W., and Richmond, M. 2004. "Bioavailability of hydrophobic organic contaminants and quality of organic carbon," Environmental Chemistry Letters, 2:77-81.

Futoma, D.J, Smith, S.R., Smith, T.E., and Tanaka, J. 1981. Polycyclic Aromatic Hydrocarbons in Water Systems. CRC Press, Boca Raton, FL, USA.

Gadde, R.R. and Leitinen, H.A. 1974. "Heavy Metal Adsorption by Hydrous Iron and Manganese Oxides," Analytical Chemistry, 46(13):2022-2026.

Ghosh, U., Gillette, J.S., Luthy, R.G., and Zare, R.N. 2000. "Microscale location, characterization, and association of polycyclic aromatic hydrocarbons on harbor sediment particles," Environmental Science & Technology, 34:1729–1736.

Ghosh, U., Zimmerman, J.R., and Luthy, R.G. 2003. "PCB and PAH Speciation amound Particle Types in Contaminated Harbor Sediments and Effects on PAH Bioavailability," Environmental Science & Technology, 37:2209-2217.

Gillis, C.A., Bonnevie, N.L., Su, S.H., Ducey, J.G., Huntley, S.L., Wenning, R.J. 1995. "DDT, DDD, and DDE contamination of sediment in the Newark Bay estuary, New Jersey," Archives of Environmental Contamination and Toxicology, 28(1):85-92.

Goring, C.A.I. 1962. "Control of Nitrification by 2-Chloro-6-(Trichloromethyl)-Pyridine," Soil Science, 93:211-218.

Goring, C.A.I. 1967. "Physical Aspects of Soil in Relation to the Action of Soil Fungicides," Annual Review of Phytopathology, 5:285-318.

Grieb, T.M., Driscoll, C.T., Gloss, S.P., Shoefield, C.L., Bowie, G.L, Porcella, D.B. 1990. "Factors Affecting Mercury Accumulation in Fish in the Upper Michigan Peninsula," Environmental Toxicology and Chemistry, 9(7):919-930.

Gustaffson, O., Haghseta, F., Chan, C., Macfarlane, J., Gschwend, P.M. 1997. "Quantification of the Dilute Sedimentary Soot Phase: Implications for PAH speciation and Bioavailability," Environmental Science & Technology, 31:203-209.

Hamaker, J.W. and Goring, C.A.I. 1972. Organic Chemicals in the Soil Environment. Marcel Dekker, New York.

Hansen, D.J., Parrish, P.R., Lowe, J.I., Wilson, A.J., and Wilson, P.D. 1971. "Chronic Toxicity, Uptake, and Retention of Aroclor® 1254 in Two Estuarine Fishes," Bulletin of Environmental Contamination and Toxicology, 6(2):113-119.

Hansen, K., Clemen, L., Ellefson, M. and Johnson, H. 2001. "Compound-Specific, Quantitative Characterization of Organic Fluorochemicals in Biological Matrices," Environmental Science & Technology, 35: 766-770.

Harris D., Horwath, W., and van Kessel, C. 2001. "Acid Fumigation of Soils to Remove Carbonates Prior to Total Organic Carbon or CARBON-13 Isotopic Analysis," Soil Science Society of America Journal, 65:1853–1856.

Hawker, D.W. and Connell, D.W. 1988. "Octanol water partition-coefficients of polychlorinated biphenyl congeners," Environmental Science & Technology, 22(4):382-287.

Haws, L. C., Su, S. H., Harris, M., Devito, M. J., Walker, N. J., Farland, W. H., Finley, B., and Birnbaum, L. S. 2006. "Development of a refined database of

mammalian relative potency estimates for dioxin-like compounds," Toxicological Science, 89:4–30.

Hay, A. 1982. The Chemical Scythe. Plenum Press, New York.

Hayduk, W. and Laudie, H. 1974. "Predicting diffusion coefficients for nonelectrolytes in dilute aqueous solutions," AICheE Journal, 20:611.

Hayes, L.A., Nevin, K.P., and Lovley, D.R. 1999. "Role of Prior Exposure on Anaerobic Degradation of Naphthalene and Phenanthrene in Marine Harbor Sediments," Organic Geochemistry, 30(8):937-945.

Hedges, J.L., and Stern, J.H. 1984. "Carbon and Nitrogen Determination of Carbonate-Containing Solids," Limnology and Oceanography, 29:657–663.

Herbes, S.E. and Allen, C.P. 1983. "Lipid Quantification of Freshwater Invertebrates: Method Modification for Microquantification," Canadian Journal of Fisheries and Aquatic Sciences, 40:1315-1317.

Hesslein, R.H. 1976. "An in Situ Sampler for Close Interval Pore Water Studies," Limnology and Oceanography, 21:912-914.

Hong, L. and Luthy, R.G. 2008. "Uptake of PAHs into polyoxymethylene and application to oil-soot (lampblack)-impacted soil samples," Chemosphere, 72(2):272-281.

Hooper, P.L., Visconti, L., Garry, P.J., Johnson, G.E. 1980. "Zinc Lowers High-Density Lipoprotein–Cholesterol Levels," Journal of the American Medical Association, 244:1960-1961.

Horne Engineering Services. 2003. Site Characterization Report for Comparative Validation of Innovative "Active Capping" Technologies for the Anacostia River, Washington, DC. Prepared for the Hazardous Substance Research Center/S&SW. http://www.hsrc-ssw.org/ana-index.html

Horne Engineering Services (Horne). 2004a. Cap Completion Report for Comparative Validation of Innovative "Active Capping" Technologies Anacostia River, Washington, DC. Prepared for the Hazardous Substance Research Center/S&SW. Retrieved on October 2, 2006 from http:www.hsrc-ssw.org/ana-index.html.

Horne Engineering Services (Horne). 2004b. Month 1 Monitoring Report Comparative Validation of Innovative "Active Capping" Technologies Anacostia River, Washington, DC. Prepared for the Hazardous Substance Research Center/S&SW. Retrieved on October 2, 2006 from http:www.hsrc-ssw.org/ana-index.html.

Horne, R.A. and Johnson, C.R. 1985. Matrix Analysis. Cambridge University Press.

Huckins, J.N., Tubergin, M.W., and Manuweera, G.K. 1990. "Semipermeable membrane devices containing model lipid: A new approach to monitoring the bioavaiiability of lipophilic contaminants and estimating their bioconcentration potential," Chemosphere, 20:533-552.

Huckins, J. N.; Petty, J. D.; Lebo, J. A.; Almeida, F. V.; Booij, K., Alvarez, D. A., Cranor, W. L., Clark, R. C., and Mogensen, B. B. 2002. "Development of the permeability/performance reference compound approach for in situ calibration of semipermeable membrane devices," Environmental Science & Technology, 36(1):85-91.

Huckins, J.N., Petty. J.D., and Booij, K. 2006. Monitors of Organic Chemicals in the Environment, Semipermeable Membrane Devices. Springer, New York, NY.

Hulburt, H.M. 1944. "Chemical Processes in Continuous-Flow Systems: Reaction Kinetics," Industrial & Engineering Chemistry, 36:1012-1017.

Hull, J.H., Jersak, J.M., McDonald, B.J. 1998. "Examination of a New Remedial Technology for Capping Contaminated Sediments: Large-Scale Laboratory Evaluation of Sediment Mixing and Cap Resistance to Erosive Forces," Remediation, 8(3):37-58.

Hull, J.H., Jersak, J.M., and Kasper, C.A. 1999. "In Situ Capping of Contaminated Sediments: Comparing the Relative Effectiveness of Sand versus Clay-Mineral Based Sediment Caps," Proceedings of the 1999 Conference on Hazardous Waste Research, 286-311.

Hyun, S., Jafvert, C., Lee, L., Rao, P. 2006. "Laboratory Studies to Characterize the Efficacy of Sand Capping a Coal Tar-Contaminated Sediment," Chemosphere, 63 (10): 1621-1631.

Imberger, J., Hamblin, P. 1982. "Dynamics of Lakes, Reservoirs, and Cooling Ponds" Annual Review of Fluid Mechanics, 14:153-187.

Isnard P, and Lambert S. 1988. "Estimating bioconcentration factors from octanol–water coefficient and aqueous solubility," Chemosphere, 17:21–34.

Jacobs, P.H. and Forstner, U. 1999. "Concept of Subaqueous Capping of Contaminated Sediments with Active Barrier Systems Using Natural and Modified Zeolites," Water Research, 33(9):2083-2087.

Jenne, E.A., 1977. "Trace element sorption by sediments and soils - sites and processes," W. Chappel and K. Petersen (Editors), Symposium on Molybdenum in the Environment. Marcel Dekker, New York, 425-553.

Jensen, S. 1966. "Report of a New Chemical Hazard," New Scientist, 32:612.

Jensen, S., Johnels, A.G., Olsson, M., and Otterland, G. 1966. "DDT and PCB in Marine Animals from Swedish Waters," Nature, 224:247-250.

Jones, E., Oliphant, T., and Peterson, P. 2001. SciPy: Open Source Scientific Tools for Python. http://www.scipy.org.

Jonker, M.T. and Koelmans, A.A. 2001. "Polyoxymethylene solid phase extraction as a partitioning method for hydrophobic organic chemicals in sediment and soot," Environmental Science & Technology, 35:3742-3748.

Jonker, M.T., van der Heijden, S.A., Kreitinger, J.P., and Hawthorne, S.B. 2007. "Predicting PAH Bioaccumulation and Toxicity in Earthworms Exposed to Manufactured Gas Plant Soils with Solid-Phase Microextraction," Environmental Science & Technology, 41:7472-7478.

Kan, A.T., Fu, G., Hunter, M.A., Tomson, M.B. 1997. "Irreversible Adsorption of Naphthalene and Tetrachlorobiphenyl to Lula and Surrogate Sediments," Environmental Science & Technology, 31:2176-2185.

Kan, A.T., Fu, G., Hunter, M.A., Chen, W., Ward, C.H., Tomson, M.B. 1998. "Irreversible Sorption of Neutral Hydrocarbons to Sediments: Experimental Observations and Predictions," Environmental Science & Technology, 32:892-902.

Kaplan, D.I. and Knox, A.S. 2004. "Enhanced Contaminant Desorption Induced by Phosphate Mineral Additions to Sediment," Environmental Science & Technology, 38:3153-3160.

Karickhoff, S.W., Brown, D.S., and Scott, T.A. 1979. "Sorption of Hydrophobic Pollutants in Natural Sediments," Water Research, 13, 241-248.

Karickhoff, S.W. 1981. "Semi-Empirical Estimation of Sorption of Hydrophobic Pollutants on Soils and Sediments," Chemosphere, 10:833-846.

Kennaway, E.L. 1930. "Further Experiments on Cancer-Producing Substances," Biochemistry, 24(2):497-504.

Klaassen, Curtis D. 2001. Casarett & Doull's Toxicology - The Basic Science of Poisons (6th Edition). McGraw-Hill, New York.

Kraaij R., Mayer P., Busser F.J.M., Bolscher M.V.H., Seinen W., Tolls J. 2003. "Measured pore-water concentrations make equilibrium partitioning work-a data analysis," Environmental Science & Technology 37:268-274.

Lambert, S.M., Porter, P.E., and Schieferstein, R.T. 1965. "Movement and Sorption of Chemicals Applied to Soil," Weeds, 13:185-190.

Lambert, S.M. 1967. "Functional Relation Between Sorption in Soil and Chemical Structure," Journal of Agricultural and Food Chemistry, 16(2):572-576.

Lampert, D.J. and Reible, D.D. 2009. "An Analytical Modeling Approach for Evaluation of Capping of Contaminated Sediments," Soil and Sediment Contamination, 18(4)470-488.

Lanphear, B.P., Vorhees, C.V., and Bellinger, D.C. 2005. Protecting Children from Environmental Toxins. PLoS Med 2, e61.

Lee, D.R. 1977. "A Device for Measuring Seepage Fluxes in Lakes and Estuaries," Limnology and Oceanography, 22(1):140-147.

Lohmann, R., MacFarlane, J.K., Gschwend, P.M. 2005. "Importance of Black Carbon to Sorption of Native PAHs, PCBs, and PCDDs in Boston and New York Harbor Sediments," Environmental Science & Technology, 39:141-148.

Lovley, D.R. 1991. "Dissimilatory Fe (III) and Mn (IV) reduction," Microbiology and Molecular Biology Reviews, 55(2):259-287.

Lu, X.X, D. D. Reible, J.W. Fleeger, and Chai, Y.Z. 2003. "Bioavailability of Desorption –Resistant Phenanthrene to the Oligochaete *Ilyodrilus templetoni*" Environmental Toxicology and Chemistry, 22:153-160.

Lu, X.X., D.D. Reible, and Fleeger, J.W. 2004a. "Relative Importance of Ingested Sediment Versus Pore Water Uptake Routes for PAHs to the Deposit-Feeding Oligochaete Ilyodrilus templetoni," Archives of Environmental Contamination and Toxicology, 47(2):207-214.

Lu, X.X., D.D Reible, and Fleeger, J.W. 2004b. "Adsorption/Desorption and Bioavailability of Sediment-Associated Benzo[a]pyrene," Environmental Toxicology and Chemistry, 23(1):57-64.

Lu, X., Reible, D.D., Fleeger, J.W. 2006. "Bioavailability of Polycyclic Aromatic Hydrocarbons in Field-Contaminated Anacostia River (Washington, DC) Sediment," Environmental Toxicology and Chemistry, 25(11):2869-2874.

Lyman, W.J, Reehl, W.F. and Rosenblatt, D.H. 1990. Handbook of Chemical Property Estimation Methods: Environmental Behavior of Organic Compounds, American Chemical Society, Washington DC.

Lyttikainen M., Pehkonen,, S., Akkanen, J., Leppanen, M., and Kukkonen, J. 2007. "Bioaccumulation and Biotransformation of Polycyclic Aromatic Hydrocarbons During Sediment Tests with Oligochaetes (Lumbriculus variegatus)." Environmental Toxicology and Chemistry, 26: 2660-2666.

Ma, M., Feng, Z., Guan, C., Ma, Y., Xu, H., Li, H. 2001. "DDT, PAH and PCB in Sediments from the Intertidal Zone of the Bohai Sea and the Yellow Sea," Marine Pollution Bulletin, 42(2):132-136.

Ma, Q., Traina, S.J., Logan, T.J., Ryan, J.A. 1993. "In Situ Lead Immobilization by Apatite," Environmental Science & Technology, 27:1803-1810.

MacKay, D. 1982. "Correlation of bioconcentration factors," Environmental Science & Technology, 16:274–278.

MacKay, D.; Shiu, W. Y.; Ma, K. C. 1992. Illustrated Handbook of Physical-Chemical Properties and Environmental Fate for Organic Chemicals, Volume 3. Lewis Publishers: Chelsea, MI.

Malusis, M. and Shackelford, C. 2002. "Theory for Reactive Solute Transport through Clay Membrane Barriers," Journal of Contaminant Hydrology 59:291-316.

Matrix Environmental and Geotechnical Services (Matrix) 2003. Final Report - Quantifying Specific Discharge across the Sediment–Water Interface within a Test Area of the Anacostia River, Washington, D.C.: a Pre-Capping Evaluation. November 2003. Submitted to Horne Engineering Services, Inc. Submitted by Matrix Environmental and Geotechnical Services, Florham Park, NJ 07932.

Matrix Environmental and Geotechnical Services (Matrix) 2004. Draft Report- Quantifying Specific Discharge across the Sediment –Water Interface within a Test Area of the Anacostia River, Washington, D.C. a Post-Capping Evaluation. July 2004. Submitted to Battelle. Submitted by Matrix Environmental and Geotechnical Services, East Hanover, NJ 07936.

Mayer, P., Vaes, W., Wijnker, F., Legierse, K., Kraaij, R., Tolls, J., and Hermans, J. 2000a. "Sensing Dissolved Sediment Porewater Concentrations of Persistent and Bioaccumulative Pollutants Using Disposable Solid-Phase Microextraction Fibers," Environmental Science & Technology, 34:5177-5183.

Mayer, P., Vaes, W. H. J., and Hermens, J. L. M. 2000b. "Sensing dissolved sediment porewater concentrations of persistent and bioaccumulative pollutants using disposable solid-phase microextraction fibers," Analytical Chemistry, 72:459-464.

McCafree, R.J., Myers, A.C., Davey, E., Morrison, G., Bender, M., Luedtke, N., Cullen, D., Froelich, P., Klinkhammer, G. 1980. "The Relation between Pore Water Chemistry and Benthic Fluxes of Nutrients and Manganese in Narragansett Bay, Rhode Island," Limnology and Oceanography, 25(1):31-44.

McDonough, K., Murphy, P., Olsta, J. Zhu, Y., Reible, D., Lowry, G. 2007. "Development of a Sorbent-Amended Thin Layer Sediment Cap in the Anacostia River," Soil & Sediment Contamination, 16(3):313-322.

McFarland V.A. 1984. "Activity-Based Evaluation of Potential Bioaccumulation from Sediments," Montgomery RL, Leach JL (eds) Dredging and Dredged Material Disposal, American Society of Civil Engineers, New York, 1:461-467.

McGroddy, S.E. and Farrington, J.W. 1995. "Sediment Porewater Partitioning of Polycyclic Aromatic Hydrocarbons in Three Cores from Boston Harbor, Massachusetts," Environmental Science & Technology, 29:1542-1550.

McNally, D.L., Mihelcic, J.R. and Lueking, D.R. 1998. "Biodegradation of Three- and Four-Ring Polycyclic Aromatic Hydrocarbons under Aerobic and Denitrifying Conditions," Environmental Science & Technology, 32:2633–2639.

Meloche, L.M, deBruyn, A.M.H., Otton, S.V., Ikonomou, M.G., and Gobas, F.A.P.C. 2009. "Assessing exposure of sediment biota to organic contaminants by thin-film solid phase microextraction," Environmental Toxicology and Chemistry, 28:247–253.

Miller, M.M., Wassik, S.P., Huang, G.L., Shiu, W.Y., MacKay, D. 1985. "Relationships between Octanol-Water Partition Coefficient and Aqueous Solubility," Environmental Science & Technology, 19:522-529.

Millington, R.J., and Quirk, J.M. 1961. "Permeability of Porous Solids," Transactions of the Faraday Society, 57:1200-1207.

Millward, R.N., Bridges, T.S., Ghosh, U., Zimmerman, J.R., Luthy, R.G. 2005. "Addition of Activated Carbon to Sediments to Reduce PCB Bioaccumulation by a Polychaete (*Neanthes arenaceodentata*) and an Amphipod (*Leptocheirus plumulosus*)," Environmental Science & Technology,39(8):2880-2887.

Miyake, M., Ishigaki, K., Suzuki, T. 1986. "Structure Refinements of Pb 2+ Ion-Exchanged Apatites by X-Ray Powder Pattern-Fitting," Journal of Solid State Chemistry, 61(2):230-235.

Moore, J.N., Ficklin, W.H., Johns, C. 1988. "Partitioning of Arsenic and Metals in Reducing Sulfidic Sediments," Environmental Science & Technology, 22:432–437.

Murphy, P., Marquette, A., Reible, D., and Lowry G.V. 2006. "Predicting the Performance of Activated Carbon-, Coke-, and Soil-Amended Thin Layer Sediment Caps," Journal of Environmental Engineering, 132(7):787-794.

Nakata, H., Kannan, K., Nasu, T., Cho, H., Sinclair, E., Takemura, A. 2006. "Perfluorinated Contaminants in Sediments and Aquatic Organisms Collected from Shallow Water and Tidal Flat Areas of the Ariake Sea, Japan: Environmental Fate of Perfluorooctane Sulfonate in Aquatic Ecosystems," Environmental Science & Technology, 40(16):4916-4921.

Namiesnik, J., Zabiegala, B., Kot-Wasik, A., Partyka, M., and Wasik, A. 2005. "Passive sampling and/or extraction techniques in environmental analysis: a review." Analytical and Bioanalytical Chemistry, 381(2):279-301.

Neuman, S.P. 1990. "Universal Scaling in Geologic Media," Water Resources Research, 26(8):1749-1758.

Nieuwveldt, F. 2009. Recipe 576934: Numerical Inversion of the Laplace Transform using the Talbot method. (Python). http://code.activestate.com/recipes/576934/.

Nimmo, D.R., Wilson, P.D., Blackman, R.R., Wilson, A.J. 1971. "Polychlorinated Biphenyl Absorbed from Sediments by Fiddler Crabs and Pink Shrimp," Nature, 231:50-52.

Nogawa, K., Kobayashi, E., Okubo, Y., Suwazono, Y. 2004. "Environmental cadmium exposure, adverse effects and preventive measures in Japan," BioMetals, 17(5):581-587.

National Research Council (NRC). 2001. A Risk-Management Strategy for PCB-Contaminated Sediments. Committee on Remediation of PCB-Contaminated Sediments, Board on Environmental Studies and Toxicology, Division on Life and Earth Studies, National Research Council. National Academy Press, Washington DC.

Palermo, M.R. 1998. "Design considerations for in-situ capping of contaminated sediments," Water Science and Technology, 37:315-321.

Palermo, M.R., S. Maynord, J. Miller, and D.D. Reible. 1998. Guidance Document for In Situ Subaqueous Capping of Contaminated Sediments, EPA 905-B96-004.

Parametrix. 1998. St. Paul Waterway Area Remedial Action and Habitat Restoration Project. Final 1998 Monitoring Report.

Parrett, K. and Blishke, H. 2005. "23-Acre Multilayer Sediment Cap in Dynamic Riverine Environment Using Organoclay as Adsorptive Capping Material," Society of Environmental Toxicology and Chemistry 26th Annual Meeting, Baltimore, MD.

Pignatello, J.J. and Xing, B. 1996. "Mechanisms of Slow Sorption of Organic Chemicals to Natural Particles," Environmental Science & Technology, 30:1-11.

Peld, M., Tonsuaado, K., Bender, V. 2004. "Sorption and Desorption of Cd 2 and Zn 2 Ions in Apatite-Aqueous Systems," Environmental Science & Technology, 35(21):5626-5631

Rabideau, A. and Khandelwal, A. 1998. "Boundary Conditions for Modeling Transport in Vertical Barriers," Journal of Environmental Engineering 124:(11)1135-1139.

Reible, D.D. and Lu, X. 2000. "Desorption, Accumulation, and Elimination of Sediment Associated Phenanthrene and Benzo[a]Pyrene to a freshwater oligochaete," Ecotoxicology, 2nd International Symposium on Contaminated Sediments, 319-324.

Reible, D.D., Lampert, D.J., Constant, D., Mutch, R., Zhu, Y. 2007. "Active Capping Demonstration in the Anacostia River in Washington DC," Remediation Journal, 17(1), 39-53.

Reible, D.D., Lu, X.X., and Blishke, H. 2005. "Organoclay for the Control of NAPLs in Sediments," Society of Environmental Toxicology and Chemistry 26th Annual Meeting, Baltimore, MD.

Renner, R. 2001. "Concern Over Perfluorinated Chemicals," Environmental Science & Technology, 35(7):154A-160A.

Reynoldson, T.B. 1987. "Interactions between Sediment Contaminants and Benthic Organisms" Hydrobiologia, 149(1):53-66.

Rockne, K.J. and Strand, S.E. 1998. "Biodegradation of Bicyclic and Polycyclic Aromatic Hydrocarbons in Anaerobic Enrichments," Environmental Science & Technology, 32:3962-3967.

Rowe, P.K. and Booker, J.R. 1985. "1-D Pollutant Migration in Soils of Finite Depth," Journal of Geotechnical Engineering, 111(4):479-499.

Rubin, H. and Rabideau, A. 2000. "Approximate Evaluation of Contaminant Transport through Vertical Barriers" Journal of Contaminant Hydrology 40: 311-333.

Rusina, T.P., Smedes, F., Klanova, J., Booij, K.S., and Holoubek, I. 2007. "Polymer selection for passive sampling: A comparison of critical properties," Chemosphere, 68:1344-1351.

Salley, J. 1954. "Experimental Carcinogenesis in the Cheek Pouch of the Syrian Hamster," Journal of Dental Research, 33(2):253-262.

Sarchet, W.V. 2008. Effects of a Thin Layer Cap on Bioavailability and Bioaccumulation in Sediments. Master's Thesis, The University of Texas at Austin.

Schaffner, L.C., Dickhut, R.M., Mitra, S., Lay, P.W., and Brouwer-Riel, C. 1997. "Effects of Physical Chemistry and Bioturbation by Estuarine Macrofauna on the Transport of Hydrophobic Organic Contaminants in the Benthos," Environmental Science and Technology, 31:3120-3125.

Schwarzenbach, R.P., Gshwend, P.M., Imboden, D.M. 2003. "Chapter 9: Sorption I: Introduction and Sorption Processes Involving Organic Matter" and "Chapter 11: Sorption III: Sorption Processes Involving Inorganic Surfaces," Environmental Organic Chemistry, 2nd Edition, Wiley & Sons, Hoboken, New Jersey, 275-330 and 387-458.

Scheunert, I., Vockel, D., Schmitzer, J., Korte, F. 1987. "Biomineralization Rates of ^{14}C-Labelled Organic Chemicals in Aerobic and Anaerobic Suspended Soil," Chemosphere, 16(5):1031-1041.

Sepic, E., Leskovsek, H., and Trier, C. 1995. "Aerobic Bacterial Degradation of Selected Polyaromatic Compounds and n-Alkanes Found in Petroleum," Journal of Chromatography A, 697(1):515-523.

Shiaris, M.P. and Sayler, G.S. 1992. "Biotransformation of PCB by Natural Assemblages of Freshwater Microorganisms" Environmental Science & Technology, 16:367-369.

Simpson, S.L., Pryor, I.D., Mewburn, B.R., Batley, G.E., Jolley, D. 2002. "Considerations for Capping Metal-Contaminated Sediments in Dynamic Estuarine Environments," Environmental Science & Technology, 36(17):3772 - 3778.

Skwarski, A.E 2008. Demonstration and Evaluation of Solid-Phase Microextraction for Assessment of Contaminant Mobility and Bioavailability. Master's Thesis. University of Texas at Austin.

Smith, R. 1982. "Contaminant Dispersion in Oscillatory Flows," Journal of Fluid Mechanics, 114:379-398.

Syracuse Research Corporation and National Oceanic and Atmospheric Administration (SRC and NOAA). 2000. "Interpretive Summary of Existing Data Relevant to Potential Contaminants of Concern within the Anacostia River Watershed," SRC#FA292.

Takeuchi, Y. and Arai, H. 1990. "Removal of Coexisting Pb^{2+}, Cu^{2+} and Cd^{2+} Ions from Water by Addition of Hydroxyapatite Powder," Journal of Chemical Engineering of Japan, 23:75–80

Tan, K., Anderson, T.A., Jackson, W.A. 2005. "Temporal and Spatial Variation of Perchlorate in Streambed Sediments: Results from In-Situ Dialysis Samplers," Environmental Pollution, 136(2):283-291.

Tessier, A., Campbell, P.G.C., and Bisson, M. 1979. "Sequential Extraction Procedure for the Speciation of Particulate Trace Metals," Analytical Chemistry, 51(7):844-851.

Tessier, A., and Turner, D.R. 1995. Metal Speciation and bioavailability in Aquatic Systems. J. Wiley, New York.

Tessier A., Fortin D., Belzile N., DeVitre R. R. and Leppard G. G. 1996. "Metal Sorption to Diagenetic Iron and Manganese Oxyhydroxides and Associated Organic Matter: Narrowing the Gap between Field and Laboratory Measurements," Geochimica et Cosmochimica Acta 60(3):387-404.

Thibodeaux, L.J. and Bosworth, W.S. 1990. "A Theoretical Evaluation of the Effectiveness of Capping PCB Contaminated New Bedford Harbor Bed Sediment, Final Report," Hazardous Waste Research Center, Louisiana State University, Baton Rouge, LA.

Thibodeaux, L.J. 1996. Environmental Chemodynamics, Chapter 5: "Chemical Exchange between Water and Adjoining Earthen Material." J. Wiley, New York.

Thibodeaux, L.J. and Duckworth, K.T. 2001. "The Effectiveness of Environmental Dredging: A Study of Three Sites." Remediation Journal, 11(3):5-33.

Thoma, G.J., Reible, D.D., Valsaraj, K.T., and Thibodeaux, L.J. 1993. "Efficiency of Capping Contaminated Bed Sediments In Situ. 2. Mathematics of Diffusion-Adsorption in the Capping Layer," Environmental Science & Technology, 27:2412-2419.

Thoms, S.R., Matisoff, G., McCall, P.L., and Wang, X. 1995. Models for Alteration of Sediments by Benthic Organisms, Project 92-NPS-2, Water Environment Research Foundation, Alexandria Virginia.

Trefethen, L.N., Weideman, J.A.C., and Schmelzer, T. 2006. Talbot quadratures and rational approximations. BIT. Numerical Mathematics, 46(3):653-670.

Trimble, T.A., You, J., Lydy, M.J. 2008. "Bioavailability of PCBs from field-collected sediments: Application of Tenax extraction and matrix-SPME techniques," Chemosphere, 71(2):337-344.

United States Department of Health and Human Services. 2005. Report on Carcinogens, Eleventh Edition; Public Health Service, National Toxicology Program.

United States Department of Health and Human Services. 2007. NTP Technical Report on the Toxicity Studies of Sodium Dichromate Dihydrate.

Upham, B. L., Deocampo, N. D., Wurl, B., and Trosko, J. E. 1998. "Inhibition of Gap Junctional Intercellular Communication by Perfluorinated Fatty Acids Is Dependent on the Chain Length of the Fluorinated Tail," International Journal of Cancer, 78:491-495.

Van den Berg, M., De Jongh, J., Poiger, H., and Olson, J. R. 1994. "The toxicokinetics and metabolism of polychlorinated dibenzo-p-dioxins (PCDDs) and dibenzofurans (PCDFs) and their relevance for toxicity," Critical Reviews in Toxicology, 24:1–74.

Van der Heijden, S.A. and Jonker, M.T. 2009. "PAH Bioavailability in Field Sediments: Comparing Different Methods for Predicting in Situ Bioaccumulation," Environmental Science & Technology, 43:3757-3763.

Van Genuchten, M.T. 1981. "Analytical solutions for chemical transport with simultaneous adsorption, zero order production and first order decay." Journal of Hydrology, 49(3):213-233.

Vinturella, A.E. Burgess, R.M., Coull, B.A., Thompson, K.M., and Shine, J.P. 2004. "Use of passive samplers to mimic uptake of polycyclic aromatic hydrocarbons by benthic polychaetes," Environmental Science & Technology, 38:1154-1160.

Walters, R.W. and Luthy, R.G. 1984. "Equilibrium Adsorption of Polycyclic Aromatic Hydrocarbons from Water onto Activated Carbon," Environmental Science & Technology, 25:1578-1584.

Wang, X.Q., Thibodeaux, L.J., Valsaraj, J.T., and Reible, D.D. 1981. "Efficiency of Capping Contaminated Bed Sediments In Situ. 1. Laboratory-Scale Experiments on Diffusion-Adsorption in the Capping Layer," Environmental Science & Technology, 18:395-403.

Watson, E.J. 1983. "Diffusion in Oscillatory Pipe Flow," Journal of Fluid Mechanics, 133:233-244.

Weber, W.J. and Miller, C.T. 1988. "Modeling the sorption of hydrophobic contaminants by aquifer materials—I. Rates and equilibria," Water Research, 22(4):457-464.

Weber W.J., LeBouf, E.J., Young, T.M., and Huang, W. 2001. "Contaminant Interactions with Geosorbent Organic Matter: Insights Drawn from Polymer Sciences," Water Research, 35, 853-868.

Wehner, J.F. and Wilhelm, R.H. 1956. "Boundary Conditions of Flow Reactor," Chemical Engineering Science, 6:89-93.

Werth, C.J. and Reinhard, M. 1997. "Effects of temperature on trichloroethylene desorption from silica gel and natural sediments. Kinetics." Environmental Science & Technology, 31:697–703.

Windom, H.L., Schropp, S.J., Calder, F.D., Ryan, J.D., Smith. R.G., Burney, L.C., Lewis, F.G., Rawlinson, C.H. 1989. "Natural Trace Metal Concentrations in Estuarine and Coastal Marine Sediments of the Southeastern United States," Environmental Science & Technology, 23:314-320.

Xu, Y., Schwartz, F.W. 1994. "Lead Immobilization by Hydroxyapatite in Aqueous Solutions," Journal of Contaminant Hydrology, 15:187-206.

You, J., Landrum, P.F., Lydy, M.J. 2006. "Comparison of Chemical Approaches for Assessing Bioavailability of Sediment-Associated Contaminants," Environmental Science & Technology, 40:6348-6353.

Young, D.R. and McDermott-Ehrlich, D. 1977. "Sediments as Sources of DDT and PCB," Southern California Coastal Water Research Project Annual Report for the Year Ended 30 June 1976.

Zeman, A.J. and Patterson, T.S. 1997. "Preliminary Results of Demonstration Capping Project in Hamilton Harbour," Water Quality Research Journal of Canada, 32(2):439-452.

Zimmerman, J.R., Ghosh, U., Millward, R.N., Bridges, T.S., Luthy, R.G. 2004. "Addition of Carbon Sorbents to Reduce PCB and PAH Bioavailability in Marine Sediments: Physicochemical Tests," Environmental Science & Technology, 38(20):5458-5464.

Vita

David Justice Lampert was born on June 1, 1978 in Alpine, TX, the son of Bruce Allan Lampert and Sandra Jean Anderson. He graduated in 1996 from Shawnee High School in Shawnee, Oklahoma and enrolled the same year at Oklahoma State University in Stillwater, OK. In May 2001 he was awarded a Bachelor of Science degree in Civil Engineering. In May of 2003, he received his Master's degree in Environmental and Water Resources Engineering at the University of Texas at Austin. After two years of working in environmental consulting, he re-enrolled in the graduate school at the University of Texas at Austin as a Doctor of Philosophy student in the Department of Civil, Architectural, and Environmental Engineering.

Permanent address: 6365 Bay Hill Drive, Abilene, TX 79606

This dissertation was typed by David Lampert.